Distribution Agreement

In presenting this thesis or dissertation as a partial fulfillment of the requirements for an advanced degree from Emory University, I hereby grant to Emory University and its agents the non-exclusive license to archive, make accessible, and display my thesis or dissertation in whole or in part in all forms of media, now or hereafter known, including display on the world wide web. I understand that I may select some access restrictions as part of the online submission of this thesis or dissertation. I retain all ownership rights to the copyright of the thesis or dissertation. I also retain the right to use in future works (such as articles or books) all or part of this thesis or dissertation.

Signature:

_____ _____

Kristen T. Thomas Date

Inhibition of the schizophrenia-associated microRNA miR-137 disrupts Nrg1α neurodevelopmental signal transduction

By

Kristen T. Thomas
Doctor of Philosophy

Graduate Division of Biological and Biomedical Sciences
Neuroscience

_____
Gary J. Bassell, Ph.D.
Advisor

_____
Yue Feng, Ph.D.
Committee Member

_____
Peng Jin, Ph.D.
Committee Member

_____
Donald Rainnie, Ph.D.
Committee Member

_____
James Q. Zheng, Ph.D.
Committee Member

Accepted:

_____
Lisa A. Tedesco, Ph.D.
Dean of the James T. Laney School of Graduate Studies

_____
Date

Inhibition of the schizophrenia-associated microRNA miR-137 disrupts Nrg1α neurodevelopmental signal transduction

By

Kristen T. Thomas
B.S., Texas A&M University, 2010

Advisor: Gary J. Bassell, Ph.D.

An abstract of
A dissertation submitted to the Faculty of the
James T. Laney School of Graduate Studies of Emory University
in partial fulfillment of the requirements for the degree of
Doctor of Philosophy

in Graduate Division of Biological and Biomedical Sciences
Neuroscience

2017

Abstract

Inhibition of the schizophrenia-associated microRNA miR-137 disrupts Nrg1α neurodevelopmental signal transduction

By Kristen T. Thomas

Defects in neural development play a well-substantiated but poorly understood role in schizophrenia etiology. Genomic studies have repeatedly associated variants in the gene encoding microRNA miR-137 with schizophrenia, but whether miR-137 contributes to the dysregulation of neurodevelopmental signal transduction in schizophrenia is unknown. Bioinformatic predictions suggest that the PI3K-Akt-mTOR branch of neuregulin (Nrg)/ErbB signaling may be particularly enriched with miR-137 targets. In the present study, we demonstrate that miR-137 regulates neuronal levels of p55γ, PTEN, Akt2, GSK3β, mTOR, and rictor. Inhibition of miR-137 ablates Nrg1α-induced increases in dendritic protein synthesis, phospho(Ser235/236)-S6, AMPA receptor subunits, and dendritic outgrowth, demonstrating a profound disruption of Nrg/ErbB signaling. Furthermore, inhibition of miR-137 blocks mTORC1-dependent responses to BDNF, including increased protein synthesis and dendritic outgrowth, while leaving mTORC1-independent S6 phosphorylation intact. Together, our results demonstrate that miR-137 regulates neuronal responses to Nrg1α and BDNF through convergent mechanisms and provide a novel mechanism by which miR-137 may regulate neural development and contribute to schizophrenia.

Inhibition of the schizophrenia-associated microRNA miR-137 disrupts Nrg1α neurodevelopmental signal transduction

By

Kristen T. Thomas
B.S., Texas A&M University, 2010

Advisor: Gary J. Bassell, Ph.D.

A dissertation submitted to the Faculty of the
James T. Laney School of Graduate Studies of Emory University
in partial fulfillment of the requirements for the degree of
Doctor of Philosophy

in Graduate Division of Biological and Biomedical Sciences
Neuroscience

2017

Acknowledgements

First, I would like to thank my mentor, Dr. Gary Bassell, for his guidance over the last five years and for allowing me to pursue a challenging and exciting project. I would also like to thank him for helping me to persevere through the more challenging times in my graduate studies: I never would have made it this far in this project without his encouragement.

I would also like to thank the current and past members of the Bassell lab for training me as a new lab member, for challenging me during scientific discussions, and for their friendship. It has been a pleasure being a part of the lab, and I hope that I have been a worthy colleague.

I would also like to thank my committee: Dr. Yue Feng, Dr. Peng Jin, Dr. Donald (Tig) Rainnie, and Dr. James Zheng. I am very grateful for their time and expertise, and it has been an honor to learn from them during my time at Emory.

I am also very grateful to have been a part of the Emory Neuroscience Program. I was very lucky to be a part of such an amazing group of smart and talented people. They have all challenged me to be a better scientist and made this experience more enjoyable than I could have imagined. I know I have made friends and memories that will last a lifetime.

Finally, I would like to thank my family and friends for encouraging me to pursue this degree and for believing in me during its many challenges. Their support has meant everything to me.

Table of Contents

Figures and Tables

Chapter 1 General Introduction

Chapter 2 miR-137 targets mRNAs encoding proteins within the PI3K-Akt-mTOR pathway

Chapter 3 Inhibition of miR-137 blocks Nrg1 signaling

Chapter 1

General Introduction

Portions of this chapter were adapted from the following manuscript:

Thomas, K.T., Anderson, B.R., Shah, N., Zimmer, S., Hawkins, D., Gu, Q., and Bassell. G.J. (2017). Inhibition of the schizophrenia-associated microRNA miR-137 disrupts Nrg1α neurodevelopmental signal transduction. Cell Rep., Revision Under Review.

1.1 miRNAs: history and significance

In 1991, Wightman et al. made an unusual observation: deletion of two small sequences in the 3'untranslated region (3'UTR) of the *lin-14* mRNA caused an abnormal accumulation of *lin-14* protein in *Caenorhabditis elegans*. The authors concluded that the deletions could not affect the stability or function of the encoded protein, rather they must function in post-transcriptional regulation of the mRNA. Normally, the authors hypothesized, an unidentified regulatory factor must bind to these sequences and repress the synthesis of the encoded protein. Two years later, the source of this regulation would be identified and become known as the first in a new class of regulatory molecules: the microRNAs.

In 1993, Lee et al. reported that the *lin-4* locus in *C. elegans* gives rise to two small RNA products: one of 22 nucleotides and one of 61 nucleotides. Both of which contain sequences complementary to seven repeated sequences in the 3'UTR sequences of *lin-14* mRNA that repress *lin-14* protein levels (Wightman et al., 1993). A model was proposed in which *lin-4* small RNAs bind to the *lin-14*-3'UTR and repress mRNA translation (Lee et al., 1993; Wightman et al., 1993). Later research would reveal that the 61 nucleotide RNA is a precursor for the functional 22 nucleotide *lin-4* RNA that mediates binding to the 3'UTR. Unfortunately, however, *lin-4* had no apparent orthologues in *Drosophila* or mammalian model systems, so the significance of this discovery would not be fully appreciated for some years.

In 2000, Reinhart et al. discovered a 21-nucleotide RNA they called *let-7* that targeted complementary regulatory sequences in the 3'UTRs of multiple mRNAs in *C. elegans*, including *lin-14*. Unlike *lin-4*, however, homologues to *let-7* were identified in a number of animal species ranging from *C. elegans* to *Drosophila* to humans (Pasquinelli et al., 2000). These small RNAs were no longer an oddity only observed in worms, but a conserved regulatory mechanism that might control human gene expression.

In 2001, three separate reports in a single issue of *Science* identified a large class of small 19-24 nucleotide noncoding RNAs present in *C. elegans*, *Drosophila melanogaster*, and

Dictyostelium discoideum (Lagos-Quintana et al., 2001; Lau et al., 2001; Lee and Ambros, 2001). These small RNAs were generated from larger 60-70 nucleotide precursors that formed stem loop structures through complementary base pairing within the precursor sequence (Hutvágner et al., 2001). Several were highly conserved across species, similar to *let-7*. The authors collectively referred to these small RNAs as microRNAs, or miRNAs, and proposed based on their similarity to *let-7*and *lin-4* that they form a new class of regulatory molecule that regulates the translation of target mRNAs through complementary base pairing.

Afterwards, the pace of miRNA research accelerated rapidly. Soon it became clear that miRNAs play a particularly critical role for the development and function of the central nervous system. Analysis of mouse tissues revealed a number of miRNAs enriched in the brain (Lagos-Quintana et al., 2002). Krichevsky et al., 2004 and Miska et al., 2004 found that miRNA expression was differentially regulated over the course of mammalian brain development, and Kim et al., 2004 identified over 80 miRNAs expressed in mammalian neurons. Disruption of Dicer, which processes pre-miRNAs to their mature form, revealed that miRNAs are collectively critical for brain morphogenesis in zebrafish (Giraldez et al., 2005). The expression of a subset of miRNAs was also found to be induced by neuronal differentiation from embryonal carcinoma cells (Sempere et al., 2004). These studies collectively suggested that miRNAs regulate brain development and neuronal function.

Then, Schratt et al., 2006 provided the first evidence of a specific miRNA-target pair that regulate synaptic function. The miRNA miR-134 was found to be specifically expressed in brain. In cultured neurons, miR-134 localizes to the postsynaptic compartment and locally regulates the translation of *Limk1* mRNA, which encodes a kinase critical for dendritic spine development. miR-134 inhibits the size of dendritic spines, and restoration of Limk1 rescues spine morphology in neurons overexpressing miR-134. miR-134, therefore, limits dendritic spine size by inhibiting the translation of target *Limk1* mRNA, demonstrating that even single miRNAs may be critical for regulation of the neural circuitry.

Studies over the course of the last decade have further emphasized the roles of miRNAs in the regulation of neural development and synaptic function, and the mammalian brain may very well rely on an arsenal of miRNAs to fine-tune every step of these processes. The sections that follow will summarize our current understanding of the miRNA biogenesis pathway and the mechanisms by which miRNAs inhibit protein synthesis. We will then discuss the neuron-specific mechanisms that regulate these processes and, conversely, how miRNAs contribute to neuronal signaling and neurodevelopmental disease.

1.2 miRNA biogenesis and mRNA targeting

miRNA biogenesis refers to the tightly regulated process by which a genomically encoded miRNA primary transcript undergoes processing to a mature, ~22 nucleotide miRNA that binds and regulates the translation of mRNA targets. The initial, primary miRNA transcript (pri-miRNA) is generated by the transcription of a miRNA gene. Approximately half of all miRNA genes are located within intergenic space (O'Carroll and Schaefer, 2013). Transcription of these genes is regulated by their own enhancers and promoters (Corcoran et al., 2009). Many of these miRNAs occur within miRNA gene clusters, in which multiple miRNA genes occur within a 0.1-50 kb span and multiple miRNAs may be transcribed within a single transcript (Lagos-Quintana et al., 2001; Lau et al., 2001). Other miRNAs (approximately 40%) are transcribed within the introns of protein coding genes, and their transcription may occur independently or in conjunction with the protein-coding host gene (Rodriguez et al., 2004). The remaining approx. 10% of miRNAs are encoded within the exons of protein coding genes (O'Carroll and Schaefer, 2013). If the miRNA is encoded in the sense direction, the transcription of the miRNA is usually shares the pattern of transcription of the host gene. The majority of pri-miRNA transcription is mediated by RNA polymerase II, which also transcribes primary mRNA transcripts, but some pri-miRNAs are transcribed by RNA polymerase III, which transcribes other

small RNAs including ribosomal and transfer RNAs (rRNA and tRNA, respectively) (Borchert et al., 2006; Cai et al., 2004; Lee et al., 2004).

During transcription, the pri-miRNA folds into one or more imperfectly paired stem loop structures. The stem loop structure is recognized by the double stranded RNA binding protein DGCR8, or Digeorge syndrome critical region 8, which recruits Drosha, a Ribonuclease III enzyme that catalyzes endonuclease cleavage of the pri-miRNA (Gregory et al., 2004; Han et al., 2004; Landthaler et al., 2004; Lee et al., 2003). Together, Drosha, DGCR8, and other proteins which play a regulatory role form the nuclear protein complex (the Microprocessor complex) that cleaves the pri-miRNA to generate a 60-70 nucleotide precursor miRNA, or pre-miRNA, which contains the characteristic stem-loop structure (Denli et al., 2004; Gregory et al., 2004). The pre-miRNA is then exported from the nucleus by Exportin-5 for further processing (Bohnsack et al., 2004; Lund et al., 2004; Yi et al., 2003).

The process above refers to the canonical pathway for miRNA biogenesis. In some cases, however, intronic miRNAs occur within introns that are small enough that they are directly exported following splicing and bypass processing by Drosha. This so called mirtron pathway was first identified in *Drosophila*, but a few examples have been described in mammals as well (Babiarz et al., 2008; Berezikov et al., 2007; Okamura et al., 2007; Ruby et al., 2007). In some cases RNA fragments derived from tRNAs or snoRNAs (small nucleolar RNAs) may also undergo processing independent of Drosha to form miRNAs (Babiarz et al., 2008; Ender et al., 2008). These Drosha-independent paths for pre-miRNA synthesis are referred to collectively as the non-canonical pathway for miRNA biogenesis.

Following exportation from the nucleus, the pre-miRNA undergoes further processing, mediated by a complex containing Dicer along with TRBP (trans-activation response RNA-binding protein) or PACT (protein activator of PKR) (Chendrimada et al., 2005; Hutvágner et al., 2001; Lee et al., 2013). Like Drosha, Dicer is a Ribonuclease III type enzyme which catalyzes endonuclease cleavage of a double stranded RNA. Dicer, however, catalyzes the biogenesis of a

mature miRNA from a pre-miRNA by removing the loop structure from the pre-miRNA to form a dsRNA product. PACT and TRBP play non-redundant roles in regulating pre-miRNA processing, and the association of Dicer with PACT or TRBP contributes to the production of different miRNAs from the same pre-miRNA (Lee et al., 2013). Both PACT and TRBP enhance Dicer's affinity for pre-miRNAs as well as Dicer's cleavage activity. Furthermore, Dicer, PACT, and TRBP help mediate the loading of one strand of the dsRNA product into the RNA-induced silencing complex (RISC) (Gregory et al., 2005).

Strand selection refers to the process by which one strand of approx. 22 nucleotides from the miRNA duplex is selected for incorporation into RISC and which strand is degraded. The thermodynamic properties of the duplex and the sequences of the two strands determine, in part, which strand is selected (Noland and Doudna, 2013). However, strand selection also differs depending on the cell-type in which miRNA biogenesis is occurring, the developmental stage, and disease state, among other variables that are not well-understood (Lee et al., 2013; Noland and Doudna, 2013). Furthermore, the presence of TRBP may lead to different strand preferences than when PACT is present. Strand selection may also be dependent on the Argonaute (Ago) protein present within RISC (Okamura et al., 2009).

The RISC refers to the Ago protein containing complex that uses the miRNA as a guide to direct the silencing of mRNA translation. The Argonautes are a group of four proteins (Ago1-4) that bind miRNAs and mediate their effects on translation. Of these, Ago2 is the only Ago with catalytic activity capable of cleaving mRNA targets (Meister et al., 2004). Interestingly, Ago2 also mediates the processing of the pre-miR-451 into its mature form (Cheloufi et al., 2010; Cifuentes et al., 2010; Yang et al., 2010). miR-451 biogenesis is thus non-canonical, Drosha-dependent, and Dicer-independent. No other miRNAs are known to undergo processing by this mechanism. However, only the loss of Ago2 is lethal in mice, suggesting that Ago2 is particularly important for mammalian development and that Ago1,3, and 4 may play redundant roles in the miRNA pathway (Alisch et al., 2007; Liu et al., 2004; Morita et al., 2007).

miRNAs recognize their mRNA targets through complementary G/C and A/U base pairing. miRNAs that are perfectly complementary to their mRNA target induce Ago2-dependent endonucleolytic cleavage of the mRNA, but this mechanism is rarely employed by mammalian miRNAs (Fabian et al., 2010). Rather, target recognition is usually mediated by nucleotides 2-7 of the miRNA, the so-called "seed sequence", which in most cases is perfectly complementary to the mRNA target sequence (Bartel, 2009). The miRNA target site is, in most cases, located within the 3' untranslated region (3'UTR) of the target mRNA, though targeting has also been reported in the 5' untranslated region (5'UTR) and protein coding sequence (CDS) (Easow et al., 2007; Ørom et al., 2008). Targeting within the 3'UTR is also thought to confer more robust translational regulation (Easow et al., 2007; Gu et al., 2009).

The miRNA biogenesis pathway generates the thousands of miRNAs currently identified in mammalian cells. Each miRNA is capable of targeting hundreds if not thousands of mRNAs. Approximately half of all known miRNAs are expressed in the brain, and deficits in miRNA biogenesis often result in neurological phenotypes (O'Carroll and Schaefer, 2013). For example, 22q11.2 deletion syndrome, also known as DiGeorge Syndrome, is caused by a microdeletion of a region on chromosome 22 that contains the Microprocessor component DGCR8 (Landthaler et al., 2004). Patients with 22q11DS are hemizygous for DGCR8 and neurological phenotypes include intellectual disability and increased risk of autism spectrum disorder (ASD) and attention-deficit/hyperactivity disorder (ADHD), and the majority of 22q11DS patients experience difficulties in adaptive functioning (Biswas and Furniss, 2016). Furthermore, approximately 1 in 4 or 5 patients with 22q11DS will develop schizophrenia. Mouse models for 22q11DS show widespread deficits in mature miRNA levels in the hippocampus (Earls et al., 2012). DGCR8 deficiency also leads to an age-dependent deficiency in thalamic miR-338-3p which disrupts thalamic inputs to the auditory cortex (Chun et al., 2014, 2016). Notably, dysregulation of these thalamocortical projections contributes to auditory hallucinations in schizophrenia patients. Interestingly, duplications in the 22q11.2 region are also associated with autism spectrum

disorders but no increased risk of schizophrenia (Wenger et al., 2016). The effects of *DGCR8* duplication on the miRNA pathway have not been explored, however.

1.3 miRNA mechanisms of action

Within the RISC, miRNAs serve the role of target recognition: the miRNA present within RISC determines which mRNAs are targeted. The Ago proteins bind the miRNA within RISC and interact with the other protein components of RISC. One of these, the GW182 family of proteins, mediates translational repression and mRNA destabilization by a number of different mechanisms (Eulalio et al., 2009). The mechanism employed in a particular instance of RISC-mediated mRNA regulation may depend on a number of factors, including the particular miRNA, Ago, and GW182 components present, as well as the cell cycle or developmental status of the cell, environmental factors, and the presence or absence of additional RISC regulatory proteins (Fabian et al., 2010).

RISC-mediated translational repression may affect the initiation, elongation, or termination stages of translation (Fabian et al., 2010). miRNAs have been shown to interfere with translation initiation by several mechanisms, including inhibition of 40S ribosomal subunit recruitment and inhibition of 80S complex formation (Mathonnet et al., 2007; Thermann and Hentze, 2007; Zdanowicz et al., 2009). GW182 may also block translation initiation by direct binding to poly(A)-binding protein (PABP) (Fabian et al., 2009). PABP binds the poly(A) tail of the mRNA and interacts with the eIF4G initiation complex to promote translation initiation. GW182 binding to PABP may either compete with eIF4G binding to PABP or cause a conformational change in PABP that disfavors eIF4G binding. RISC may also interfere with translation elongation by causing premature termination and ribosome drop-off (Petersen et al., 2006). PABP also interacts with the translation termination factor eRF3, and it has been proposed that GW182 binding to PABP also interferes with translation termination by blocking PABP-eRF3 interactions (Fabian et al., 2010; Uchida et al., 2002).

miRNAs may also destabilize mRNAs. GW182 interactions with PABP may recruit the CCR4-NOT1 deadenylase complex to the poly(A) tails of RISC-targeted mRNAs (Behm-Ansmant et al., 2006). Deadenylation occurs via the 3'-5' exoribonuclease activity of the complex. Shortening of the poly(A) tail promotes removal of the 5' cap of the mRNA, which subsequently leaves the mRNA vulnerable to 5'-3' exonucleolytic digestion. Shortening of the poly(A) tail also interferes with translation initiation, so miRNAs may simultaneously inhibit the translation of the mRNA and destabilize the mRNA. However, miRNAs may also repress translation without destabilizing the target mRNA (Filipowicz et al., 2008).

RISC activity is also modulated by mRNA binding proteins (mRNABPs). mRNABPs may stimulate or inhibit miRNA activity by altering the secondary structure of the target mRNA or competing with miRNAs for a common target site. For example, HuR binding to mRNAs causes RISC to dissociate from the mRNA, which stabilizes and promotes the translation of the mRNA target (Kundu et al., 2012). Pumillio1 (PUM1) promotes miR-221 and miR-222 binding to the 3'UTR of p27 mRNA by inducing a change in the 3'UTR structure that makes the miRNA target site accessible and represses p27 translation (Kedde et al., 2010).

miRNA-mRNABP interactions also play a role in stimulus induced translation, which is particularly important in neuronal signaling and the regulation of synaptic plasticity. For example, miR-125a and FMRP, fragile x mental retardation protein, both target the 3'UTR of *Dlg4* mRNA in neurons (Muddashetty et al., 2011). Under basal conditions, FMRP is phosphorylated and inhibits translation by a miR-125a-dependent mechanism. However, when group 1metabotropic glutamate receptors (mGluR1/5), which induce a form of synaptic plasticity known as long term depression, are stimulated, FMRP is dephosphorylated and relieves *Dlg4* mRNA of translational repression by miR-125a-RISC. Therefore, both miR-125a and FMRP are necessary for this bidirectional regulation of *Dlg4* mRNA translation in neurons.

Furthermore, dysregulation of miRNA-mRNABP interactions may contribute to neurodevelopmental disorders, such as Fragile X Syndrome (FXS), which is caused by the loss of

FMRP. FXS is associated with intellectual disability and increased risk of autism spectrum disorders and epilepsy, among other neurological symptoms (Tsiouris and Brown, 2004). The translation of mRNAs involved in synaptic plasticity, including *Dlg4*, is dysregulated under basal conditions and insensitive to stimulus induced translation in mouse models of FXS (Muddashetty et al., 2007; Qin et al., 2005; Weiler et al., 2004). FMRP also interacts with protein components of RISC at the genetic and molecular levels (Jin et al., 2004). Future experiments examining the mechanisms of miRNA-mediated regulation of gene expression may yield further insight into FXS and other neurodevelopmental disorders.

1.4 miRNAs play diverse roles in the regulation and dysregulation of neuronal signaling

The human brain contains over 100 billion individual neurons which together mediate its diverse functions, including perception, motor control, emotional processing, learning and memory, executive function, and even consciousness. Every one of these functions requires rapid communication between neurons in distant brain regions. Much of this communication involves neurotransmitter signaling at the estimated 100 trillion synaptic connections in the human brain, and this classical synaptic activity is further modulated by growth factors and other signals at synaptic and extra-synaptic sites. Recent research suggests that miRNAs may fine-tune every step of this process, from the synthesis of pre-synaptic signaling molecules to the transduction of post-synaptic signals, and that miRNAs are critical for the initial formation of the neural circuitry during brain development as well as the induction of long-lasting changes in the synaptic architecture during synaptic plasticity. In the following sections, we will highlight the diverse roles of miRNAs in classical neurotransmitter and growth factor signaling and in the formation and modulation of the neural circuitry. We will focus on validated miRNA-mRNA target interactions and on the direct effects of miRNA regulation, which are more predictable across model systems than downstream changes induced by protein-protein interactions.

1.4.1 miRNAs regulate neuronal signaling

Classical neurotransmission begins with the synthesis of a neurotransmitter and packaging of the neurotransmitter into presynaptic vesicles. miRNAs might regulate these processes by targeting the mRNAs that encode the enzymes that catalyze neurotransmitter synthesis (e.g. glutamate decarboxylase which synthesizes GABA from glutamate), by targeting the mRNAs that encode peptide neurotransmitters (e.g. corticotropin-releasing hormone), or by targeting the membrane proteins which package neurotransmitter into vesicles (e.g. the vesicular glutamate transporters, VGLUT1-3). The central nervous system utilizes over 100 different neurotransmitters, but to date very few studies have demonstrated a role for miRNAs in the regulation of neurotransmitter synthesis and packaging. For example, miR-130a and miR-206 target *Tac1* mRNA, which encodes the neuropeptide Substance P, in neurons derived from mesenchymal stem cells (Greco and Rameshwar, 2007). Also, Chen et al., 2016 recently demonstrated that miR-210 is upregulated by status epilepticus and that multiple genes involved in GABA (gamma-aminobutyric acid) signaling, including the glutamate decarboxylase GAD65, were downregulated following status epilepticus. Furthermore, inhibition of miR-210 blocked the effects of status epilepticus on GAD65 and other GABA related proteins, consistent with miR-210 inhibiting the synthesis of these proteins. However, miR-210 may have mediated its effects by inducing the apoptosis of GABAergic neurons, rather than by targeting mRNAs related to GABA signaling. Further research is necessary to validate whether *GAD2* mRNA, which encodes GAD65, is a direct target of miR-210.

By contrast, several miRNAs have been identified that directly target the mRNAs that encode growth factors. The 3'UTR of *BDNF* mRNA, which encodes brain-derived neurotrophic factor (BDNF), appears to be particularly important for regulating stimulus-induced BDNF synthesis in neurons (Lau et al., 2010). miR-26a and miR-26b both target the 3'UTR of *BDNF* mRNA in HeLa cells (Caputo et al., 2011). Whether these miRNAs regulate BDNF levels in neurons remains to be examined. Similarly, miR-206 directly targets the 3'UTR of mouse *Bdnf*

mRNA and inhibits BDNF protein synthesis in the Neuro2A cell line (Lee et al., 2012). miR-206 was elevated in the brains of Alzheimer's disease (AD) model mice and in the temporal cortex of AD patients, and inhibition of miR-206 in AD mice improved memory function. Together, these data suggest that dysregulation of miRNAs that target growth factors may contribute to neurological disease and provide a novel therapeutic target for the treatment of these diseases.

Some growth factors, such as the neuregulins, are synthesized as transmembrane precursors that undergo proteolytic process to release a soluble extracellular signaling domain. Others, such as BDNF, are packaged into vesicles and released into the extracellular space via the secretory pathway. The role of miRNAs in these processes is currently unknown. However, miRNAs have been shown to regulate the release of vesicles containing neurotransmitters by targeting mRNAs that encode proteins within the secretory pathway. For example, miR-153 regulates SNAP-25, a core protein of the SNARE complex which mediates calcium induced vesicle fusion with the plasma membrane and the release of neurotransmitter into the synaptic cleft (Wei et al., 2013). Overexpression of miR-153 inhibits the synaptic vesicle cycle at the zebrafish neuromuscular junction, whereas inhibition of miR-153 enhances the synaptic vesicle cycle. Furthermore, miR-153 activity significantly regulates the movement of zebrafish embryos, presumably by regulating the release of acetylcholine at neuromuscular junctions.

miRNAs that regulate presynaptic calcium signaling also affect neurotransmitter release. For example, miR-25 and miR-185 both target the sarco(endo)plasmic reticulum ATPase SERCA2, which maintains calcium levels in the presynaptic endoplasmic reticulum (Earls et al., 2012). When either miRNA is reduced, such as in 22q11DS model mice, SERCA2 levels are elevated, which in turn elevates calcium levels in the presynaptic cytosol and increases neurotransmitter release. Deficits in these miRNAs are thought to contribute to spatial memory deficits in 22q11DS mice. Bioinformatic predictions suggest that miRNAs might also regulate presynaptic vesicle release by targeting presynaptic calcium channels, which allow the

depolarization-induced influx of calcium that triggers neurotransmitter release (Lambert et al., 2010). This mechanism has yet to be explored experimentally, however.

Following the release of a neurotransmitter or growth factor into the extracellular space, the signaling molecule binds and activates receptors in the postsynaptic/receiving neuron. The signaling effects of many neurotransmitters are terminated by reuptake of the neurotransmitter into the presynaptic or surrounding cells via neurotransmitter transporters, and miRNAs may potentiate neurotransmission by inhibiting these transporters. For example, miR-16 targets SERT, the serotonin transporter which terminates serotonergic signaling (Baudry et al., 2010). Interestingly, the selective serotonin reuptake inhibitor (SSRI) fluoxetine increases miR-16 and reduces SERT expression in the raphe nuclei, and miR-16 overexpression mimics the anti-depressant effects of fluoxetine in mouse models of depression. Alternatively, neurotransmission may also be terminated by enzymes that degrade the neurotransmitter within the synaptic cleft, and miRNAs that target these enzymes are also predicted to potentiate neurotransmission. For example, miR-132 inhibits the expression of acetylcholinesterase, the enzyme that catalyzes the hydrolysis of acetylcholine at the neuromuscular junction and in the central nervous system (Shaked et al., 2009; Shaltiel et al., 2013). Stress paradigms elevate mouse hippocampal levels of miR-132, reduce acetylcholinesterase levels, and impair performance in hippocampus-dependent tasks, such as the Morris water maze, suggesting that miR-132 may contribute to cognitive deficits following exposure to stressful stimuli (Shaltiel et al., 2013). Together, these studies suggest that miRNAs play a significant role in regulating the termination of neurotransmission by multiple mechanisms. Whether miRNAs also function in the termination of neuronal growth factor signaling has not been examined.

miRNAs regulate a number of neurotransmitter receptors in the central nervous system, including glutamate, GABA, serotonin, dopamine, and acetylcholine receptors and/or receptor subunits (Higa et al., 2014). In some cases, a single miRNA may target multiple neurotransmitter receptors with opposing effects on neuronal activity. miR-181a, for example, targets both the

AMPA (α-amino-3-hydroxy-5-methyl-4-isoxazolepropionic acid) receptor subunit GluA2 and the $GABA_A$α-1 receptor subunit (Saba et al., 2012; Sengupta et al., 2013). AMPA receptors mediate most fast excitatory neurotransmission in the central nervous system by allowing an influx of sodium ions in response to glutamate binding at the cell surface, which depolarizes the neuron and increases the likelihood that the neuron will fire an action potential. By contrast $GABA_A$ receptors mediate fast inhibitory neurotransmission in the central nervous system by allowing an influx of chloride ions in response to GABA binding, which hyperpolarizes the neuron and reduces the likelihood that the neuron will fire an action potential. miR-181a, therefore, targets receptors with opposing effects on neuronal excitability. Overexpression of miR-181a in primary hippocampal neurons reduces the volume and density of dendritic spines (Saba et al., 2012), suggesting that miR-181a may preferentially regulate excitatory neurotransmission in this cell type. It is feasible, however, that miR-181a may preferentially regulate inhibitory neurotransmission or balance excitatory/inhibitory inputs in other cell types or developmental time points. These studies suggest that knowing a single target of a miRNA may not be sufficient to predict the effects of miRNA activity on neuronal signaling.

miRNAs can also regulate intrinsic neuronal excitability by targeting ion channels that are voltage gated, rather than ligand gated. miR-129 inhibits synthesis of Kv1.1 and miR-324 inhibits synthesis of Kv4.2, both of which are subunits of voltage-gated potassium channels that open in response to membrane depolarization and allow an outflux of potassium ions (Gross et al., 2016; Raab-Graham et al., 2006). These channels limit the frequency and propagation of action potentials, and the loss of either channel increases seizure susceptibility in mouse models. Kainic acid-induced status epilepticus was recently shown to increase miR-324-5p association with RISC component Ago2 and to recruit *Kcnd2* mRNA (which encodes Kv4.2) to RISC (Gross et al., 2016). Inhibition of miR-324-5p delays seizure onset following kainic acid injection into the mouse amygdala and reduces kainic acid-induced cell death in cultured hippocampal neurons and in the hippocampus *in vivo*. Furthermore, inhibition of miR-324-5p blocks kainic-acid

induced downregulation of Kv4.2 in primary neurons, and inhibition of miR-324-5p fails to delay seizure onset in *Kcnd2* knockout mice, suggesting that increased Kv4.2, and presumably reduced intrinsic excitability, contribute to the neuroprotective effects of inhibition of miR-324-5p. These studies suggest that by regulating intrinsic excitability miRNAs not only regulate the likelihood that a neuron will respond to a given excitatory signal by firing an action potential but also regulate neuronal vulnerability to seizures and seizure-induced neuronal loss.

miRNAs can also regulate neuronal ion channels and cell surface receptors by targeting proteins that regulate their surface expression, internalization, or degradation. For example, miR-125a regulates PSD-95 synthesis in primary neurons (Muddashetty et al., 2011). PSD-95 directly interacts with AMPA receptor regulatory proteins to stabilize AMPA receptor surface expression (Yudowski et al., 2013). Changes in miR-125a activity are, therefore, expected to affect AMPA receptor surface levels, but this has yet to be verified. In addition, miR-146a-5p regulates the synthesis of dendritic microtubule-associated protein 1B (MAP1B), which regulates group 1 mGluR-induced AMPA receptor endocytosis (Chen and Shen, 2013). Overexpression of miR-146a-5p blocks mGluR-dependent AMPA receptor endocytosis, as measured by surface GluA1 protein levels. When miR-146a-5p is inhibited, AMPA receptor endocytosis is enhanced without affecting total GluA1 protein levels, and synaptic transmission (measured by mEPSC frequency) is depressed by a MAP1B-dependent mechanism. It is feasible that miRNA-mediated inhibition of mRNAs encoding cell surface receptors provides greater specificity for targeting specific receptor subunits or receptor types, whereas miRNA targeting of mRNAs that encode proteins like PSD-95 and MAP1B with the potential to interact with multiple surface receptors may provide a mechanism for coordinating the surface levels of classes of receptors.

Ion channels regulate neuronal signaling in part by regulating the membrane potential and the likelihood that the neuron will fire an action potential. Metabotropic neurotransmitter receptors (e.g. the mGluRs and other G-protein couple receptors) and growth factor receptors, by contrast, signal through intracellular protein cascades mediated by kinases, phosphatases, and

second messenger systems. miRNAs can regulate signaling responses to these ligands by targeting the mRNAs that encode these downstream protein components. For example, miR-126 regulates phosphoinositide-3-kinase (PI3K) downstream of insulin-like growth factor 1 (IGF-1) by targeting the mRNAs that encode insulin receptor substrate 1(IRS-1) and the PI3K regulatory subunit p85β (Guo et al., 2008; Kim et al., 2014; Ryu et al., 2011; Zhang et al., 2008; Zhu et al., 2011). In neuroblastoma cell lines, overexpression of miR-126 impairs IGF-1 induced cell proliferation and increases sensitivity to the neurotoxic agent 6-OHDA, while inhibition of miR-126 enhances the protective effects of IGF-1 against cell death (Kim et al., 2014). Overexpression of miR-126 in primary neurons also reduces the neuroprotective effects of BDNF, nerve growth factor (NGF), and IGF-1 and increases neuronal vulnerability to amyloid beta (Aβ) induced neurotoxicity (Kim et al., 2016). Furthermore, overexpression of miR-126 reduces IGF-1-induced increases in Akt and p85β; both of which mediate PI3K signaling downstream of IGF-1 (Kim et al., 2016). Together, these studies demonstrate that miR-126 regulates multiple proteins downstream of growth factor signaling and regulates neuronal responses to multiple growth factors. Furthermore, miR-126 levels are increased in dopaminergic neurons in the brains of Parkinson's disease patients, suggesting that dysregulation of miRNA activity may contribute to deficits in growth factor signaling and to neuronal cell death in neurodegenerative disease (Kim et al., 2014).

Neuronal signaling may very well be sensitive to changes in miRNA activity at every stage of signal transduction. Furthermore, single miRNAs may regulate multiple steps within multiple signaling pathways. The examination of single miRNA targets may therefore be insufficient to predict the effects of changes in miRNA activity in neuronal signaling, and the effects of miRNAs on neuronal signaling may very well differ across developmental stages, cell types, brain regions, and disease states. Further research is needed to elucidate the many roles of miRNAs in the regulation of neuronal signaling and to elucidate how miRNA dysregulation may contribute to signaling deficits in neurological disease.

1.4.2 Neuronal signaling regulates the miRNA pathway

While miRNAs certainly play a role in regulating neuronal signal transduction, miRNA activity is also attuned to changes in neuronal signaling. Neuronal activity may very well regulate every step of the miRNA biogenesis pathway as well as miRNA interactions with target mRNAs by a multitude of mechanisms. Ultimately, regulation of miRNA activity allows neuronal signaling to fine-tune the translation of target mRNAs with a high degree of spatial, temporal, and sequence specificity. In the following section, we will summarize our current understanding of the mechanisms by which neuronal signaling regulates miRNA activity and how disruption of these mechanisms may contribute to neurological disease.

miRNA biogenesis begins with the transcription of miRNA genes in the nucleus. The transcription factor cAMP-reponse binding protein (CREB) stimulates transcription in response to increased neuronal activity, neurotrophin signaling, and other factors. Vo et al., 2005 identified a CREB binding site upstream of *MIR132* and demonstrated that transcription of the brain-enriched miRNA miR-132 is rapidly induced by BDNF signaling in primary cortical neurons. Activation of hippocampal neurons in response to pilocarpine injection or various environmental stimuli also rapidly and robustly increases pri-miR-132 *in vivo* (Nudelman et al., 2010). High frequency stimulation also induces transcription of *MIR132* in the adult rat dentate gyrus by an mGluR-dependent mechanism (Wibrand et al., 2010). Similarly, the transcription factor myocyte enhancing factor 2 (Mef2) induces transcription of the miR-379-410 cluster in response to KCl or BDNF stimulation in cultured neurons (Fiore et al., 2009).

Neuronal signaling may also regulate pri-miRNA processing by the nuclear Microprocessor complex. Woldemichael et al., 2016 recently demonstrated that protein phosphatase 1 (PP1) selectively inhibits the processing of pri-miRNAs for miR-182, miR-96, and miR-183. Inhibition of PP1 during training on a novel object recognition task significantly enhances miR-182 and miR-183 levels in the hippocampus, and both inhibition of PP1 and

overexpression of miR-182/183 increase long term memory (Woldemichael et al., 2016). The mechanism by which PP1 regulates pri-miRNA processing has not been identified.

Whether neuronal signaling regulates the export of pre-miRNAs from the nucleus has not been examined. Similarly, whether the transport of pre-miRNAs to axons, dendrites, or synapses is regulated by neuronal activity remains unknown. Dendritic targeting of pre-miR-134 is mediated by DEAH-box helicase DHX36 recognizing and binding a specific sequence in the terminal loop of the pre-miRNA (Bicker et al., 2013). Whether DHX36 activity, or the activity of other proteins that mediate miRNA transport, is regulated by neuronal activity is currently unknown.

Because the pre-miRNA is inactive, regulation of the processing of the pre-miRNA to its mature form and the incorporation of the mature miRNA into RISC are critical for the regulation of miRNA activity in neurons and other cell types. NMDA receptor activity increases dendritic miR-501-3p by a transcription- and miRNA transport-independent mechanism, suggesting that NMDA receptor activity stimulates the Dicer-dependent processing of pre-miR-501 to mature miR-501-3p (Hu et al., 2015). Lugli et al., 2005 proposed a model by which NMDA receptor activity increases intracellular calcium, activating calpain I which in turn enhances synaptic Dicer activity by freeing it from the postsynaptic density. Whether this model explains NMDA receptor induced miR-501-3p activity is unknown, however. BDNF also increases miRNAs in cultured neurons but by increasing TRBP phosphorylation (Huang et al., 2012), which in turn stabilizes TRBP and Dicer and enhances miRNA biogenesis (Paroo et al., 2009). Interestingly, BDNF also reduces the levels of a subset of miRNAs, the let-7 family of miRNAs, by inducing the expression of the RNA binding protein Lin28, which binds the terminal loop of the pre-miRNA and protects it from Dicer-mediated cleavage (Huang et al., 2012).

Neuronal activity also regulates mature miRNA activity by several mechanisms, including the degradation of mature miRNAs, the degradation of RISC protein components, and post-translational modification of RISC protein components. miRNA half-lives vary greatly, and

the mechanisms that regulate miRNA degradation are unclear (O'Carroll and Schaefer, 2013). Within the retina miRNA turnover was found to be faster in neuronal cells than in nonneuronal cells (Krol et al., 2010). Neuronal activity and glutamatergic signaling significantly increase miRNA turnover and may stimulate the degradation of miRNAs in neurons as a means of rapidly inducing changes in mRNA translation (Krol et al., 2010). Kinjo et al., 2016 found that XRN-2 mRNA was increased in the rat hippocampus following status epilepticus, while PAPD4 mRNA was reduced. XRN-2, 5'-3' exonuclease 2, mediates the degradation of miRNAs (Chatterjee and Grosshans, 2009). PAPD4, also known as GLD-2, is an atypical poly(A) polymerase that adds a single 3' adenine to mature miRNAs and promotes their stability (Katoh et al., 2009). XRN-2 upregulation and PAPD4 downregulation should synergistically promote the degradation of mature miRNAs, therefore. However, Kinjo et al., 2016 found that the effects of status epilepticus on XRN-2 and PAPD4 protein levels differed across regions of the hippocampus and neuronal subtypes. For example, parvalbulin positive interneurons accumulated PAPD4 in the hippocampal CA1 and hilus, suggesting status epilepticus-induced miRNA stabilization, while PAPD4 levels in excitatory neurons were unaffected. The significance of these findings is currently unclear, and further research is needed to elucidate the mechanisms by which neuronal activity affects miRNA turnover.

Neuronal activity can also stimulate mRNA translation by inducing the degradation of protein components of RISC. In *Drosophila* neuronal activity stimulates mRNA translation by promoting the degradation of Armitage, an RNA helicase within RISC that is homologous to mammalian MOV10 (Ashraf et al., 2006). Degradation of Armitage releases RISC targeted mRNAs from miRNA-mediated translational repression and induces synaptic protein synthesis underlying memory formation. Similarly, NMDA receptor activity induces the proteasome-dependent degradation of MOV10 and stimulates dendritic local protein synthesis in murine primary hippocampal neurons (Banerjee et al., 2009). This mechanism may provide a means of

specifically stimulating protein synthesis at activated synapses and likely affects all RISC-targeted mRNAs at a given synapse.

The protein components of RISC may also undergo neuronal signaling-dependent modifications that affect miRNA-mediated translational repression. Phosphorylation of Ago2 at S824–S834 is induced by miRNA-mediated binding to an mRNA target and is required for miRNA-mediated translational silencing (Golden et al., 2017). However, dephosphorylation rapidly occurs following mRNA target association, and phosphorylation inhibits Ago2 association with target mRNAs. Whether this phosphorylation is regulated by neuronal activity is currently unknown. Phosphorylation of Ago2 at additional residues in turn regulates miRNA maturation, miRNA guide strand loading, and translational repression (Horman et al., 2013; Shen et al., 2013; Zeng et al., 2008). p38 signaling during neuronal differentiation induces Ago2 phosphorylation at Tyr529, which causes Ago2 to release the miRNA let-7a and stimulates translation of let-7a target mRNAs (Patranabis and Bhattacharyya, 2016). Ago2 phosphorylation or other post-translational modifications induced by neuronal activity have not yet been examined in mature neurons.

Finally, neuronal signaling affects miRNA targeting by regulating the mRNA binding proteins that cooperate with, antagonize, and/or compete with miRNAs to regulate mRNA translation. For example, Muddashetty et al., 2011found that group 1 mGluR signaling induces *Dlg4* mRNA translation by stimulating the dephosphorylation of FMRP, which in turn causes miR-125a to release *Dlg4* mRNA and relieves RISC-mediated translation repression. Under basal conditions, Ago2 association with *Dlg4* mRNA is significantly reduced in synaptic fractions derived from cortex of *Fmr1* knockout mice, suggesting that phosphorylated FMRP may facilitate miR-125a binding to *Dlg4* mRNA. In another example, HuD and miR-129 compete to regulate Kv1.1 mRNA translation (Sosanya et al., 2013). When mTORC1 signaling is active, miR-129 binds to Kv1.1 mRNA and inhibits its translation. When mTORC1 is inhibited by rapamycin, however, HuD binds Kv1.1 mRNA and miR-129 binding is inhibited, thus stimulating Kv1.1

protein synthesis. The regulation of mRNA binding proteins by neuronal activity thus provides a mechanism by which neuronal activity can bidirectionally regulate the translation of specific mRNAs.

Neuronal signaling therefore regulates miRNA biogenesis, degradation, targeting, and activity by a diverse arsenal of molecular mechanisms that are important for the temporal and spatial control of mRNA translation. Future research may further explore how these processes operate *in vivo* and contribute to behavior and cognition as well as whether dysregulation of these processes contributes to neurological disease.

1.4.3 miRNAs regulate the neuronal circuitry

The development of the mammalian brain involves the formation of trillions of connections between neurons. This process is highly regulated, and the axons of developing neurons must traverse great distances under the guidance of extracellular cues to navigate to their final targets and form synaptic connections, usually on the dendrites of the target cells. Dendrites also undergo outgrowth and branching and extend dendritic spines under the regulation of extracellular cues. Newly formed spines may then mature or collapse depending on synaptic inputs. As previously discussed, miRNAs play a critical role in regulating neuronal signal transduction. miRNAs also regulate the processes that guide the formation of the neuronal circuitry, thereby regulating which neurons communicate with one another, as well as synaptic plasticity, thereby regulating the strength of those connections.

The axon growth cone is a highly dynamic structure on the tip of the developing axon that guides the path of the axon in response to extracellular cues. The roles of only a few individual miRNAs have been verified in axon guidance. For example, in *C. elegans* the miRNA *lin-4* regulates the synthesis of the transcription factor *lin-14* in anterior ventral microtubule (AVM) neurons, which in turn regulates long-range guidance of AVM axons toward the nerve ring (Zou et al., 2012). miRNAs may also act locally, within axons and growth cones to regulate

axon guidance. The translational machinery, including mRNAs and miRNAs, localize to the growth cone, and local protein synthesis within the growth cone plays a critical role in axon guidance. Over 100 miRNAs have been identified that localize to the axons of developing primary cortical neurons (Sasaki et al., 2014). Several of these miRNAs are enriched in axons and growth cones relative to the cell body, suggesting a mechanism exists for targeting specific miRNAs to these compartments. In *Xenopus*-derived primary spinal neurons, miR-134 localizes to the growth cone and regulates axon turning toward BDNF attractive cues in the environment, and BDNF-induced axon turning is disrupted in neurons in which miR-134 is overexpressed or inhibited (Han et al., 2011). Interestingly, miR-134 regulates the synthesis of LIM kinase 1 (Schratt et al., 2006), which regulates actin polymerization within the growth cone. In developing murine cortical neurons, miR-9 localizes to axons where it inhibits basal and BDNF-induced axonal branching and outgrowth by inhibiting the synthesis of Map1B, which regulates microtubule stability (Dajas-Bailador et al., 2012). By contrast, miR-132 promotes axon extension in dorsal root ganglion neurons by targeting the mRNA for Rasa1, a known regulator of the cytoskeleton (Hancock et al., 2014). Together, these studies suggest that miRNA regulation of cytoskeletal architecture may play a key role in regulating axon outgrowth and the formation of the neuronal circuitry.

miRNA regulation of the cytoskeleton also contributes to miRNA regulation of dendrite outgrowth. miR-124, for example, promotes dendritic outgrowth by inhibiting RhoG, a small GTPase that regulates the actin cytoskeleton (Franke et al., 2012). However, miR-124, in conjunction with miR-9, also stimulates dendritic outgrowth by inhibiting the GTP binding protein Rap2a (Xue et al., 2016). Overexpression of miR-124 together with miR-9 thereby increases Akt signaling and GSK3β phosphorylation, which has previously been shown to increase dendritic outgrowth (Rui et al., 2013). Together, these studies demonstrate that miR-124 promotes dendritic outgrowth through the inhibition of multiple mRNA targets and through diverse molecular mechanisms.

Similarly, miR-9, in addition to targeting Rap2a, stimulates dendritic outgrowth by inhibiting the RE1-silencing transcription factor (REST), also known as neuron-restrictive silencer factor (NRSF) (Giusti et al., 2014; Packer et al., 2008). REST inhibits the transcription of a network of neuron-specific genes and is normally lost over the course of neuronal differentiation (Ballas and Mandel, 2005), but the mechanism by which REST inhibits neurite outgrowth is unknown.

miRNA targets that regulate later stages of neuronal gene expression can also affect dendrite outgrowth. For example, miR-214 stimulates dendritic outgrowth by inhibiting the schizophrenia-associated protein quaking (Irie et al., 2016). Quaking, in turn, regulates the splicing, turnover, and translation of its own target mRNAs, some of which presumably regulate dendritic outgrowth; but the specific mechanism by which quaking inhibits dendritic outgrowth also remains unclear. Finally, miR-185 promotes dendritic outgrowth and the loss of miR-185 in 22q11.2DS may contribute to structural deficits in the cortices of mouse models and human patients (Xu et al., 2012). miR-185 does so in part by targeting Mirta22, a newly identified protein of unknown function which co-localizes with the Golgi apparatus, and miR-185 predicted targets are enriched for Golgi-related functions, many of which are dysregulated in the brains of 22q11.2DS model mice. Jan and Jan, 2010 speculated that the Golgi outposts in the dendrites contribute to dendritic outgrowth by modulating neuronal signaling. Further research is needed to determine the mechanism(s) by which miR-185 and dysregulation of the Golgi apparatus contribute to neuronal deficits in 22q11.2DS, however.

Finally, miRNAs regulate the neuronal circuitry by regulating the formation, morphology, and plasticity of synapses. As one example, miR-132 regulates all three. miR-132 stimulates synapse formation by inhibiting p250GAP, a Rho family GTPase-activating protein (Impey et al., 2010; Wayman et al., 2008). miR-132 upregulation over the course of neuronal development in culture mirrors the gradual increase in synapse number, and inhibition of miR-132 reduces the density of dendritic spines (Impey et al., 2010). p250GAP inhibits spine

formation by inhibiting Rac1-induced changes to the actin cytoskeleton necessary for spine formation. miR-132 increases Rac1 activity by inhibiting p250GAP synthesis, thereby increasing the formation of dendritic spines. miR-132 also increases the width of dendritic spines, so miR-132 promotes the maturation in addition to the formation of dendritic spines (Edbauer et al., 2010; Impey et al., 2010). Overexpression of miR-132 also, however, inhibits both long term potentiation (LTP) and long term depression (LTD) in the perirhinal cortex and impairs object recognition memory (Scott et al., 2012). Inhibition of experience-induced changes in miR-132 activity also blocks ocular dominance plasticity in the visual cortex (Mellios et al., 2011; Tognini et al., 2011). Together, these studies demonstrate that the temporal control of neuronal miR-132 expression is critical for proper synaptic function, synaptic plasticity, and memory formation.

miRNAs play a critical in regulating the formation and maintenance of the neuronal circuitry, from neurite outgrowth to experience-dependent changes in synaptic strength. The loss of even single miRNAs can disrupt neuronal structure and impair cognition, and single miRNAs can regulate these processes by diverse molecular mechanisms. Unsurprisingly, dysregulation of miRNAs critical to neuronal signaling has been linked to neurodevelopmental, neurodegenerative, and psychiatric disease; but the mechanisms by which miRNA activity contributes to disease etiology are only beginning to emerge. In the following sections we will consider one specific miRNA, miR-137, that has been linked to the regulation of pre- and postsynaptic signaling as well as neuronal maturation and several forms of synaptic plasticity. More intriguingly, miR-137 dysregulation has been linked to intellectual disability, autism, bipolar disorder, depression, and schizophrenia, suggesting that miR-137 is critical for human brain function.

1.5 The schizophrenia-associated miRNA miR-137 regulates neuronal signaling

1.5.1 miR-137 and 1p21.3 deletion syndrome

Remarkably, the first human studies to examine miR-137 provided the first definitive evidence that dysregulation of a single miRNA can significantly impact human brain function. Animal studies had demonstrated that miRNAs were important for neuronal function, and human studies investigating 22q11DS suggested that broad dysregulation of the miRNA pathway contributes to neurodevelopmental disorders. However, prior to 2011 no mutations in miRNA genes had been associated with neurological or cognitive dysfunction.

Carter et al., 2011 identified a novel hemizygous microdeletion syndrome affecting the 1p21.3 region in 4 individuals from 3 families that presented with autism spectrum disorder (ASD) and severe speech delay. Two of the 4 patients also presented with intellectual disability. At the time, the authors attributed the cognitive symptoms to the loss of *DPYD* which encodes dihydropyrimidine dehydrogenase, an enzyme involved in pyrimidine catabolism. However, loss-of-function mutations in *DPYD* had previously been described in human patients, and the *DPYD* mutation patients lacked the cognitive dysfunction noted in the 1p21.3 microdeletion patients (van Kuilenburg et al., 2010). Willemsen et al., 2011 then identified 5 additional 1p21.3 microdeletion patients, all with mild to moderate intellectual disability and 3 with features of ASD, and identified the genomic regions affected in each patient using genome-wide array analysis. The shortest region of overlap present in all patients included *DPYD* but also, within an intron, *MIR137*. Furthermore, lymphoblastoid cell lines (LCLs) derived from the 1p21.3 patients expressed significantly lower levels of mature miR-137 and increased expression of validated miR-137 targets. By contrast, plasma pyrimidine levels were unaffected, suggesting no deficiency in pyrimidine metabolism.

Analysis of human brain tissue also revealed that miR-137 expression increases over the course of human neurodevelopment, and miR-137 is highly expressed in the human cortex, hippocampus, and other brain regions critical for cognition (Willemsen et al., 2011). Later studies

revealed that miR-137 is enriched in neurons rather than glia and more highly expressed in CamKII-positive glutamatergic neurons in mouse brain (He et al., 2012; Jovičić et al., 2013). Willemsen et al., 2011 concluded that the loss of miR-137 specifically contributes to the intellectual disability, ASD, and other cognitive phenotypes observed in 1p21.3 microdeletion patients, therein providing the first evidence that mutations, in this case a hemizygous deletion, in miRNA genes contribute to human cognitive function and dysfunction. To date, 12 patients with 9 independent 1p21.3 microdeletions have been described in the literature (Tucci et al., 2016). The smallest region of overlap shared by all 9 microdeletions includes only *MIR137*, confirming that the loss of miR-137 underlies the shared cognitive phenotypes described in these patients.

1.5.2 miR-137 and schizophrenia

Schizophrenia is a debilitating psychological disorder with no cure, poorly understood etiology, and complex underlying genetics. The symptoms of schizophrenia usually emerge during adolescence or early adulthood and generally fall into three broad categories: positive, negative, and cognitive (Tandon et al., 2009). Positive symptoms include auditory and visual hallucinations, delusions, and other distortions of reality. Negative symptoms refer to the loss or blunting of conative and affective functions. Specific negative symptoms include anhedonia (the loss of pleasure), reduced social drive, and apathy. Cognitive symptoms vary widely but include disorganized thoughts and depression. Across patients, the symptoms of schizophrenia are highly heterogeneous, with different patients experiencing different combinations and severities of symptoms. Antipsychotic therapies generally only treat the positive symptoms. The lifetime prevalence of schizophrenia is approximately 0.7%, with an annual incidence of an average of 15 per 100,000 people-years (Tandon et al., 2008). Schizophrenia therefore poses a substantial global economic burden, with schizophrenia associated costs in the United States estimated at $60 billion in 2013 alone (Chong et al 2016).

Twin studies suggest that schizophrenia is highly heritable (approximately 81% heritable) (Sullivan et al., 2003). Yet the dysfunction of no single gene can explain all symptoms of schizophrenia or the presence of schizophrenia in all patients; and rare, common, and *de novo* variants have all been linked to schizophrenia susceptibility. Furthermore, genetic variants that have been linked to schizophrenia often also contribute to other neurodevelopmental or psychiatric disorders, including ASD, bipolar disorder, and intellectual disability (Sullivan et al., 2012).

In 2011, a genome-wide association study (GWAS) identified 5 novel schizophrenia associated loci within the following genes: *TCF4*, *CACNA1C*, *CSMD1*, *C10orf26*, and *MIR137* (Ripke et al., 2011). The variant near *MIR137* is within the putative primary transcript of miR-137 (pri-miR-137). Furthermore, TCF4, *CACNA1C*, *CSMD1*, and *C10orf26* encode validated mRNA targets of miR-137 (Kwon et al., 2011). *ZNF804A*, another miR-137 target, nearly met genome-wide significance (Kim et al., 2012; Ripke et al., 2013). Later GWAS studies confirmed and emphasized the association between schizophrenia and *MIR137* (Ripke et al., 2013, 2014). Most notably, in an analysis of 36,989 cases and 113,075 controls, Ripke et al., 2014 identified 108 schizophrenia associated loci that met genome-wide significance: the *MIR137* locus showed the second strongest association. Interestingly, the rare allele (G) at the schizophrenia associated locus rs1625579 identified by Ripke et al., 2011 appears to be protective against schizophrenia relative to the more common allele (T).

Whether miR-137 loss- or gain-of-function contributes to schizophrenia remains unclear. Guella et al., 2013 found that healthy individuals homozygous for the risk associated T allele have lower levels of miR-137 in the dorsolateral prefrontal cortex relative to carriers of the protective G allele. However, no genotype-associated differences were observed in the tissue from schizophrenia patients. Strazisar et al., 2014 identified two novel functional variants in *MIR137* with higher frequencies in schizophrenia and bipolar disorder patients relative to control subjects. The variants are predicted to alter the secondary structure of pri-miR-137 to interfere

with processing by the miRNA biogenesis machinery. Furthermore, constructs containing the two variants each led to significantly reduced miR-137 expression relative to wild-type *MIR137* constructs when transfected into SH-SY5Y cells, suggesting that these variants may lead to lower miR-137 levels in patients. Duan et al., 2014 also identified a rare schizophrenia- and bipolar disorder-associated single nucleotide polymorphism (SNP) in the enhancer element for *MIR137*. Reporter assays in neuroblastoma cell lines suggest that the SNP reduces enhancer activity by greater than 50%, suggesting that the SNP may reduce *MIR137* transcription *in vivo*. Warburton et al., 2015 recently found that the rs1625579 SNP identified by Ripke et al., 2011is linked to (i.e. in strong linkage disequilibrium with) a second SNP, rs2660304 that lies within the promoter region of *MIR137*. Reporter assays in SH-SY5Y cells suggest that the risk associated SNP at rs2660304 inhibits transcription, suggesting that the rs2660304 risk allele, and by extension the rs1625579 risk allele, may reduce synthesis of miR-137 *in vivo*.

All of the studies above suggest that miR-137 loss-of-function contributes to schizophrenia etiology. However, Siegert et al., 2015 reported significantly increased miR-137 levels in neurons derived from fibroblasts from individuals with 4 schizophrenia-associated SNPs, including the previously described SNPs at rs1625579 and rs2660304. This study suggests that miR-137 gain-of-function may also contribute to schizophrenia. Further research is needed to determine how variation in *MIR137* affects miR-137 activity.

Similarly, the mechanism by which miR-137 dysregulation might contribute to schizophrenia remains unclear. One of the hallmark morphological features of schizophrenia is enlargement of the cerebral ventricles (Johnstone et al., 1976). Schizophrenia patients often show associated deficits in total brain volume and particularly in gray matter structures (Haijma et al., 2013). Three early studies found no association between the schizophrenia-associated allele of *MIR137* and macroscopic brain structure, including gray matter volume, white matter volume, hippocampal volume, amygdala volume, caudate nucleus volume, putamen volume, and total brain volume, in healthy individuals (Cousijn et al., 2014; Li and Su, 2013; Rose et al., 2014).

The risk allele also does not appear to affect brain volume in schizophrenia patients (Rose et al., 2014). However, Lett et al., 2013 reported that individuals with schizophrenia who were also homozygous for the risk associated T allele display reduced white matter integrity throughout the brain as well as enlarged ventricles and smaller hippocampi, whereas TG and GG individuals with schizophrenia showed no such deficits. Kuswanto et al., 2015 also found that individuals with schizophrenia with the TT genotype display reduced white matter integrity in the right orbitofrontal cortex and in the left striatum. These studies suggest that miR-137 may influence brain structure in individuals with schizophrenia but not in healthy individuals.

The *MIR137* rs1625579 locus may also predict the severity of several symptoms in schizophrenia patients. The risk-associated TT genotype, for example, predicts greater negative symptom severity, poor attention, and reduced processing speed in schizophrenia patients (Kuswanto et al., 2015). In a Chinese Han population of schizophrenia patients, Ma et al., 2014 found that the TT genotype is also associated with a slight impairment of working memory. Schizophrenia patients with the TT genotype also display hyperactivation of the dorsolateral prefrontal cortex during a working memory task (van Erp et al., 2014), suggesting functional inefficiency in this brain region which may contribute to deficits in performance during demanding working memory tasks. By contrast, Cummings et al., 2013 reported that the T allele is associated with cognitive deficits involving attentional control and episodic memory, independent of schizophrenia diagnosis.

Two recent studies have examined how the *MIR137* risk locus interacts with risk variants at loci associated with miR-137 target mRNAs. In these studies, a polygenic “risk score” was calculated based on variation at miR-137 target loci. Cosgrove et al., 2017 reported that higher risk scores are associated with impairments in episodic and working memory as well as lower intelligence quotient. Furthermore, in health individuals, higher risk scores are associated with increased activation in the right inferior occipital gyrus during a spatial working memory task. Wright et al., 2016 also found that schizophrenia patients with the TT risk genotype show

decreases in gray matter concentration with increased risk scores in the temporal, occipital, and parietal lobes, whereas G allele carriers show increased gray matter concentration and healthy subjects show no correlation between gray matter concentration and risk score.

These studies suggest that variation at *MIR137* and miR-137 target genes interact to influence brain structure and cognition in schizophrenia patients and may influence brain structure in healthy individuals as well. These studies also highlight the need to consider the effects of miR-137 targets when considering the relationship between miR-137 and schizophrenia. Hauberg et al., 2016 recently reported that genes associated with schizophrenia are more likely to encode targets of miRNAs and that schizophrenia associated genes are most enriched within the predicted target sets for miR-9, miR-485-5p, and miR-137, respectively. Additional research regarding the role of miR-137 in neuronal function suggests that miR-137 may play a particularly important role in regulating neuronal signaling, neuronal maturation, and synaptic plasticity, all of which are likely to be dysregulated in schizophrenia.

1.5.3 miR-137 in neuronal signaling and synaptic function

The first mechanism by which miR-137 regulates neuronal signaling is by targeting proteins essential for the release of neurotransmitter from the axon terminus (Siegert et al., 2015). Neurotransmitters are packaged into presynaptic vesicles within the axon terminus and released in response to action potential-induced influx of calcium. Bioinformatic predictions suggest that miR-137 may target over 20 proteins involved in vesicle trafficking. Siegert et al., 2015 validated the mRNAs that encode complexin-1 (Cplx1), N-ethylmaleimide-sensitive fusion protein (Nsf), synapsin-3 (Syn3), and synaptotagmin-1 (Syt1) as bona fide targets of miR-137. Overexpression of miR-137 reduces the levels of these proteins in the mossy fiber–CA3 pathway, reduces the number of vesicles in the active zone of the mossy fiber presynaptic terminal *in vivo,* and reduces the amplitude of the response evoked in mossy fiber-CA3 synapses by sustained low frequency stimulation of dentate granule cells. Overexpression of miR-137 in the dentate gyrus also impairs

presynaptic LTP, a form of synaptic plasticity that involves increased neurotransmitter release from the mossy fiber axon terminal, and impairs hippocampus-dependent learning. By contrast, inhibition of miR-137 increases target protein levels, increases vesicle number in the active zone, and increases the induction of mossy fiber LTP. These results suggest that miR-137 plays a critical role in regulating presynaptic vesicle dynamics, thereby regulating synaptic signal transduction and synaptic plasticity.

miR-137 also regulates postsynaptic signaling by several mechanisms. First, miR-137 targets a number of extracellular signaling receptors. For example, miR-137 regulates the Notch signaling pathway, which regulates cellular inflammation and apoptosis, by targeting the receptor Notch1 (Shi et al., 2017). Downregulation of miR-137 during oxygen glucose deprivation stimulates Notch signaling and enhances cell injury in rat primary hippocampal neurons. Also, Zhao et al., 2013 found that miR-137 targets mRNA encoding the NMDA receptor subunit GluN2A and inhibits GluN2A synthesis in PC12 cells. In *Drosophila*, miR-137 also regulates the levels of NMDAR2 mRNA, which is homologous to mammalian GluN2A, as well as the mRNAs for the GABA receptors GABA-B-R3 and GABA-B-R1 and the dopamine receptor D2R (Kong et al., 2015). Furthermore, miR-137 levels are upregulated in Parkinson's disease model flies and these mRNA targets are significantly downregulated, suggesting that miR-137 may contribute to signaling defects in this model system. miR-137 also regulates glutamatergic signaling by targeting the AMPA receptor subunit GluA1 (Olde Loohuis et al., 2015). mGluR5 signaling transiently increases miR-137 levels in primary hippocampal neurons, and this increase in miR-137 inhibits AMPAR signaling and allows mGluR-dependent long term depression (LTD) at CA3-CA1 synapses. Conversely, inhibition of endogenous miR-137 inhibits mGluR-dependent LTD expression, suggesting that miR-137 is necessary for this form of synaptic plasticity.

miR-137 also targets intracellular proteins that regulate signaling downstream of receptor activation. For example, miR-137 is predicted to regulate proteins involved in glucocorticoid receptor signaling, and inhibition of miR-137 in rat primary cortical neurons regulates mRNAs,

such as COX2, DUSP1, DUSP4, EGR2, and SGK1, that encode proteins involved in this signaling pathway, i.e. cyclooxygenase 2, dual specificity phosphatase 1 and 4, early growth response 2, and serum/glucocorticoid regulated kinase 1 (Vallès et al., 2014). Together with several previously validated miR-137 targets (CACNA1C, TCF4, and ZNF804A), these proteins may form a miR-137 target protein network that regulates glucocorticoid signaling. Whether miR-137 activity actually regulates neuronal responses to glucocorticoid signaling remains unknown, however.

miR-137 also affects neuronal signaling by regulating the formation of the neural circuitry. Overexpression of miR-137 in newly formed neurons in the dentate gyrus inhibits dendritic outgrowth *in vivo*, while inhibition of miR-137 significantly enhances outgrowth (Smrt et al., 2010). Overexpression of mindbomb 1 (Mib1), a direct target of miR-137, blocks the effects of miR-137 overexpression on dendritic outgrowth, suggesting that miR-137 regulates neuronal maturation, in part, by regulating Mib1. Interestingly, Mib1 is an E3 ubiquitin ligase that regulates late phase LTP as well as learning and memory, in part, by promoting the ubiquitination and internalization of Notch receptors (Yoon et al., 2012). In *Drosophila*, Mib1 also positively regulates the synaptic localization of GluRIIA, GluRIIB, and GluRIIC receptors, which are homologues of AMPA receptors (Sturgeon et al., 2016). The studies suggest that miR-137 may regulate Notch and glutamatergic signaling by multiple mechanisms.

miR-137 also targets the mRNA that encodes the signaling ligand bone morphogenic protein 7 (BMP7) (Yang et al., 2015), which regulates dendritic outgrowth in sympathetic neurons (Courter et al., 2016). Interestingly, miR-137 also targets mRNA encoded by the schizophrenia-associated gene *TCF4* (Kwon et al., 2011). TCF4 is a transcription factor which regulates neuron migration during the formation of the cerebral cortex by inhibiting *BMP7* transcription (Chen et al., 2016b). miR-137 may therefore regulate BMP signaling through both the direct targeting of *BMP7* mRNA and by regulating BMP7 transcription, suggesting a novel mechanism by which miR-137 might regulate neuron migration and maturation.

As previously discussed, miR-137 regulates the neural circuitry by regulating several forms of synaptic plasticity. miR-137 also regulates the formation of dendritic spines. Smrt et al., 2010 found that overexpression of miR-137 reduces the density of dendritic spines in newly formed neurons in the dentate gyrus, and Olde Loohuis et al., 2015 found that inhibition of miR-137 increases dendritic spine density in primary hippocampal neurons. miR-137 also inhibits the unsilencing of synapses in cultured neurons, presumably by inhibiting the synthesis of AMPA receptor subunit GluA1. Olde Loohuis et al., 2015 also reported that neither overexpression nor inhibition of miR-137 affects the percentage of mature spines, suggesting that miR-137 may regulate the formation but not the maturation of dendritic spines. While several validated targets of miR-137, e.g. Cdc42 (Liu et al., 2011; Scott et al., 2003), regulate the formation of dendritic spines, the target(s) responsible for miR-137's effects on spine density remain unknown.

Taken together, these studies suggest that at a single synapse miR-137 might regulate presynaptic vesicle release, the availability of receptors at the cell surface, downstream signaling, and the induction of synaptic plasticity. miR-137 may also regulate the outgrowth of the dendrites and the formation of the synapse itself. The loss of miR-137 in 1p21.3 microdeletions, and perhaps in schizophrenia, may cause neuronal dysfunction by a number of mechanisms. Further research is needed, however, to determine how dysregulation of miR-137 associated signaling might contribute to the etiology of these neurodevelopmental diseases.

1.5.4 miR-137 target predictions and pathway analyses

Though these studies have shed considerable light on the role of miR-137 in neuronal signaling, mRNA target predictions suggest that miR-137 might yet play a much larger role. This thesis sought to investigate whether miR-137 might target signaling pathways previously implicated in schizophrenia. We first conducted a DAVID analysis on predicted miR-137 targets from TargetScan to identify pathways in which miR-137 targets were enriched. The results of this analysis are shown in **Table 1.1**. These pathways included neuregulin (Nrg)/ErbB signaling

(p=0.00089), neurotrophin signaling (p=0.019), and long term potentiation (p=0.033). Among these three, enrichment of only the Nrg/ErbB signaling pathway remained significant following Benjamini-Hochberg correction for multiple comparisons (p=0.025). Notably, many predicted miR-137 targets fell within the phosphoinositide-3-kinase (PI3K)-Akt-mechanistic target of rapamycin (mTOR) branch of Nrg/ErbB signaling, as shown in **Table 1.2**. A complete list of miR-137 target predictions for these pathways is given in **Fig. 1.1** and the proposed relationship between targets relevant to the PI3K-Akt-mTOR branch of Nrg signaling is shown in **Fig. 1.2**.

miR-137 has previously been shown to regulate LTP and other forms of synaptic plasticity by several molecular mechanisms. miR-137 has also been studied within the context of neuronal differentiation and neurogenesis. The mechanisms by which miR-137 contributes to other stages of neurodevelopment, such as when primary neurite outgrowth and early synaptogenesis are underway, by contrast remain largely unknown. Neurotrophin signaling and Nrg/ErbB signaling have been shown to regulate dendritic outgrowth through several mechanisms, including stimulation of the PI3K-Akt-mTOR pathway. Dysregulation of the Nrg/ErbB pathway in particular is also strongly linked to schizophrenia through genetic studies. We, therefore, decided to examine the relationship between miR-137 and Nrg/ErbB signaling.

1.6 Dissertation Hypothesis and Objectives

We hypothesized that miR-137 regulates PI3K-Akt-mTOR-dependent responses to Nrg/ErbB neurodevelopmental signaling. We undertook the studies described in subsequent chapters with the following objectives: 1) to identify and validate novel mRNA targets of miR-137 in the Nrg/ErbB pathway, 2) to determine whether miR-137 is necessary for Nrg/ErbB signal transduction, 3) to determine whether Nrg/ErbB signaling regulates miR-137 activity, 4) to examine whether miR-137 regulates Nrg-induced neurite outgrowth, 5) to determine whether miR-137 specifically regulates PI3K-Akt-mTOR-dependent responses to Nrg/ErbB signaling, 6) to determine whether miR-137 regulates PI3K-Akt-mTOR-dependent responses to other

extracellular signals, such as neurotrophins, or whether miR-137 might uniquely regulate the Nrg/ErbB pathway.

1.7 Materials and methods

Bioinformatic analysis

miR-137 targets were identified using TargetScan (v6.2). The Functional Annotation Tool within DAVID (Database for Annotation, Visualization, and Integrated Discovery, v6.7) was used to identify signaling pathways in which miR-137 targets were enriched. Pathways of interest were visualized using KEGG pathway maps within DAVID. Target sites within mRNAs of interest were identified using TargetScan (v6.2) or miRmap (http://mirmap.ezlab.org/app/).

1.8 Figures

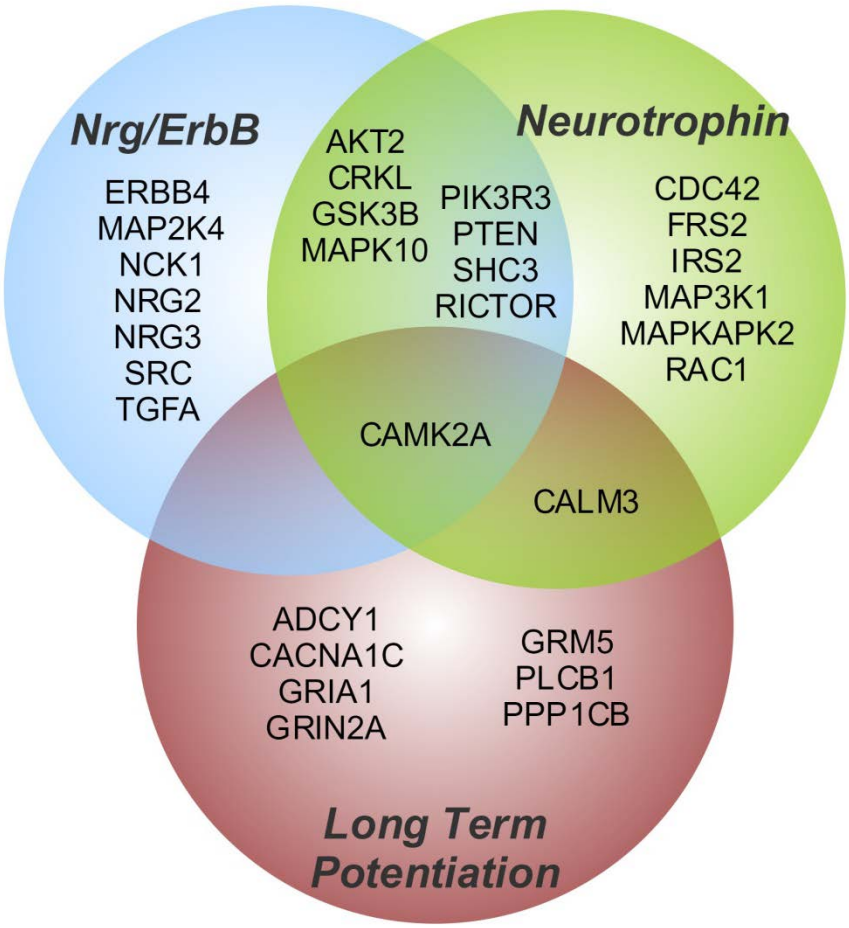

Figure 1.1 miR-137 targets within the Nrg/ErbB, BDNF, and LTP pathways

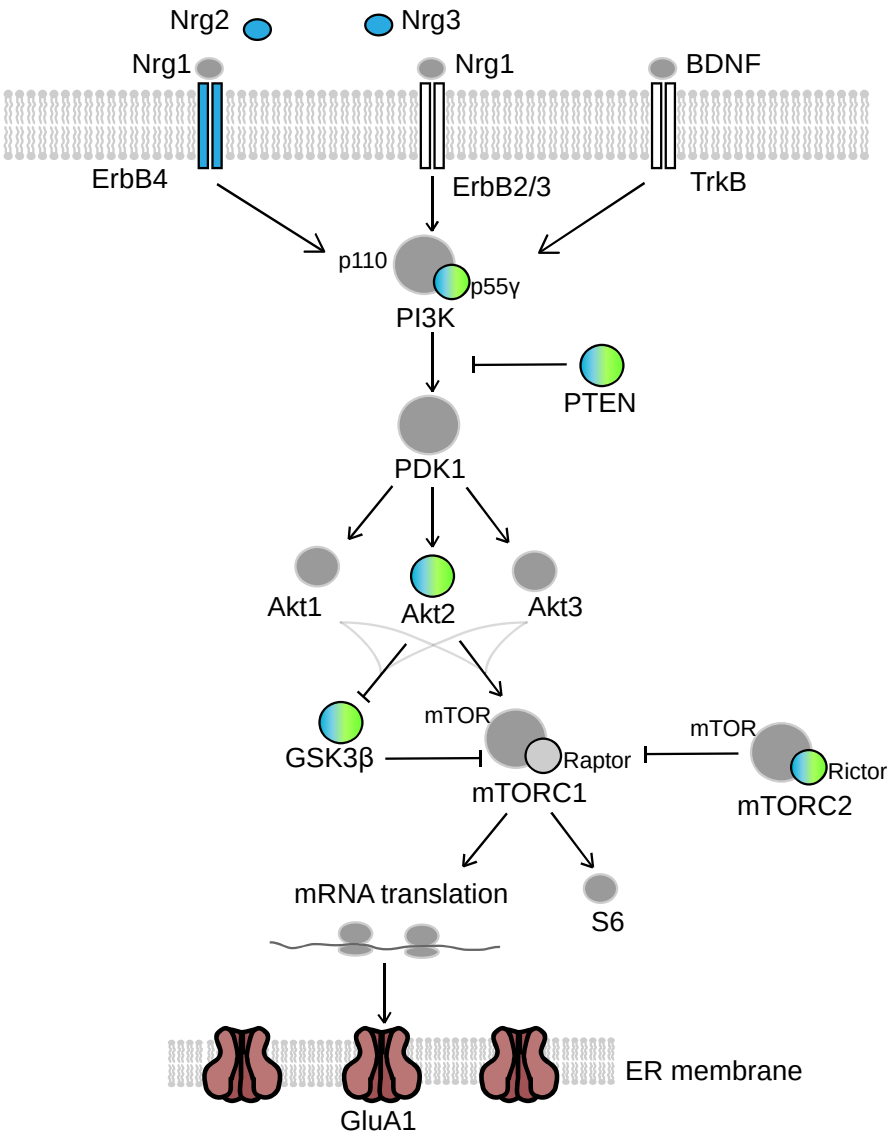

Figure 1.2 Proposed relationship between miR-137 targets within the PI3K-Akt-mTOR branch of Nrg/ErbB signaling. Proteins encoded by predicted miR-137 targets are shown in colors corresponding to their position within the Venn Diagram in Fig.1.1.

1.9 Tables

KEGG Pathway Term	Count	P-Value	Benjamini-Hochberg P-Value
MAPK signaling pathway	33	2.2E-05	3.1E-03
Axon guidance	21	2.2E-05	1.6E-03
Calcium signaling pathway	24	9.0E-05	4.2E-03
Hypertrophic cardiomyopathy (HCM)	14	7.1E-04	2.5E-02
ErbB signaling pathway	14	8.9E-04	2.5E-02
Dilated cardiomyopathy	14	1.5E-03	3.5E-02
GnRH signaling pathway	14	2.7E-03	5.3E-02
Adipocytokine signaling pathway	11	3.5E-03	6.0E-02
Insulin signaling pathway	16	7.3E-03	1.1E-01
Ubiquitin mediated proteoysis	16	8.4E-03	1.1E-01
Arrhythmognenic right ventribular cardiomyopathy	11	8.7E-03	1.1E-01
Gap junction	12	9.6E-03	1.1E-01
Focal adhesion	20	1.5E-02	1.5E-01
Neurotrophin signaling pathway	14	1.9E-02	1.8E-01
Melanogenesis	12	2.0E-02	1.8E-01
Endocytosis	18	2.5E-02	2.0E-01
Long-term potentiation	9	3.3E-02	2.4E-01
Wnt signaling pathway	15	3.9E-02	2.7E-01
Colorectal cancer	10	4.2E-02	2.7E-01
Type II diabetes melllitus	7	4.4E-02	2.7E-01
Pancreatic cancer	9	4.4E-02	2.6E-01

Table 1.1 miR-137 targets are enriched in pathways relevant to neuronal signaling

miR-137 target sites within human mRNAs were identified using TargetScan (v6.2) and pathway enrichment was analyzed by DAVID analysis. Counts refer to the number of miR-137 targets in a given pathway identified by TargetScan.

mRNA	Protein	mRNA Target Site	Prediction Tool	Experimental Evidence
AKT2	Akt2	5' ...UAUUUGUACGGUACAAGCAAUAA... ||||||| 3' GAUGCGCAUAAGAAUUCGUUAUU	TargetScan	Liu et al., 2014
ERBB4	ErbB4	5' ...UUGGAUUUUGAAUCAAGCAAUAU... ||||||| 3' GAUGCGCAUAAGAAUUCGUUAUU	TargetScan	None
GSK3B	Gsk3β	5' ...UCUUUUUGAAGAAAAAGCAAUAU... ||||||| 3' GAUGCGCAUAAGAAUUCGUUAUU	TargetScan	None
NRG2	Nrg2	5' ...GUGUAUUCCCCUUUUAGCAAUAA... |||||| ||||||| 3' GAUGCGCAUAAGAAU----UCGUUAUU	TargetScan	None
NRG3	Nrg3	5' ...GUUCAUUUGGAAUAAAGCAAUAU... ||||||| 3' GAUGCGCAUAAGAAUUCGUUAUU	TargetScan	None
PIK3R3	p55γ	5' ...UGCAAUAAAGACAUUGCAAUAAA... |||||| 3' GAUGCGCAUAAGAAUUCGUUAUU	TargetScan	Sang et al., 2016
PTEN	PTEN	5' ...AAAGUAAAUGAAAAAAUGUGCAAUAAU... |||||| 3' GAUGCGCAUAAGAAUUCGUUAUU	miRMap	Lyu et al., 2016
RICTOR	Rictor	5' ...AAGCACAGAUCAUUAAGCAAUAA... ||||||| 3' GAUGCGCAUAAGAAUUCGUUAUU	TargetScan	None

Table 1.2 Predicted miR-137 targets within the PI3K-Akt-mTOR branch of Nrg/ErbB signaling

miR-137 target sites within human mRNAs were identified using TargetScan (v6.2) unless otherwise indicated. Where miR-137 was predicted to target multiple sites, only the highest scored site is shown.

Chapter 2

miR-137 targets mRNAs encoding proteins within the PI3K-Akt-mTOR pathway

Portions of this chapter were adapted from the following manuscript:

Thomas, K.T., Anderson, B.R., Shah, N., Zimmer, S., Hawkins, D., Gu, Q., and Bassell. G.J. (2017). Inhibition of the schizophrenia-associated microRNA miR-137 disrupts Nrg1α neurodevelopmental signal transduction. Cell Rep., Revision Under Review.

2.1 Introduction

Our bioinformatic analysis found that many of the predicted miR-137 targets within the Nrg/ErbB pathway fell within the PI3K(phosphoinositide-3-kinase)-Akt-mTOR(mechanistic target of rapamycin) branch of Nrg/ErbB signaling (**Figure 1.1** and **Table 1.1**). The PI3K-Akt-mTOR pathway plays a critical role in not only cellular growth, autophagy, differentiation, and cellular survival throughout the body (Hawkins et al., 2006; Laplante and Sabatini, 2009), but also plays brain-specific roles in cortical lamination, neurite outgrowth, dendritic spine development, synaptic plasticity, and learning and memory (Crino, 2016; Gross and Bassell, 2014). Furthermore, defects in PI3K-Akt-mTOR signaling underlie some forms of intellectual disability and autism and may contribute to schizophrenia (Crino, 2016; Gross and Bassell, 2014; Law et al., 2012). We sought to validate novel miR-137 targets within the PI3K-Akt-mTOR pathway and to evaluate the effects of miR-137 activity on the levels of these targets within neurons.

2.1.1 The PI3K-Akt-mTOR pathway: general structure and function

Activation of the PI3K-Akt-mTOR pathway usually begins with the binding of a ligand (e.g. a growth factor, antigen, or hormone) to a receptor tyrosine kinase (RTK) or G-protein-coupled receptor (GPCR) (Hawkins et al., 2006). Within the context of Nrg/ErbB signaling, the Nrg's (e.g. Nrg 1) bind and induce the homo- or heterodimerized of ErbB receptor (e.g. ErbB4 homodimer or ErbB2/3 heterodimers). ErbB4 and ErbB3 both possess tyrosine kinase activity that leads to phosphorylation of tyrosine residues within the cytosolic domain of the receptor and activation of PI3K (Mei and Nave, 2014).

The PI3Ks are a family of primarily lipid kinases defined by their ability to phosphorylate the 3-position of the inositol ring within a phosphoinositide substrate (Hawkins et al., 2006). The class I PI3Ks, rather than class II or III, mediate Nrg/ErbB and neurotrophin signaling. PI3K exists as a heterodimer consisting of one catalytic subunit (the p110 subunit) and one regulatory

subunit (Hawkins et al., 2006). Specifically, the p110δ catalytic subunit mediates the majority of ErbB4 signaling (Law et al., 2012), and it is capable of interacting with any one of the following regulatory subunits: p50α, p55α, p85α, p85β, and p55γ. Upon receptor activation, the regulatory subunit binds phosphotyrosine residues within YXXM (tyrosine-any amino acid-any amino acid-methionine) motifs and activates the catalytic subunit of PI3K, which then catalyzes the conversion of phosphatidylinositol(PtdIns)(4,5)P_2 to PtdIns(3,4,5)P_3 (Hawkins et al., 2006). This reaction is reversed by PTEN (phosphatase and tensin homolog), which thereby inhibits PI3K signaling (Hawkins et al., 2006). PtdIns(3,4,5)P_3 serves as a docking site for PI3K effector proteins, including PDK1 (phosphoinositide-dependent kinase-1) and Akt (also known as protein kinase B, or PKB), which mediate downstream signaling (Crino, 2016; Hawkins et al., 2006).

Both PDK1 and Akt directly bind PtdIns(3,4,5)P_3, and activation of PI3K thereby brings these proteins into close proximity, alters Akt's conformation, and allows PDK1 to activate Akt by phosphorylating it at Thr308 (Hawkins et al., 2006). Akt kinases are encoded by three genes (*AKT1*, *AKT2*, and *AKT3*), and Akt1/2/3 all respond to class I PI3K signaling. Upon activation, Akt phosphorylates a number of downstream targets, including TSC (the tuberous sclerosis complex), the transcription factor FOXO, and glycogen synthase kinase 3 (GSK3) (Hawkins et al., 2006).

Among these targets, TSC mediates downstream PI3K-Akt-mTOR signaling. TSC consists of TSC1 and TSC2 proteins, both of which are required for proper function of the complex (Crino, 2016). Akt phosphorylates TSC2 and inhibits TSC activity. TSC acts as a Rheb-GAP (GTPase activating protein) and stimulates the conversion of Rheb-GTP (active form) to Rheb-GDP (inactive form) (Han and Sahin, 2011). When active, Rheb-GTP stimulates the serine/threonine kinase mTOR within mTOR complex 1 (mTORC2) (Crino, 2016; Laplante and Sabatini, 2009). TSC thereby functions as a potent inhibitor of mTORC1, and inhibition of TSC by Akt relieves mTORC1 of TSC-mediated repression, thereby activating mTORC1 (Laplante and Sabatini, 2009).

mTOR functions within two distinct complexes: mTOR complex 1 and mTOR complex 2 (mTORC1 and mTORC2, respectively). mTORC1 mediates downstream PI3K-Akt-mTOR signaling and stimulates some cellular responses, including increased protein synthesis and cell growth, and inhibits other cellular responses, such as autophagy (Crino, 2016). mTORC1 also receives PI3K-independent inputs from the GATOR complex (GTPase-activating proteins toward Rags 1, which inhibits mTORC1 in response to reduced amino acid availability) and AMPK (5' adenosine monophosphate-activated protein kinase, which activates TSC in response to reduced ATP, or adenosine triphosphate) (Crino, 2016). mTORC1 thereby integrates information from multiple sources regarding the cellular resources available for cellular growth, survival, protein synthesis, motility, and other energy-consuming cellular processes; and downstream signals from mTORC1 either stimulate these processes or stimulate cellular conservancy, autophagy, or other processes that conserve or increase the availability of limited resources (Laplante and Sabatini, 2009). Among the downstream targets of mTORC1 are S6K1 (ribosomal protein S6 kinase 1) and EIF4EBP1 (eukaryotic initiation factor 4E binding protein 1) (Crino, 2016). mTORC1-induced stimulation of S6K1 and inhibition of EIF4EBP1 act synergistically to increase protein synthesis.

In addition to the canonical PI3K-Akt-mTOR pathway described above, GSK3 and mTORC2, among other kinases and phosphatases, also regulate mTORC1 activity. GSK3, which exists in α and β isoforms, is a downstream target of Akt and was recently shown to inhibit mTORC1 activity during brain development (Ka et al., 2014). mTORC2 is defined by the presence of rictor rather than raptor, the obligate component of mTORC1 (Laplante and Sabatini, 2009). mTORC2 plays a critical role in regulating PI3K-Akt-mTOR signaling by phosphorylating Akt at the Ser473 residue, which is required for Akt activation (Sarbassov et al., 2005). mTORC2 thereby plays a secondary role in mTORC1 activation, but mTORC2 also inhibits mTORC1 by competing with mTORC1 for shared protein components (e.g. mTOR) (Chen et al., 2011). Inhibition of rictor thereby increases mTORC1 activity, whereas overexpression of rictor inhibits mTORC1 activity (Sarbassov et al., 2004, 2005). Independent of its role in regulating PI3K-Akt-

mTOR signaling, mTORC2 also regulates changes in cytoskeletal structure and motility (Laplante and Sabatini, 2009).

2.1.2 The PI3K-Akt-mTOR pathway in neuronal signaling

In addition to the ubiquitous functions of the PI3K-Akt-mTOR pathway described above, this pathway also plays specific roles in neuronal signaling and development. For example, PI3K-Akt-mTOR signaling regulates the proliferation, migration, and differentiation of neural and glial progenitors during brain development (Crino, 2016). Normal mTORC1 and mTORC2 activity are required for normal dendritic outgrowth and arborization (Crino, 2016). PI3K-Akt-mTOR signaling also regulates dendritic spine morphology and synaptic plasticity, making this critical for several forms of learning and memory (Crino, 2016; Han and Sahin, 2011).

PI3K-Akt-mTOR pathway components also localize to dendrites where they locally transduce extracellular signals, e.g. BDNF, and regulate translation of dendritic and synaptically localized mRNAs (Crino, 2016; Gross et al., 2010). Local translation allows the postsynaptic compartment to rapidly and specifically respond to synaptic signaling. If a neuron must first transduce a signal to the nucleus, induce transcription, and then transport the mRNA or protein to the site of signal initiation, a significant delay occurs between signal initiation and postsynaptic changes in protein expression, during which time the original signal may have dissipated from the site of signal initiation. Local translation near the site of signal initiation allows the neuron to respond significantly faster and specifically near this site of initiation, and local changes in protein levels are essential for some forms of synaptic plasticity (Leal et al., 2014; Liu-Yesucevitz et al., 2011; Swanger and Bassell, 2013). Neurons possess an arsenal of RNA-binding and associated proteins to regulate this process, and dysregulation of local translation underlies synaptic deficits associated with Fragile X Syndrome and other neurological disorders (Bassell and Warren, 2008; Liu-Yesucevitz et al., 2011; Sutton and Schuman, 2005; Swanger and Bassell,

2013). Neurons depend on the dendritic localization of proteins within signaling pathways, including PI3K-Akt-mTOR pathway components, for local transduction of the original signal.

2.1.3 The PI3K-Akt-mTOR pathway in neurodevelopmental disease

Given the importance of PI3K-Akt-mTOR signaling for neuronal function, it is not surprising that mutations in genes encoding PI3K-Akt-mTOR pathway component have been linked to numerous neurological and neurodevelopmental disorders. Dysregulation of signaling, however, leads to highly divergent phenotypes and disorders, and the consequences of dysregulated PI3K-Akt-mTOR signaling for brain function depend on numerous factors, including whether signaling is enhanced or inhibited, the developmental stage at which the disruption occurs, and the region of the brain in which the disruption occurs (Crino, 2016).

Neurodevelopmental disorders associated with defects in PI3K-Akt-mTOR signaling include tuberous sclerosis complex (TSC), intellectual disability, fragile x syndrome, autism spectrum disorders (ASDs), megalencephaly (a condition in which the brain is abnormally enlarged due to enhanced cell proliferation), and epilepsy (Crino, 2016).

TSC is a dominantly inherited disorder caused by loss-of-function mutations in *TSC1* or *TSC2*, which encode the components of the TSC protein complex, which inhibits mTORC1 activity (Crino, 2016; Han and Sahin, 2011). TSC-causing mutations lead to constitutively active mTORC1 in *in vitro* and *in vivo* models of TSC, and enhanced mTORC1 is evident in patient brain tissue samples (Crino, 2016). Although patient mutations affect multiple organ symptoms, over 90% of patients display neurological symptoms (Han and Sahin, 2011).

Fragile X Syndrome (FXS) is caused by a trinucleotide expansion in the *FMR1* gene, which prevents production of the protein product, an RNA-binding protein known as fragile x mental retardation protein (FMRP). Known FMRP targets include mRNAs encoding critical PI3K-Akt-mTOR pathway components, including the PI3K catalytic subunit p110β and the PI3K

enhancer PIKE (Gross et al., 2010, 2015a, 2015b). Loss of FMRP enhances the synthesis of both proteins and increases downstream mTORC1 signaling in mouse models of FXS.

Symptoms of both TSC and FXS include intellectual disability, autism, and epilepsy, all of which are common features of disorders with enhanced PI3K-Akt-mTOR signaling (Crino, 2016). Whether PI3K-Akt-mTOR signaling defects also contribute to non-syndromic forms of autism remains unclear, though a recent report demonstrated enhanced activity of the PI3K catalytic subunit p110δ and enhanced S6 phosphorylation, which occurs downstream of mTORC1, in lymphoblastoid cell lines derived from individuals with autism (Poopal et al., 2016).

Dysregulation of PI3K-Akt-mTOR signaling may also contribute to schizophrenia (SCZ) A single nucleotide polymorphisms (SNP) in *AKT3* was recently associated with SCZ with genome-wide significance (Ripke et al., 2014). Furthermore, some lymphoblastoid cell lines derived from SCZ patients display enhanced p110δ activity and impaired p110δ-dependent signaling (Law et al., 2012). Small molecule inhibitors of p110δ also rescue cognitive deficits in a mouse model of schizophrenia (Papaleo et al., 2016). Furthermore, the antipsychotic haloperidol stimulates mTORC1 signaling, dendrite outgrowth, and mRNA translation in primary striatal neurons (Bowling et al., 2014). Together, these data suggest that pharmacological targeting of the PI3K-Akt-mTOR pathway may have therapeutic utility in some SCZ patients.

Interestingly, mutations that enhance PI3K and Akt activity often lead to phenotypes that are reversible by inhibitors that target downstream mTORC1 (Crino, 2016). This suggests that although PI3K and Akt have mTORC1-independent effects, mTORC1 serves as a common signaling node within the pathway, and drugs that target mTORC1 may hold therapeutic utility for a wide range of disorders caused by defects in upstream signaling.

2.1.4 miR-137 and the PI3K-Akt-mTOR pathway

Previous studies have demonstrated miR-137's ability to regulate multiple kinases within the PI3K-Akt-mTOR pathway (summarized in **Table 1.1**). For example, miR-137 directly targets

AKT2 mRNA and inhibits tumor growth in hepatocellular carcinoma by inhibiting Akt2-mTOR signaling (Liu et al., 2014). miR-137 also targets mRNA encoding cyclooxygenase-2, which stimulates PI3K-Akt-mTOR signaling by inhibiting PTEN (Cheng et al., 2014; Li et al., 2011). However, miR-137 overexpression also reduces PTEN levels in primary mouse neurons (Lyu et al., 2016). miR-137 may, therefore, exhibit both stimulating and inhibitory effects on PI3K-Akt-mTOR pathway activity. More work is needed to examine miR-137's role in regulating multiple mRNA targets that encode PI3K-Akt-mTOR pathway components in neurons.

2.1.5 Chapter 2 hypothesis and objectives

In Chapter 1, we identified *PIK3R3, PTEN, AKT2, GSK3B,* and *RICTOR* mRNAs as potential targets of miR-137. Of these, only *AKT2* and *PIK3R3* have been previously validated, but the ability of miR-137 to regulate endogenous protein levels in neurons has not been assessed. We hypothesized that miR-137 also targets the 3'UTRs of *PTEN, GSK3B,* and *RICTOR* mRNAs and thereby regulates the endogenous levels of PTEN, GSK3β, and rictor proteins in neurons.

2.2 Results

To validate miR-137 targets within the PI3K-Akt-mTOR pathway, we first conducted a series of luciferase reporter assays in the Neuro2A cell line and western blots in primary cortical neurons to validate the following predicted targets: p55γ, PTEN, Akt2, GSK3β, and rictor. This list includes proteins that stimulate (i.e. p55γ and Akt2) and proteins that inhibit mTORC1 signaling (i.e. PTEN, GSK3β, and rictor).

All luciferase assays utilized human 3'UTR sequences, which allow us to assess the significance of specific human mRNA sequences for regulation by miR-137. For all luciferase assays, Neuro2A cells were transfected with three constructs: 1) a plasmid encoding firefly or *Renilla* luciferase with the attached 3'UTR of interest, 2) a plasmid encoding firefly or *Renilla* luciferase without any 3'UTR to control for differences in transfection efficiency, and 3) a

plasmid to overexpress pre-miR-137, an LNA inhibitor specific to miR-317, or the relevant control. In some cases, a single plasmid contained firefly and *Renilla* luciferase under the control of independent promoters. We predicted that overexpression of miR-137 would reduce 3'UTR reporter activity, whereas inhibition of miR-137 would increase reporter activity.

Our western blot experiments allow us to assess whether miR-137 regulates endogenous protein levels within neurons and in some cases to evaluate changes in post-translational modifications (i.e. phosphorylation). For overexpression experiments, neurons were transfected prior to plating with a plasmid encoding pre-miR-137 and protein levels were assessed at DIV6 or 7 (see **Supplemental Fig. 2.1** for validation of the pre-miR-137 overexpression plasmid). For inhibition experiments, neurons were transfected on DIV11 or 12 with an LNA inhibitor specific to miR-137 and protein levels were assessed after 3 days (DIV14 or 15, respectively). We predicted that overexpression of miR-137 would reduce 3'UTR reporter activity and reduce levels of the mRNA targeted-protein of interest, whereas inhibition of miR-137 would increase reporter activity and increase levels of the target protein.

2.2.1 miR-137 negatively regulates neuronal p55γ levels

P55γ functions as a regulatory subunit of PI3K and is encoded by *PIK3R3* mRNA in humans. We found that overexpression of miR-137 reduced *PIK3R3*-3'UTR reporter activity (**Fig. 2.1A**) while inhibition of miR-137 increased *PIK3R3*-3'UTR reporter activity (**Fig. 2.1B**), as expected for a miR-137 target mRNA and consistent with a previous report (Sang et al., 2016). Using western blots, we found that overexpression of miR-137 had no effect on p55γ (**Fig. 2.1C**), but inhibition of miR-137 significantly increased p55γ protein levels in primary cortical neurons (**Fig. 2.1D**). Together these data demonstrate that miR-137 regulates p55γ protein levels in neurons, likely by targeting the 3'UTR of *PIK3R3* mRNA.

2.2.2 miR-137 negatively regulate neuronal PTEN levels

Overexpression of miR-137 has previously been shown to reduce PTEN levels in primary neurons (Lyu et al., 2016). Whether *PTEN* functions as a direct target of miR-137 has not been previously examined however. We found that overexpression of miR-137 also reduced *PTEN*-3'UTR reporter activity (**Fig. 2.2A**) while inhibition of miR-137 had no effect (**Fig. 2.2B**). Similarly, overexpression of miR-137 reduced PTEN protein levels in primary neurons (**Fig. 2.2C**), as previously described, while inhibition of miR-137 had no effect (**Fig. 2.2D**). These data suggest that while miR-137 may be capable of targeting *PTEN* mRNA and inhibiting PTEN protein synthesis, miR-137 present at basal, endogenous levels may play little role in regulating PTEN synthesis.

2.2.3 miR-137 negatively regulates neuronal Akt2 levels

AKT2 has previously been validated as a miR-137 target (Liu et al., 2014), but whether miR-137 regulates Akt2 levels in neurons has not been evaluated. We, therefore, chose not to perform luciferase assays with the *AKT2*-3'UTR. Consistent with miR-137 targeting *AKT2* mRNA in neurons, we found that overexpression of miR-137 reduced Akt2 protein levels (**Fig. 2.3A**) and that inhibition of miR-137 increased Akt2 protein levels (**Fig. 2.3B**).

2.2.4 miR-137 negatively regulates neuronal GSK3β levels

GSK3β lies downstream of Akt signaling but is also capable of negatively regulating mTORC1 signaling (**Fig. 1.1**) (Ka et al., 2014). We conducted luciferase assays with *GSK3B*-3'UTR reporters that we purchased in two fragments: the first containing nucleotides 11-2510 and the second containing nucleotides 2293-4835 of the human *GSK3B*-3'UTR sequence. Each fragment contains at least one predicted miR-137 target site, and both reporters showed reduced activity following miR-137 overexpression (**Fig. 2.4A**). Neither, however, were affected by

inhibition of miR-137 (**Fig. 2.4B**), suggesting miR-137 may not target the *GSK3B*-3'UTR in Neuro2A cells under basal conditions. In primary cortical neurons, overexpression of miR-137 reduced GSK3β protein levels without affecting phosphorylation at the Ser9 site (**Fig. 2.4C**) while inhibition of miR-137 increased GSK3β protein levels without affecting phosphorylation (**Fig. 2.4D**). Together these data demonstrate that miR-137 likely targets the 3'UTR of *GSK3B* mRNA and regulates GSK3β protein synthesis in neurons.

2.2.5 miR-137 negatively regulates neuronal rictor levels

Rictor is an obligate component of mTORC2 (Sarbassov et al., 2004). While overexpression of miR-137 had no effect on *RICTOR*-3'UTR reporter activity (**Fig. 2.5A**), inhibition of miR-137 increased reporter activity by almost 100% (**Fig. 2.5B**), suggesting that the *RICTOR*-3'UTR is strongly targeted by miR-137 in Neuro2A cells. By contrast, overexpression of miR-137 reduced rictor protein levels in primary cortical neurons (**Fig. 2.5C**), while inhibition of endogenous miR-137 had no effect (**Fig. 2.5D**), suggesting miR-137 may play little role in regulating rictor protein levels in neurons under basal conditions.

2.2.6 miR-137 negatively regulates neuronal mTOR levels

Though mTOR is not a predicted target of miR-137, previous reports suggest that miR-137 negatively regulates mTORC1 activity by inhibiting Akt2 (Liu et al., 2014). Our data suggest that both negative and positive regulators of mTORC1 signaling are targeted by miR-137, however, so we next used western blots to determine whether miR-137 regulates mTOR protein levels or phosphorylation in primary neurons. Overexpression of miR-137 in primary cortical neurons significantly reduced mTOR protein levels without affecting phosphorylation at the Ser2448 site, which is involved in both mTORC1 and mTORC2 signaling (**Fig. 2.6A**). Inhibition of endogenous miR-137 had no effect on mTOR protein levels or phosphorylation (**Fig. 2.6B**). Notably, our western blot data with rictor, which directly interacts with mTOR as part of

mTORC2, closely resemble those obtained for mTOR, suggesting that changes in rictor levels may contribute to the loss of mTOR with miR-137 overexpression.

2.3 Discussion

We addressed the hypothesis that miR-137 regulates proteins within the PI3K-Akt-mTOR pathway. Specifically, our bioinformatics predictions (**Fig. 1.1** and **Table 1.1**) suggested that p55γ, PTEN, Akt2, GSK3β, and rictor may be encoded by target mRNAs containing miR-137 binding sites within their 3'UTRs. Each potential target was assessed by four different assays: 1) luciferase assays with the 3'UTR of interest and miR-137 overexpression, 2) luciferase assays with the 3'UTR of interest and inhibition of miR-137, 3) western blots for the protein of interest with miR-137 overexpression, and 4) western blots for the protein of interest with inhibition of miR-137. We expected that miR-137 overexpression would reduce reporter activity and target protein levels while inhibition of miR-137 would increase reporter activity and target protein levels. We found that miR-137 targets the human 3'UTR sequence of *PIK3R3*, *PTEN*, *RICTOR*, and *GSK3B* mRNAs and regulates mTOR, p55γ, PTEN, Akt2, rictor, and GSK3β protein levels in primary neurons. Surprisingly, miR-137 did not consistently regulate any of these targets by all four measures. The effects of miR-137 appear to differ between Neuro2A cells and neurons, to differ depending upon whether miR-137 is present at endogenous levels or artificially overexpressed, and perhaps to differ based on affinity to different 3'UTRs.

In the case of p55γ, our luciferase assays consistently demonstrated that miR-137 targets the *PIK3R3*-3'UTR and inhibition of miR-137 significantly increased p55γ protein levels in neurons. However, overexpression of miR-137 had no effect on p55γ levels in neurons. One possible explanation for this observation is that the miR-137 binding site in the 3'UTR of *Pik3r3* mRNA in mouse neurons is saturated under basal conditions, so increased levels of miR-137 do not lead to increased binding. Alternatively, our overexpression and inhibition experiments were

conducted at different time points (DIV6-7 for overexpression and DIV14-15 for inhibition). miRNAs often have different mRNA targets at different stages of development (Bartel, 2009), due to changes in the availability of high affinity targets, differences in pre-mRNA processing, and due to differences in mRNA binding protein levels and miRNAs that compete for available binding sites on the mRNA target. It is possible that miR-137 targets *Pik3r3* only at later stages of neuronal development.

The *PTEN* 3'UTR contains a poorly conserved miR-137 binding site (TargetScan v7.0). Only miR-137 overexpression affected reporter or endogenous protein levels, suggesting that endogenous levels of miR-137 may not target the *PTEN*-3'UTR, but binding may occur when miR-137 is increased, such as when glutamate stimulates mGluR signaling in the hippocampus (Olde Loohuis et al., 2015).

Rictor also behaved inconsistently in our assays. Our 3'UTR only responded to inhibition of miR-137, suggesting that the *RICTOR*-3'UTR may be strongly bound by miR-137 in Neuro2A cells. However, only miR-137 overexpression affected rictor protein levels in neurons, suggesting that miR-137 may not target the mRNA under basal conditions. The inconsistencies in our results may be due to several causes: 1) miR-137 may have a higher affinity for the human *RICTOR*-3'UTR than for the mouse *Rictor*-3'UTR, 2) the miR-137 binding site may be more accessible, even saturated, in Neuro2A cells but inaccessible in neurons due to differences in mRNA binding proteins or competing miRNAs, or 3) rictor levels are reduced in neurons as a secondary consequence of miR-137 targeting another protein that regulates rictor, not because miR-137 targets *Rictor* mRNA directly.

GSK3β responded as predicted for a miR-137 target by all but one measure. Inhibition of miR-137 had no effect on 3'UTR reporter activity. However, miR-137 overexpression reduced reporter activity, and both overexpression and inhibition of miR-137 regulated GSK3β protein levels. Together, these data suggest that miR-137 targets *Gsk3b* mRNA in neurons, but that basal

levels of miR-137 may not target the *GSK3B*-3'UTR in Neuro2A cells. These inconsistencies may be due to several causes: 1) differences between Neuro2A cells and neurons in binding site accessibility or 2) differences in miR-137 binding affinity for the human *GSK3B*-3'UTR and mouse *Gsk3b*-3'UTR.

All of these possibilities could be addressed using a series of mRNA pulldown experiments, followed by qRT-PCR measurement of associated miR-137. As described in (Hassan et al., 2013), biotinylated DNA oligonucleotide probes complementary to the mRNA of interest may be added to neuronal lysate. The probes then bind the mRNA of interest, and probe, mRNA, and associated miRNAs may be precipitated with streptavidin coated beads. This method allows measurement of endogenous mRNA-miRNA interactions and may be used to measure these interactions in neurons at different developmental timepoints (e.g. DIV6 compared with DIV14), in the presence of different environmental signals (e.g. increased mGluR signaling), and in neurons from different species (e.g. human iPSC-derived neurons compared with mouse primary neurons). These experiments should allow the identification of bona fide miR-137 targets under a variety of conditions.

Additionally, future experiments should identify specific miR-137 target sites within *PIK3R3*, *PTEN*, *GSK3B*, and *RICTOR* mRNAs. One option is to mutagenize or remove the bioinformatically predicted target site from the mRNA sequence of interest and repeat the luciferase assays. Either manipulation should ablate or reduce the effect of miR-137 overexpression or inhibition on reporter activity.

Finally, future experiments should address whether miR-137 similarly impacts proteins within the PI3K-Akt-mTOR pathway that are not encoded by miR-137 targets. We observed that overexpression of miR-137 reduced mTOR protein levels, although mTOR is not encoded by a predicted miR-137 target according to TargetScan, miRmap, or other target prediction tools. Other proteins may respond similarly to miR-137 targets due to interactions with miR-137 target proteins, or some may respond conversely as a way of normalizing basal PI3K-Akt-mTOR

pathway activity. Some candidates for these studies include catalytic subunits of PI3K, e.g. p110β, orthologues of Akt2, e.g. Akt1 and Akt3, and other mTORC1/2 components (e.g. raptor).

Together, our data suggest that miR-137 regulates multiple kinases and phosphatases within the PI3K-Akt-mTOR pathway. miR-137 and the PI3K-Akt-mTOR pathway have been independently linked to schizophrenia, intellectual disability, and autism; and both regulate dendritic outgrowth and synaptic plasticity. miR-137 target mRNAs that encode PI3K-Akt-mTOR pathway components provide a promising mechanism by which alterations in miR-137 activity might cause or contribute defects in PI3K-Akt-mTOR signaling that ultimately lead to neurodevelopmental abnormalities and disease. However, our data thus far do not address whether miR-137 regulates the activity of the pathway or the ability of the pathway to respond to changes in cellular signaling. These questions will be addressed in **Chapter 3**.

2.4 Materials and Methods

Neuro2A cell cultures

Neuro2A cells, a mouse neuroblastoma cell line, were cultured as previously described (Williams et al., 2016).

Primary hippocampal and cortical neuron cultures

Primary hippocampal and cortical neuron cultures were prepared from C57BL/6J mouse embryos of either sex on embryonic day 17 as described by Williams et al., 2016. Animal protocols were approved by the Institutional Animal Care and Use Committee at Emory University. For western blot experiments, neurons were plated at a density of 150,000 cells per well in a 12-well plate. All dishes were coated with 1 mg/mL poly-l-lysine (Sigma, P2636) dissolved in borate buffer (40 mM boric acid, 15 mM sodium tetraborate, pH 8.5) overnight at 37°C.

Plasmids and LNA inhibitors

The pre-miR-137 overexpession (OE) plasmid used in experiments with neurons was generated by cloning the pre-miR-137 sequence a purchased Origene construct into the FUGW plasmid. Briefly, pre-miR-137 sequence was cut from the Origene construct using SalI and XhoI restriction enzymes, and the FUGW plasmid was cut with EcoRI. Overhangs were filled by T4 DNA polymerase prior to ligation. Insert sequence and flanking sites were confirmed by sequencing. Overexpression of miR-137 was confirmed by transfecting Neuro2A cells at 100% confluence (12-well plate) with 1 μg FUGW-pre-miR-137OE plasmid or FUGW control, extracting miRNAs using Trizol and measuring miR-137 levels by qRT-PCR.

Negative control A (199006-011) and miR-137 targeting (4101446-011) fluorescein-conjugated locked nucleic acid (LNA) inhibitors were purchased from Exiqon.

For Neuro2A cell luciferase assay experiments, pre-miR-137 was overexpressed using the human miR-137 overexpression plasmid from Origene (MI0000454). Overexpression was confirmed by qRT-PCR (data not shown). The control construct was generated by removing the pre-miR-137 sequence using SalI and XhoI restriction enzymes, blunting the ends with T4 DNA polymerase, and ligating the ends. Removal of the pre-miR-137 sequence was confirmed by sequencing.

To generate the *PIK3R3*-3'UTR and *RICTOR*-3'UTR constructs for luciferase assays, the human *PIK3R3*-3'UTR and *RICTOR*-3'UTR sequences were cut from the pLightSwitch_3UTR backbone (SwitchGear Genomics, S814084 and S814333, respectively) using NheI and FseI restriction enzymes. The 3'UTRs were then cloned pGL3-promoter (Promega) using the XbaI and FseI restriction sites.

Transfections

Neuro2A cells were transfected with Lipofectamine 2000 per manufacturer's instructions. For miR-137 overexpression western blot experiments, cortical neurons were transfected by

nucleofection using the Lonza Nucleofector Kit for Mouse Neurons per manufacturer's instructions prior to plating, and neurons were lysed on DIV6 or 7. For western blot experiments using LNA (locked nucleic acid) inhibitors, neurons were transfected on DIV11 or DIV12 with 75 nM LNA inhibitor (final concentration) by magnetofection using Neuromag (Oz Biosciences, NM50200) per manufacturer's instructions, and neurons were lysed after 3 days (on DIV14 or DIV15, respectively).

RNA isolation, cDNA synthesis, and qPCR

For RNA quantitation, cells were lysed in Trizol (ThermoFisher Scientific) and RNA was isolated per manufacturer's instructions. cDNA was generated from total RNA using qScript microRNA cDNA synthesis kit (Quanta, #95107-025) for miRNAs per manufacturer's instructions. Quantitative PCR was then performed using LightCycler SYBR Green I reagent (Roche) in a LightCycler real-time PCR system using the following primers. For miR-137 and miR-125a, the forward primer was identical to the mature miRNA sequence, and the reverse primer was the PerfeCTa Universal PCR primer, provided by the qScript microRNA cDNA synthesis kit. Relative RNA levels were assessed using primer-specific standard curves and normalization to an internal control.

Luciferase assays

Neuro2A cells were transfected at 70% confluence with Lipofectamine 2000 per manufacturer's instructions along with 1) plasmids expressing firefly and/or *Renilla* luciferase (see below) and 2) an LNA inhibitor to inhibit miR-137 activity (75 nM final concentration), a plasmid to overexpress miR-137 (Origene, 1 μg/mL final concentration), or the relevant control. firefly and *Renilla* luciferase activities were assessed 24 hrs after transfection using the Dual-Glo Luciferase Assay System (Promega, E2940).

For experiments with *RICTOR*- and *PIK3R3*-3'UTRs, the UTR of interest was cloned downstream of firefly luciferase within the pGL3-promoter plasmid (Promega). The pGL3-3'UTR plasmid was transfected at a final concentration of 0.25 μg/mL. Each plasmid was co-transfected with pRL-CMV (Promega) at a final concentration of 0.05 μg/mL. Firefly luciferase activity was normalized to *Renilla* luciferase activity within each well to control for differences in transfection efficiency.

For experiments with the *PTEN*-3'UTR, Neuro2A cells were transfected with 0.25 μg/mL psi-Check2-*PTEN*-3'UTR (a gift from Pier Pandolfi, AddGene, 50936), which contains the human *PTEN*-3'UTR downstream of the *Renilla* luciferase coding sequence (Taylor et al., 2011). The psi-Check2 backbone encodes firely luciferase under an independent promoter. *Renilla* luciferase activity was normalized to firefly luciferase activity to control for differences in transfection efficiency between wells.

For experiments with *GSK3B*-3'UTRs, Neuro2A cells were transfected with 0.25 μg/mL plasmid containing the human *GSK3B*-3'UTR split into two overlapping sequences, each downstream of firefly luciferase within the pEZX-MT06 backbone (Genecopoeia, HmiT054075-MT06). The pEZX-MT06 backbone encodes *Renilla* luciferase under an independent promoter. Firefly luciferase activity was normalized to *Renilla* luciferase activity to control for differences in transfection efficiency between wells.

Western blots

High density cortical neurons were lysed in lysis buffer (50 mM Tris-HCl, 150 mM NaCl, 5 mM $MgCl_2$, 1% NP40, pH 7.4, supplemented with protease and phosphatase inhibitors). Protein concentrations were measured by BCA assay (ThermoFisher Scientific, # 23227). Eight micrograms of protein per sample were resolved by SDS-polyacrylamide gel electrophoresis and transferred to a nitrocellulose membrane. Blots were blocked in Odyssey Blocking Buffer (PBS) (LI-COR, #927-40000) and incubated overnight at 4°C in primary antibodies diluted in a 1:1 mix

of blocking buffer and PBS-Tween-0.1%. Blots were incubated in secondary antibodies diluted in PBS-Tween-0.1% 1 hr at room temperature. All washes were performed in PBS-Tween-0.1%. Blots were viewed on a LI-COR Odyssey blot scanner. All bands were below saturation. Protein levels were assessed by quantitative densitometry using ImageJ, normalized to the average band intensity within each biological replicate, and normalized to a loading control.

Antibodies

The following primary antibodies and dilutions were used for Western blot experiments: mouse monoclonal anti-β-actin (Abcam, ab6276, 1:8000), rabbit polyclonal anti-β-tubulin III (Sigma-Aldrich, T2200, 1:10,000), rabbit monoclonal anti-phospho-mTOR (Ser2448) (Cell Signaling, #5536, 1:250), mouse monoclonal anti-mTOR (Cell Signaling, #4517, 1:1000), rabbit polyclonal anti-phospho-GSK3β (Ser9) (Cell Signaling, #9336, 1:1000), mouse monoclonal anti-GSK3β (Abcam, ab93926, 1:1000), rabbit monoclonal anti-Akt2 (Cell Signaling, #2964, 1:500), rabbit monoclonal anti-p55γ (Abcam, ab186612, 1:1000), rabbit monoclonal anti-PTEN (Cell Signaling, #9559, 1:1000), and rabbit polyclonal anti-rictor (Cell Signaling, #2140, 1:250). The following secondary antibodies were used for infrared fluorescence detection of Western blots: donkey anti-rabbit (LI-COR, #926-32213, 1:10,000) and donkey anti-mouse (LI-COR, #926-68022, 1:20,000).

Statistical Analyses

For each experiment, data were derived from a minimum of three independent biological replicates. Each biological replicate represents neurons obtained from the pooled embryos of one pregnant mouse, i.e. three biological replicates represent cultures from three different dams. All experimental conditions were represented within each biological replicate. Statistical analyses and graphs were prepared in GraphPad Prism (version 7). For all experiments α was set at 0.05.

See figure legends for specific statistical tests. For luciferase assays only, outliers were identified using Grubb's test and removed before further analysis.

2.5 Figures

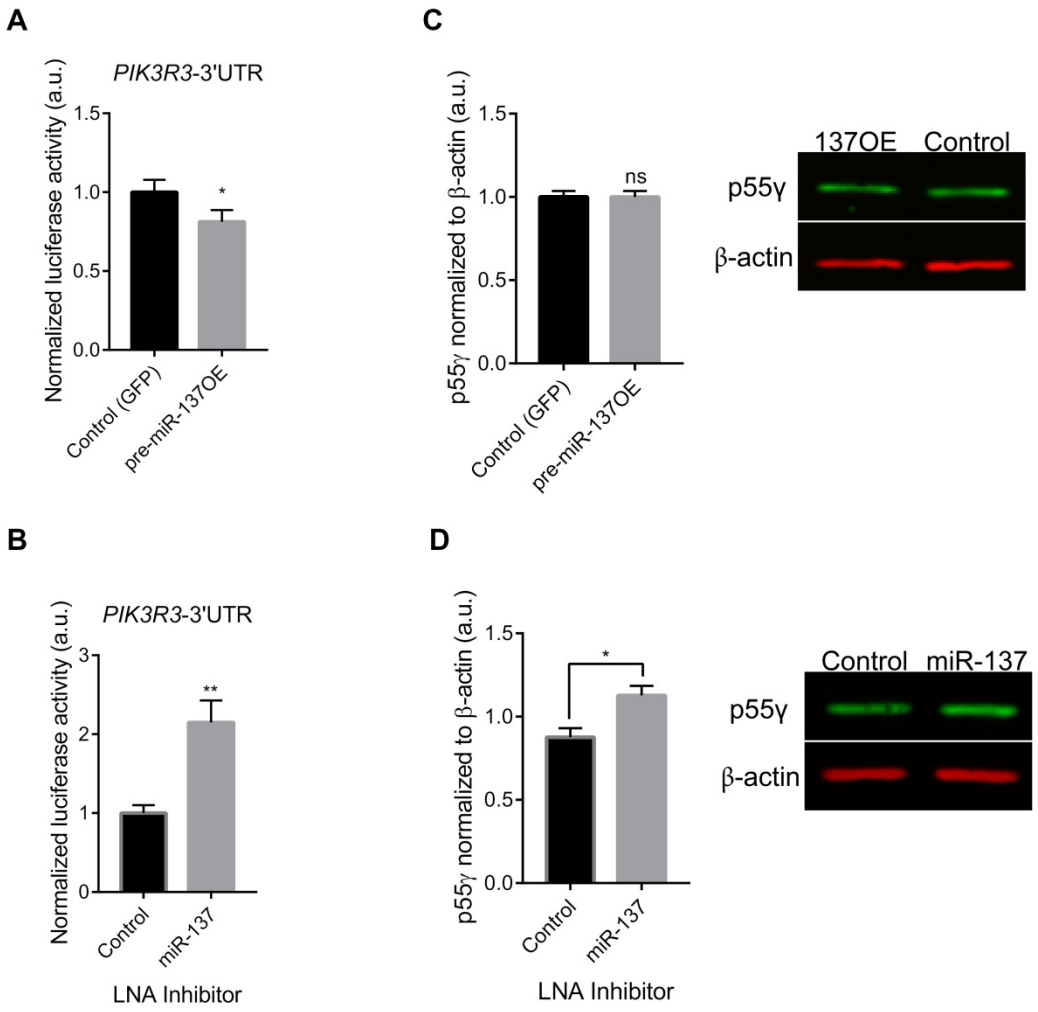

Figure 2.1 miR-137 targets the *PIK3R3*-3'UTR and regulates neuronal p55γ protein. (**A**) Overexpression of pre-miR-137 reduces *PIK3R3*-3'UTR luciferase reporter activity in Neuro2A cells (paired t-test, *p<0.05, n=5). (**B**) Inhibition of miR-137 increases *PIK3R3*-3'UTR luciferase reporter activity in Neuro2A cells (paired t-test, **p<0.01, n=4). (**C**) Overexpression of pre-miR-137 does not affect p55γ protein levels in DIV6-7 primary cortical neurons (paired t-test, not significant, n=6). (**D**) Inhibition of miR-137 increases p55γ protein levels in DIV14-15 primary cortical neurons (paired t-test, *p<0.05, n=6). Representative western blots are shown to the right. Data are shown as mean ± SEM.

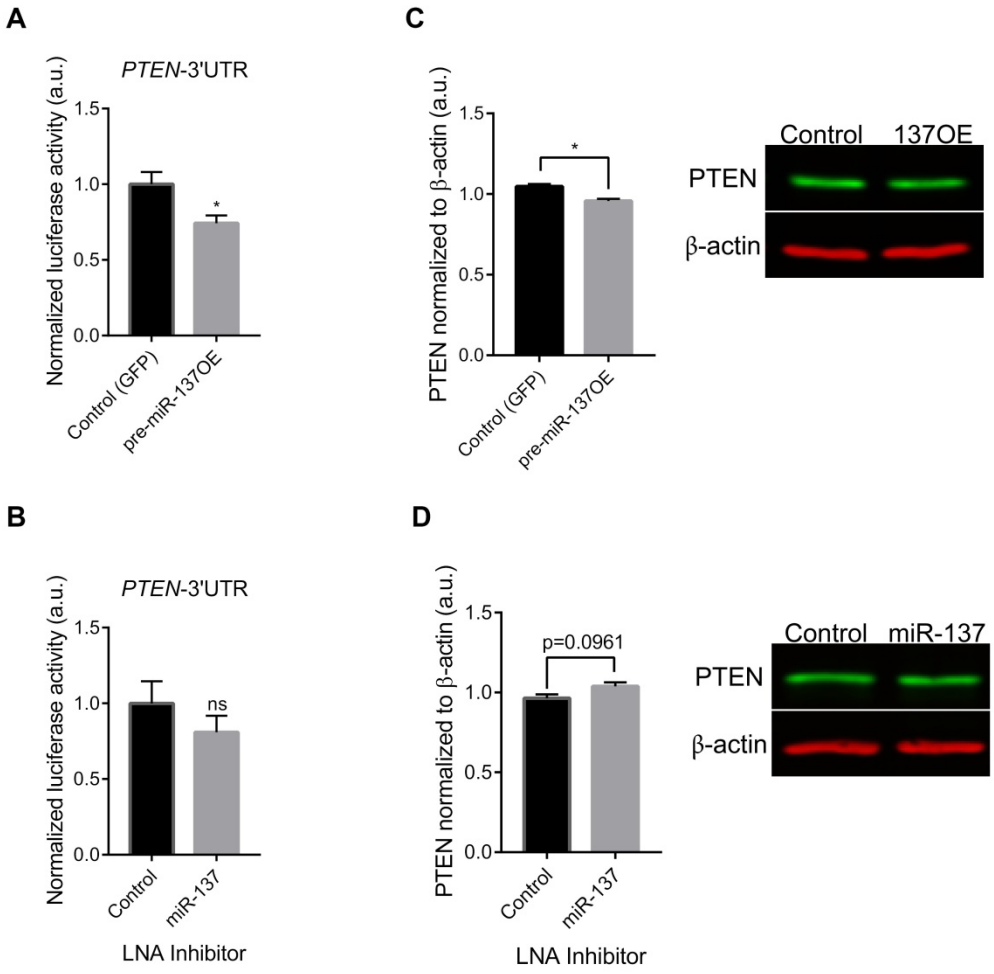

Figure 2.2 miR-137 targets the *PTEN*-3'UTR and regulates neuronal PTEN protein. (**A**) Overexpression of pre-miR-137 reduces *PTEN*-3'UTR luciferase reporter activity in Neuro2A cells (paired t-test, *p<0.05, n=5). (**B**) Inhibition of miR-137 does not affect *PTEN*-3'UTR luciferase reporter activity in Neuro2A cells (paired t-test, not significant, n=4). (**C**) Overexpression of pre-miR-137 reduces PTEN protein levels in DIV6-7 primary cortical neurons (paired t-test, *p<0.05, n=7). (**D**) Inhibition of miR-137 does not affect PTEN protein levels in DIV14-15 primary cortical neurons (paired t-test, not significant, n=6). Representative western blots are shown to the right. Data are shown as mean ± SEM.

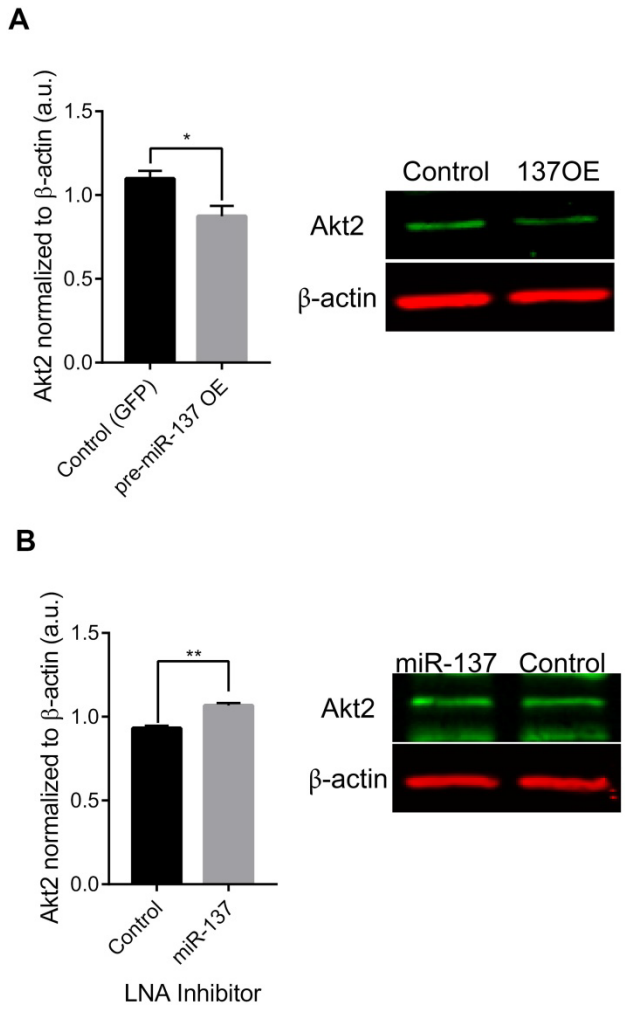

Figure 2.3 miR-137 regulates neuronal Akt2 protein. (**A**) Overexpression of pre-miR-137 reduces Akt2 protein levels in DIV6-7 primary cortical neurons (paired t-test, *p<0.05, n=8). (**B**) Inhibition of miR-137 increases Akt2 protein levels in DIV14-15 primary cortical neurons (paired t-test, **p<0.01, n=6). Representative western blots are shown to the right. Data are shown as mean ± SEM.

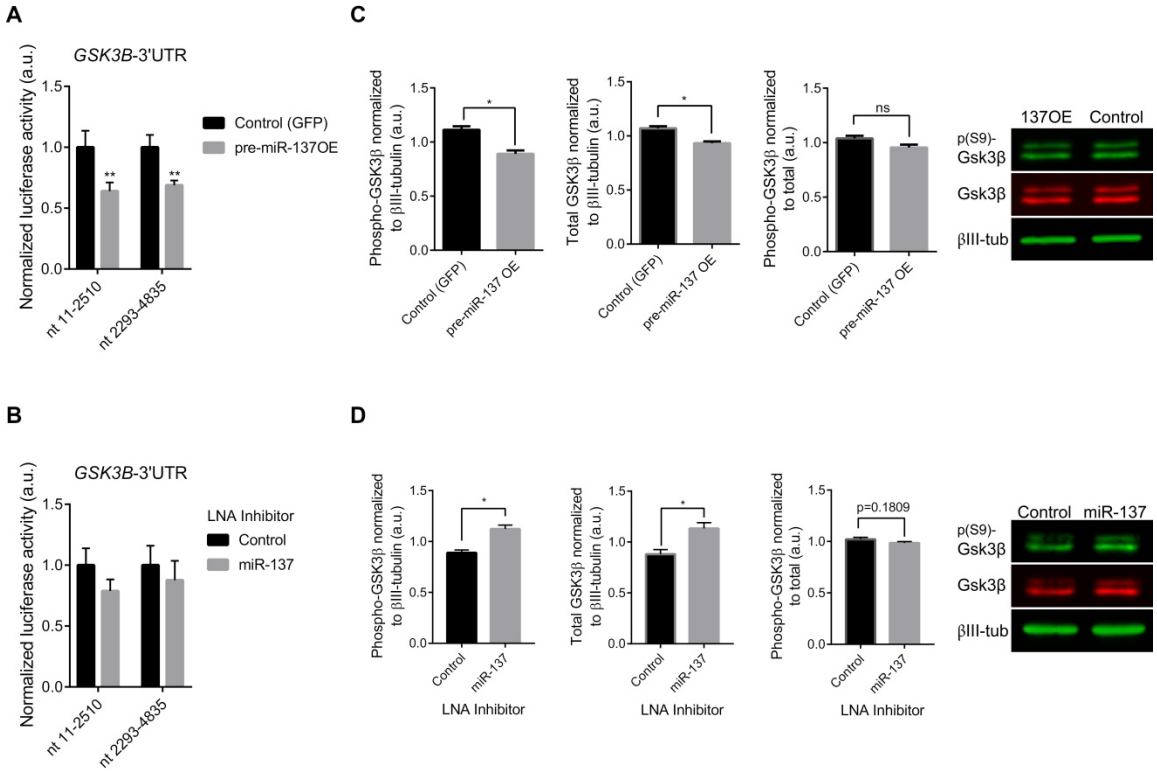

Figure 2.4 miR-137 targets the *GSK3B*-3'UTR and regulates neuronal GSK3β protein levels without affecting phosphorylation at Ser9. (**A**) Overexpression of pre-miR-137 reduces the activities of two *GSK3B*-3'UTR luciferase reporters in Neuro2A cells (Sidak's test, **p<0.01, n=5). (**B**) Inhibition of miR-137 does not affect the activities of either of two *GSK3B*-3'UTR luciferase reporters in Neuro2A cells (Sidak's test, not significant, n=4). (**C**) Overexpression of pre-miR-137 reduces GSK3β protein levels without affecting phosphorylation (Ser9) in DIV6 primary cortical neurons (paired t-test, *p<0.05, n=4). (**D**) Inhibition of miR-137 increases GSK3β protein levels without affecting phosphorylation (Ser9) in DIV14-15 primary cortical neurons (paired t-test, *p<0.05, n=5). Representative western blots are shown to the right. Data are shown as mean ± SEM.

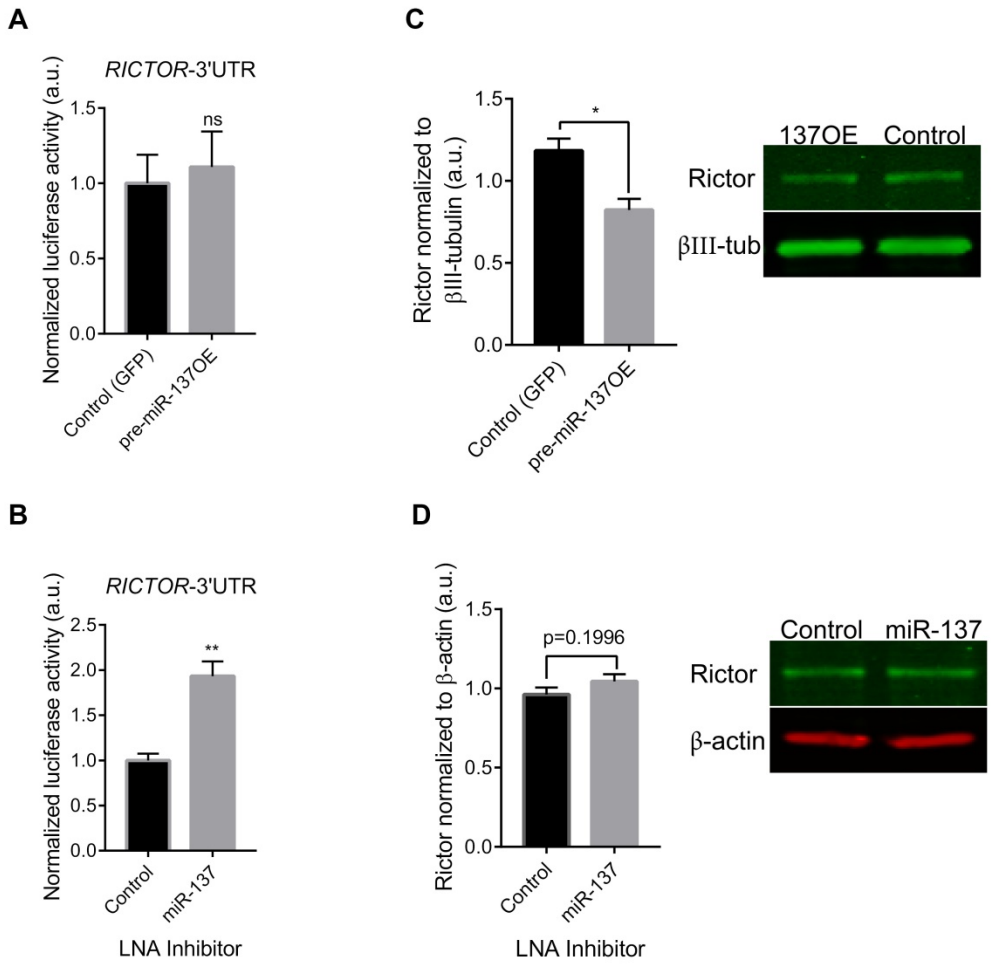

Figure 2.5 miR-137 targets the *RICTOR*-3'UTR and regulates neuronal rictor protein. (**A**) Overexpression of pre-miR-137 does not affect *RICTOR*-3'UTR luciferase reporter activity in Neuro2A cells (paired t-test, not significant, n=5). (**B**) Inhibition of miR-137 increases *RICTOR*-3'UTR luciferase reporter activity in Neuro2A cells (paired t-test, **p<0.01, n=4). (**C**) Overexpression of pre-miR-137 reduces rictor protein levels in DIV6-7 primary cortical neurons (paired t-test, *p<0.05, n=5). (**D**) Inhibition of miR-137 does not affect rictor protein levels in DIV14-15 primary cortical neurons (paired t-test, not significant, n=6). Representative western blots are shown to the right. Data are shown as mean ± SEM.

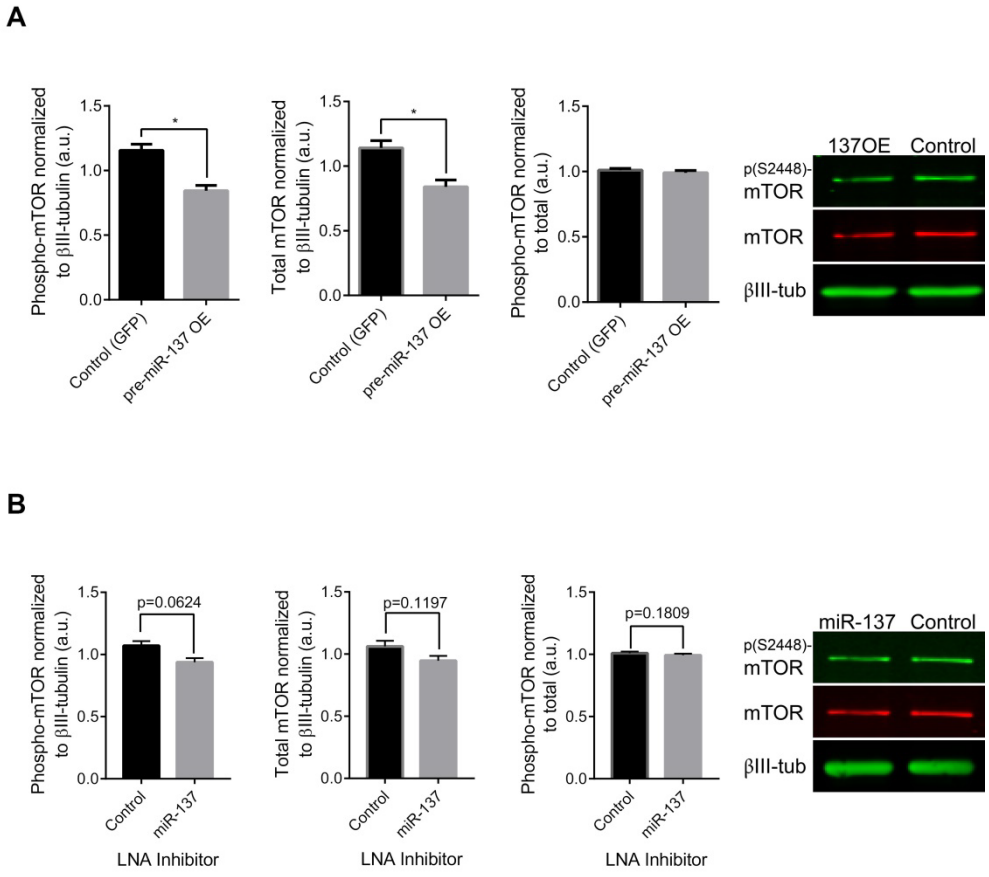

Figure 2.6 miR-137 regulates neuronal mTOR levels but not phosphorylation at Ser2448. (**A**) Overexpression of pre-miR-137 reduces mTOR protein levels without affecting phosphorylation (Ser2448) in DIV6 primary cortical neurons (paired t-test, *p<0.05, n=5). (**B**) Inhibition of miR-137 does not affect mTOR protein levels or phosphorylation (Ser2448) in DIV14-15 primary cortical neurons (paired t-test, not significant, n=5). Representative western blots are shown to the right. Data are shown as mean ± SEM.

2.6 Supplemental Figures

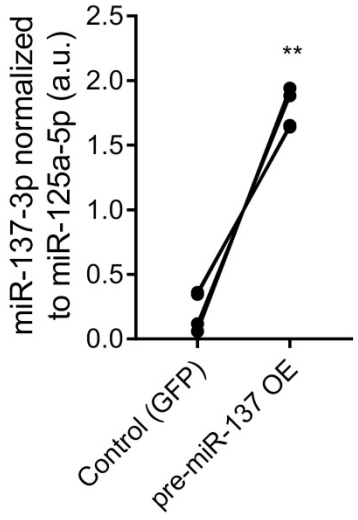

Supplemental Figure 2.1 Validation of pre-miR-137 overexpression plasmid used in neuronal experiments. Neuro2A cells transfected with the pre-miR-137 OE plasmid overexpress miR-137-3p relative to miR-125a-5p, as measured by qRT-PCR (paired t-test, **p<0.01, n=4). Individual data points and pairings are shown.

Chapter 3

Inhibition of miR-137 blocks Nrg1 signaling

Portions of this chapter were adapted from the following manuscript:

Thomas, K.T., Anderson, B.R., Shah, N., Zimmer, S., Hawkins, D., Gu, Q., and Bassell. G.J. (2017). Inhibition of the schizophrenia-associated microRNA miR-137 disrupts Nrg1α neurodevelopmental signal transduction. Cell Rep., Revision Under Review.

3.1 Introduction

Predicted miR-137 targets are significantly enriched within the neuregulin (Nrg)/ErbB signaling pathway, which plays a critical role in regulating neural development and synaptic plasticity. Dysregulation of Nrg/ErbB signaling, and particularly Nrg1/ErbB4 signaling, has been repeatedly linked to psychiatric disorders, including schizophrenia, depression, and bipolar disorder (Mei and Nave, 2014). Furthermore, stimulation of PI3K-Akt-mTOR signaling downstream of Nrg/ErbB promotes neurite outgrowth (Krivosheya et al., 2008) and ion channel synthesis (Yao et al., 2013) among other responses. In Chapter 2, we observed that miR-137 regulates the levels of key proteins within the PI3K-Akt-mTOR signaling pathway. We hypothesized that miR-137 would also regulate PI3K-Akt-mTOR-dependent responses to Nrg/ErbB signaling.

3.1.1 The Nrg/ErbB pathway: general structure and function

The neuregulins are a family of epidermal growth factor (EGF)-like proteins expressed from six separate human genes (*NRG1-6*) (Mei and Nave, 2014). Each genes gives rise to a multitude of isoforms through alternative splicing: *NRG1*, for example, give rise to at least 31 different isoforms (Mei and Xiong, 2008). Nrgs in their mature form begin as immature transmembrane proteins (pro-Nrgs), with the N-terminus, which contains the EGF-like domain, extending extracellularly (Mei and Nave, 2014). Proteolytic cleavage releases the soluble extracellular domain, which is the mature form of Nrg. The extracellular domain of Nrg may be of either the alpha (α) or beta (β) form, which consist of related but distinct EGF-like domains and possess different affinities for ErbB receptors (Wen et al., 1994). Soluble Nrg then binds to and induces the homo- or heterodimerization of the ErbB family of receptor tyrosine kinases, which mediate canonical downstream signaling (Mei and Nave, 2014).

The ErbB receptor tyrosine kinases (RTKs) are expressed from four separate genes (*ERBB1-4*) which share homology with the EGF receptor (EGFR), also known as ErbB1 (Mei

and Nave, 2014). Of these, Nrg1 only interacts with ErbB2, ErbB3, and ErbB4. ErbB4 is the only receptor among these three that both binds Nrg and possesses RTK activity (Mei and Nave, 2014). ErbB2 can bind ligands but lacks RTK activity and can only activate downstream signaling through the formation of heterodimers with ErbB3 or ErbB4 (Mei and Xiong, 2008). By contrast, ErbB3 cannot bind ligand but possesses RTK activity and can activate downstream signaling through the formation of heterodimers with ErbB2 or ErbB4 (Mei and Xiong, 2008). Therefore, only the following ErbB receptor dimers mediate Nrg1 signaling: ErbB4-ErbB4, ErbB2-ErbB4, ErbB3-ErbB4, and ErbB2-ErbB3.

During canonical Nrg1/ErbB signaling, Nrg1 induces ErbB homo- or heterodimerization and activates the receptor's RTK activity. Resulting phosphotyorsine residues then serve as docking sites for adapter proteins or enzymes which mediate downstream signaling. PI3K-Akt-mTOR signaling and Raf-MEK-ERK signaling are frequently activated by ErbB receptors, but ErbB receptors can activate additional downstream kinases, including JNK, CDK5, Fyn, and Pyk2 (Mei and Xiong, 2008). In the case of ErbB4, ErbB4 consists of four different splicing isoforms, which are each capable of triggering distinct downstream signaling cascades. For example, only the Cyt-1-containing isoforms of ErbB4, which contain a motif that binds the PI3K regulatory subunit, activate PI3K signaling (Kainulainen et al., 2000). Downstream signaling from ErbB receptors alter transcription and mRNA translation, causing long lasting changes in cellular activities (Mei and Xiong, 2008).

Nrg1 also engages in noncanonical signaling involving its intracellular domain. Following proteolytic cleavage of the extracellular domain, the intracellular domain may undergo further proteolytic processing, releasing the intracellular domain to translocate to the nucleus (Bao et al., 2003; Mei and Nave, 2014). Within the nucleus, the intracellular domain can interact with transcription factors (Bao et al., 2003) and activate transcription of *PSD95* and other gene targets (Bao et al., 2004).

3.1.2 The Nrg/ErbB pathway in neural development and function

Nrg/ErbB signaling regulates multiple aspects of neural development, including the assembly of neural circuitry, myelination of neuronal axons, synapse formation, and synaptic plasticity (Mei and Nave, 2014). Among these, we will focus on the assembly of neural circuitry and synapse formation, with some discussion of synaptic plasticity.

Nrg/ErbB signaling is critical for multiple aspects of GABAergic circuitry formation. First, Nrg/ErbB signaling directs the migration of interneurons from the ganglionic eminences (the origin of new interneurons) into the cerebral cortex (Mei and Xiong, 2008). During interneuron migration, ErbB4 receptors on the migrating neuron respond to Nrg guidance cues in the environment (López-Bendito et al., 2006; Mei and Xiong, 2008). Whether these cues are primarily attractive of repulsive is unclear. Interestingly, the migration of some of these interneurons towards the diencephalon forms a corridor, which helps guide the entry of the axons that form the thalamocortical projections into the telencephalon (López-Bendito et al., 2006). Developing thalamocortical axons then rely on additional Nrg1-ErbB4 signaling interactions to guide their path through the telencephalon and to their final destinations in the developing cerebral cortex (López-Bendito et al., 2006). When fully formed, thalamocortical projections relay sensory and motor information form the thalamus to the cerebral cortex.

Nrg1 signaling stimulates the outgrowth and branching of axons from primary cortical GABAergic interneurons. Nrg1 signaling in GABAergic interneurons also promotes dendritic outgrowth. Gerecke et al., 2004 reported that Nrg1β increases dendritic branching in primary hippocampal neurons by stimulating ERK and through a PI3K-independent mechanism. By contrast, Krivosheya et al., 2008 reported that Nrg1β/ErbB4 signaling increases the number of primary neurites (presumably by increasing the number of primary dendrites) in GABAergic primary hippocampal neurons while inducing the loss of mature neurites and that inhibition of PI3K blocked completely blocked Nrg1β's effects on neurite formation. Cahill et al., 2012 reported that Nrg1β induces dendrite outgrowth in mature GABAergic primary cortical neurons

by activating kalirin-7, a Rac-guanine nucleotide exchange factor that interacts with postsynaptic density protein 95 (PSD95) in dendrites. Whether any or all of these mechanisms contribute to neurite outgrowth *in vivo* remains to be seen.

Nrg1/ErbB4 signaling also directs the formation of excitatory synapses on GABAergic neurons. Abe et al., 2011 found that peripheral administration of Nrg1 significantly increased surface GluA1 immunoreactivity in parvalbumin-positive GABAergic interneurons, which express ErbB4, and increased GluA1 within synaptic fractions prepared from Nrg-treated mouse cortices. These data suggest that Nrg1 regulates AMPAR expression and surface localization *in vivo*. Furthermore, Ting et al., 2011 found that Nrg1-ErbB4 interactions in primary cultured GABAergic interneurons promote ErbB interactions with PSD95, which stabilizes PSD95 and which could, in turn, stabilize AMPAR at the cell surface. Notably, Nrg1 treatment increased both the number at size of PSD95 immunoreactive puncta suggesting that Nrg1 increases both the formation and maturation of excitatory synapses. Deletion of ErbB4 also reduced the frequency and size of miniature excitatory postsynaptic currents (mEPSCs), demonstrating that ErbB4 is necessary for normal excitatory synaptogenesis in cultured interneurons.

Nrg1 and ErbB4 both continue to be expressed postnatally and throughout adulthood. In the adult brain, Nrg1 localizes to specific lamina of the cortex, with Type I and Type II Nrg1 confined to layers 2, 3, and 6b and Type III in layer 5 (Mei and Xiong, 2008). Types I, II, and III are also found in the hippocampus, piriform cortex, and the reticular nucleus of the thalamus (Mei and Xiong, 2008). In adulthood, ErbB4 expression is confined to GABAergic interneurons, and ErbB4 is most highly expressed in brain regions enriched with interneurons, such as the intercalated masses of the amygdala. ErbB4 also localizes to layers 2-6b in the cortex (Mei and Xiong, 2008).

In adulthood, Nrg1/ErbB4 signaling regulates several forms of neurotransmission and synaptic plasticity. Several reports suggest that ErbB4 localizes to excitatory synapses on GABAergic interneurons, and stimulation of Nrg1/ErbB4 strengthens these synapses and

increases the activity of GABAergic interneurons (Mei and Nave, 2014; Mei and Xiong, 2008). Others suggest that Nrg enhances GABA release from interneurons by acting on presynaptic ErbB4 receptors. By either model, Nrg1/ErbB4 signaling enhances GABAergic activity and inhibits pyramidal neurons onto which these interneurons synapse. Both models are also consistent with the observation that Nrg1 treatment suppresses the induction of long term potentiation (LTP) in Schaffer Collateral-CA1 synapses in hippocampal slice cultures, whereas treatments that cause Nrg1/ErbB4 hypofunction enhance LTP (Mei and Nave, 2014; Mei and Xiong, 2008).

Nrg1/ErbB4 signaling also regulates additional forms of neurotransmission. For example, Nrg1 stimulates dopamine release in the midbrain by acting on ErbB4 receptors expressed on dopaminergic neurons (Yurek et al., 2004). Nrg1 treatment in midbrain slices also activates PI3K-Akt-mTOR signaling and stimulates metabotropic glutamate receptor 1 (mGluR1) synthesis, thereby enhancing mGluR1-activated currents (Ledonne et al., 2014). In cerebellar granule neurons, Nrg1 signaling also stimulates PI3K-Akt-mTOR signaling and the synthesis of the voltage gated potassium channel subunit Kv4.2, which regulates intrinsic neuronal excitability (Yao et al., 2013).

In summary, Nrg/ErbB signaling is critical for multiple stages of neural development and for the regulation of neuronal activity and synaptic plasticity into adulthood. It is therefore unsurprising that Nrg/ErbB signaling dysfunction contributes to neurodevelopmental and psychiatric disease.

3.1.3 The Nrg/ErbB pathway in psychiatric disease

Genetic association and genome wide association studies (GWASs) have repeatedly linked genes in the Nrg/ErbB pathway with psychiatric diseases, including schizophrenia, bipolar disorder, and major depressive disorder (Mei and Nave, 2014). Of these, schizophrenia appears to have to strongest link to the Nrg/ErbB pathway, and single nucleotide polymorphisms in many of

the genes encoding Nrg (*NRG1*, *NRG2*, *NRG3,* and *NRG6)* and all of the genes encoding ErbB receptors (*EGFR*, *ERBB2*, *ERBB3,* and *ERBB4*) have been linked to schizophrenia (Mei and Nave, 2014).

The research examining whether Nrg/ErbB hyper- or hypofunction contributes to schizophrenia has produced mixed results (Reviewed in Mei and Nave, 2014). Studies examining Nrg1 protein levels have reported reduced Type I Nrg1 in the brains of schizophrenia patients. Interestingly, postmortem studies suggest that the density of Nrg1β-positive neurons is increased in schizophrenia subjects while the density of Nrg1α-positive neurons is significantly reduced (Bernstein et al., 2013; Bertram et al., 2007). However, most studies examining mRNA levels have reported increased mRNA within the hippocampus and/or prefrontal cortex of schizophrenia patients, and *ERBB4* mRNA may also be elevated in the prefrontal cortex of schizophrenia patients.

An intriguing series of studies identified a particular isoform of ErbB4 containing the CYT-1 domain, which is required to activate PI3K, that was elevated in the dorsolateral prefrontal cortex of schizophrenia patients (Law et al., 2012). Elevated p110δ, the PI3K catalytic subunit that mediates ErbB4 signaling, was also reported in patients with a particular *ERBB4* schizophrenia risk haplotype (Law et al., 2012). Lymphoblastoid cell lines derived from schizophrenia patients with the *ERBB4* risk haplotype also displayed increased *ERBB4* mRNA encoding the CYT-1 domain and increased *PIK3CD* and *PIK3R3* mRNAs, which encode p110δ and the p55γ regulatory subunit of PI3K respectively(Law et al., 2012). Nrg1α-induced PI3K signaling is also impaired in patient-derived LCLs, suggesting PI3K-Akt-mTOR signaling in response to Nrg1 may be impaired in schizophrenia patients.

3.1.4 Chapter 3 hypothesis and objectives

In Chapter 2, we demonstrated that miR-137 regulates the levels of multiple proteins within the PI3K-Akt-mTOR pathway, which is one of the signaling cascades stimulated by

Nrg/ErbB signaling. Therefore, we hypothesized that miR-137 would regulate PI3K-Akt-mTOR dependent responses to Nrg/ErbB signaling in neurons. The experiments that follow were undertaken with the following objectives: 1) to identify novel mTORC1-dependent responses to Nrg1α, 2) to determine whether miR-137 regulates basal mTORC1 activity, 3) to determine whether miR-137 is required for Nrg/ErbB signaling, and 4) to determine whether Nrg/ErbB signaling, in turn, regulates miR-137 activity.

3.2 Results

In the following experiments, we examine the effects of altered miR-137 activity on three well-defined responses to increased PI3K-Akt-mTOR signaling in neurons: 1) increased phosphorylation of the ribosomal protein S6, 2) increased protein synthesis, and 3) increased dendritic outgrowth. We used primary hippocampal and primary cortical neurons for all experiments, as indicated in figure legends.

3.2.1 Nrg1α increases dendritic phospho-S6 by an ErbB receptor-dependent mechanism

We treated primary hippocampal neurons with a soluble form of the Nrg1α EGF-like domain for 30 min and measured changes in dendritic proteins by quantitative immunofluorescence (qIF). The experimental timeline in **Fig. 3.1** applies to experiments examining phospho-S6 and/or mRNA translation. We found that Nrg1α significantly increased dendritic levels of phospho(Ser235/236)-S6 as well as total S6, without affecting the ratio of phospho- to total S6 (**Fig. 3.2**). S6 is phosphorylated by S6K1 downstream of mTORC1 signaling (Laplante and Sabatini, 2009), so increased phospho-S6 is consistent with increased PI3K-Akt-mTOR signaling. mTORC1 also stimulates ribosome biogenesis, including the transcription of ribosomal RNAs and the translation of ribosomal proteins, which may account for the increase in total S6 in dendrites (Iadevaia et al., 2012).

We also confirmed that Nrg1α acts through ErbB receptors to increase phospho-S6. Because pharmacological inhibitors specific for different ErbB receptor subunits (e.g. ErbB4) have not been developed, we treated primary neurons with the pan-ErbB inhibitor PD158780 for 30 min prior to treatment with Nrg1α. Consistent with Nrg1α mediating its effects through ErbB receptors, we found that PD158780 blocked all effects of Nrg1α on dendritic phospho- and total S6 levels (**Fig. 3.2**).

3.2.2 Nrg1α increases dendritic phospho-S6 and mRNA translation by a miR-137 dependent mechanism

To evaluate the integrity of Nrg/ErbB signaling when endogenous miR-137 is inhibited, we transduced primary hippocampal neurons on DIV2 with a lentivirus containing a previously described miR-137 sponge construct (Olde Loohuis et al., 2015). The miR-137 sponge sequesters endogenous miR-137 and promotes translation of endogenous mRNA targets. On DIV6 (up to DIV9, specific ages reported in figure legends), we treated neurons Nrg1α for 30 min and measured changes in dendritic S6 by quantitative qIF.

Again, we found that Nrg1α treatment significantly and consistently increased dendritic phospho(Ser235/236)-S6 (**Fig. 3.3**) , but whether this was primarily due to an increase in S6 phosphorylation or to an increase in total S6 levels differed between experiments (**Fig. 3.2** compared to **Fig. 3.3A-D**). We, therefore, chose dendritic phospho-S6, rather than total S6 or the ratio of phospho- to total S6, as our primary measure of signaling integrity.

We found that in neurons expressing the miR-137 sponge, Nrg1α no longer stimulated dendritic phospho-S6 (**Fig. 3.3**). By contrast, in one experiment we observed a significant reduction in phospho-S6 in response to Nrg1α in neurons expressing the miR-137 sponge, demonstrating a requirement for endogenous miR-137 in neuronal Nrg1α signaling.

S6 phosphorylation is often correlated with mRNA translation, so we hypothesized Nrg1α would stimulate mRNA translation in a miR-137-dependent manner. We used

puromycylation to label newly synthesized proteins which were then detected by qIF with a puromycin-specific antibody as depicted in **Fig. 3.1**. Nrg1α increased dendritic protein synthesis in control neurons, but this response was ablated in neurons expressing the miR-137 sponge (**Fig. 3.3E-G**). Puromycylation was translation- and puromycin-dependent, but our negative controls for puromycylation had no impact on phospho-S6 (**Fig. 3.3H-J**).

3.2.3 Nrg1α increases dendritic phospho-S6 and mRNA translation by an mTORC1-dependent mechanism

S6 phosphorylation at the Ser235/236 sites may also occur downstream of Erk signaling (Roux et al., 2007). To confirm Nrg-acts through mTORC1 to increase dendritic phospho-S6 and mRNA translation, we treated primary hippocampal neurons with the mTORC1 inhibitor rapamycin prior to Nrg1α treatment. Dendritic phospho-S6 was reduced by 80% with rapamycin, while total S6 was not affected by rapamycin (**Fig. 3.4A-D**). Rapamycin pre-treatment ablated the Nrg1α-induced increases in phospho-S6 (**Fig. 3.4**) and dendritic protein synthesis (**Figure 3.4E-G**). Together, these results demonstrate that Nrg1α-induced increases in dendritic phospho-S6 and protein synthesis require endogenous mTORC1 activity, mirroring the requirement for endogenous miR-137 activity.

3.2.4 Nrg1α increases dendritic MAP2 by a miR-137-dependent mechanism

Interestingly, Gong et al., 2006 reported that MAP2 synthesis in response to tetanic stimulation requires mTORC1 activity in hippocampal slices. MAP2 promotes dendritic outgrowth and branching (Audesirk et al., 1997; Chamak et al., 1987; Harada et al., 2002), and altered MAP2 expression may contribute to mTORC1-induced dendritic outgrowth (examined later in this chapter). We found that acute Nrg1α treatment increased dendritic MAP2 in DIV6 hippocampal neurons in a miR-137-dependent manner (**Fig. 3.5A-B**). Inhibition of miR-137 had no effect on dendrite diameter (**Fig. 3.5C**). Our results suggest that Nrg1α may increase MAP2

synthesis by stimulating mTORC1 and are consistent with our hypothesis that miR-137 regulates mTORC1-dependent Nrg1α signaling.

By contrast, we found that Nrg1α reduces GSK3β phosphorylation at the Ser9 site in primary hippocampal neurons (**Supp. Fig. 3.1**). Inhibition of miR-137 had not effect on Nrg-induced loss of Ser9 phosphorylation, demonstrating that some Nrg1α signaling remains intact in miR-137 sponge expressing neurons. Inhibition of miR-137 also increased dendritic GSK3β total protein levels, consistent with our hypothesis that miR-137 directly targets and inhibits the translation of *GSK3B* mRNA (explored in Chapter 2).

3.2.5 Nrg1α does not affect total or dendritic levels of miR-137

Our data suggest miR-137 regulates Nrg/ErbB signal transduction. Nrg1α may also regulate protein synthesis by altering miR-137 levels (**Supp. Fig. 3.2**). Nrg1α had no effect on total or dendritic miR-137 levels (**Supp. Fig. 3.3**), though miR-137 localizes to the dendrites of primary neurons by DIV6 (**Supp. Fig. 3.3B-C**), suggesting miR-137 may act locally within dendrites to mediate its effects on Nrg1α signal transduction.

3.2.6 Nrg1α increases dendritic outgrowth by an ErbB-dependent mechanism

The PI3K-Akt-mTOR pathway, Nrg1 signaling, and miR-137 activity are known regulators of dendritic outgrowth (Cahill et al., 2012; Gerecke et al., 2004; Krivosheya et al., 2008; Kumar et al., 2005; Smrt et al., 2010). We treated primary neurons on DIV2 with 10 nM Nrg1α or vehicle control and assessed dendritic complexity on DIV4 by Sholl analysis. The experimental timeline in **Fig. 3.6A** applies to all of the morphology experiments that follow. In Sholl analysis, a series of concentric circles of increasing diameter is drawn around the neuron of interest, starting at the cell body and continuing until the end of the longest dendrite (**Fig. 3.6B-C**). The number of times the dendritic arbor is intersected by each circle is then recorded for

statistical analysis, with increased intersections interpreted as increased dendritic complexity (**Fig. 3.6D-E**).

We found that Nrg1α promoted dendritic outgrowth in primary cortical neurons (**Fig. 3.7**).Concurrent treatment with PD158780 completely blocked Nrg1α-induced dendritic outgrowth, consistent with Nrg1α acting through ErbB receptors.

3.2.7 Nrg1α increases dendritic outgrowth by a miR-137-dependent mechanism

We hypothesized that inhibition of miR-137 might block Nrg1α-induced dendritic outgrowth. We found that the miR-137 sponge independently increased dendritic outgrowth (consistent with Smrt et al., 2010); however, Nrg1α significantly reduced dendritic outgrowth in both cortical and hippocampal neurons expressing the miR-137 sponge (**Fig. 3.8A-F**). Furthermore, Nrg1α did not significantly increase dendritic outgrowth in cortical neurons overexpressing miR-137 (**Fig. 3.8G-I**). Together, these results demonstrate that Nrg1α stimulates dendritic outgrowth by a miR-137- dependent mechanism.

3.2.8 Nrg1α increases dendritic outgrowth by an mTOR-dependent mechanism

Nrg1β has been shown to stimulate dendritic outgrowth through multiple mechanisms, including not only increased PI3K signaling but also increased Erk signaling. In order to examine whether Nrg1α increases dendritic outgrowth through an mTOR dependent mechanism, we treated cells with the mTORC1 inhibitor rapamycin concurrently with Nrg1α. We found that rapamycin both reduced dendritic outgrowth and blocked Nrg1α-induced dendritic outgrowth (**Fig. 3.9**). As with acute Nrg1α stimulation, we also found that our 2d treatment with Nrg1α had no effect on miR-137 levels (**Supp. Fig. 3.4**).

With extended treatments, rapamycin may also inhibit mTORC2 activity in some cell types, and whether rapamycin can regulate mTORC2 in neurons has not been examined (Sarbassov et al., 2006). We conclude that Nrg1α stimulates dendritic outgrowth by an mTOR-,

but not necessarily mTORC1-, dependent mechanism. Our data are consistent, however, with our hypothesis that miR-137 disrupts the PI3K-Akt-mTOR branch of Nrg1 signaling.

3.2.9 Nrg1β increases dendritic outgrowth by a miR-137-dependent mechanism

Nrg1α and Nrg1β may act on different time courses and activate different downstream signaling pathways (Eckert et al., 2009; Wen et al., 1994). As mentioned above, Nrg1β has previously been shown to stimulate dendritic outgrowth by multiple, and some of them mTOR-independent, mechanisms. We found that inhibition of miR-137 blocked Nrg1β-induced dendritic outgrowth (**Fig. 3.10**), demonstrating that miR-137 is necessary for some aspects of Nrg1β signaling as well. However, in contrast to our data with Nrg1α, Nrg1β did not reduce dendritic outgrowth in neurons expressing the miR-137 sponge. This suggests that signaling responses to different forms of Nrg1 may be somewhat differently impacted by inhibition of miR-137.

3.3 Discussion

In the present study, we tested the hypothesis that miR-137 regulates Nrg1α neurodevelopmental signal transduction. We found that inhibition of miR-137 blocked Nrg1α-induced increases in phospho-S6 and mRNA translation in the dendrites of primary hippocampal neurons and also blocked Nrg1α-induced dendritic outgrowth. We conclude that inhibition of miR-137 profoundly disrupts Nrg1α signal transduction in primary neurons.

3.3.1 The role of Nrg1α

The EGF-like domain of Nrg exists in two forms: an alpha form and a beta form. The alpha and beta forms of Nrg1 differ in their affinity for ErbB4 receptors and in their ability to stimulate downstream signaling (Eckert et al., 2009). To date, the majority of research concerning the role of Nrg1 signaling in neuronal function has focused on Nrg1β, leaving the Nrg1α form largely unstudied (Bernstein and Bogerts, 2013). However, Nrg1α is highly expressed in neurons

in the human pre- and perinatal brain, including pyramidal neurons and interneurons in multiple regions of the cerebral cortex and hippocampus (Bernstein et al., 2006). Nrg1α expression decreases over the course of human brain maturation, but Nrg1α-positive interneurons remain evident in the human adult cortex and hippocampus, among other brain regions (Bernstein et al., 2006; Connor et al., 2009). Interestingly, the density of Nrg1α-positive neurons is significantly reduced in the cortex of schizophrenia patients (Bernstein et al., 2013; Bertram et al., 2007), and Nrg1α-induced activation of PI3K signaling is impaired in LCLs derived from schizophrenia patients (Law et al., 2012). Together, these studies suggest that Nrg1α signaling may be particularly important for human brain development and for the etiology of schizophrenia (Bernstein and Bogerts, 2013).

Our data demonstrate several novel roles for Nrg1α in neuronal function. Specifically, we found that Nrg1α stimulate S6 phosphorylation, mRNA translation, MAP2, and dendritic outgrowth. Furthermore, Nrg1α stimulates these responses through the mTORC1 pathway and by a miR-137-dependent mechanism. Further research is needed to elucidate the roles of Nrg1α in neuronal function and in the etiology of schizophrenia.

The receptor(s) responsible for the Nrg1α-dependent responses examined in this study have yet to be determined and may be a topic of future research. Nrg/ErbB signaling in excitatory neurons remains largely unexamined, as previous studies have shown that within the adult mouse hippocampus ErbB4 is exclusively expressed by parvalbumin-positive GABAergic interneurons. The majority of neurons in our culture system are likely to be excitatory pyramidal neurons, however, and the responses we describe are unlikely to be restricted to GABAergic neurons, which make up a relatively small proportion of our neuronal population. Within primary neurons, ErbB4 expression may be more widespread, particularly at the DIV4-9 time points addressed in this study (Gerecke et al., 2004). ErbB2 and ErbB3 are also expressed in primary neurons and have previously been shown to mediate Nrg1β-induced changes in DISC1 expression (Seshadri et

al., 2010). Whether Nrg1α preferentially targets specific forms of ErbB receptor or neuronal subtypes remains to be seen.

3.3.2 Significance for schizophrenia

We observed that Nrg1α-induced mRNA translation was ablated in neurons in which miR-137 was inhibited. Whether dysregulated translation also contributes to schizophrenia has only recently begun to be addressed; however, dysregulated mRNA translation has been tied to other neurodevelopmental disorders, including autism spectrum disorders such as Fragile X Syndrome (Swanger and Bassell, 2013). A recent study with patient-derived olfactory cells reported reduced mRNA translation in cells derived from schizophrenia patients (English et al., 2015). Furthermore, the antipsychotic haloperidol stimulates mTORC1 signaling and mRNA translation in primary striatal neurons (Bowling et al., 2014). Whether dysregulated miR-137, Nrg/ErbB, or mTORC1 signaling contribute to defects in mRNA translation in schizophrenia patients should be an interesting topic for future research.

We also observed that inhibition of miR-137 blocked Nrg1α-induced dendritic outgrowth. Though less well-documented than dendritic spine loss, several studies suggest that subpopulations of neurons within the cerebral cortex of schizophrenia patients may have reduced dendritic complexity (Broadbelt et al., 2002; Kalus et al., 2002; Rosoklija et al., 2000). Furthermore, the antipsychotics haloperidol and olanzapine promote neurite outgrowth in primary neurons (Bowling et al., 2014; Zhang et al., 2016). Whether dysregulated miR-137, Nrg/ErbB, or mTORC1 signaling alter neurite outgrowth in schizophrenia patients should be an interesting topic for future research as well.

Drugs that target the PI3K-Akt-mTOR pathway, particularly the p110δ subunit of PI3K which mediates ErbB4 signaling, have been proposed as potential schizophrenia treatments (Gross and Bassell, 2014; Papaleo et al., 2016). Nrg1α-induced PI3K activation is significantly reduced in LCLs derived from schizophrenia patients (Law et al., 2012), indicating that Nrg1α

signaling may be disrupted in schizophrenia in a manner similar to that described in the present study. Future investigation of the role of dysregulated Nrg/ErbB signaling and miR-137 in schizophrenia may provide further support for therapeutic strategies targeting PI3K-Akt-mTOR signaling and other molecular and developmental mechanisms underlying schizophrenia.

3.3.3 Model

We propose the following model by which miR-137 regulates Nrg1 signaling (**Fig. 3.11**). Nrg1α binds ErbB receptors at the surface of dendrites, leading to downstream activation of PI3K, Akt, and mTORC1, respectively. Activation of mTORC1 promotes S6 phosphorylation, increases translation of mRNAs, and enhances dendritic outgrowth in developing neurons. When miR-137 is chronically inhibited, synthesis of proteins such as p55γ, Akt2 and GSK3β is enhanced and renders the pathway unresponsive to further stimulation by an unknown mechanism. Basal S6 phosphorylation and mRNA translation were unaffected by inhibition of miR-137, suggesting that miR-137 does not affect the balance of stimulation and inhibition of PI3K-Akt-mTOR signaling under basal conditions.

While we did not identify one specific miR-137 target within the PI3K-Akt-mTOR pathway responsible for the defects in Nrg1α signaling we observed, we propose that changes in any one of these targets may be sufficient to disrupt downstream signaling within the pathway. For example, altered GSK3β activity is sufficient to alter dendritic morphology in neurons (Llorens-Martín et al., 2013), while increased Akt2 protein levels are sufficient to increase mTOR and S6 kinase phosphorylation and promote cell migration and adhesion in hepatocellular carcinoma (Liu et al., 2014). Interestingly, miR-137 overexpression was recently shown to impair presynaptic synaptic plasticity and vesicle release by reducing the levels of several presynaptic proteins including synaptotagmin-1 (Syt-1), complexin-1, and Nsf; and restoration of Syt-1 only partially rescued these defects (Siegert et al., 2015). As miR-137 regulates multiple proteins

within the PI3K-Akt-mTOR pathway, rescue of any one protein is likely to only partially restore Nrg1α signal transduction.

3.3.4 Alternative mechanism

Changes in miRNA activity are often a critical component of signal transduction. For example, extracellular signals may alter miRNA levels by stimulating or inhibiting their synthesis from precursors (Huang et al., 2012). Group 1 mGluR signaling has previously been shown to increase miR-137 levels in primary hippocampal neurons, and this increase is necessary for mGluR-dependent long term depression (LTD) (Olde Loohuis et al., 2015). Extracellular signals may also regulate miRNA transport into dendrites (Bicker et al., 2013). We predicted that Nrg1α might reduce dendritic miR-137 by either mechanism, relieving target mRNAs of miR-137 repression and allowing protein synthesis (**Supp. Fig. 3.2**). However, we found that Nrg1α had no effect on either total or dendritic levels of miR-137 in primary neurons (**Supp. Fig. 3.3**).

Alternatively, extracellular signals may also affect RNA binding proteins that alter mRNA secondary structures and accessibility of miRNA target sites (Kedde et al., 2010; Kundu et al., 2012; Sosanya et al., 2013) or promote miRNA release from RISC with subsequent miRNA degradation (Banerjee et al., 2009; Muddashetty et al., 2011). Interestingly, Nrg1 signaling is disrupted in lymphoblasts derived from Fragile X Syndrome patients, who lack the RNA binding protein FMRP which has previously been shown to interact with RISC and regulate miRNA-mRNA interactions in response to mGluR signaling (Jin et al., 2004; Kovács et al., 2014; Muddashetty et al., 2011). Future studies may examine whether Nrg1α alters RISC structure, RISC composition, or miRNA activity to promote mRNA translation. However, Nrg1α increased the levels of MAP2 (**Fig. 3.5**), which is unlikely to be expressed from a direct miR-137 mRNA target, while having no effect on GSK3β, a likely miR-137 target (**Supp. Fig. 3.1)**. Any effects of Nrg1α on miR-137-mRNA target interactions appear insufficient to explain changes in protein

levels we observed in response to Nrg1α signaling. However, further work is needed to determine the mechanism by which Nrg1α stimulates mRNA translation.

3.4 Materials and Methods

Primary hippocampal and cortical neuron cultures

Primary neurons were cultured as described in Chapter 2. For quantitative immunofluorescence experiments, neurons were plated at a density of 500,000 cells in a 10-cm dish containing twenty 15-mm coverslips. For morphology experiments, neurons were plated at a density of 200,000 cells in a 10-cm dish containing twenty 15-mm coverslips. Two hours after plating, coverslips were flipped into a 6-well plate (2 coverslips/well) containing secondary glia in conditioned neurobasal media containing B27 and glutamax. All coverslips were coated with 1 mg/mL poly-l-lysine (Sigma, P2636) dissolved in borate buffer (40 mM boric acid, 15 mM sodium tetraborate, pH 8.5) overnight at 37°C.

Drug treatments

For acute stimulation experiments, neurons were treated on DIV6-9 for 30 min with 14 μM (100 ng/mL) of a soluble form of the extracellular domain of Nrg1α (R&D Systems, #296-HR-050) immediately prior to puromycylation or fixation. For morphology experiments, neurons were treated on DIV2 for 48 hrs with 10 nM (0.07 ng/mL) Nrg1α or Nrg1β (R&D Systems, 396-HB-050). For acute rapamycin stimulation experiments, neurons were treated with 200 nM rapamycin (Sigma-Aldrich, R0395) or an equal volume of dimethyl sulfoxide (DMSO) for 30 min prior to Nrg1α treatment and remained in media with Nrg1α. For morphology experiments, neurons were treated with 100 nM rapamycin or an equal volume of DMSO concurrent with Nrg1α treatment. For acute treatment experiments, neurons were treated with 200 nM of the pan-ErbB inhibitor PD158780 (Tocris, 2615) or an equal volume of DMSO for 30 min prior to Nrg1α treatment and remained in solution with Nrg1α. For morphology experiments, neurons were

treated with 100 nM PD158780 or an equal volume of DMSO concurrent with Nrg1α treatment on DIV2. For anisomycin experiments, neurons were treated for 1 hr with 40 μM anisomycin prior to puromycylation.

Plasmids and lentiviruses

FUGW (Control GFP) and miR-137 sponge plasmids were previously described (Olde Loohuis et al., 2015). The pre-miR-137 overexpession (OE) plasmid used in experiments with neurons was generated as described in Chapter 2. All lentiviruses were generated by Emory University's Viral Vector Core.

Transfections and transductions

For morphology experiments, cortical neurons were transfected by nucleofection using the Lonza Nucleofector Kit for Mouse Neurons per manufacturer's instructions prior to plating. Hippocampal and cortical neurons were transduced by adding 1 μL lentivirus (2 x 10^6 infectious units) directly to each well of a 6-well plate containing secondary glia and primary neurons on coverslips. Transductions were performed on DIV1 for western blot and morphology experiments or on DIV2 for DIV6-9 quantitative immunofluorescence experiments. Lentivirus remained in solution until neurons were fixed or lysed.

RNA isolation, cDNA synthesis, and qPCR

RNA isolation, cDNA synthesis, and qPCR were performed as described in Chapter 2.

Immunofluorescence

Neurons were fixed for 15 min at room temperature in 4% paraformaldehyde in PBS. Coverslips were then rinsed in PBS and blocked in IF blocking solution (PBS, 5% normal donkey serum, 0.1% bovine serum albumin, 0.1% Triton X-100, pH 7.4). Coverslips were incubated in

primary (overnight, 4°C) and secondary antibodies (1 hr, room temperature) diluted in IF blocking solution. Where indicated, Rhodamine phalloidin (ThermoFisher, R415, 1:20) was added to secondary antibody solutions. Nuclei were stained with DAPI (10 min, 37°C, 1:1000 in PBS). Excess antibodies and DAPI were removed by PBS washes and the coverslips were mounted for imaging.

Antibodies

The following primary antibodies and dilutions were used for immunofluorescence experiments: rabbit polyclonal anti-MAP2 (EMD Millipore, AB5622, 1:500), mouse monoclonal anti-MAP2 (Sigma-Aldrich, M1406, 1:500), mouse monoclonal anti-tau-1 (EMD Millipore, PC1C6, 1:500), rabbit polyclonal anti-phospho-S6 (Ser235/236) (Cell Signaling, #2211, 1:250), and mouse monoclonal anti-S6 (Cell Signaling, #2317, 1:100). The following secondary antibodies and dilutions were used for detection: donkey anti-mouse Alexa Fluor 488, donkey anti-rabbit Cy3, and donkey anti-mouse Cy5 (Jackson Immunoresearch, 1:500). Mouse monoclonal anti-puromycin (DSHB, PMY-2A4, 1:250) was used for puromycylation experiments.

Puromycylation

Puromycylation was performed as described by Graber et al., 2013 with the following modifications: puromycin was added to neurons at a concentration of 4.17 μg/mL and detected with mouse anti-puromycin antibody diluted 1:250.

Fluorescence in situ hybridization

Primary cortical neurons were treated 15 min with 14 μM Nrg1α then fixed and processed for microRNA FISH using locked nucleic acid (LNA) probes (Exiqon) as previously

described (Sasaki et al., 2013). Probe sequences are given in **Supplemental Figure 3.3**. Coverslips were incubated in LNA probes overnight at 57°C.

Image acquisition

Images were acquired using a Nikon Eclipse inverted microscope equipped with a cooled CCD camera (Photometrics). All qIF experiments utilized a 60x Plan-Neofluar Objective (Nikon, 1.4 numerical aperture), and all morphology experiments utilized a 40x Plan-Neofluar Objective (Nikon, 1.3 numerical aperture). Imaging conditions were constant within experiments, and all experimental groups were imaged within each session. Exposure times were kept below saturation for quantitative analysis. Z-series were acquired at 0.2 μm steps (10-12 total steps).

Image analysis

For quantitative analysis, image stacks were deconvolved using AutoQuant X3 software and a 3-D blind algorithm. Quantification of FISH and qIF signals was performed using Imaris v7 software. Quantification of dendritic morphology was performed using ImageJ (version 1.48s) with NeuronJ and Sholl Analysis plug-ins.

For all quantitative immunofluorescence experiments, one to three dendritic regions of interest approximately 40 μm in length and beginning 25 μm from the cell body were traced for each neuron using the surface function in Imaris. For all quantitative imaging experiments, total signal within the dendritic region of interest was normalized to the volume.

For measurements of dendritic diameter, one to three dendritic regions of interest approximately 40 μm in length and beginning 25 μm from the cell body were traced for each neuron using the FilamentTracer function in Imaris. Dendrites were defined based on MAP2 immunofluorescence. The average diameter of the dendrite within the region of interest was recorded without normalization.

For dendritic morphology experiments, the MAP2 channel was thresholded and dendrites were traced using the NeuronJ plugin in ImageJ (version 1.48s). During tracing, dendrites were identified as neurites that were positive for MAP2 staining and negative for the axonal marker Tau-1 in the source image. Tracings were then analyzed using ImageJ's Sholl Analysis plug-in. Intersections were measured starting 10 μm from the center of the cell body and every 1 μm thereafter until the end of the longest dendrite was reached. Data are displayed first by the resulting "intersections vs distance" curve, and also by summing the total number of intersections for each neuron and normalizing to average number of intersections for neurons in the control group.

Within biological replicates, all quantitative immunofluorescence and total intersections (morphology) measurements were normalized to the average of the control group within that replicate (e.g. "Control(GFP)/Control(Vehicle)" or "DMSO/Control(Vehicle)").

Statistical analyses

For each experiment, data were derived from a minimum of three independent biological replicates. Each biological replicate represents neurons obtained from the pooled embryos of one pregnant mouse, i.e. three biological replicates represent cultures from three different dams. All experimental conditions were represented within each biological replicate. Statistical analyses and graphs were prepared in GraphPad Prism (version 7). For all experiments α was set at 0.05. See figure legends for specific statistical tests.

3.5 Figures

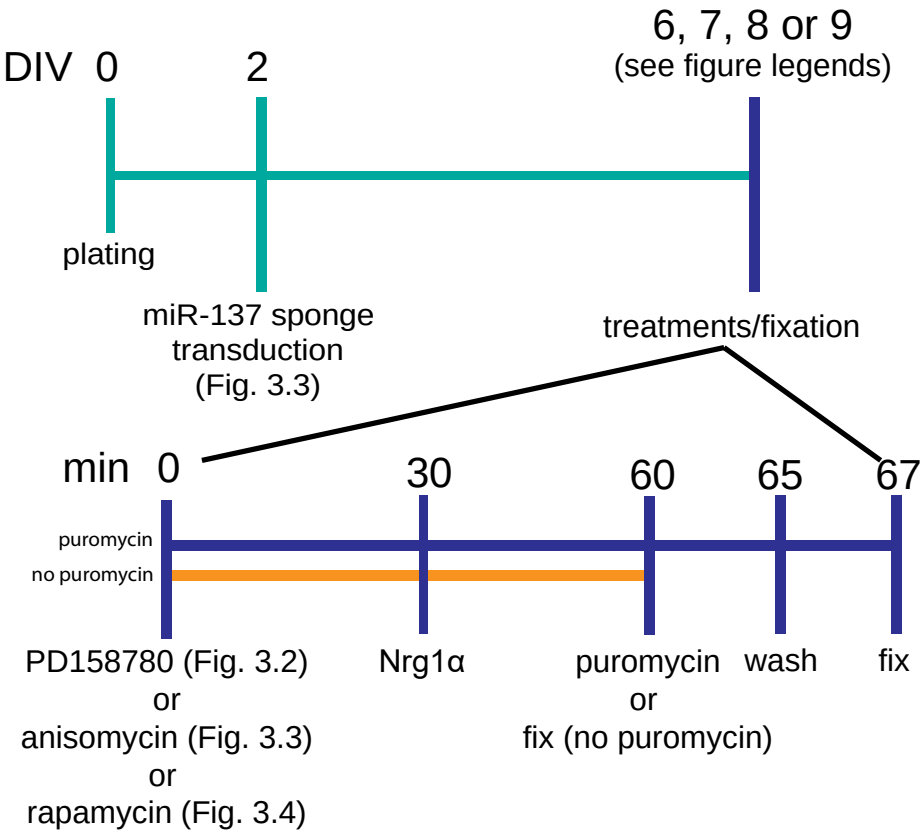

Figure 3.1 Timeline for experiments using acute Nrg1α stimulation. The figure above presents an experimental timeline for the quantitative immunofluorescence and puromycylation experiments presented in **Figures 3.2-3.4**.

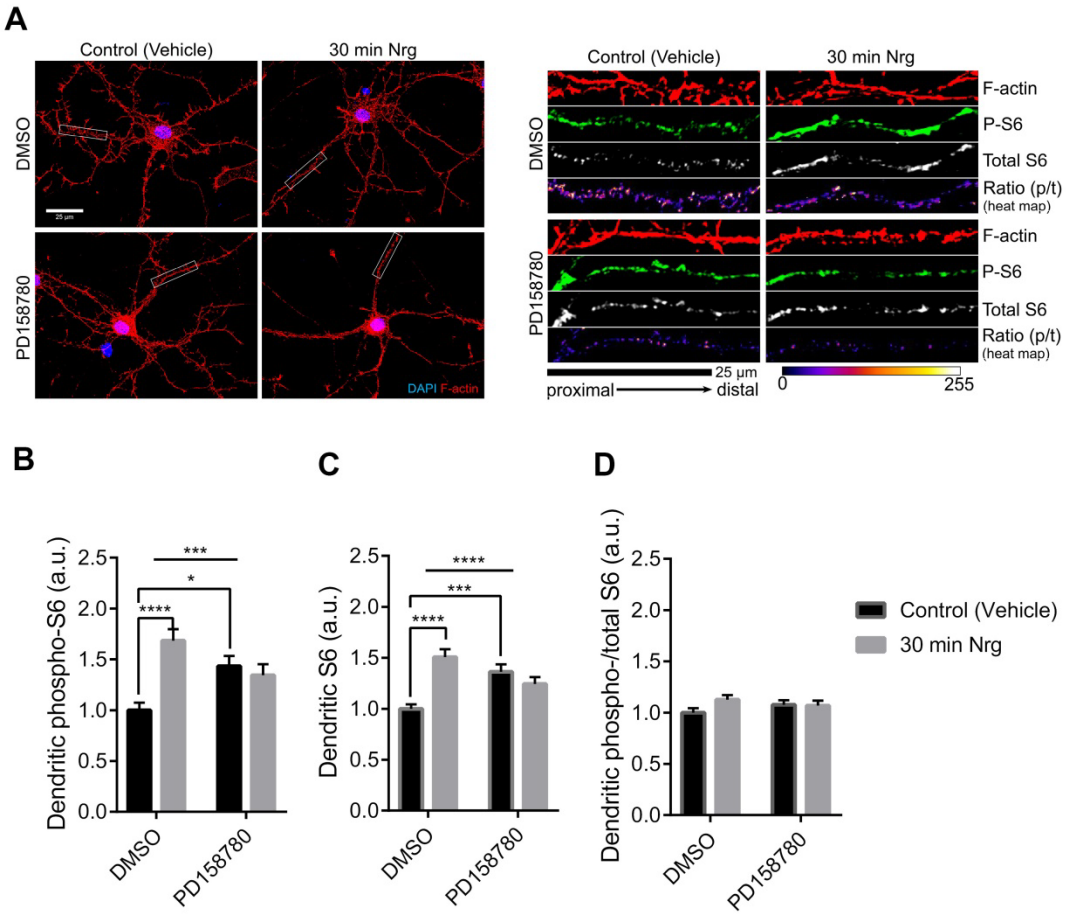

Figure 3.2 Nrg1α increases dendritic phospho(Ser235/236)-S6 by an ErbB receptor-dependent mechanism. Nrg1α treatment increases phospho(Ser235/236) and total S6 levels in DIV6 primary hippocampal neurons. Both responses are ablated in neurons pre-treated (30 min) with the pan-ErbB receptor inhibitor PD158780. Representative neurons and dendritic regions of interest are shown in (**A**). Dendritic phospho-S6 is quantified in (**B**) (Two-way ANOVA, p(Nrg)=0.0034, ***p(interactive)=0.0001; Sidak's test, ****p<0.0001, *p<0.05; n=60 cells/condition from 3 biological replicates). Total S6 is quantified in (**C**) (Two-way ANOVA, p(Nrg)=0.0040, ****p(interactive)<0.0001; Sidak's test, ****p<0.0001, ***p<0.001; n=60 cells/condition from 3 biological replicates). The ratio of phospho- to total S6 is quantified in (**D**) (Two-way ANOVA, not significant, n=60 cells/condition from 3 biological replicates). Data are shown as mean ± SEM. Scale bars are 25 µm for whole cell and dendrite images.

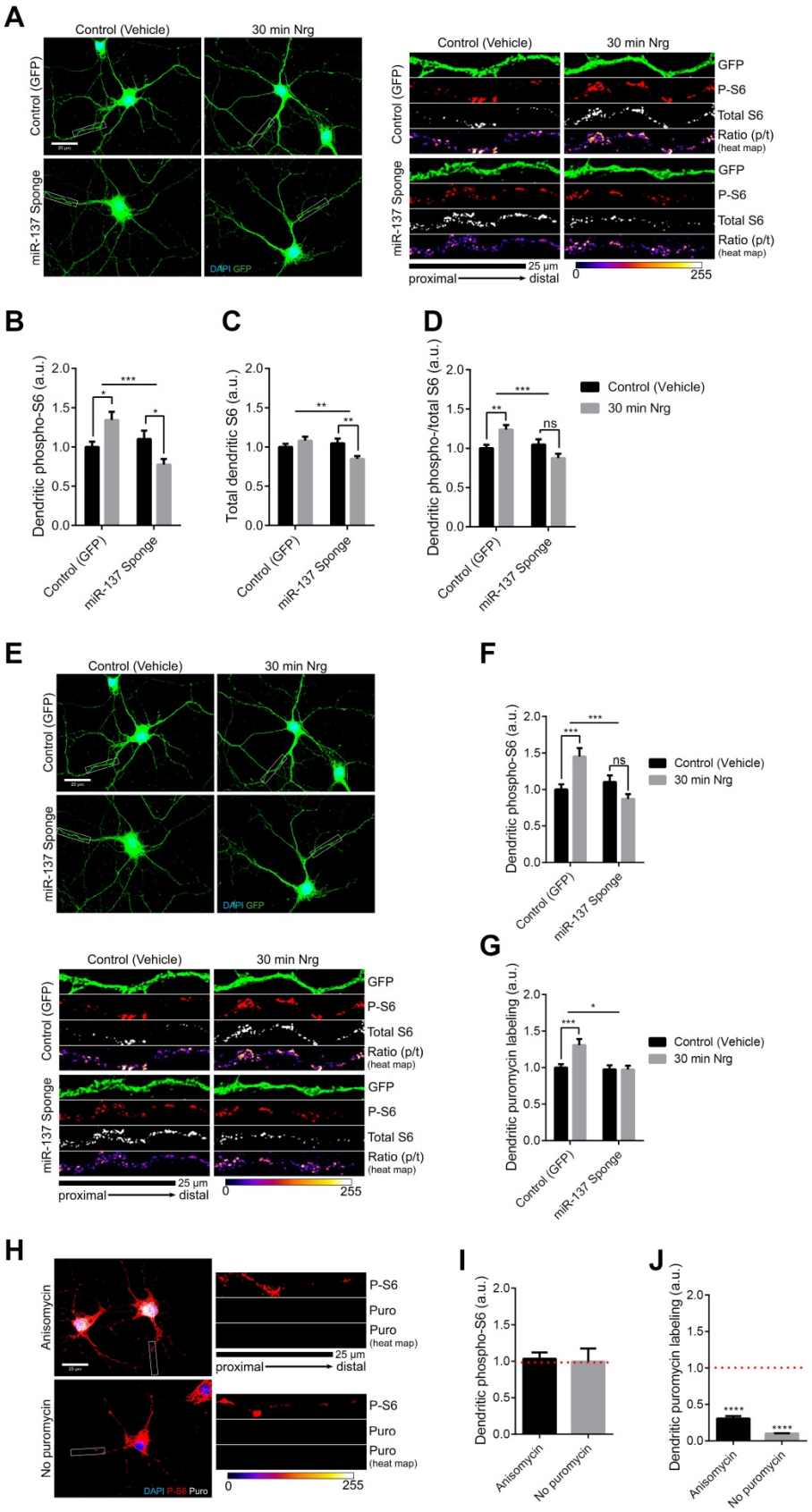
A
Control (Vehicle)
30 min Nrg
Control (GFP)
miR-137 Sponge
DAPI GFP
GFP
P-S6
Total S6
Ratio (p/t)
(heat map)
25 µm
proximal
distal
0
255
B
Dendritic phospho-S6 (a.u.)
C
Total dendritic S6 (a.u.)
D
Dendritic phospho-/total S6 (a.u.)
ns
Control (Vehicle)
30 min Nrg
E
F
G
Dendritic puromycin labeling (a.u.)
H
Anisomycin
No puromycin
Puro
DAPI P-S6 Puro
I
J
****

Figure 3.3 Inhibition of miR-137 blocks Nrg1α-induced increases in dendritic phospho(Ser235/236)-S6 and mRNA translation. (**A-D**) Nrg1α treatment increases dendritic S6 phosphorylation (Ser235/236) without affecting total S6 protein levels in DIV6 primary hippocampal neurons. In neurons expressing the miR-137 sponge, Nrg1α significantly reduces dendritic phospho- and total S6 protein levels. Representative neurons and dendritic regions of interest are shown in **A**. Dendritic phospho-S6 is quantified in **B** (Two-way ANOVA, p(virus)=0.0102, ***p(interactive)=0.0003; Sidak's test, *p<0.05; n=59-60 cells/condition from 3 biological replicates). Total dendritic S6 is quantified in **C** (Two-way ANOVA, **p(interactive)=0.0038; Sidak's test, **p<0.01; n=59-60 cells/condition from 3 biological replicates. The ratio of phospho- to total dendritic S6 is quantified in **D** (Two-way ANOVA, p(virus)=0.0063; ***p(interactive)=0.0005; Sidak's test, **p<0.01; n=59-60 cells/condition from 3 biological replicates). (**E-J**) Inhibition of miR-137 blocks Nrg1α-induced increases in dendritic phospho(Ser235/236) and protein synthesis in DIV7-9 primary hippocampal neurons. Protein synthesis was measured by puromycylation. Representative neurons and dendritic ROIs are shown in **E**. Phospho(S235/236)-S6 is quantified in **F** (Two-way ANOVA, p(sponge)=0.0070,***p(interactive)=0.0001; Sidak's test, ***p<0.001; n=60 cells/condition from 3 biological replicates). Dendritic puromycin incorporation is quantified in **G** (Two-way ANOVA, p(sponge)= 0.0038, p(Nrg)=0.0136, *p(interactive)=0.0123; Sidak's test, ***p<0.001; n=60 cells/condition from 3 biological replicates). Pretreatment with the translation inhibitor anisomycin or not adding puromycin had no effect on phospho-S6 (**I**) but blocked the majority of the puromycylation signal (**J**, one sample t-test, ****p<0.0001, n=18 cells/condition from 3 biological replicates). Representative neurons and dendritic ROIs are shown in **H**. Data are shown as mean ± SEM. Scale bars are 25 μm for whole cell and dendrite images.

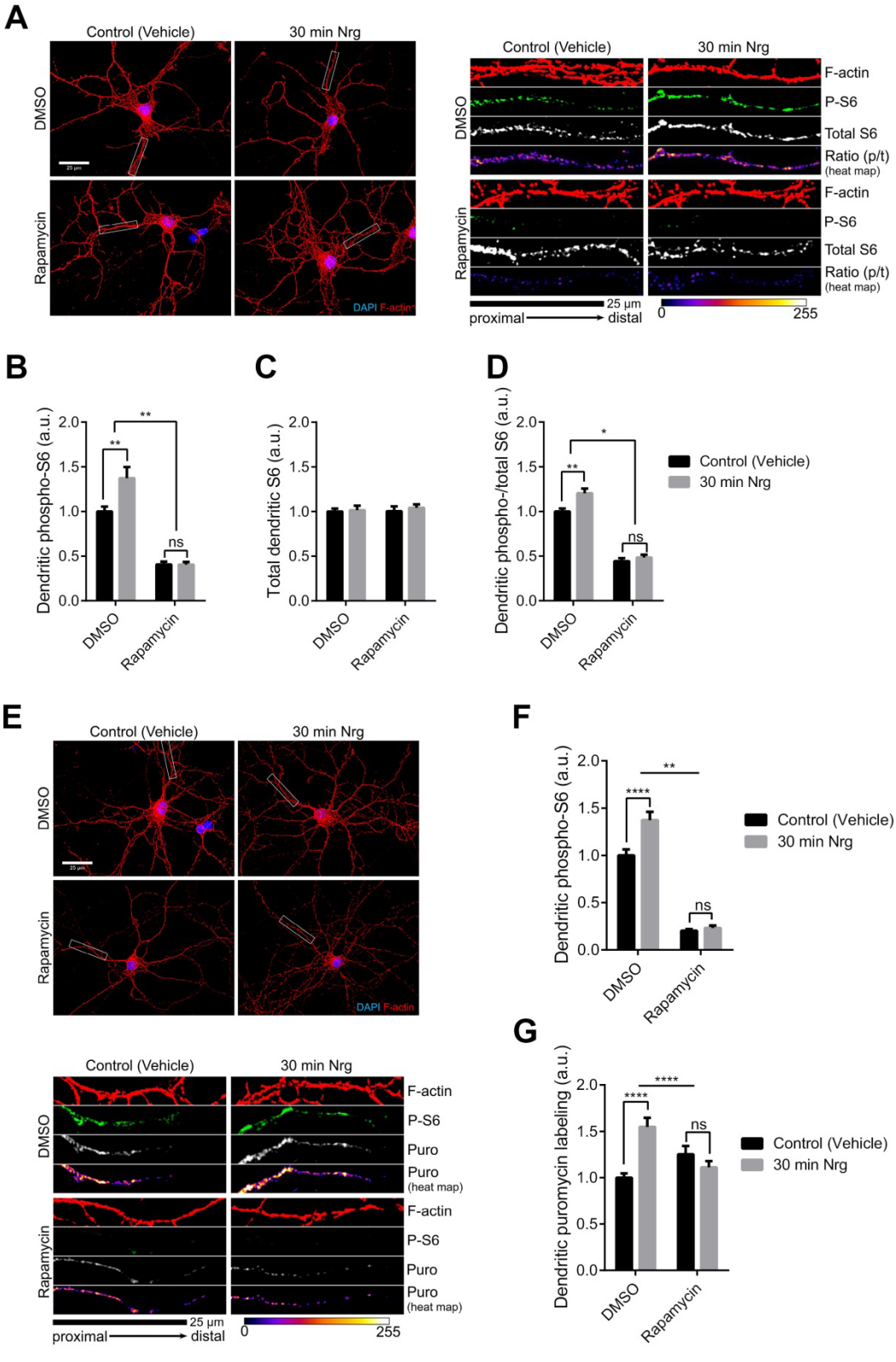
A
Control (Vehicle)
30 min Nrg
DMSO
Rapamycin
DAPI F-actin
F-actin
P-S6
Total S6
Ratio (p/t)
(heat map)
25 µm
proximal
distal
0
255
B
Dendritic phospho-S6 (a.u.)
C
Total dendritic S6 (a.u.)
D
Dendritic phospho-/total S6 (a.u.)
Control (Vehicle)
30 min Nrg
E
Puro
F
Dendritic phospho-S6 (a.u.)
G
Dendritic puromycin labeling (a.u.)

Figure 3.4 Inhibition of mTORC1 blocks Nrg1α-induced increases in dendritic phospho(Ser235/236)-S6 and mRNA translation. (**A-D**) Pre-treatment with the mTORC1-inhibitor rapamycin blocks Nrg1α-induced S6 phosphorylation (Ser235/236) without affecting total S6 levels in the dendrites of DIV6 primary hippocampal neurons. Representative neurons and ROIs are shown in **A**. Dendritic phospho-S6 is shown in **B** (Two-way ANOVA, p(rapamycin)<0.0001, p(Nrg)=0.0099, **p(interactive)=0.0094; Sidak's test, **p<0.01; n=78 cells/condition from 4 biological replicates). Total dendritic S6 is quantified in **C** (Two-way ANOVA, not significant; n=78 cells/condition from 4 biological replicates). The ratio of phospho- to total S6 in dendrites is quantified in **D** (Two-way ANOVA, p(rapamycin)<0.0001, p(Nrg)=0.0017; *p(interactive)=0.0326; Sidak's test, **p<0.01; n=78 cells/condition from 4 biological replicates). (**E-G**) Inhibition of mTORC1 blocks Nrg1α-induced increases in dendritic phospho(Ser235/236) and protein synthesis. DIV6-7 hippocampal neurons were treated with rapamycin 30 min prior to Nrg treatment. Representative neurons and dendritic ROIs are shown in **E**. Quantification of phospho(S235/236)-S6 is shown in **F** (Two-way ANOVA, p(rapamycin)<0.0001, p(Nrg)=0.0005, **p(interactive)=0.0027; Sidak's test, ****p<0.0001; n=60 cells/condition from 3 biological replicates). Quantification of puromycylation is shown in **G** (Two-way ANOVA, p(Nrg)=0.0099, ****p(interactive)<0.0001; Sidak's test, ****p<0.0001; n=60 cells/condition from 3 biological replicates). Data are shown as mean ± SEM. Scale bars are 25 μm.

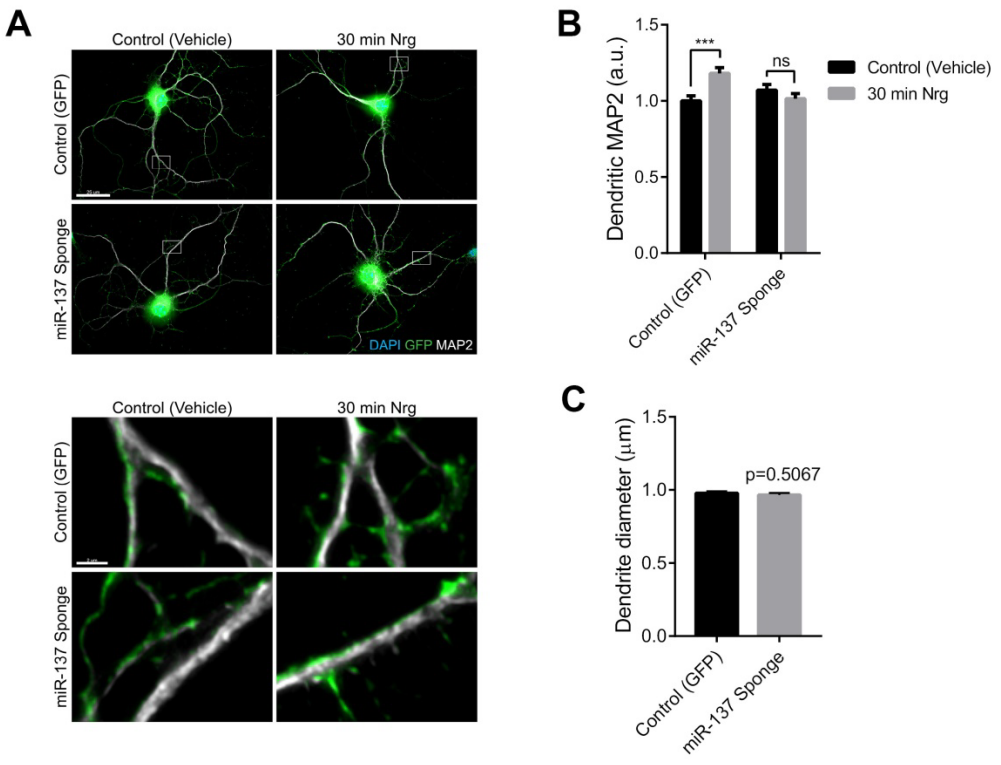

Figure 3.5 Nrg1α increases dendritic MAP2 by a miR-137-dependent mechanism. Inhibition of miR-137 blocks Nrg1α stimulation of dendritic MAP2 protein levels in DIV6 primary hippocampal neurons without affecting dendrite diameter. Representative neurons and dendritic regions of interest are shown in **A**. Quantification of MAP immunofluorescence is shown in **B** (Two-way ANOVA, p(interactive)=0.0010; Sidak's test, ***p<0.001; n=80 cells/condition from 4 biological replicates). Dendritic diameters for Control (GFP) and miR-137 Sponge expressing neurons (only vehicle treatment, no Nrg) are shown in **C** (student's t-test, not significant, n=80 cells/condition from 4 biological replicates). Scale bars are 25 μm for whole cell and 2 μm for dendrite images. Data are shown as mean ± SEM.

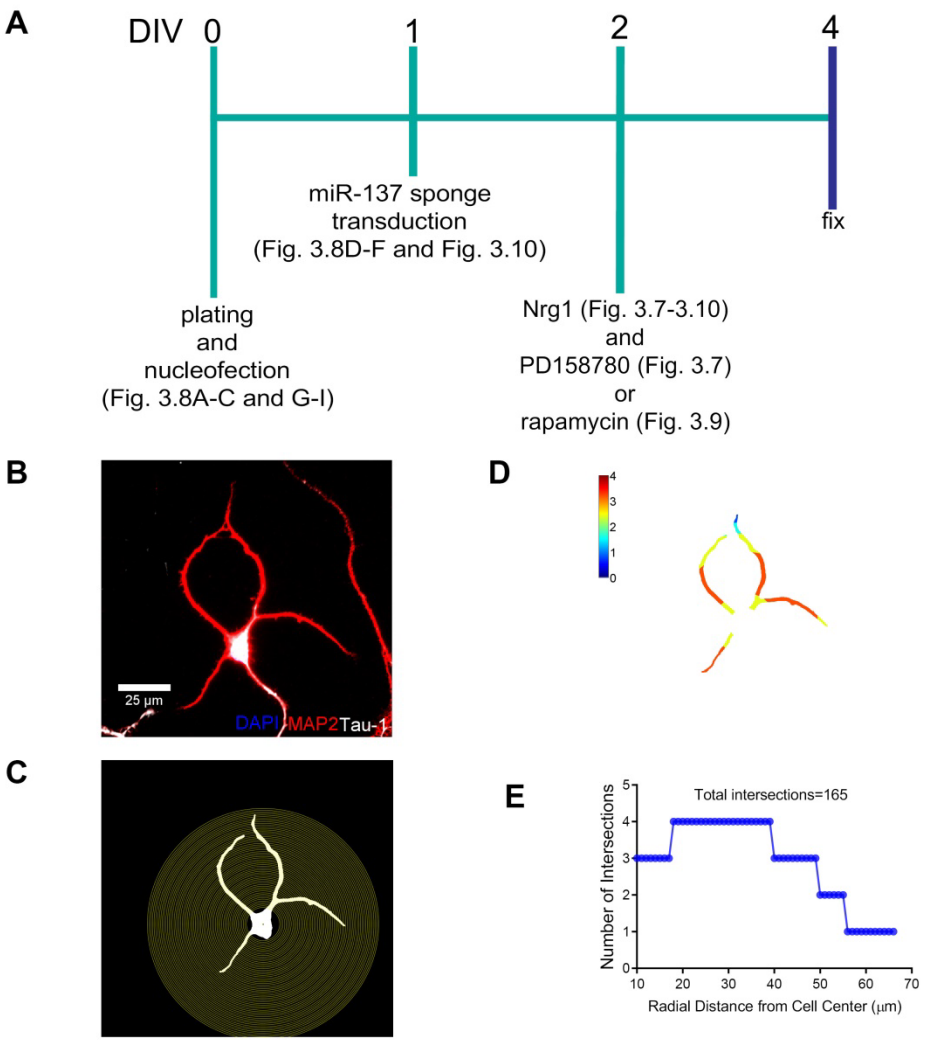

Figure 3.6 Experimental timeline and Sholl methodology for Nrg1α morphology experiments. An experimental timeline for **Figure 3.6-3.10** is shown in **A**. A DIV4 cortical neuron stained for MAP2 and tau-1 is shown in **B** to demonstrate several steps of Sholl analysis. In **C**, the dendritic arbor of the neuron has been traced and concentric circles have been drawn as needed for Sholl analysis. The circles begin 10 µm and continue every 1 µm until the end of the longest dendrite. For every circle, the number of intersections is counted. In **D**, the dendritic arbor is color-coded according to the number of intersections at each radius of the intersecting concentric circles. This data is graphed in **D**.

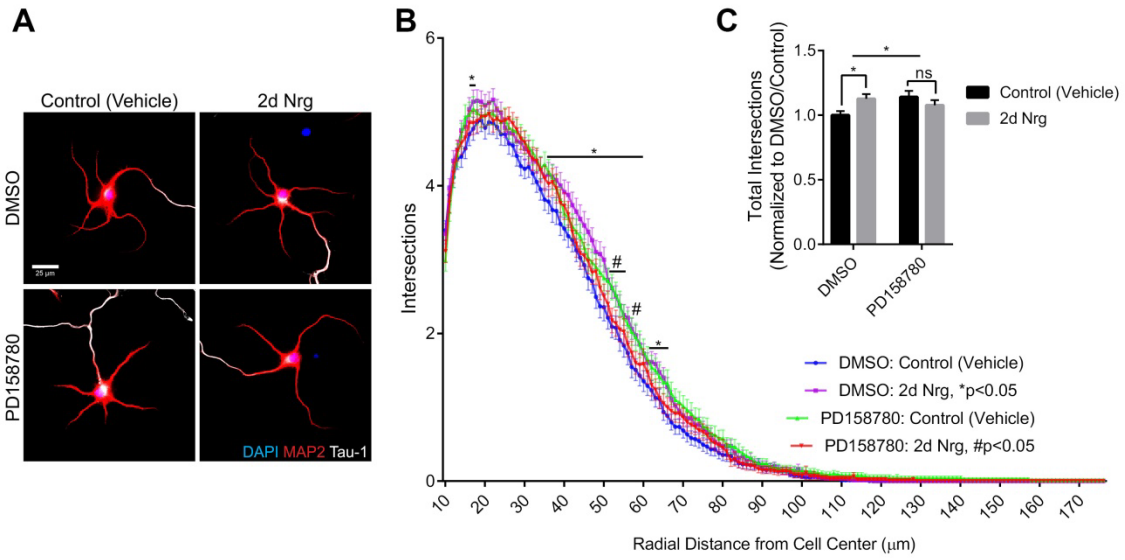

Figure 3.7 Nrg1α increases dendritic outgrowth in DIV4 primary cortical neurons by an ErbB receptor-dependent mechanism. The pan-ErbB receptor inhibitor PD158780 (or DMSO, vehicle control) was added to neurons concurrently with Nrg treatment. Representative neurons are shown in **A**. Scale bars are 25 μm. Quantification of dendritic complexity by Sholl anslysis is shown in **B** (intersections vs distance from cell center, Sidak's test, *p<0.05: DMSO/Nrg vs DMSO/Control (Vehicle), #p<0.05: PD158780/Nrg vs PD158780/Control (Vehicle); n=79-80 cells/condition from 4 biological replicates) and **C**(total number of intersections normalized to DMSO/Control (Vehicle), *p(interactive)=0.0155; Sidak's test, *p<0.05; n=79-80 cells/condition from 4 biological replicates). Data are shown as mean ± SEM.

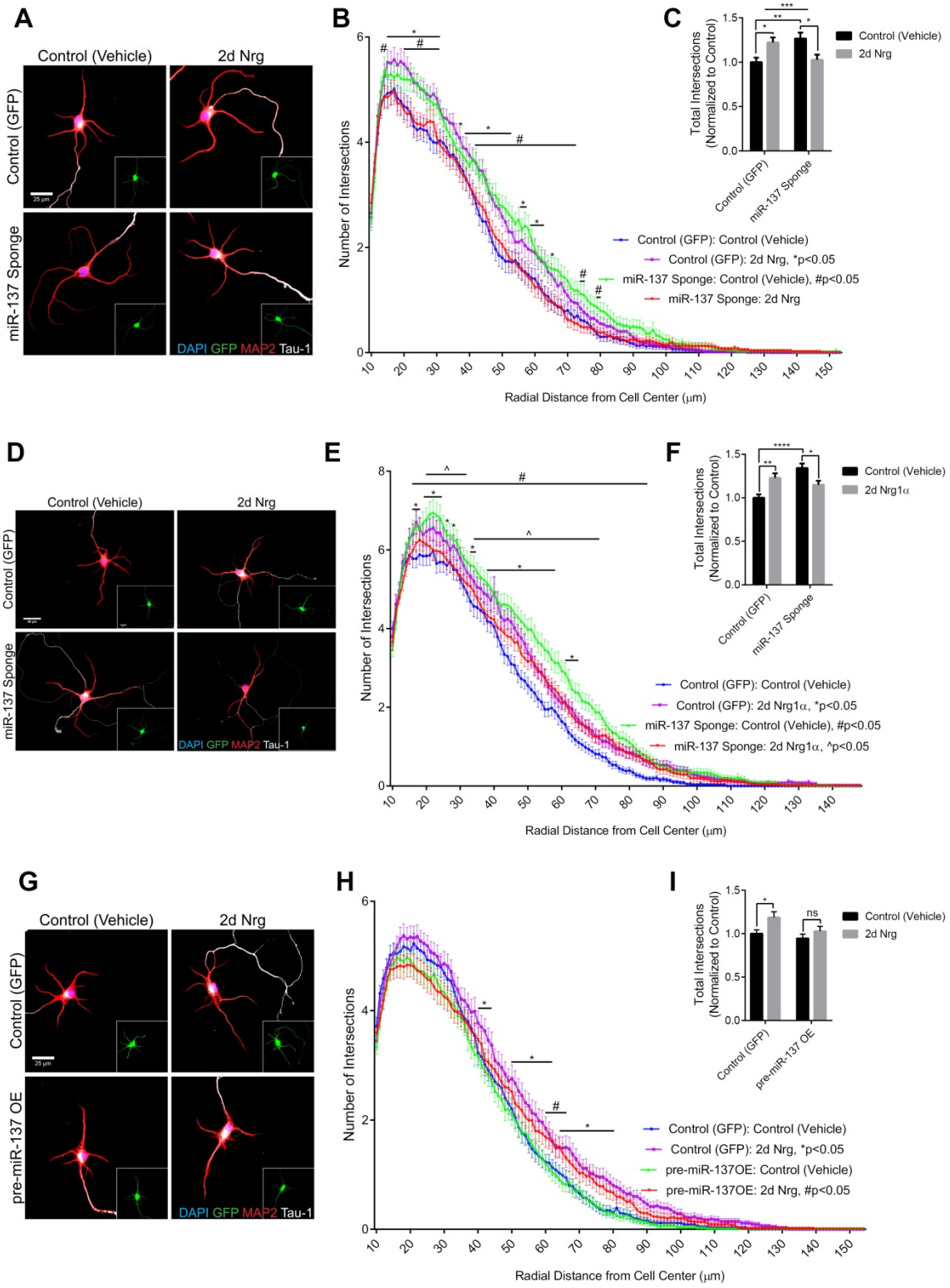
A
Control (Vehicle)
2d Nrg
Control (GFP)
miR-137 Sponge
DAPI GFP MAP2 Tau-1
B
Number of Intersections
Radial Distance from Cell Center (μm)
Control (GFP): Control (Vehicle)
Control (GFP): 2d Nrg, *p<0.05
miR-137 Sponge: Control (Vehicle), #p<0.05
miR-137 Sponge: 2d Nrg
C
Total Intersections (Normalized to Control)
Control (Vehicle)
2d Nrg
Control (GFP)
miR-137 Sponge
D
Control (Vehicle)
2d Nrg
Control (GFP)
miR-137 Sponge
DAPI GFP MAP2 Tau-1
E
Number of Intersections
Radial Distance from Cell Center (μm)
Control (GFP): Control (Vehicle)
Control (GFP): 2d Nrg1α, *p<0.05
miR-137 Sponge: Control (Vehicle), #p<0.05
miR-137 Sponge: 2d Nrg1α, ^p<0.05
F
Total Intersections (Normalized to Control)
Control (Vehicle)
2d Nrg1α
Control (GFP)
miR-137 Sponge
G
Control (Vehicle)
2d Nrg
Control (GFP)
pre-miR-137 OE
DAPI GFP MAP2 Tau-1
H
Number of Intersections
Radial Distance from Cell Center (μm)
Control (GFP): Control (Vehicle)
Control (GFP): 2d Nrg, *p<0.05
pre-miR-137OE: Control (Vehicle)
pre-miR-137OE: 2d Nrg, #p<0.05
I
Total Intersections (Normalized to Control)
Control (Vehicle)
2d Nrg
ns
Control (GFP)
pre-miR-137 OE

Figure 3.8 Nrg1α increases dendritic outgrowth by a miR-137-dependent mechanism. (**A-C**) Nrg1α and inhibition of miR-137 independently increase dendritic outgrowth in DIV4 primary cortical neurons, but inhibition of miR-137 reverses the effects of Nrg1α. Representative neurons are shown in **A**. Dendritic outgrowth was assessed by Sholl analysis as shown in **B** (intersections vs distance from cell center; Sidak's test, *p<0.05: Control/Nrg vs Control/Control (Vehicle), #p<0.05: miR-137 Sponge vs Control (GFP); n=60 cells/condition from 3 biological replicates) and **C** (total number of intersections, normalized to Control (GFP/Vehicle); Two-way ANOVA, ****p(interactive)<0.0001; Sidak's test, *p<0.05, **p<0.01; n=60 cells/condition from 3 biological replicates). **(D-F**) Inhibition of miR-137 reverses Nrg1α-induced dendritic outgrowth in DIV4 primary hippocampal neurons. Representative neurons are shown in **D**. Scale bars are 25 μm. Quantification of dendritic complexity by Sholl analysis is shown in **E** (intersections vs distance from cell center, Sidak's test, *p<0.05: Control/Nrg vs Control/Control (Vehicle), #p<0.05: miR-137 Sponge/Control (Vehicle) vs Control/Control (Vehicle), ^p<0.05: miR-137 Sponge/Nrg vs miR-137 Sponge/Control (Vehicle); n=58 cells/condition from 3 biological replicates) and **F** (total number of intersections normalized to Control/Control (Vehicle), Two-way ANOVA, p(Sponge)=0.0056, ****p(interactive)<0.0001; Sidak's test, *p<0.05, **p<0.01; n=58 cells/condition from 3 biological replicates). (**G-I**) Overexpression of pre-miR-137 disrupts Nrg1α-induced dendritic outgrowth in DIV4 primary cortical neurons. Representative neurons are shown in **G**. Quantification of dendritic complexity by Sholl analysis is shown in **H** (intersections vs distance from cell center; Sidak's test, *p<0.05: Control/Nrg vs Control/Control (Vehicle, #p<0.05: pre-miR-137OE/Nrg vs pre-miR-137OE/Control (Vehicle); n=69-70 cells/condition from 4 biological replicates) and **I** (total number of intersections, normalized to Control (GFP/Vehicle); Two-way ANOVA, p(Nrg)=0.0149; Sidak's test, *p<0.05; n=69-70 cells/condition from 5 biological replicates). Data are shown as mean ± SEM. Scale bars are 25 μm.

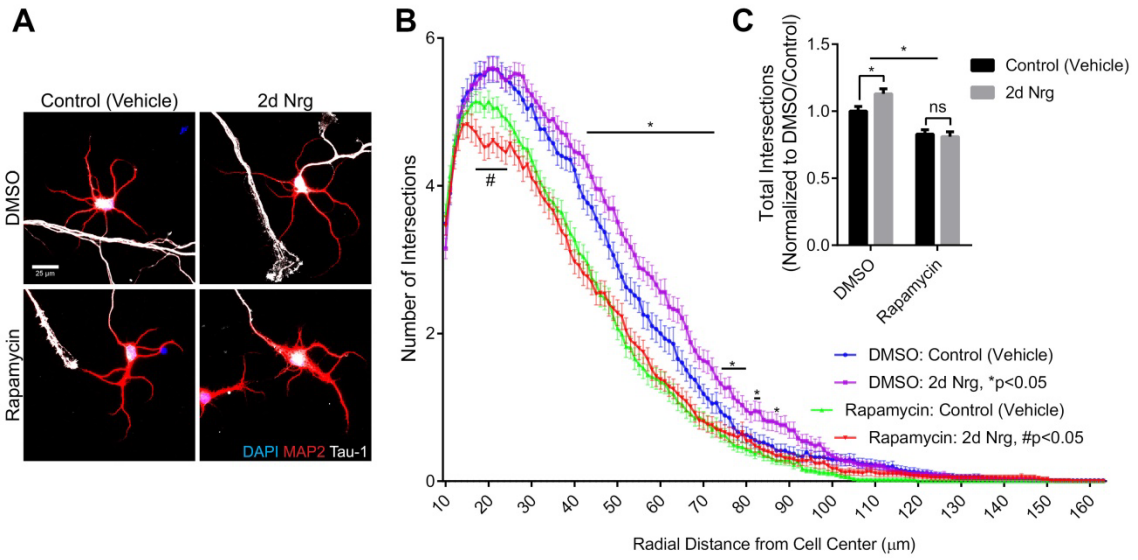

Figure 3.9 Inhibition of mTOR blocks Nrg1α-induced dendritic outgrowth. Co-treatment with rapamycin blocks Nrg1α-induced dendritic outgrowth in DIV4 primary cortical neurons. Representative neurons are shown in **A**. Quantification of dendritic complexity by Sholl analysis is shown in **B** (intersections vs distance from cell center; Sidak's test, *p<0.05: DMSO/Nrg vs DMSO/Control; #p<0.05: Rapamycin vs Control (Vehicle); n=99-100 cells/condition from 5 biological replicates) and **C** (Total number of intersections, normalized to DMSO/Control (Vehicle); Two-way ANOVA, p(rapamycin)<0.0001, p(interactive)=0.0357; Sidak's test, *p<0.05; n=99-100 cells/condition from 5 biological replicates). Data are shown as mean ± SEM. Scale bars are 25 μm.

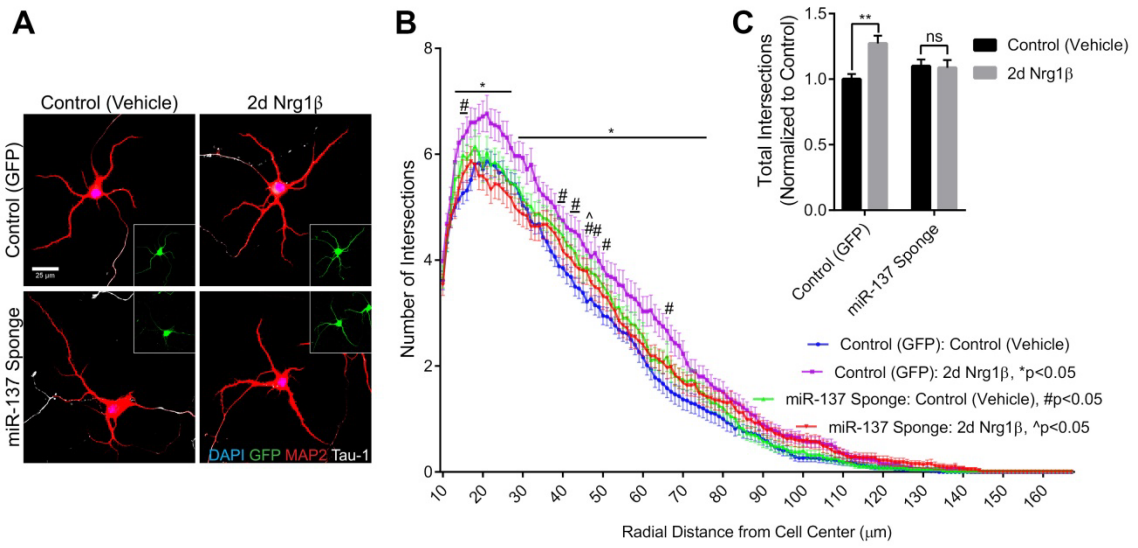

Figure 3.10 Inhibition of miR-137 blocks Nrg1β-induced dendritic outgrowth. Nrg1β does not stimulate dendritic outgrowth in primary hippocampal neurons expressing the miR-137 sponge. Representative neurons are shown in **A**. Scale bars are 25 μm. Quantification of dendritic complexity by Sholl analysis is shown in **B** (intersections vs distance from cell center, Sidak's test, *p<0.05: Control/Nrg vs Control/Control (Vehicle), #p<0.05: miR-137 Sponge/Control (Vehicle) vs Control/Control (Vehicle), ^p<0.05: miR-137 Sponge/Nrg vs Control/Control (Vehicle); n=60 cells/condition from 3 biological replicates) and **C** (total number of intersections normalized to Control/Control (Vehicle), Two-way ANOVA, p(Nrg)=0.0142, p(interactive)=0.0070; Sidak's test, **p<0.01; n=60 cells/condition from 3 biological replicates). Data are shown as mean ± SEM. Scale bars are 25 μm.

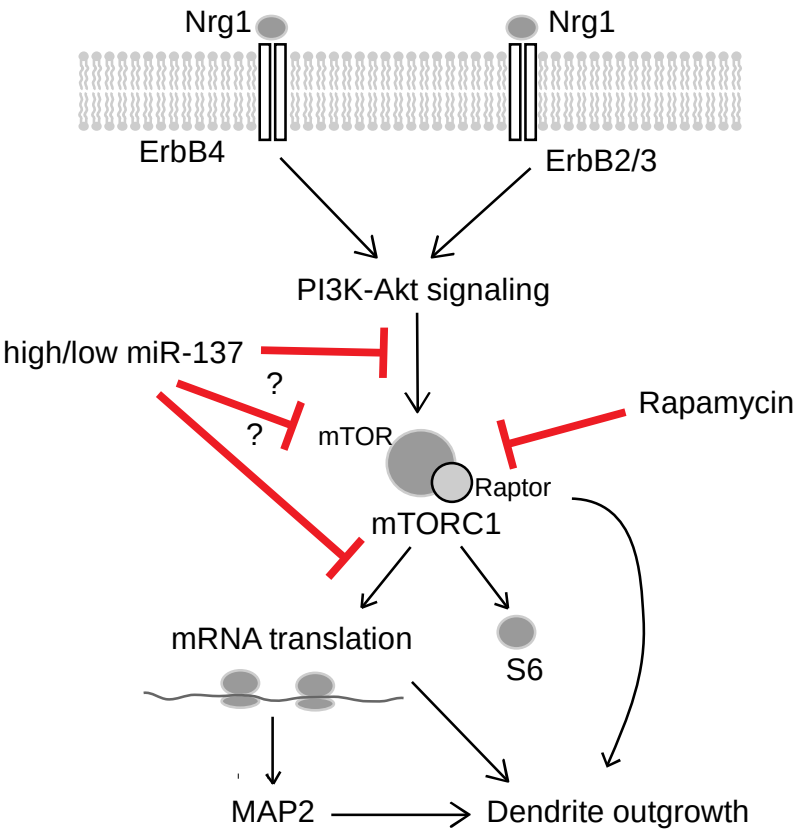

Figure 3.11 Model for miR-137 regulating Nrg1α signal transduction

We propose that in the presence of normal miR-137 levels, Nrg1 binds to ErbB receptors to activate PI3K-Akt signaling, which stimulates mTORC1 and increases mRNA translation, phospho-S6, MAP2, and dendrite outgrowth. Rapamycin blocks responses to Nrg1 by strongly inhibiting mTORC1 activity. When miR-137 activity is inhibited and when miR-137 is overexpressed, Nrg1 can no longer stimulate mRNA translation and other mTORC1-dependent responses. Altered miR-137 may affect mTORC1 signaling through at least three separate mechanisms: 1) by blocking upstream signaling from the PI3K-Akt pathway, 2) by directly interfering with mTORC1 structure or function, or 3) by interfering with downstream targets of mTORC1. Our current data do not provide sufficient information to determine which mechanism contributes to miR-137's effects on Nrg/ErbB signal transduction.

3.6 Supplemental Figures

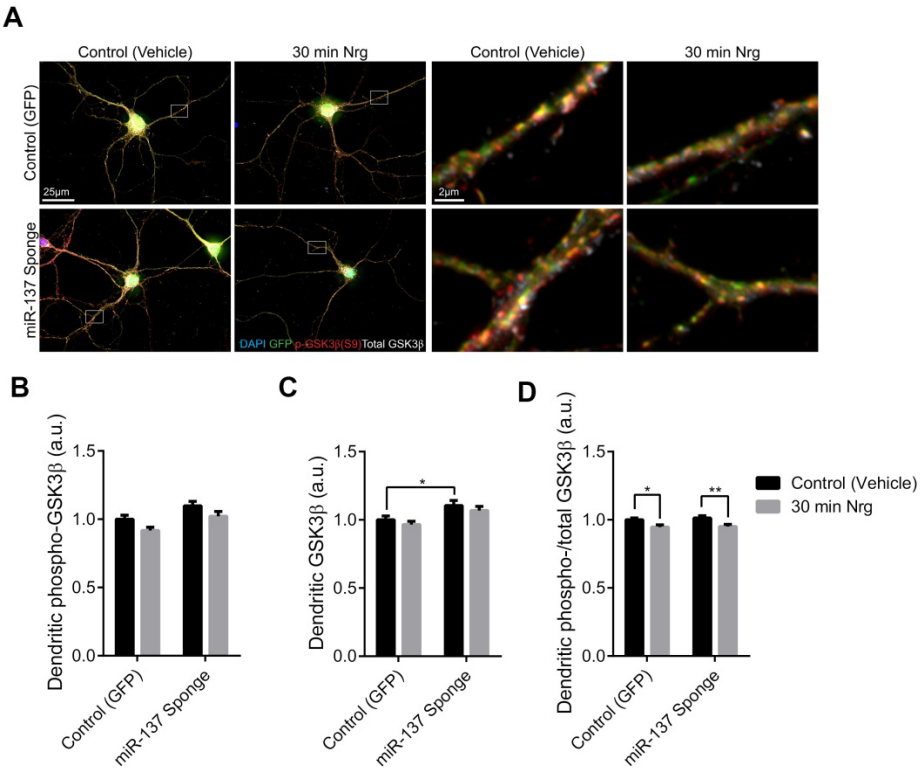

Supplemental Figure 3.1 Inhibition of miR-137 increases dendritic GSK3β without blocking Nrg1α-induced dephosphorylation at Ser9. Dendritic levels of GSK3β were significantly increased in DIV6 primary hippocampal neurons expressing the miR-137 sponge. Nrg1α reduced phosphorylation at Ser9 in neurons, regardless of whether neurons expressed the miR-137 sponge. Representative neurons and dendritic ROIs are shown in **A**. Scale bars are 25 μm for whole cell and 2 μm for dendrite images. Quantification of dendritic phospho(Ser9)-GSK3β is shown in **B** (Two-way ANOVA, p(sponge)= 0.0009, p(Nrg)= 0.0095; Sidak's test, not significant; n=80 cells/condition from 4 biological replicates). Quantification of total dendritic GSK3β is shown in **C** (Two-way ANOVA, p(sponge)= 0.0007; Sidak's test, *p<0.05; n=80 cells/condition from 4 biological replicates). Quantification of the ratio of phospho- to total GSK3β is shown in **C** (Two-way ANOVA, p(Nrg)= 0.0002; Sidak's test, *p<0.05, **p<0.01; n=80 cells/condition from 4 biological replicates). Data are shown as mean ± SEM.

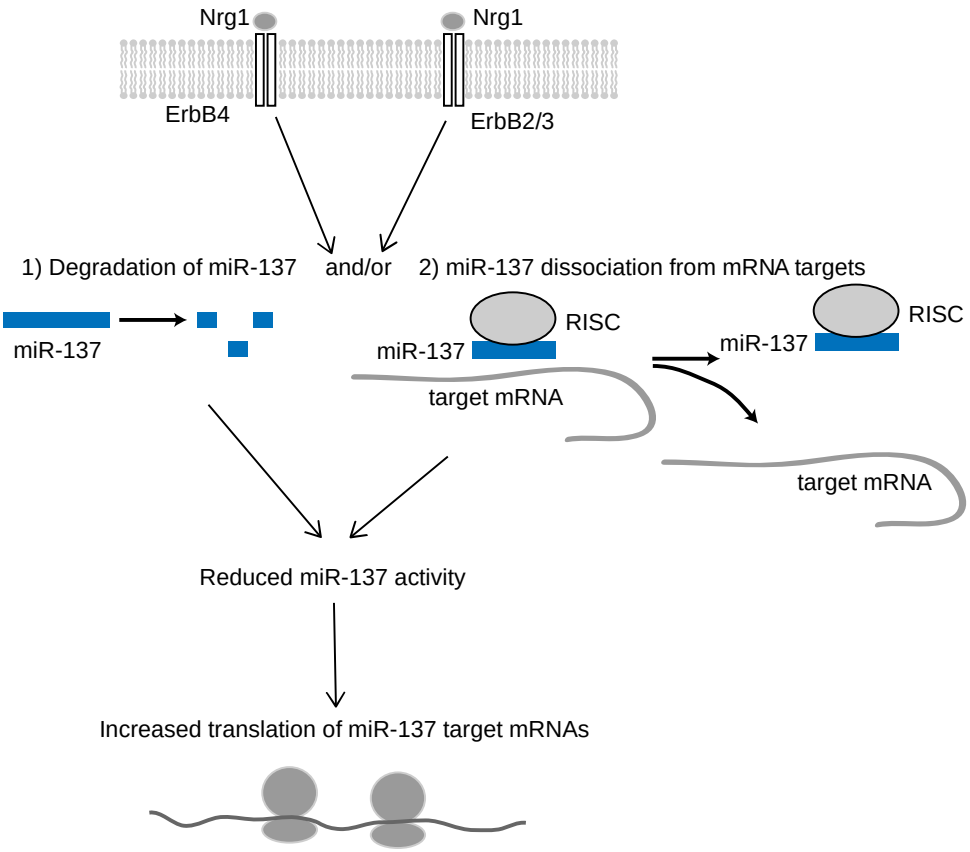

Supplemental Figure 3.2 Model for Nrg1α regulating miR-137 levels or activity

Nrg1α might also stimulate mRNA translation by inhibiting miR-137 activity by either or the mechanisms illustrated above. First, Nrg/ErbB signaling could induce the degradation of miR-137. Second, Nrg/ErbB signaling could cause the dissociation of miR-137 from its target mRNAs. Additional potential mechanisms (not depicted), include the degradation of protein components of RISC, reduced miR-137 synthesis from pre-miR-137, reduced miR-137 transport into dendrites, among others. All would have the outcome of reducing miR-137 mediated inhibition of its targets mRNAs and increased translation of miR-137 target mRNAs.

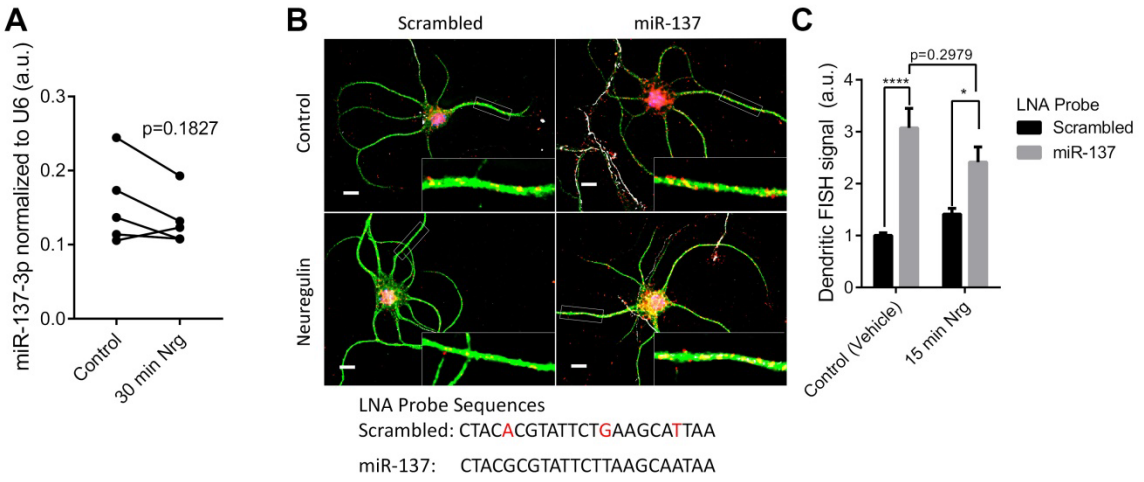

Supplemental Figure 3.3 Acute Nrg1α treatment does not affect total or dendritic levels of miR-137. (**A**) 30 min treatment with Nrg1α does not alter miR-137 levels in DIV6 primary cortical neurons when measured by qRT-PCR (paired t-test). Individual data points and pairings are shown. (**B-C**) Pre- and/or mature miR-137 localizes to the dendrites of DIV6 primary cortical neurons, however dendritic levels are not affected by Nrg1α stimulation. Representative neurons and dendritic ROIs are shown in (**B**). Scale bars are 10 μm. DAPI is shown in blue, MAP2 in green, Tau-1 in gray, and LNA FISH puncta are shown in red. LNA probe sequences are given below. Quantification of dendritic FISH signal intensity is shown in (**C**) (Two-way ANOVA, p(LNA probe)<0.0001; Sidak's test, *p<0.05, **p<0.01; n=32-34 cells/ condition from 3 biological replicates). Data are shown as mean ± SEM.

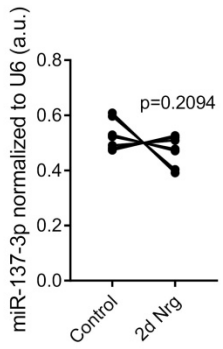

Supplemental Figure 3.4 Two-day Nrg1α treatment does not affect miR-137 levels. DIV2-4 Nrg1α treatment has no effect on miR-137 levels in primary cortical neurons (paired t-test, not significant, n=7). Individual data points and pairings are shown.

Chapter 4

Regulation of AMPA receptor subunits by miR-137 and Nrg1α

Portions of this chapter were adapted from the following manuscript:

Thomas, K.T., Anderson, B.R., Shah, N., Zimmer, S., Hawkins, D., Gu, Q., and Bassell. G.J. (2017). Inhibition of the schizophrenia-associated microRNA miR-137 disrupts Nrg1α neurodevelopmental signal transduction. Cell Rep., Revision Under Review.

4.1 Introduction

In Chapter 3, we demonstrated that Nrg1α stimulates mRNA translation in the dendrites of primary hippocampal neurons by an mTORC1- and miR-137-dependent mechanism. We next sought to identify a specific protein whose synthesis is induced by Nrg1α by a miR-137-dependent mechanism. Previous studies have demonstrated that Nrg1/ErbB4 signaling regulates AMPA receptor surface levels (Cahill et al., 2013), suggesting that Nrg1 may promote the synthesis of AMPA receptor subunits. Single nucleotide polymorphisms within the *GRIA1* gene are also associated with schizophrenia with genome wide significance (Ripke et al., 2014). Therefore, we chose GluA1 as our candidate for studying the interactions between Nrg1α and miR-137 in the regulation of neuronal protein synthesis. During the course of our experiments, miR-137 was demonstrated to target the 3'UTR of human *GRIA1* mRNA (Olde Loohuis et al., 2015), consistent with our findings to be presented below.

4.1.1 AMPAR subunits: general structure and function

AMPA receptors mediate the majority of the brain's fast excitatory neurotransmission. Each receptor consists of four subunits (GluA1-4, encoded by *GRIA1*-*GRIA4*) that may be homo- or heteromeric, with GluA1/2 and GluA2/3 receptors being most common in the hippocampus (Traynelis et al., 2010). Subunits are synthesized and assembled into tetrameric receptors on the endoplasmic reticulum and exported through the secretory pathway to the plasma membrane. Each receptor contains four functional domains: 1) an extracellular amino-terminal domain, 2) an extracellular ligand binding domain, which binds synaptic glutamate, 3) a transmembrane domain, which contains the ion channel pore, and 4) a carboxy-terminal domain, which regulates synaptic delivery of AMPA receptors (Traynelis et al., 2010). When activated by glutamate, the ion channel pore opens, allowing an influx of sodium ions (and calcium ions in AMPA receptors lacking a GluA2 subunit) into the neuron, which promotes depolarization and increases the likelihood that a neuron will fire an action potential.

AMPA receptors are the major determinant of synaptic responsiveness and are critical for the regulation of neuronal activity. Therefore, the number of AMPA receptors present at the surface of a synapse is tightly controlled in all aspects, including the transcription of the *GRIA1-4* genes, the splicing and RNA editing of mRNA transcripts, the trafficking of mRNAs into dendrites, the synthesis of new AMPA receptor subunits, the assembly of subunits into functional tetramers, the trafficking of AMPA receptors through the secretory pathway to the cell surface, the internalization of activated receptors, and receptor degradation (Bredt and Nicoll, 2003). We will focus on the post-transcriptional mechanisms that regulate AMPA receptor subunit synthesis.

Early in neural development, AMPA receptors are diffusely expressed in the dendrites, but as neurons mature, AMPA receptors become increasingly localized to dendritic spines and excitatory post-synaptic sites (Rao et al., 1998). The transcripts or all four AMPA receptor subunits (*Gria1*-4) localize to synapses within the rat hippocampus (Cajigas et al., 2012). Furthermore, *Gria1* and *Gria2* transcripts localize to dendrites in murine primary cortical and hippocampal neurons (Ju et al., 2004) and in the cortex and hippocampus *in vivo* (Muddashetty et al., 2007). In primary neurons, these transcripts undergo local mRNA translation in dendrites, and GluA1 and GluA2 local protein synthesis has been demonstrated in transected dendrites (Ju et al., 2004). GluA1 synthesis in particular is regulated by a number of extracellular signals including BDNF, NMDA receptor activation, and mGluR signaling (Fortin et al., 2012; Ju et al., 2004; Muddashetty et al., 2007). GluA1 synthesis in response to LTP-inducing stimuli may also contribute to the enlargement and maturation of spines in response to increased synaptic activity (Fortin et al., 2010, 2012). GluA1 synthesis also contributes to homeostatic synaptic plasticity. When neuronal activity is blocked, increased GluA1 synthesis leads to increased surface levels of GluA1 homomeric receptors, which are permeable to calcium as well as sodium, and leads to a compensatory increase in synaptic strength (Sutton et al., 2006).

GluA1 in particular also plays a critical role in driving neuronal maturation. Neuronal maturation refers to all of the processes by which newly formed neurons extend axons and

dendrites, undergo synaptogenesis, and join together to form the neural circuitry. Reductions in GluA1 reduce dendritic outgrowth both in primary neurons and in newly formed neurons *in vivo*, whereas overexpression of GluA1 increases dendritic outgrowth (Guo et al., 2015).

In summary, GluA1 synthesis plays a critical role in the regulation of synaptic plasticity and neural development. Unsurprisingly, dysregulation of GluA1 has been tied to several neurodevelopmental disorders.

4.1.2 AMPAR subunits in neurodevelopmental disease

Dysregulation of GluA1 may contribute to a number of neurological disorders, including depression, epilepsy, Alzheimer's disease, and several neurodevelopmental disorders (Zhang and Abdullah, 2013). Here, we will focus on the relationship between GluA1 and the following neurodevelopmental disorders: Fragile X Syndrome, Rett syndrome, and schizophrenia.

Dysregulated AMPAR activity may also contribute to dysregulated neuronal activity in Fragile X Syndrome (FXS), a neurodevelopmental disorder characterized by intellectual disability and, in many patients, seizures and/or autism. FXS is caused by the loss of the mRNA binding protein FMRP (fragile X mental retardation protein) which regulates stimulus-induced mRNA translation in dendrites and dendritic spines. Interestingly, mGluR-induced translation of both *Gria1* and *Gria2* mRNAs is dysregulated in primary neurons derived from mouse models of FXS (Muddashetty et al., 2007). FMRP has also been shown to enhance neuronal maturation by increasing the delivery of GluA1-containing AMPA receptors to the cell membrane (Guo et al., 2015). The translation of *Dlg4* mRNA, which encodes PSD-95, is also dysregulated in mouse models of FXS (Muddashetty et al., 2007, 2011). PSD-95 localizes to the postsynaptic density in excitatory synapses, where it stabilizes AMPA receptors at the cell surface and regulates AMPA receptor endocytosis. Whether dysregulated AMPA receptor subunit synthesis or localization contribute to cognitive deficits, epilepsy, or other features of FXS remains to be seen.

Rett syndrome, like FXS, is a monogenic neurodevelopmental disorder associated with intellectual disability and autism. Rett syndrome is caused by the loss of MeCP2, a transcriptional regulator that also binds mRNAs and regulates their processing and, perhaps, their transport. A recent study found that synaptic GluA1 localization and AMPA receptor currents were enhanced in a mouse model of Rett syndrome (Li et al., 2016). However, neurons from mice lacking MeCP2 failed to increase synaptic GluA1 trafficking when neuronal activity was increased and failed to express LTP (Li et al., 2016). These data suggest that dysregulation of GluA1 may contribute to cognitive deficits and other neurological phenotypes in Rett syndrome.

Schizophrenia is also characterized by deficits in glutamatergic signaling. Most of these deficits have been attributed to dysregulation of NMDA receptors (Coyle, 2006). However, recent studies suggest that AMPA receptors may contribute to schizophrenia as well. Single nucleotide polymorphisms in *GRIA1* are associated with schizophrenia with genome-wide significance (Ripke et al., 2014). *Gria1* mRNA levels may also be elevated in pyramidal neurons within the dorsolateral prefrontal cortex of schizophrenia patients (O'Connor and Hemby, 2007). *Gria1* knockout mice also show deficits in short term habituation, while schizophrenia patients show deficits in habituation of the startle reflex (Barkus et al., 2014). The molecular mechanism by which GluA1 contributes to schizophrenia is unknown, however.

Interestingly, Rett syndrome and FXS patients often display both intellectual disability and autism, and patients with microdeletions encompassing *MIR137* also display mild to moderate intellectual disability and, in some patients, autism (Willemsen et al., 2011). While Nrg/ErbB signaling has not been linked to autism, Nrg/ErbB signaling, miR-137, and GluA1 have all been linked to schizophrenia through genomic studies of schizophrenia patients (Mei and Nave, 2014; Ripke et al., 2011, 2013, 2014). We hypothesized that miR-137, GluA1, and Nrg/ErbB signaling might contribute to neurodevelopmental disorders, particularly schizophrenia, through a common molecular mechanism.

4.1.3 Regulation of GluA1 by miR-137

A previous study demonstrated that miR-137 directly targets the 3'UTR of human *GRIA1* mRNA at the site indicated in **Fig. 4.1** (Olde Loohuis et al., 2015). Furthermore, miR-137 regulates total GluA1 and GluA2 protein levels as well as GluA1 surface levels at synapses in rat primary hippocampal neurons. miR-137 also inhibits the unsilencing of synapses during neuronal maturation, presumably by inhibiting GluA1 synthesis. mGluR5 activity also leads to increased miR-137 synthesis from pre-miR-137, which may then contribute to reduced surface AMPA receptor levels (a hallmark of long term depression, LTD) by inhibiting GluA1 synthesis. miR-137 also inhibits dendritic outgrowth (Smrt et al., 2010), whereas GluA1 stimulates dendritic outgrowth (Guo et al., 2015). This suggests that GluA1 may at least partly underlie miR-137's effects on neuronal maturation. mTORC1 activity also stimulates GluA1 synthesis *in vivo* (Slipczuk et al., 2009). Our data in Chapter 2 suggest that miR-137 driven changes in mTORC1 activity might provide an additional mechanism by which miR-137 might regulate GluA1 synthesis.

4.1.4 Regulation of AMPAR subunits by Nrg1/ErbB signaling

Nrg1 signaling regulates AMPAR stability and surface expression. For example, treating DIV28 primary cortical neurons for 3 days with 5 nm Nrg1β significantly increases surface GluA1 without affecting total GluA1 protein levels (Cahill et al., 2013). The same study found that 2 day treatment with Nrg1β also significantly increased GluA1 content in spines, as well as the number and size of dendritic spines suggesting increased neuronal maturation, consistent with increased GluA1 expression. Peripheral administration of Nrg1 also increases synaptic GluA1 *in vivo* (Abe et al., 2011).

ErbB4 expression at the cell surface also stabilizes AMPA receptors at the cell surface and promotes the enlargement of dendritic spines (Li et al., 2007). ErbB4 also directly interacts with PSD-95 (Garcia et al., 2000). Together, these data suggest that Nrg1 signaling might

increase AMPA receptors at the cell surface and in spines by enhancing ErbB4-PSD95 interactions.

Alternatively, Nrg1 signaling has previously been shown to stimulate the synthesis of mGluR1 and of Kv4.2 (Ledonne et al., 2014; Yao et al., 2013), both of which are transmembrane proteins that regulate neuronal activity. Nrg1 signaling also stimulates PI3K-Akt-mTOR signaling (Mei and Nave, 2014), which has previously been shown to stimulate GluA1 synthesis. We, therefore, hypothesized that Nrg1 signaling would promote GluA1 synthesis in neurons.

4.1.5 Chapter 4 hypothesis and objectives

In Chapter 3, we demonstrated that miR-137 regulates PI3K-Akt-mTOR-dependent responses to Nrg1 signaling, including Nrg1-induced dendritic protein synthesis. We hypothesize that Nrg1 stimulates GluA1 synthesis in dendrites by a miR-137-dependent mechanism as well. The experiments that follow were undertaken with the following objectives: 1) validate mouse *Gria1* mRNA as a miR-137 target, 2) determine if Nrg1α stimulates GluA1 synthesis, 3) determine whether miR-137 regulates Nrg1α-induced Glua1 synthesis, 4) determine whether Nrg1α regulates miR-137 binding to *Gria1* mRNA.

4.2 Results

4.2.1 miR-137 targets the mouse Gria1-3'UTR

A previous study indicated that miR-137 directly targets *Gria1* mRNA in rat neurons. Given that the miR-137 target site is well conserved in mammals, we hypothesized that miR-137 would similarly target *Gria1* mRNA in mouse neurons. To test this hypothesis, we cloned the 3’UTR of mouse *Gria1* downstream of firefly luciferase and used luciferase assays to measure changes in reporter activity in response to miR-137 manipulation. We found that overexpressing miR-137 repressed *Gria1*-3’UTR reporter activity without affecting an *Actb*-3’UTR reporter in

Neuro2A cells (**Fig. 4.1A**). Conversely, a miR-137-specific locked nucleic acid (LNA) inhibitor increased *Gria1*-3'UTR reporter activity, also without affecting the *Actb*-3'UTR (**Fig. 4.1B**). Mutation of the miR-137 binding site ablated the effects of miR-137 inhibition (**Fig. 4.1C-D**). These results are consistent with the hypothesis that miR-137 regulates *Gria1* mRNA translation in a 3'UTR site- and sequence-specific manner.

To determine whether miR-137 directly interacts with *Gria1* mRNA, we measured miRNA pulldown with a biotinylated mouse *Gria1* mRNA sequence and streptavidin coated beads *in vitro*. We found that miR-137, miR-92a-3p, and miR-128 all associated with *Gria1* mRNA (**Fig. 4.2**) Mutation of the miR-137 binding site ablated most miR-137 association with *Gria1* without affecting miR-128, which is predicted to target a more distal site within the 3'UTR (**Fig. 4.2**). Mutation of the miR-137 binding site also slightly reduced association of miR-92a-3p, which is predicted to target an overlapping site.

We then examined whether miR-137 would regulate GluA1 protein levels in primary cortical neurons. We first nucleofected primary cortical neurons prior to plating with a plasmid to overexpress pre-miR-137 and lysed the neurons on DIV6. We found that overexpression of pre-miR-137 significantly reduced GluA1 and GluA2 protein levels, without affecting β-actin (**Fig. 4.3A-C**). We next transfected primary cortical neurons with a miR-137-specific LNA inhibitor on DIV12, lysed cells on DIV15 then used western blots to measure changes in GluA1 and GluA2 levels. We found that the miR-137 inhibition significantly increased both GluA1 and GluA2 levels in primary cortical neurons (**Fig. 4.3D-E**). GluA2 is not predicted to be a miR-137 target (TargetScan v6.2), however GluA2 has also previously been shown to be regulated by miR-137 activity (Olde Loohuis et al., 2015). Taken together, these results are consistent with our model that miR-137 directly targets *Gria1* mRNA and regulates its translation in mouse primary neurons.

4.2.2 Nrg1α increases total GluA1/2 protein levels in neurons

Our data in Chapter 3 demonstrated that Nrg1α increases total protein synthesis in dendrites. Nrg1 signaling increases surface AMPA receptor levels (Cahill et al., 2013), but whether increased synthesis of subunits, e.g. GluA1, contributes to this increase is unknown. We treated DIV6 cortical neurons 30 min with Nrg1α and lysed the neurons for western blots and qRT-PCR analysis of AMPAR subunit protein and mRNA levels, respectively. Nrg1α increased total GluA1 and GluA2 protein levels (**Fig. 4.4A**) without affecting mRNA levels (**Fig. 4.4B**), consistent with our hypothesis that Nrg1α increases AMPAR subunit synthesis.

4.2.3 Nrg1α increases GluA1/2 protein by a miR-137-dependent mechanism

In Chapter 3, we demonstrated that inhibition of miR-137 blocked Nrg1α-induced total protein synthesis in dendrites. We hypothesized that inhibition of miR-137 would block Nrg1α-induced changes in AMPAR levels and/or synthesis as well. As in Chapter 3, we transduced DIV2 primary hippocampal neurons with lentivirus containing a miR-137 sponge and treated the neurons on DIV6 or DIV7 with Nrg1α for 30 min. Using qIF, we found that Nrg1α increased dendritic GluA1 and GluA2 protein, and this response was blocked by the miR-137 sponge (**Fig. 4.5**).

To determine whether the increase in GluA1 was due to new protein synthesis, we used puromycylation followed by proximity ligation assay to detect endogenous, newly synthesized GluA1 following Nrg1α treatment as depicted in **Fig. 4.6A**. Nrg1α significantly increased dendritic GluA1 synthesis, but the miR-137 sponge ablated Nrg1α-induced GluA1 synthesis (**Fig. 4.6B, D**). The PLA signal was translation- and puromycin-dependent (**Fig. 4.6C, E**). Together, these results demonstrate that Nrg1α regulates AMPAR subunits by a miR-137-dependent mechanism.

Surprisingly, we found that the miR-137 sponge did not increase dendritic GluA1 or GluA2 in the dendrites of primary neurons when measured by qIF (data not shown) and did not

increase dendritic GluA1 protein synthesis under basal conditions (**Fig. 4.6D**), as would be expected for GluA1, a validated miR-137 target. The conflict between the imaging and biochemistry data may indicate that miR-137 is capable of regulating GluA1 protein synthesis, but that the effects of the miR-137 sponge on mTOR signaling are dominant in regulating GluA1 synthesis at this developmental timepoint (DIV6-7).

Our previous data (Chapters 2 and 3) suggest that inhibition of miR-137 blocks Nrg1α-induced GluA1 synthesis by disrupting PI3K-Akt-mTOR signal transduction. An additional mechanism by which Nrg1α might induce GluA1 synthesis by a miR-137-dependent mechanism is for Nrg1α to relieve *Gria1* mRNA of translational repression by miR-137. Nrg1α might cause the degradation of miR-137, for example, or cause miR-137-RISC to dissociate from *Gria1* mRNA. The miR-137 binding site might also become inaccessible when PI3K-Akt-mTOR signaling is stimulated. To test this hypothesis, we treated neurons with Nrg1α, lysed them, and added biotinylated *Gria1* mRNA to the Nrg-stimulated lysate. We then allowed endogenous miR-137 from the Nrg-stimulated lysate to assemble on the biotinylated mRNA, precipitated the biotinylated mRNA and associated miRNAs with streptavidin coated beads, and measured the precipitated RNAs by qRT-PCR. We found that Nrg1α had no effect on miR-137's ability to assemble on *Gria1* mRNA in vitro, demonstrating that the miR-137 binding site was accessible (**Supp. Fig. 4.1**).

4.3 Discussion

To date, hundreds of loci have been associated with schizophrenia; many of which regulate neuronal development and synaptic function. *MIR137, GRIA1,* and *NRG1* have previously been associated with schizophrenia through independent genetic studies. Whether their gene products interact at the molecular level in a common schizophrenia-associated pathway, however, was unknown. We tested the hypothesis that miR-137 regulates Nrg1α-induced

AMPAR synthesis. We found that miR-137 directly targets the *Gria1*-3'UTR and regulates GluA1 and GluA2 protein levels in mouse neurons. Nrg1α also increases dendritic and total GluA1 and GluA2 protein levels and stimulate dendritic GluA1 protein synthesis by a miR-137-dependent mechanism. Our data presented in Chapters 2 and 3 demonstrate that miR-137 regulates the PI3K-Akt-mTOR pathway and mTORC1-dependent responses to Nrg1α, including Nrg1α-induced protein synthesis. We propose the following model (**Fig. 4.7**). When miR-137 is present at normal levels, Nrg1α stimulates the mTORC1-dependent translation of multiple mRNAs, including *Gria1* mRNA. Nrg1α stimulates the translation of both miR-137 target and miR-137 non-target mRNAs. When miR-137 is inhibited, however, Nrg1α cannot stimulate PI3K-Akt-mTOR signaling and Nrg1α-induced GluA1 synthesis is impeded.

4.3.1 miR-137 regulates the AMPAR subunits GluA1 and GluA2

A previous study demonstrated that miR-137 targeted *Gria1* mRNA in primary rat hippocampal neurons (Olde Loohuis et al., 2015). For the present study, we further validated *Gria1* mRNA as a miR-137 target in primary mouse cortical neurons, confirming that this interaction is intact in multiple species (**Fig. 4.1-4.2**). Because GluA1 upregulation is associated with the formation of calcium-permeable AMPA receptors, we were interested to find that miR-137 also regulates GluA2 protein levels (**Fig. 4.3**), indicating miR-137 may regulate AMPAR levels rather than subunit composition or calcium permeability. Whether miR-137 directly targets *Gria2* mRNA remains to be determined.

We predicted that inhibition of miR-137 would increase basal GluA1 synthesis in the dendrites of primary hippocampal neurons. However, we found that GluA1 synthesis was slightly reduced (**Fig. 4.4**). The conflict between our GluA1 synthesis data and our western blot data suggests that miR-137 may regulate GluA1 synthesis by multiple mechanisms: not only through direct miR-137-*Gria1* mRNA interactions, but also as a downstream consequence of miR-137's regulation of other mRNA targets. In Chapter 2, we demonstrated that miR-137 targets multiple

proteins within the PI3K-Akt-mTOR pathway. mTORC1 plays a well-documented role in the regulation of GluA1 synthesis. We propose that miR-137's effects on PI3K-Akt-mTOR signaling may be more important for the regulation of GluA1 protein synthesis, even under basal signaling conditions.

Interestingly, miR-137 is also predicted to target *Gria4*, which encodes AMPAR subunit GluA4, as well as an NMDA receptor subunit (GluN2A, encoded by *Grin2a* mRNA) and metabotropic glutamate receptors (mGluR5 and mGluR2, encoded by *Grm5* and *Grm2* mRNA, respectively). Of these, only *Grin2a* and *Gria1* are validated mRNA targets (Olde Loohuis et al., 2015; Zhao et al., 2013). The glutamate hypothesis of schizophrenia posits that glutamatergic signaling is dysregulated in the brains of schizophrenia patients. Targeting of multiple glutamatergic receptor subunits by miR-137 provides a mechanism by which dysregulated miR-137 might contribute to abnormal glutamatergic signaling that warrants further examination.

4.3.2 Nrg1α, miR-137, and GluA1 regulate dendritic outgrowth and synaptic plasticity: a shared mechanism?

Inhibition of miR-137 and overexpression of GluA1 have both been demonstrated to increases dendritic outgrowth by independent studies (Guo et al., 2015; Smrt et al., 2010). Whether miR-137's interactions with *Gria1* drive miR-137's effects on dendritic outgrowth, remains to be determined. Similarly, Nrg1α signaling increases dendritic outgrowth and GluA1 synthesis, suggesting that enhanced GluA1 synthesis may contribute to Nrg1α-induced dendritic outgrowth. Inhibition of miR-137 blocks Nrg1α-induced dendritic outgrowth (Chapter 3) as well as Nrg1α-induced GluA1 synthesis. Nrg1α-induced GluA1 synthesis may also underlie Nrg-induced dendritic outgrowth as well as miR-137's ability to regulate Nrg-induced dendritic outgrowth.

Our data have interesting implications for the regulation of synaptic plasticity by miR-137 and Nrg1. Nrg1β has previously been shown to enhance GluA1 surface levels (Abe et al.,

2011; Cahill et al., 2013), but whether this response is dependent on new protein synthesis has not been examined. The Nrg1 receptor ErbB4 directly interacts with postsynaptic density protein 95 (PSD-95), a postsynaptic scaffolding protein that is essential for the function of AMPARs at the surface of dendritic spines (Garcia et al., 2000). Nrg1 might stabilize AMPAR subunits, including GluA1 and GluA2, by an ErbB4-PSD95 interaction-dependent mechanism that is independent of new protein synthesis. Nrg1 might also regulate GluA1 through the regulation of mGluR synthesis. Nrg1 has previously been shown to stimulate mGluR synthesis (Ledonne et al., 2014). mGluR signaling stimulates new GluA1 synthesis (Ju et al., 2004; Muddashetty et al., 2007). The experiments in the present chapter using Nrg1α were conducted using DIV6-7 primary neurons, which are undergoing synaptogenesis but lack mature dendritic spines. Given the strong link between dysregulated synaptic plasticity and neurodevelopmental disorders, particularly schizophrenia, future studies may examine whether Nrg1α also induces GluA1 synthesis by a miR-137 dependent mechanism in more mature neurons and whether this contributes to the regulation of synaptic plasticity by Nrg/ErbB signaling.

4.3.3 Implications for neurodevelopmental disorders

The link between miR-137 and schizophrenia remains unclear. Several *MIR137* variants have been associated with schizophrenia, but how they affect miR-137 activity appears to vary. Several patient SNPs increase miR-137 production (Siegert et al., 2015). Other schizophrenia-associated *MIR137* variants appear to reduce miR-137 levels, however (Strazisar et al., 2014). Interestingly, *MIR137* variants have also been associated with autism, bipolar disorder, and intellectual disability (Duan et al., 2014; Smoller, 2013; Willemsen et al., 2011). Changes in Nrg/ErbB signaling and GluA1 levels have similarly been associated with multiple neurodevelopmental disorders (Mei and Nave, 2014).

Our results link the schizophrenia associated gene products Nrg1α, miR-137, and GluA1 together in a common translational control pathway. Our results suggest that changes in miR-137

activity or in Nrg/ErbB signaling may have similar consequences for neuronal development and consequently may contribute to the pathogenesis of schizophrenia and other neurodevelopmental disorders through a shared molecular mechanism.

4.4 Materials and Methods

Primary hippocampal and cortical neuron cultures

Primary neurons were cultured as described in Chapers 2 and 3.

Drug treatments

Nrg1α and anisomysyn treatments were performed as described in Chapter 3.

Puromycylation and proximity ligation assay

Puromycylation was performed as described in Chapter 3.

Plasmids and lentiviruses

Neurons were nucleofected with the pre-miR-137 overexpression plasmid or control (FUGW) plasmid as described in Chapter 2. Neurons were transduced with miR-137 sponge containing virus on DIV2 as described on Chapter 3. Neurons were transfected with miR-137-specific or negative control LNA inhibitors as described in Chapter 2.

The mouse *Kcnd2*-3'UTR sequence was PCR amplified from pCMV-Kv4.2 (Origene, MC206092), and NheI restriction sites were added using the following primers: 5' ATGGCTAGCGACAATTGCCGCAGGTCT 3' and 5' ATGGCTAGCTCCTGTTCAAGCATGCACA 3' (reverse). The 3'UTR was then cloned into pGL3-promoter using the XbaI restriction site, as the XbaI and Nhe1 enzymes create overhangs

compatible for ligation. The *Actb*-3'UTR firefly luciferase plasmid was previously described (Muddashetty et al., 2011).

RNA isolation, cDNA synthesis, and qPCR

RNA isolation was performed as described in Chapter 2. cDNA synthesis for miRNAs and qPCR for miRNAs were also performed as described in Chapter 2. cDNA synthesis for mRNAs was performed using the qScript cDNA SuperMix kit (Quanta, #95048-025). Quantitative PCR was then performed using LightCycler SYBR Green I reagent (Roche) in a LightCycler real-time PCR system using the following primers: *Gria1* (5' GACTGTGAATCAGAACGCCTCAA 3', 5' AAGTCAATGTCCATGAAGCCCAG 3'), *Gria2* (5' GCGACCTGACCTCAAAGGAG 3', 5' TGATAGCAGTCACCTGCCAC 3'), and *Actb* (5' GGCTTCGCGGGCGACGA 3', 5' GCCACACGCAGCTCATTGTAG 3'). Relative RNA levels were assessed using primer-specific standard curves and normalization to an internal control. Gria1 and Gria2 mRNAs were normalized to Actb mRNA.

Luciferase assays

Luciferase assays were performed as described in Chapter 2, with the following modifications. Neuro2A cells were transfected with 1.6 μg/well *Kcnd2*-3'UTR firefly luciferase reporter plasmid, 1.6 μg/well *Gria1*-3'UTR firefly luciferase reporter plasmid, or 1.11 μg/well *Actb*-3'UTR firefly luciferase reporter plasmid. All wells also received 0.05 μg/well *Renilla* luciferase plasmid. Firefly luciferase activity was normalized to *Renilla* luciferase activity for all wells.

Western blots

Western blots were performed as described in Chapter 2.

Quantitative immunofluorescence

Quantitative immunofluorescence was performed as described in Chapter 3.

Puromycylation and Proximity Ligation Assay

Puromycylation was performed as described by Graber et al., 2013 with the following modifications: puromycin was added to neurons at a concentration of 4.17 μg/mL and detected with mouse anti-puromycin antibody diluted 1:250. Proximity ligation assays were performed as described by tom Dieck et al., 2015 using the Duolink In Situ Detection Reagents Red kit (Sigma-Aldrich, DUO92008).

Antibodies

The following primary antibodies and dilutions were used for Western blot experiments: mouse monoclonal anti-β-actin (Abcam, ab6276, 1:8000), rabbit polyclonal anti-β-tubulin III (Sigma-Aldrich, T2200, 1:10,000), rabbit polyclonal anti-GluA1 (EMD Millipore, AB1504, 1:1000), and mouse monoclonal anti-GluA2 (EMD Millipore, MAB397, 1:1000). The following secondary antibodies were used for infrared fluorescence detection of Western blots: donkey anti-rabbit (LI-COR, #926-32213, 1:10,000) and donkey anti-mouse (LI-COR, #926-68022, 1:20,000).

The following primary antibodies and dilutions were used for immunofluorescence experiments: rabbit polyclonal anti-GluA1 (EMD Millipore, PC246, 1:10) and mouse monoclonal anti-GluA2 (EMD Millipore, MAB397, 1:250). The following secondary antibodies and dilutions were used for detection: donkey anti-rabbit Cy3 and donkey anti-mouse Cy5 (Jackson Immunoresearch, 1:500). The following primary antibodies and dilutions were used for puromycylation and proximity ligation assay experiments: mouse monoclonal anti-puromycin (DSHB, PMY-2A4, 1:250) and rabbit polyclonal anti-GluA1 (EMD Millipore, AB1504, 1:200).

Image acquisition and analysis

Image acquisition was performed as described in Chapter 3. Image analysis for qIF experiments was performed as descried in Chapter 3 with the following modifications for PLA experiments. For PLA experiments, background fluorescence was subtracted in the PLA channel, and the surface function in Imaris was used to create a surface within each dendritic region of interest that encompassed the PLA puncta. For all quantitative imaging experiments, total signal within the dendritic region of interest was normalized to the volume. Within biological replicates, all quantitative immunofluorescence measurements were normalized to the average of the control group within that replicate (i.e. "Control(GFP)/Control(Vehicle)"). Normalization was done to the average of the "miR-137 Sponge/Control(Vehicle)" condition for total dendritic GluA1/2 measurements only.

In vitro transcription and biotinylated RNA pulldown

In vitro transcription was performed as described in Chapter 2. For pulldown experiments with Nrg-treated neurons and wild-type Gria1 biotinylated mRNA, DIV6 cortical neurons were treated 15 min with 100 ng/mL Nrg1α or an equal volume of PBS (vehicle control). Neurons were immediately lysed in lysis buffer (10mM TrisHCl, 150 mM NaCl, 5 mM EDTA, 1% triton, 0.20%SDS, pH 7.4; supplemented with protease inhibitors and SuperaseIN, modified from Sosanya et al 2013). Protein concentration was measured by Bradford assay. Cell extract containing 40 μg protein was mixed with 4 μg biotinylated Gria1 mRNA and brought to a final volume of 400 μL using reaction buffer (10 mM Hepes, 150 mM NaCl, 3 mM MgCl2, 2.50% glycerol, 0.50% NP-40, 0.2 mg/mL yeast tRNA, 5 mM EDTA, pH 7.4; supplemented with protease inhibitors and Superase IN, modified from Sosanya et al 2013) and incubated 1 hr rotating at room temperature. Reaction mixture was added to 40 μL NeutrAvidin beads (pre-washed with reaction buffer) and incubated 1 hr rotating at room temperature. Beads were

washed three times with reaction buffer and biotinylated mRNA and associated mRNAs were then pulled down by centrifugation and extracted with Trizol prior to quantification by qPCR.

Statistical analyses

Statistical analyses were performed as described in Chapter 2 and 3.

4.5 Figures

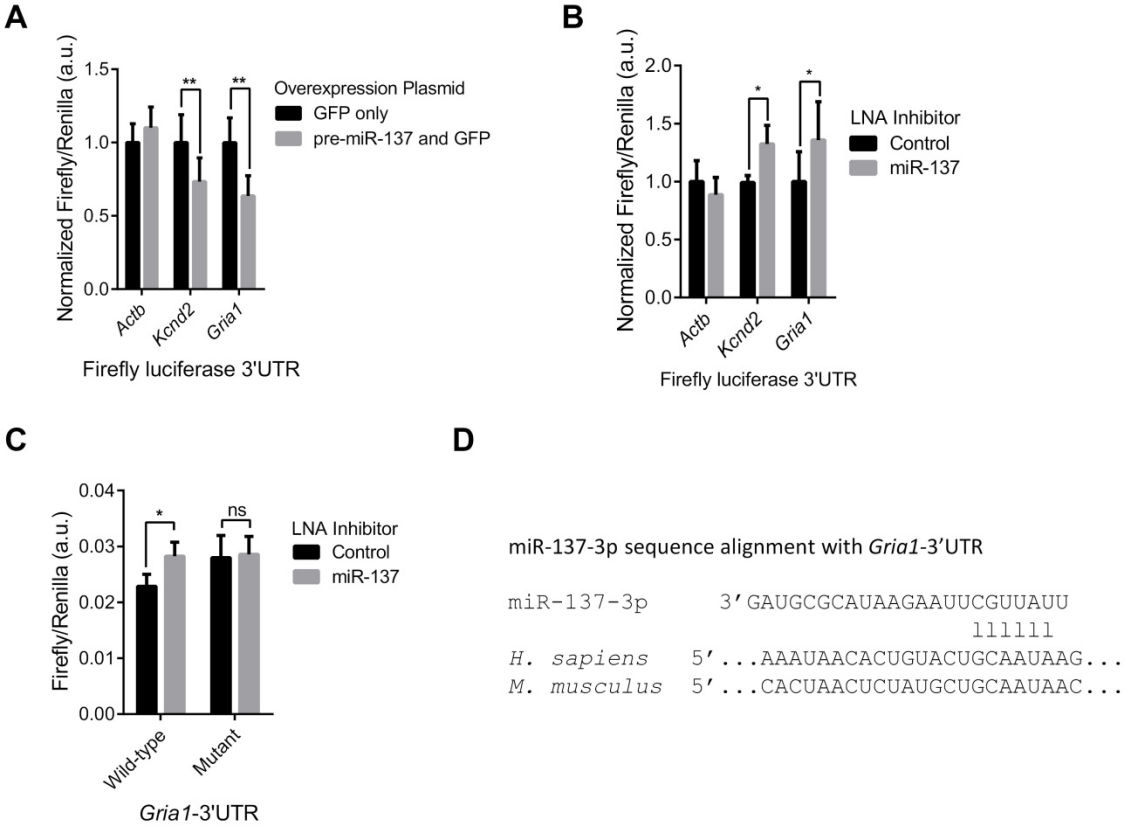

Figure 4.1 miR-137 inhibits *Gria1*-3'UTR luciferase reporter activity. (**A**) Overexpression of pre-miR-137 reduces mouse *Gria1*- and *Kcnd2*-3'UTR luciferase reporter activities without affecting a negative control, *Actb*-3'UTR reporter in Neuro2A cells (Sidak's test, **p<0.01, n=4). (**B**) Inhibition of miR-137 increases mouse *Gria1* and *Kcnd2*-3'UTR luciferase reporter activities without affecting a negative control, *Actb*-3'UTR reporter in Neuro2A cells (Sidak's test, *p<0.05, n=5). (**C**) The effect of miR-137 inhibition is ablated by mutation of the predicted miR-137 target site (Two-way ANOVA, p(LNA)=0.0209, *p(interactive)=0.0411; Sidak's test, *p<0.05, n=7). miR-137 sequence alignment with the mouse *Gria1* and human *GRIA1*-3'UTRs is shown in **D**. Data are shown as mean ± SEM.

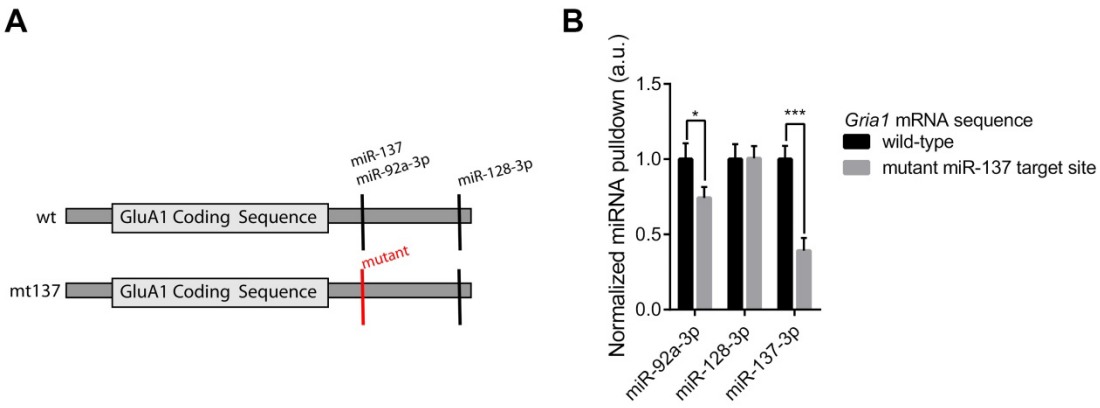

Figure 4.2 miR-137 associates with *Gria1* mRNA *in vitro* in a site and sequence-specific manner. (**A**) Schematic shows the relative positions of miR-137, miR-92a, and miR-128 predicted binding sites in the *Gria1*-3'UTR.Mutation of the miR-137 target site (relative position shown in **A**) significantly reduces miR-137 and miR-92a association with mouse *Gria1* mRNA when measured by a biotinylated mRNA pulldown assay (**B**, Two-way ANOVA, p(3'UTR)=0.0007, p(miRNA)=0.1323, p(interactive)=0.0009; Sidak's test, *p<0.05, ***p<0.001; n=4 biological replicates). Data are shown as mean ± SEM.

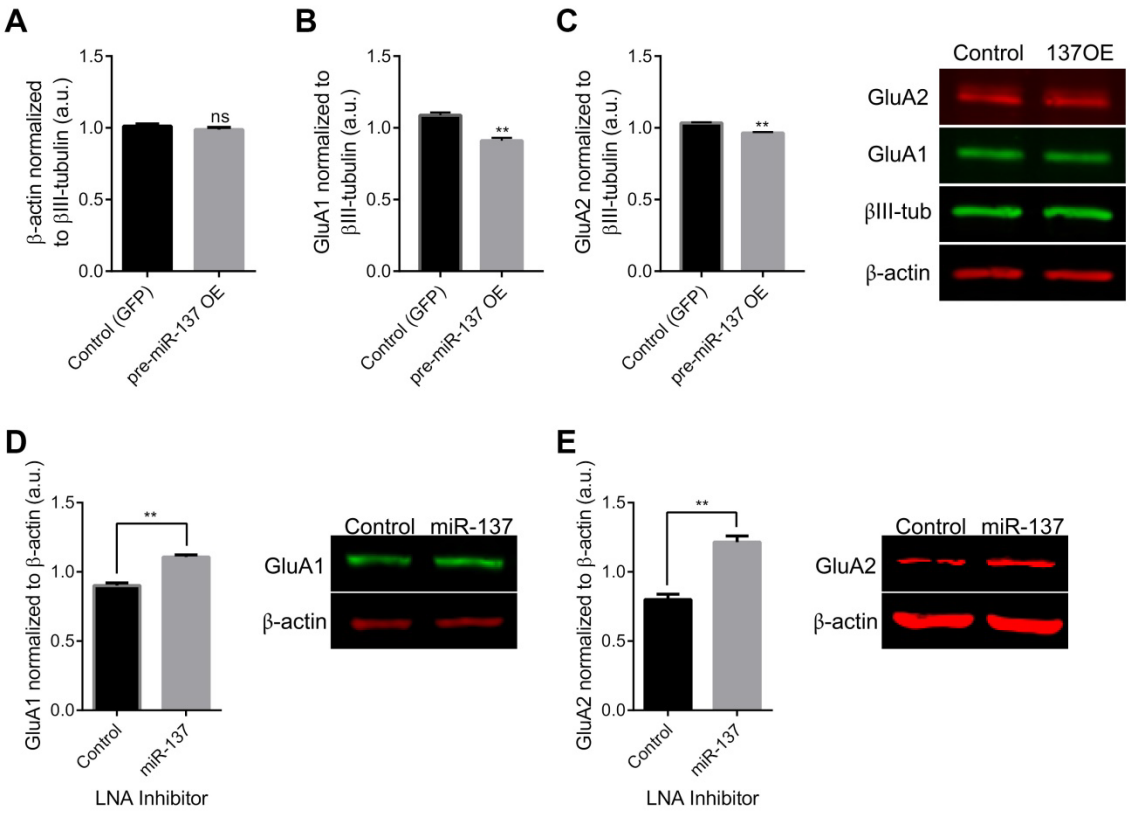

Figure 4.3 miR-137 inhibits GluA1 and GluA2 protein levels in cortical neurons. (**A**) Overexpression of pre-miR-137 does not affect β-actin protein levels in DIV6 primary cortical neurons (paired t-test, not significant, n=4). (**B**) Overexpression of pre-miR-137 reduces GluA1 protein levels in DIV6 primary cortical neurons (paired t-test, **p<0.01, n=5). (**C**) Overexpression of pre-miR-137 reduces GluA2 protein levels in DIV6 primary cortical neurons (paired t-test, **p<0.01, n=5). (**D**) Inhibition of miR-137 increases GluA1 protein levels in DIV15 primary cortical neurons (paired t-test, **p<0.01, n=4). (**E**) Inhibition of miR-137 increases GluA2 protein levels in DIV15 primary cortical neurons (paired t-test, **p<0.01, n=6). Representative western blots are shown to the left or right. Data are shown as mean ± SEM.

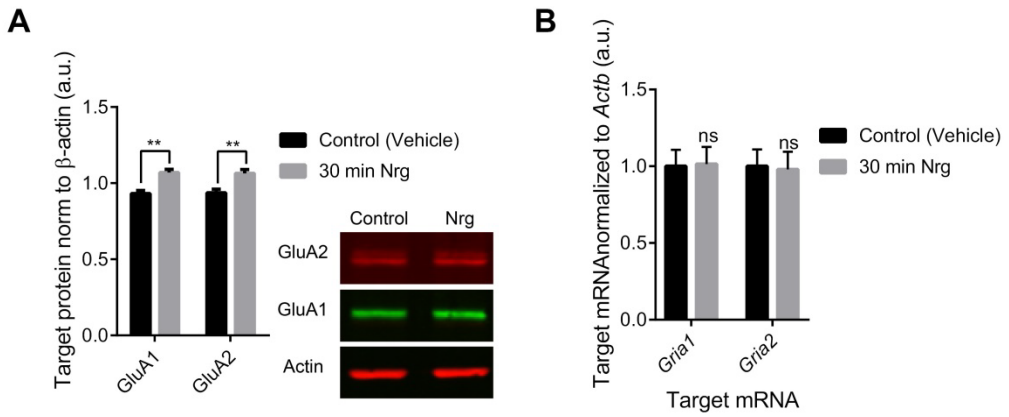

Figure 4.4 Nrg1α increases GluA1 and GluA2 protein levels without affecting mRNA levels. (**A**) Nrg1α significantly increases GluA1 and GluA2 protein levels in DIV6 primary cortical neurons (Sidak's test, **p<0.01, n=5). Representative western blots are shown to the right. (**B**) Nrg1α does not affect *Gria1* or *Gria2* mRNA levels in DIV6 primary cortical neurons (Sidak's test, not significant, n=5). Data are shown as mean ± SEM.

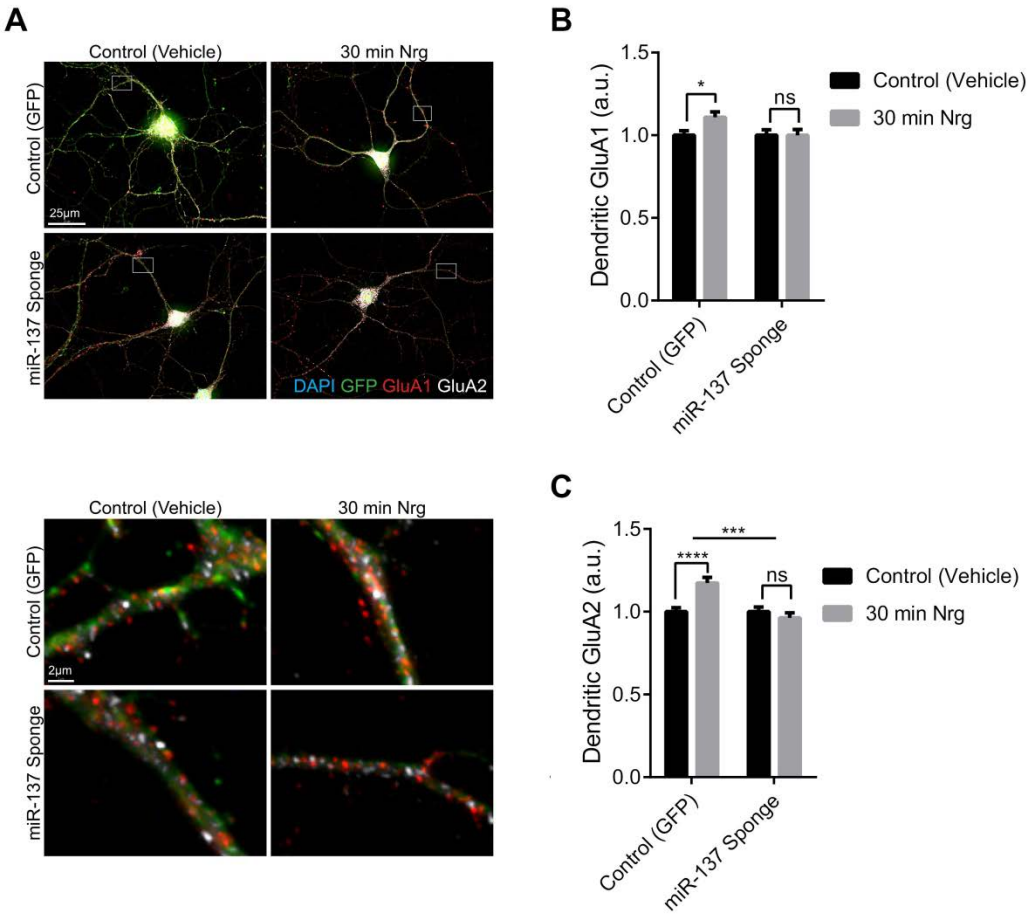

Figure 4.5 Inhibition of miR-137 blocks Nrg1α-induced increases in dendritic GluA1 and GluA2. Stimulation of dendritic GluA1 and GluA2 protein levels by Nrg1α is ablated by inhibition of miR-137 in DIV6 primary hippocampal neurons. Representative neurons and dendritic ROIs are shown in **A**. Quantification of GluA1 and GluA2 are shown in **B** and **C**, respectively (**B**, Sidak's test, *p<0.05, n=79-80 cells/condition from 4 biological replicates; **C,** Two-way ANOVA, p(sponge)= 0.0003, p(Nrg)=0.0184, ***p(interactive)=0.0003; Sidak's test, ****p<0.0001; n=79-80 cells/condition from 4 biological replicates). Scale bars are 25 μm for whole cell and 2 μm for dendrite images. Data are shown as mean ± SEM.

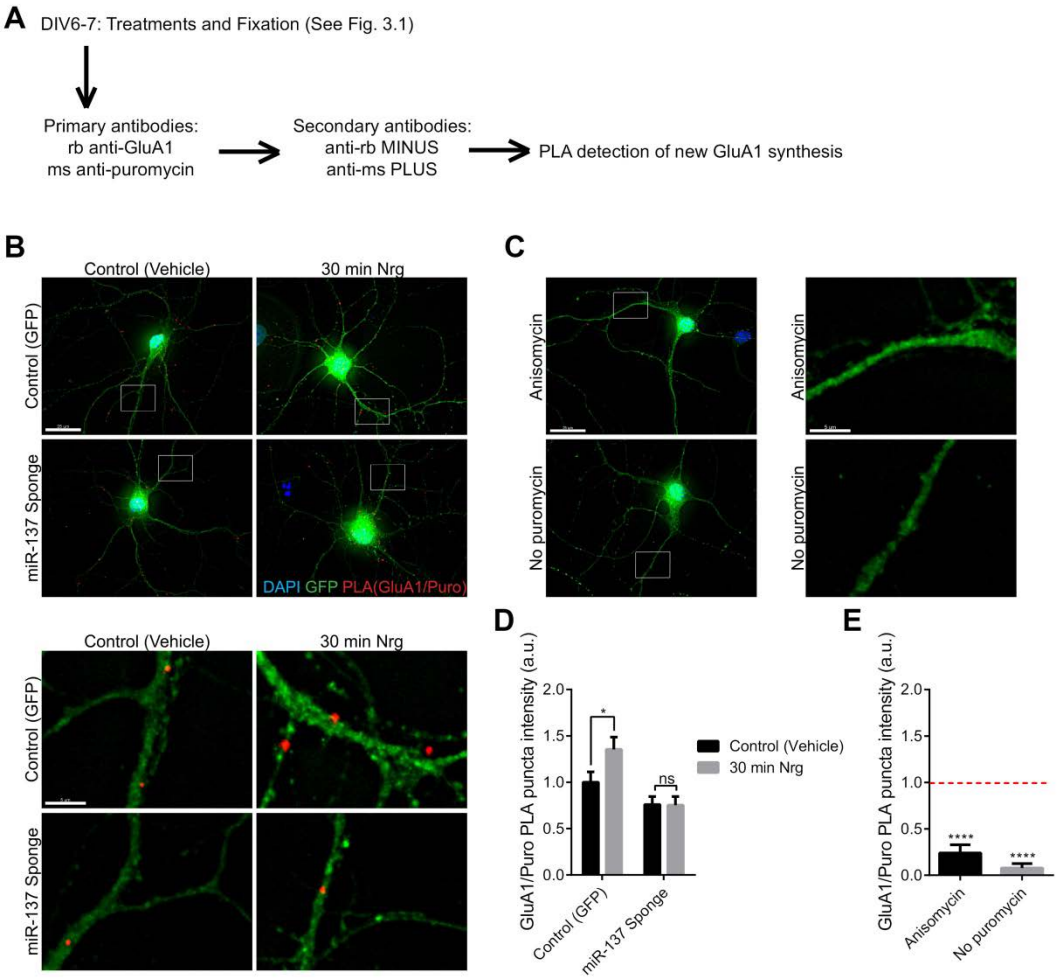

Figure 4.6 Inhibition of miR-137 blocks Nrg1α induced GluA1 synthesis. GluA1 synthesis was measured in DIV6-7 primary hippocampal neurons by puromycylation of nascent proteins and proximity ligation assay (PLA), as shown in **A**. Representative neurons and dendritic ROIs are shown in **B**. Quantification of PLA puncta intensity is shown in **D** (Two-way ANOVA, p(sponge)=0.0001; Sidak's test, *p<0.05; n=70-71 cells/condition from 4 biological replicates). For quantification, the sum of the intensities of the PLA puncta was normalized to the dendritic volume within each ROI. The PLA signal was sensitive to anisomycin and dependent on puromycin (**C,** representative neurons and ROIs; **E**, one sample t-test, ****p<0.0001, n=18 cells/condition from 3 biological replicates). Scale bars are 25 μm for whole cell and 3 μm for dendrite images. Data are shown as mean ± SEM.

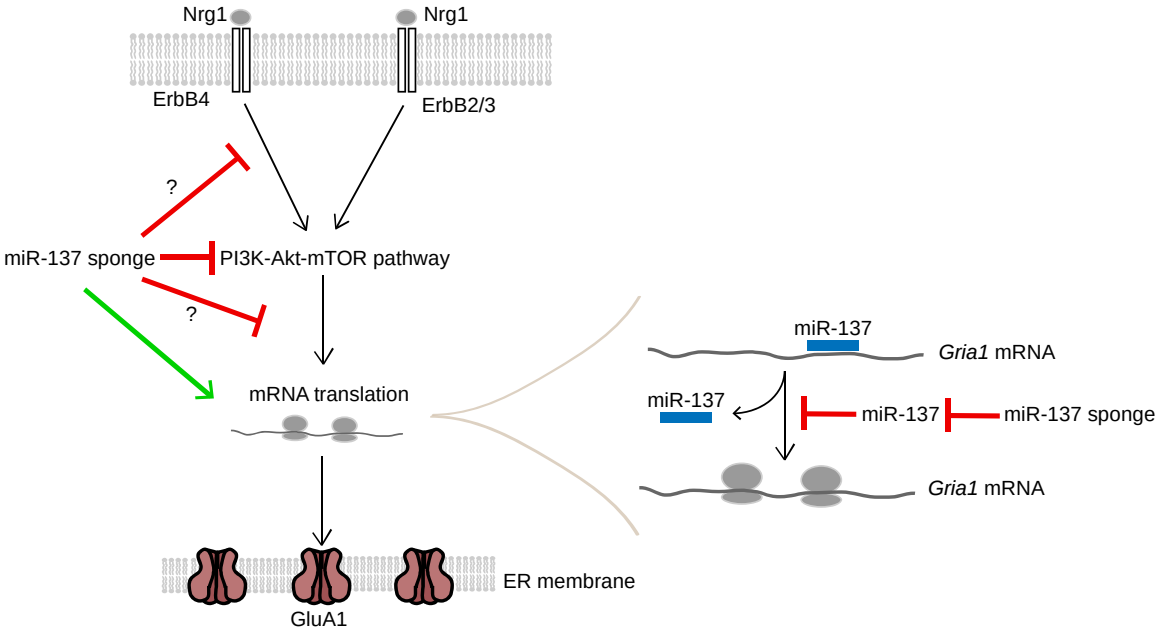

Figure 4.7 Model for miR-137 regulating Nrg1α-induced changes in GluA1 levels

We propose the model above to explain how Nrg1α stimulates GluA1 synthesis by a miR-137-dependent mechanism. In control neurons, Nrg1α binds ErbB receptors and stimulates the PI3K-Akt-mTOR pathway which stimulates the translation of mRNAs, including *Gria1*. Increased *Gria1* translation increases GluA1 protein levels. In neurons expressing the miR-137 sponge, Nrg1α can no longer stimulate the PI3K-Akt-mTOR pathway and/or mTORC1-dependent protein synthesis, and therefore cannot stimulate GluA1 synthesis. An additional mechanism by which miR-137 regulates GluA1 protein synthesis is by directly targeting the 3'UTR of *Gria1* mRNA. The miR-137 sponge relieves *Gria1* of miR-137-mediated translational repression. Whether Nrg1α regulates miR-137 binding to *Gria1* or other mRNA targets of miR-137 remains unknown.

4.6 Supplemental Figures

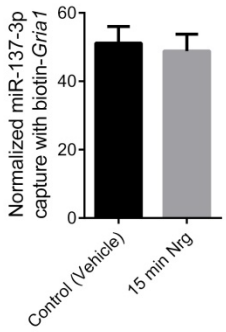

Supplemental Figure 4.1 Nrg1α does not affect miR-137's ability to assemble on *Gria1* mRNA *in vitro*. DIV6 primary cortical neurons were treated 15 min with Nrg1α before lysis, then miR-137's ability to bind *Gria1* mRNA *in vitro* was measured by biotinylated mRNA pulldown assay (paired t-test, not significant, n=4). Bound miR-137 was normalized to miR-137 input as well as to *Gria1* mRNA pulldown. Data are shown as mean ± SEM.

Chapter 5

miR-137 regulates mTOR-dependent responses to BDNF

Portions of this chapter were adapted from the following manuscript:

Thomas, K.T., Anderson, B.R., Shah, N., Zimmer, S., Hawkins, D., Gu, Q., and Bassell. G.J. (2017). Inhibition of the schizophrenia-associated microRNA miR-137 disrupts Nrg1α neurodevelopmental signal transduction. Cell Rep., Revision Under Review.

5.1 Introduction

In Chapter 3, we demonstrated that miR-137 regulates Nrg/ErbB signaling in neuronal dendrites. Our bioinformatic predictions in Chapter 1 indicate that miR-137 targets may also be enriched in neurotrophin signaling, suggesting that miR-137 may regulate neurotrophin signaling as well. The neurotrophins are a class of signaling molecules that regulate neuronal maturation, neuron survival, synapse maturation, and synaptic plasticity, among other CNS processes. Of the neurotrophins, the role of brain-derived neurotrophic factor (BDNF) in synaptic function and neuropsychiatric disease is best characterized. Furthermore, like Nrg/ErbB signaling, BDNF mediates many of its effects by activating the PI3K-Akt-mTOR pathway, which we previously showed to be regulated by miR-137 (Chapter 2). In the present chapter, we examine whether miR-137 regulates BDNF signaling and Nrg/ErbB signaling by a conserved mechanism: through the regulation of proteins within the PI3K-Akt-mTOR pathway.

5.1.1 BDNF signaling: general structure and function

Like Nrg, BDNF is synthesized as a precursor that then undergoes enzymatic processing to create its active form. The first precursor, prepro-BDNF, undergoes regulated processing to pro-BDNF (Autry and Monteggia, 2012). Pro-BDNF is secreted in an activity-dependent manner along with enzymes that cleave pro-BDNF to form mature BDNF (Lessmann et al., 2003). Both pro-BDNF and mature BDNF participate in neuronal signaling, with pro-BDNF acting on p75 receptors to regulate apoptosis and mature BDNF acting on tropomyosin related kinase B (TrkB) receptors to initiate a number of neurotrophic signaling cascades (Autry and Monteggia, 2012; Koshimizu et al., 2010; Levine et al., 1995). Like the ErbB receptors, TrkB receptors are receptor tyrosine kinases that dimerize upon ligand binding and undergo autophosphorylation of tyrosine residues which then serve as docking sites for downstream signaling kinases that initiate signaling cascades(Autry and Monteggia, 2012; Levine et al., 1995). One of these signaling cascades is the phospholipase C γ (PLC γ) pathway, which activates phosphokinase C and regulates the release

of calcium from intracellular stores and induces rapid changes in neural activity (Yoshii and Constantine-Paton, 2010). Also like ErbB receptors, TrkB can activate ERK signaling and PI3K-Akt-mTOR pathway signaling (Reviewed in Chapter 2) to induce long term changes in transcription, translation, and synaptic strength (Yoshii and Constantine-Paton, 2010).

In the developing brain, BDNF regulates the outgrowth of axons and dendrites, the formation of the neural circuitry, the formation of synapses, and neuronal survival (Yoshii and Constantine-Paton, 2010). In the mature brain, BDNF regulates excitatory and inhibitory synapses and regulates the conversion of early phase LTP to late phase LTP (Panja and Bramham, 2014). BDNF-induced protein synthesis in dendrites and synapses may be particularly important for long lasting changes in synaptic strength (late LTP) (Panja and Bramham, 2014). Unsurprisingly, disruption of BDNF signaling in animal models during early stages of development impairs neural development, whereas disruption of BDNF in adulthood impairs learning and memory. Interestingly, BDNF signaling in adulthood also regulates cognition and mood. BDNF is therefore implicated in a wide range of neurodevelopmental and psychiatric disorders, including schizophrenia, major depression, Rett syndrome, and addiction (Autry and Monteggia, 2012).

5.1.2 BDNF in neurodevelopmental disease

We will focus on the role of BDNF in the neurodevelopmental disorders Rett syndrome and schizophrenia.

Rett syndrome is caused by the loss of MeCP2, a transcription-regulating protein. *BDNF* is among the transcriptional targets of MeCP2, and mouse models of Rett syndrome display reduced BDNF protein levels in the cortex and cerebellum concurrent with the onset of Rett syndrome-like phenotypes (Chang et al., 2006). Overexpression of BDNF delays the onset of phenotypes in mouse models of Rett syndrome, whereas deletion of BDNF leads to earlier symptom onset (Chang et al., 2006). BDNF overexpression also rescues morphological and

synaptic deficits in primary hippocampal neurons derived from Rett syndrome model mice (Sampathkumar et al., 2016). Furthermore, a recent study demonstrated that glatiramer acetate, which stimulates BDNF secretion, significantly improved gait velocity in patients with Rett syndrome (Djukic et al., 2016). Only ten patients were included in this preliminary study, however, and larger scale studies are needed to further evaluate the therapeutic utility of glatiramer acetate and other BDNF-based therapies in the treatment of Rett syndrome. Together, these data suggest that dysregulation of BDNF may contribute to the Rett syndrome symptoms in patients and that restoration of BDNF signaling provides a potential therapeutic strategy for the treatment of Rett syndrome.

BDNF may also play a role in schizophrenia etiology, but whether BDNF plays a causative or merely incidental role remains unknown (Autry and Monteggia, 2012). A recent meta-analysis of studies examining serum levels of BDNF in schizophrenia patients concluded that there was moderate quality evidence for reduced serum BDNF in schizophrenia (Green et al., 2011). While some studies demonstrate increased BDNF protein in cortical or hippocampal tissue from schizophrenia patient, others report the opposite (Autry and Monteggia, 2012). Whether these conflicting results are due to the effects of antipsychotics on BDNF levels or other confounding variables is unclear, and antipsychotics also appear to have diverse effects on BDNF expression (Autry and Monteggia, 2012). Animal models also suggest that BDNF may contribute to schizophrenia (Angelucci et al., 2005). Reduced BDNF protein levels were observed in the cortices of rats that underwent long term amphetamine administration, an animal model of schizophrenia which displays psychosis-related behaviors and has predictive validity for antipsychotics (Angelucci et al., 2007). Furthermore, mice with reduced BDNF expression show deficits in spatial and contextual learning tasks and in other behavioral measures relevant to schizophrenia (Autry and Monteggia, 2012). These animal models suggest that BDNF signaling deficits may contribute to positive and cognitive symptoms of schizophrenia, but further studies

are needed to clarify how BDNF does so in animal models and whether BDNF does so in schizophrenia patients.

5.1.3 Chapter 5 hypothesis and objectives

In Chapter 3, we demonstrated that inhibition of miR-137 blocks mTORC1-dependent responses to Nrg/ErbB signaling. In Chapter 2, we also demonstrated that miR-137 targets multiple proteins within the PI3K-Akt-mTOR pathway, suggesting that miR-137 regulation of the PI3K-Akt-mTOR pathway underlies miR-137's ability to regulate Nrg/ErbB signaling. However, miR-137 is also predicted to target mRNAs encoding two Nrgs (Nrg2 and Nrg3) as well as the Nrg1 receptor ErbB4. It is therefore possible that miR-137's effects on PI3K-Akt-mTOR pathway components had no effect on Nrg/ErbB signaling and that the effects of miR-137 can be attributed to changes in Nrgs and/or ErbB receptors. If this were the case, we would predict that miR-137 would specifically regulate PI3K-Akt-mTOR signaling downstream of Nrg/ErbB signaling and not downstream of neurotrophins, such as BDNF. Neither BDNF nor its receptor TrkB are encoded by predicted miR-137 targets, but BDNF signaling through TrkB does activate PI3K-Akt-mTOR signaling, similarly to Nrg1/ErbB signaling.

We hypothesized that inhibition of miR-137 would block PI3K-Akt-mTOR-dependent responses to BDNF. The experiments that follow were undertaken with the following objectives: 1) to determine whether miR-137 regulates BDNF signaling or whether miR-137 uniquely regulations Nrg/ErbB signaling and 2) to determine whether miR-137 specifically regulates PI3K-Akt-mTOR-dependent signaling or whether miR-137 regulates all responses to Nrg/ErbB and/or BDNF signaling.

5.2 Results

BDNF is known to stimulate dendritic outgrowth, S6 phosphorylation, and mRNA translation in neurons, all responses that we observed to Nrg1α in Chapter 3. In the following

experiments, we examine whether these responses are dependent on mTORC1 activity and miR-137 activity in primary hippocampal neurons.

5.2.1 BDNF stimulates dendritic outgrowth by an mTOR- and miR-137-dependent mechanism

To examine the effects of miR-137 on BDNF-induced dendritic outgrowth, we treated DIV2 neurons with BDNF, fixed the neurons on DIV4, and quantified dendritic complexity by Sholl analysis, as described in Chapter 4. Similar to our observations with Nrg1α, BDNF significantly and consistently increased dendritic outgrowth in hippocampal neurons under control conditions (**Fig. 5.1**). BDNF also had no effect on miR-137 levels (**Supp. Fig. 5.1**). In our first experiment, we treated neurons with rapamycin concurrent with BDNF treatment to inhibit mTOR activity. We found that rapamycin ablated BDNF-induced dendritic outgrowth (**Fig. 5.1A-C**), demonstrating that BDNF induces dendritic outgrowth through an mTOR-dependent mechanism.

We next transduced primary hippocampal neurons on DIV1 with a lentivirus containing a miR-137 sponge construct. As reported in Chapter 4, inhibition of miR-137 increased basal dendritic outgrowth, but BDNF treatment reduced dendritic outgrowth in neuron expressing the miR-137 sponge (**Fig. 5.1D-F**). Similar to our observations with Nrg1α, we conclude that inhibition of miR-137 blocks BDNF-induced dendritic outgrowth.

We then transduced primary hippocampal neurons on DIV1 with a lentivirus containing a pre-miR-137 overexpression construct. Overexpression of miR-137 did not significantly affect dendritic outgrowth under basal conditions, but it did block BDNF-induced dendritic outgrowth (**Fig. 5.1G-I**).We conclude that BDNF stimulates dendritic outgrowth by an mTOR- and miR-137-dependent mechanism.

5.2.2 BDNF stimulates S6 phosphorylation by an mTOR- and miR-137-independent mechanism

We previously reported that Nrg1α increases dendritic phospho(Ser235/236)-S6 by a miR-137- and mTORC1-dependent mechanism in primary hippocampal neurons (Chapter 3). We predicted that BDNF would stimulate dendritic phospho-S6 by a similar mechanism.

We first treated DIV7 primary hippocampal neurons with BDNF for 30 min following pretreatment with rapamycin and measured changes in phospho(Ser235/236)-S6 and total S6 in dendrites using qIF. Surprisingly, we found that even in the presence of rapamycin BDNF increased dendritic phospho-S6 by approximately 50% without affecting total S6 (**Fig. 5.2A-C**). BDNF also increased S6 phosphorylation (the ratio of phospho- to total S6) in the presence of rapamycin (**Fig. 5.2D**). We conclude that, unlike Nrg1α, BDNF stimulates dendritic phospho-S6 through an mTORC1-independent mechanism.

We next inhibited miR-137 by transducing DIV2 primary hippocampal neurons with lentivirus containing the miR-137 sponge, treated neurons on DIV7-9 with BDNF for 30 min, and measured changes in phospho- and total S6 by qIF. We found that BDNF increased dendritic phospho-S6 and S6 phosphorylation in control neurons as well as in neurons expressing the miR-137 sponge (**Fig. 5.2E-H**). Neither treatment affected total dendritic S6 levels. We conclude that, unlike Nrg1α, BDNF stimulates dendritic phospho-S6 through a miR-137-independent mechanism. These data suggest that BDNF stimulates S6 phosphorylation through an alternative pathway, such as ERK signaling (Roux et al., 2007), and this branch of BDNF signaling may be intact in neurons expressing the miR-137 sponge.

5.2.3 BDNF stimulates mRNA translation in dendrites by a miR-137-dependent mechanism

BDNF has previously been shown to stimulate mRNA translation in neurons by an mTORC1-dependent mechanism (Schratt et al., 2004). We transduced DIV7 primary hippocampal neurons with the miR-137 sponge and treated them for 10 min with BDNF on

DIV14. Dendritic protein synthesis was then measured by puromycylation as described in Chapter 3. For experimental timeline, see **Fig. 5.3A.** We found that BDNF stimulated protein synthesis in control DIV14 hippocampal neurons but not in neurons expressing the miR-137 sponge (**Fig. 5.3B-C**), consistent with our hypothesis that miR-137 regulates the PI3K-Akt-mTOR branch of BDNF signaling,

5.3 Discussion

In the present chapter, we examined the hypothesis that miR-137 regulates PI3K-Akt-mTOR-dependent responses to BDNF. We found that BDNF stimulated dendritic outgrowth by an mTOR and miR-137-dependent mechanism, similar to Nrg1α-induced dendritic outgrowth reported in Chapter 3. BDNF also stimulated dendritic protein synthesis by a miR-137-depedent mechanism, and a previous study demonstrated that BDNF stimulates dendritic protein synthesis by an mTORC1-dependent mechanism. In Chapter 3, we demonstrated that Nrg1α increased dendritic phospho(Ser235/236)-S6 by a miR-137 and mTORC1-dependent mechanism. By contrast BDNF-induced S6 phosphorylation is insensitive to rapamycin, and therefore mTORC1-independent, and insensitive to the miR-137 sponge, and therefore miR-137 independent. These data support several conclusions.

First, miR-137 regulates not only Nrg/ErbB signaling, but also BDNF signaling. In Chapter 1, we reported that predicted miR-137 targets were enriched in both the Nrg/ErbB and neurotrophin signaling pathways, but predicted miR-137 targets were more highly enriched in Nrg/ErbB signaling. This is partially due to the observation that two forms of Nrg (Nrg2 and Nrg3) and the receptor ErbB4 are encoded by predicted miR-137 targets. If miR-137 does target these signaling components unique to Nrg/ErbB signaling, they may be necessary and sufficient for miR-137 to regulate Nrg/ErbB signaling. For example, if miR-137 regulates the synthesis of ErbB4 receptors, changes in miR-137 activity may regulate the surface availability of ErbB4, which may be sufficient to regulate all downstream signaling. However, we found that miR-137

also regulates BDNF signaling, which is not directly influenced by Nrg2, Nrg3, or ErbB4, suggesting that even if miR-137 regulates these proteins, they are not necessary for miR-137 to regulate neuronal signal transduction.

Second, it is likely that miR-137 regulates Nrg/ErbB signaling and BDNF signaling by a conserved mechanism. In Chapter 1, we demonstrated that many of the predicted miR-137 targets within the Nrg/ErbB signaling pathway would also affect neurotrophin signaling. In Chapter 2, we demonstrated that miR-137 regulates the levels of many of these proteins, including p55γ, Akt2, GSK3β, and rictor, which all regulate PI3K-Akt-mTOR signaling. We propose that miR-137's ability to regulate these proteins underlies the effects of miR-137 on both Nrg/ErbB and BDNF signaling.

Finally, we conclude that miR-137 does not regulate all responses to Nrg/ErbB and BDNF signaling, but rather only those that filter through the mTOR pathway. In Chapter 3, we observed that Nrg1α reduced GSK3β phosphorylation at Ser9, independent miR-137 activity. In the present chapter, we observed that BDNF induced S6 phosphorylation independent of miR-137 activity and independent of mTORC1 activity. Together, these data support at least two conclusions. First, receptors for Nrg1α and BDNF are present at the cell surface and are activated by ligand binding. Second, some downstream signaling is intact in neurons expressing the miR-137 sponge. We do not know why Nrg1α reduced phosphorylation of GSK3β, since Nrg/ErbB signaling activates Akt, which should increase GSK3β phosphorylation. Presumably, another pathway that induces dephosphorylation is also activated by Nrg/ErbB signaling. BDNF-induced S6 phosphorylation is likely due to ERK signaling, which also promotes S6 phosphorylation at Ser235/236 (Roux et al., 2007). Our data therefore suggest that ERK signaling downstream of BDNF is independent of miR-137 activity and intact in neurons expressing the miR-137 sponge. We propose that miR-137 regulates the PI3K-Akt-mTOR pathway downstream of Nrg/ErbB signaling and BDNF signaling by directly targeting proteins that mediate PI3K-Akt-mTOR signaling.

5.3.1 Future directions

Several questions remain regarding the regulation of BDNF signaling by miR-137. First, does overexpression of miR-137 affect BDNF-induced S6 phosphorylation or mRNA translation? We found that overexpression of miR-137 blocked BDNF-induced dendritic outgrowth, suggesting that miR-137 overexpression disrupts BDNF signaling. Furthermore, mTORC1 signaling and protein synthesis contribute to dendritic outgrowth (Kumar et al., 2005). If both were intact in neurons overexpressing miR-137, we would expect for BDNF-induced dendritic outgrowth to be at least partly intact. We therefore predict that overexpression of miR-137 will also disrupt BDNF-induced S6 phosphorylation and mRNA translation, but this must be examined experimentally.

Future experiments should also address whether miR-137 regulates BDNF-induced changes in GluA1. In Chapter 3, we demonstrated that Nrg1α-induced GluA1 synthesis was miR-137-dependent. BDNF has previously been shown to stimulate GluA1 synthesis by an mTORC1-dependent mechanism (Fortin et al., 2012). We therefore predict that inhibition of miR-137 will block BDNF-induced GluA1 synthesis. Interestingly, ERK signaling regulates AMPA receptor phosphorylation and trafficking, and ERK signaling may not be affected by changes in miR-137 activity (Patterson et al., 2010). Future experiments should therefore address how miR-137 regulates BDNF-induced changes in not only GluA1 protein synthesis but also phosphorylation, channel conductivity, localization, and trafficking.

BDNF-induced protein synthesis may be particularly critical for late phase LTP and for several forms of learning and memory (Leal et al., 2014; Panja and Bramham, 2014). miR-137's ability to regulate BDNF-induced protein synthesis might also suggest that miR-137 is critical for these processes as well. For example, BDNF activates mTORC1 signaling during multiple phases of memory consolidation during an inhibitory avoidance task, and inhibition of BDNF signaling blocks mTORC1-dependent synthesis of proteins critical for memory formation (including GluA1) and hinders memory retention (Slipczuk et al., 2009). miR-137 may also prove critical

for BDNF-induced protein synthesis during memory consolidation and prove critical for memory retention.

5.3.2 Significance for neurodevelopmental disorders

Dysregulation of BDNF signaling may contribute to Rett syndrome etiology, and restoration of BDNF may have therapeutic utility for the treatment of Rett syndrome. MeCP2 regulates the transcription of BDNF and the loss of MeCP2 leads to the loss of BDNF in mouse models of Rett syndrome (Chang et al., 2006). Interestingly, miR-137 expression is significantly higher in neural stem cells derived from *Mecp2*-deficient mice (Szulwach et al., 2010). We demonstrated that miR-137 overexpression inhibits BDNF-induced dendritic outgrowth. Together, these data suggest that miR-137 overexpression may contribute to deficits in BDNF signaling and dendritic morphology in Rett syndrome.

Dysregulation of miR-137 and BDNF may also contribute to schizophrenia. We observed that both overexpression and inhibition of miR-137 disrupted BDNF-induced dendritic outgrowth. As previously discussed in Chapter 3, several studies suggest that dendritic complexity may be reduced in some cortical neurons in schizophrenia patients. Our data suggest that changes in miR-137 activity in schizophrenia patients may contribute to deficits in dendritic outgrowth by disrupting BDNF signaling.

Both Rett syndrome and schizophrenia are also associated with deficits in synaptic plasticity (Stephan et al., 2006; Zoghbi and Bear, 2012). miR-137 has already been shown to be critical for presynaptic LTP and for mGluR-dependent LTD in the hippocampus (Olde Loohuis et al., 2015; Siegert et al., 2015), demonstrating that miR-137 regulates multiple forms of synaptic plasticity. Our data examining BDNF-induced protein synthesis provide a novel mechanism by which miR-137 might contribute to synaptic plasticity, particularly late phase LTP. Whether this also contributes to deficits in synaptic plasticity in neurodevelopmental and psychiatric disease will be an interesting topic for future research.

5.4 Materials and Methods

Primary hippocampal and cortical neuron cultures

Primary neurons were cultured as described in Chapers 2 and 3.

Drug treatments

For acute stimulation experiments, neurons were treated for 30 min (S6 experiments) or 10 min (puromycylation) with 100 ng/mL BDNF (PeproTech, #450-02) immediately prior to puromycylation or fixation. For morphology experiments, neurons were treated DIV2-4 with 0.07 ng/mL BDNF. For acute rapamycin stimulation experiments, neurons were treated with 200 nM rapamycin (Sigma-Aldrich, R0395) or an equal volume of dimethyl sulfoxide (DMSO) for 30 min prior to BDNF treatment and remained in media with BDNF. For morphology experiments, neurons were treated with 100 nM rapamycin or an equal volume of DMSO concurrent with BDNF treatment.

Puromycylation

Puromycylation was performed as described in Chapter 3.

Plasmids and lentiviruses

Neurons were transduced with lentivirus containing miR-137 sponge or pre-miR-137 overexpression constructs on DIV1 for morphology experiments, on DIV2 for qIF experiments with DIV7-9 neurons, or on DIV7 for DIV14 puromycylation experiments. Hippocampal neurons were transduced by adding 1 μL lentivirus (2×10^6 infectious units) directly to each well of a 6-well plate containing secondary glia and primary neurons on coverslips.

RNA isolation, cDNA synthesis, and qPCR

RNA isolation, miRNA cDNA synthesis, and qRT-PCR were performed as described in Chapter 2.

Quantitative immunofluorescence

Quantitative immunofluorescence was performed as described in Chapter 3.

Puromycylation

Puromycylation was performed as described by Graber et al., 2013 with the following modifications: puromycin was added to neurons at a concentration of 4.17 μg/mL and detected with mouse anti-puromycin antibody diluted 1:250.

Antibodies

The following primary antibodies and dilutions were used for immunofluorescence experiments: rabbit polyclonal anti-MAP2 (EMD Millipore, AB5622, 1:500), rabbit polyclonal anti-phospho-S6 (Ser235/236) (Cell Signaling, #2211, 1:250), and mouse monoclonal anti-S6 (Cell Signaling, #2317, 1:100). The following secondary antibodies and dilutions were used for detection: donkey anti-mouse Alexa Fluor 488, donkey anti-rabbit Cy3, and donkey anti-mouse Cy5 (Jackson Immunoresearch, 1:500). The mouse monoclonal anti-puromycin (DSHB, PMY-2A4, 1:250) primary antibody was used for puromycylation experiments.

Image acquisition and analysis

Image acquisition and analysis was performed as described in Chapter 3.

Statistical analyses

Statistical analyses were performed as described in Chapter 3.

5.5 Figures

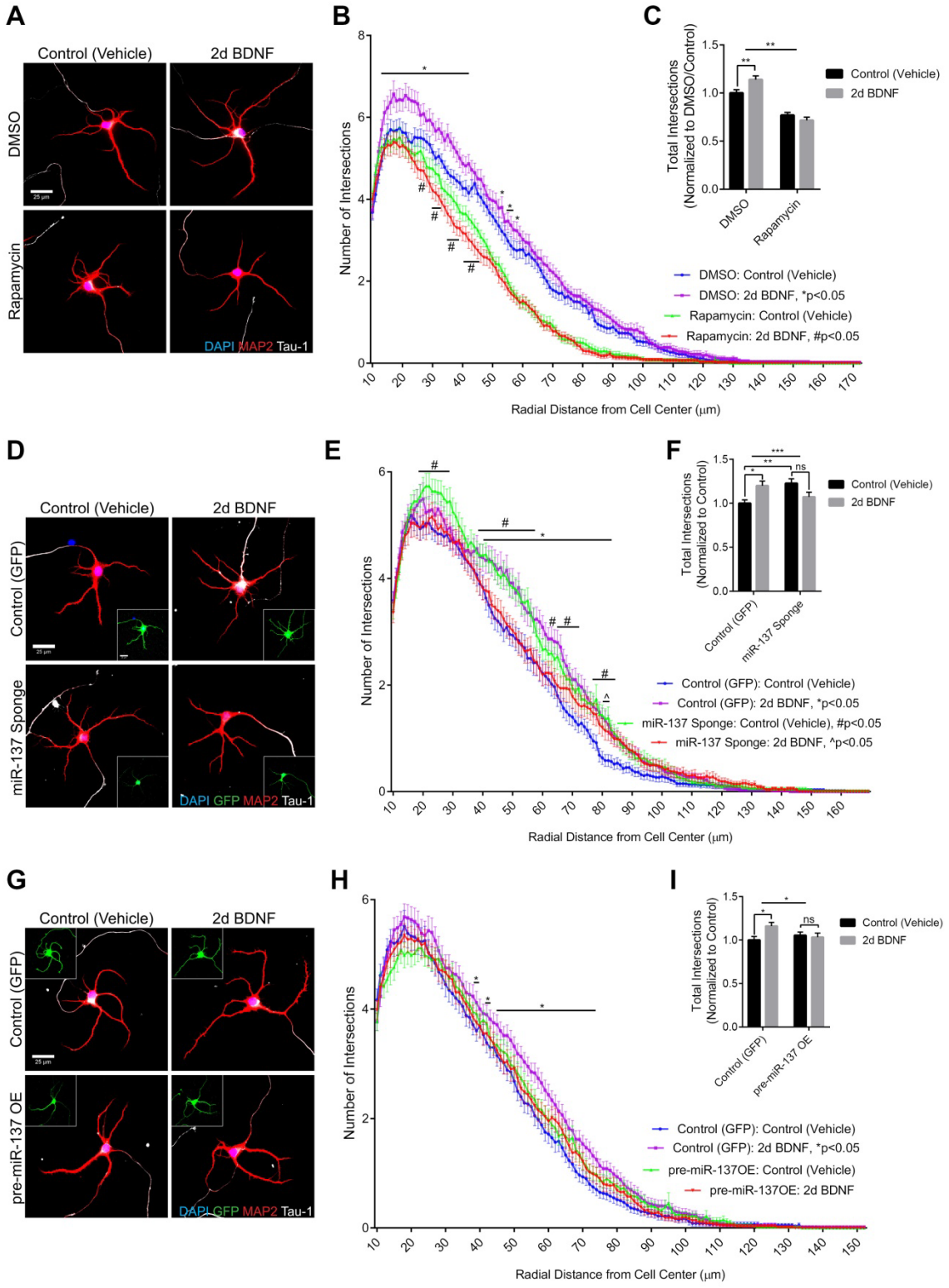
A
Control (Vehicle)
2d BDNF
DMSO
Rapamycin
DAPI MAP2 Tau-1
B
Number of Intersections
Radial Distance from Cell Center (μm)
DMSO: Control (Vehicle)
DMSO: 2d BDNF, *p<0.05
Rapamycin: Control (Vehicle)
Rapamycin: 2d BDNF, #p<0.05
C
Total Intersections (Normalized to DMSO/Control)
DMSO
Rapamycin
Control (Vehicle)
2d BDNF
D
Control (Vehicle)
2d BDNF
Control (GFP)
miR-137 Sponge
DAPI GFP MAP2 Tau-1
E
Number of Intersections
Radial Distance from Cell Center (μm)
Control (GFP): Control (Vehicle)
Control (GFP): 2d BDNF, *p<0.05
miR-137 Sponge: Control (Vehicle), #p<0.05
miR-137 Sponge: 2d BDNF, ^p<0.05
F
Total Intersections (Normalized to Control)
Control (GFP)
miR-137 Sponge
Control (Vehicle)
2d BDNF
G
Control (Vehicle)
2d BDNF
Control (GFP)
pre-miR-137 OE
DAPI GFP MAP2 Tau-1
H
Number of Intersections
Radial Distance from Cell Center (μm)
Control (GFP): Control (Vehicle)
Control (GFP): 2d BDNF, *p<0.05
pre-miR-137OE: Control (Vehicle)
pre-miR-137OE: 2d BDNF
I
Total Intersections (Normalized to Control)
Control (GFP)
pre-miR-137 OE
Control (Vehicle)
2d BDNF

Figure 5.1 BDNF stimulates dendritic outgrowth by an mTOR- and miR-137-dependent mechanism. (**A-C**) Co-treatment with rapamycin blocks BDNF-induced dendritic outgrowth in DIV4 primary hippocampal neurons. Representative neurons are shown in **A**. Quantification of dendritic complexity by Sholl analysis is shown in **B** (intersections vs distance from cell center; Sidak's test, *p<0.05: DMSO/BNDF vs DMSO/Control, #p<0.05: Rapamycin/BDNF vs Rapamycin/Control; n=60 cells/condition from 3 biological replicates) and **C** (total number of intersections, normalized to DMSO/Control; Two-way ANOVA, p(rapamycin)<0.0001, **p(interactive)<0.0041; Sidak's test, **p<0.01; n=60 cells/condition from 3 biological replicates). (**D-F**) Inhibition of miR-137 blocks BDNF-induced dendritic outgrowth in DIV4 primary hippocampal neurons. Representative neurons are shown in **D**. Quantification of dendritic complexity by Sholl analysis is shown in **E** (intersections vs distance from cell center; Sidak's test, *p<0.05: Control/BDNF vs Control/Control (Vehicle), #p<0.05: miR-137 Sponge/Control (Vehicle) vs Control/Control (Vehicle), ^p<0.05: miR-137 Sponge/BDNF vs Control/Control (Vehicle); n=59-60 cells/condition from 3 biological replicates) and **F** (total number of intersections, normalized to Control (GFP/Vehicle); Two-way ANOVA, ***p(interactive)=0.0004; Sidak's test, *p<0.05, **p<0.01; n=59-60 cells/condition from 3 biological replicates). (**G-I**) Overexpression of pre-miR-137 blocks BDNF-induced dendritic outgrowth in DIV4 primary hippocampal neurons. Representative neurons are shown in **G**. Quantification of dendritic complexity by Sholl analysis is shown in **H** (intersections vs distance from cell center; Sidak's test, *p<0.05: Control/BNDF vs Control/Control (Vehicle); n=60 cells/condition from 3 biological replicates) and **I** (total number of intersections, normalized to Control (GFP/Vehicle); Two-way ANOVA, *p(interactive)=0.0334; Sidak's test, *p<0.05; n=60 cells/condition from 3 biological replicates). Data are shown as mean ± SEM. Scale bars are 25 μm.

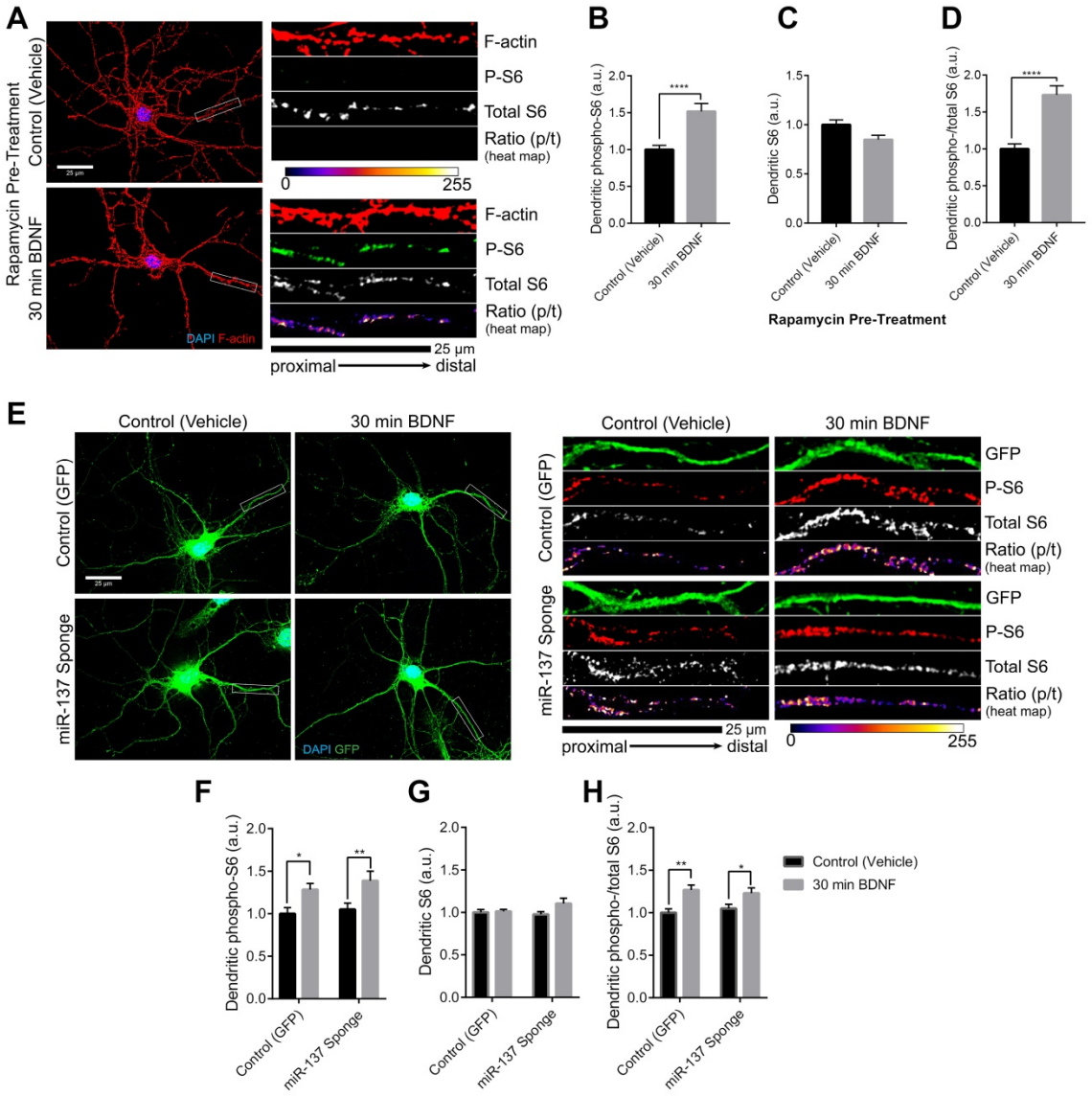

Figure 5.2 BDNF stimulates S6 phosphorylation by an mTOR- and miR-137-independent mechanism. (**A-D**) BDNF-induced S6 phosphorylation (Ser235/236) is not dependent on mTORC1 in DIV7 primary hippocampal neurons. Neurons were treated with rapamycin for 30 min prior to the addition of BDNF. Representative neurons are shown in **A**. Quantification of dendritic phospho-S6 is shown in **B** (student's t-test, ****p<0.0001, n=58-60 cells/condition from 3 biological replicates). Quantification of total dendritic S6 is shown in **C** (student's t-test, not significant, n=58-60 cells/condition from 3 biological replicates). The ratio of phospho- to total dendritic S6 is shown in **D** (student's t-test, ****p<0.0001, n=58-60 cells/condition from 3

biological replicates). (**E-H**) Inhibition of miR-137 does not affect BNDF-induced S6 phosphorylation (Ser235/236) in DIV7-9 primary hippocampal neurons. Representative neurons are shown in **E**. Quantification of dendritic phospho-S6 is shown in **F** (Two-way ANOVA, $p(BNDF)<0.001$; Sidak's test, $*p<0.05$, $**p<0.01$; n=59-60 cells/condition from 3 biological replicates). Quantification of total dendritic S6 is shown in **G** (Two-way ANOVA, not significant, n=59-60 cells/condition from 3 biological replicates). The ratio of phospho- to total dendritic S6 is shown in **H** (Two-way ANOVA, $p(BDNF)<0.0001$; Sidak's test, $*p<0.05$, $**p<0.01$; n=59-60 cells/condition from 3 biological replicates). Data are shown as mean ± SEM. Scale bars are 25 μm.

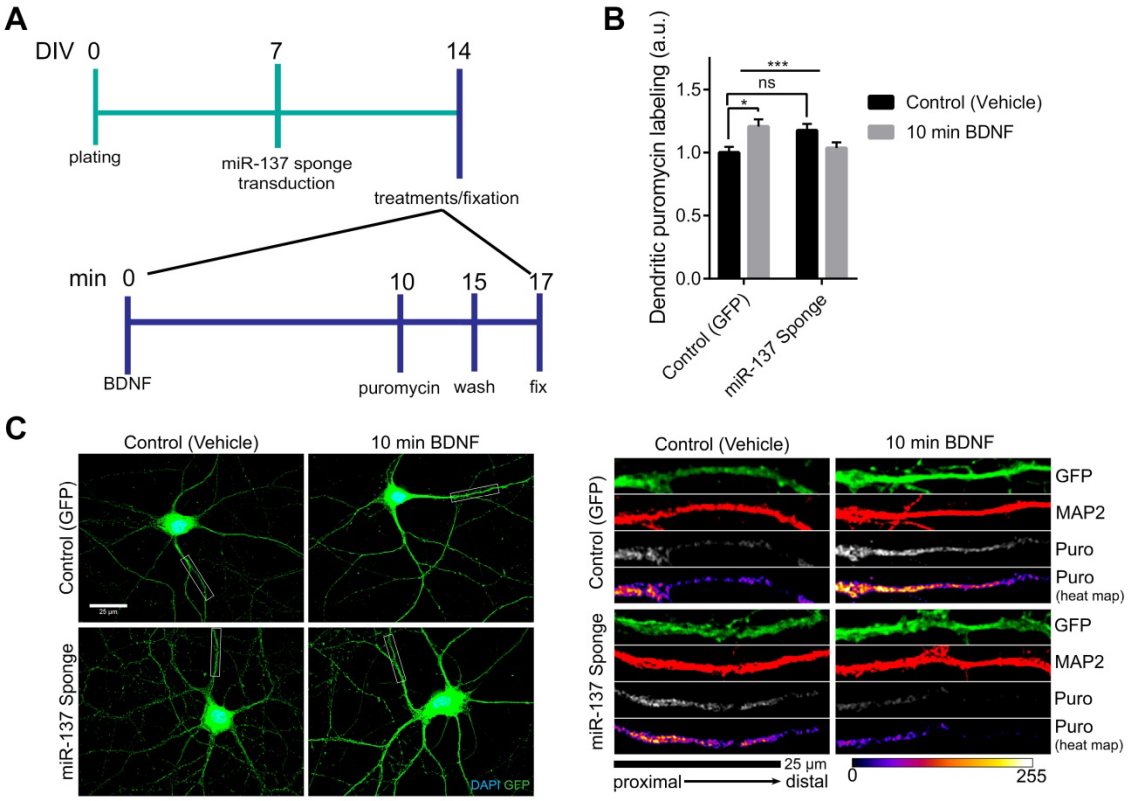

Figure 5.3 BDNF stimulates mRNA translation in dendrites by a miR-137-dependent mechanism. (**A**) This experimental timeline applies to the experiments in (**B-C**). Neurons were treated for 10 min with BDNF prior to puromycylation of nascent proteins. Representative neurons are shown in **B**. Quantification of dendritic puromycylation is shown in **C** (Two-way ANOVA, ***p(interactive)=0.0007; Sidak's test, *p<0.05; n=60 cells/condition from 3 biological replicates). Data are shown as mean ± SEM. Scale bars are 25 µm.

5.6 Supplemental Figures

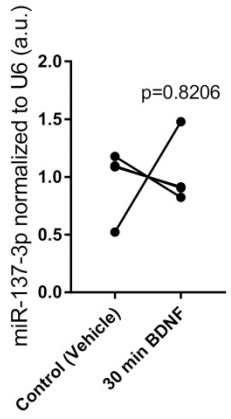

Supplemental Figure 5.1 30 min treatment with BDNF does not affect miR-137 levels in cortical neurons. DIV7 primary cortical neurons were treated 30 min with BDNF before lysis in Trizol (paired t-test, not significant, n=4). Individual data points and pairings are shown.

Chapter 6

General Discussion

Portions of this chapter were adapted from the following manuscript:

Thomas, K.T., Anderson, B.R., Shah, N., Zimmer, S., Hawkins, D., Gu, Q., and Bassell. G.J. (2017). Inhibition of the schizophrenia-associated microRNA miR-137 disrupts Nrg1α neurodevelopmental signal transduction. Cell Rep., Revision Under Review.

6.1 Summary

In the present study, we tested the hypothesis that miR-137 regulates PI3K-Akt-mTOR-dependent responses to Nrg/ErbB neurodevelopmental signaling. We found that miR-137 regulates the levels of key proteins within the PI3K-Akt-mTOR pathway, specifically the PI3K regulatory subunit p55γ, PTEN, Akt2, GSK3β, rictor, and mTOR. Some of these appear to be encoded by mRNA targets of miR-137. We found that inhibition of miR-137 blocks Nrg1α-induced increases in phospho-S6, mRNA translation, and GluA1 synthesis in the dendrites of primary hippocampal neurons and also blocks Nrg1α-induced dendritic outgrowth. Furthermore, inhibition of miR-137 blocks mTORC1-dependent responses to BDNF, specifically mRNA translation and dendritic outgrowth, while leaving mTORC1-independent S6 phosphorylation intact. By contrast, we found no evidence that Nrg1α or BDNF signaling regulates miR-137 activity. Together, these results suggest that miR-137 regulates responses to multiple signaling ligands but may selectively regulate the PI3K-Akt-mTOR branch of Nrg/ErbB and neurotrophin signaling.

6.2 A novel role for miR-137 in neuronal signaling and neurodevelopment

In Chapter 1, we explored the multifaceted roles of miR-137 in neuronal signaling. Specifically within the context of signaling at a glutamatergic synapse, miR-137 may regulate signal transduction through a variety of mechanisms. First, miR-137 inhibits the trafficking of glutamate-containing vesicles within the axon terminus by inhibiting the synthesis of Cplx1, Nsf, Syn3, and Syt1 (Siegert et al., 2015). At the surface of the postsynaptic neuron, miR-137 inhibits the expression of GluA1, GluN2A, and perhaps other surface proteins, such as ErbB4, which modulate glutamatergic signaling (Olde Loohuis et al., 2015; Vallès et al., 2014; Zhao et al., 2013). The work presented in this dissertation demonstrates that miR-137 also regulates signal transduction downstream of ErbB and neurotrophin receptors by targeting proteins within the

PI3K-Akt-mTOR pathway. In **Fig. 6.1**, we propose a new model for miR-137-dependent regulation of neuronal signaling.

6.3 Significance for schizophrenia and other neurodevelopmental disorders

Without examining miR-137 within the context of disease models, we can only speculate whether our findings have true significance for schizophrenia and other neurodevelopmental disorders. However, our finding that miR-137 regulates pathways implicated in neurodevelopmental disease suggest that dysregulation of miR-137 may lead to dysregulation of these pathways *in vivo* and thus contribute to the etiology of these disorders.

6.3.1 miR-137 and 1p21.3 microdeletion syndrome

The rare 1p21.3 microdeletion syndrome is caused by the hemizygous loss of miR-137 and results in intellectual disability and/or autism in most patients (Willemsen et al., 2011). We found that inhibition of miR-137 blocks Nrg1α and BDNF signaling in primary neurons, suggesting that the reduction of miR-137 observed in patients with 1p21.3 microdeletions may interfere with Nrg and BDNF signaling and contribute to neurological defects in these patients. The loss of Nrg- and BDNF-induced dendritic outgrowth, for example, may contribute to structural defects in the brains of microdeletion carriers. Histology experiments have not been conducted on the brains of 1p21.3 microdeletion patients, however, so it is unknown whether such defects occur. The loss of miR-137 was also previously shown to enhance presynaptic LTP in mossy fiber-CA1 synapses in mouse models and to inhibit postsynaptic LTD in CA1-CA3 synapses (Olde Loohuis et al., 2015; Siegert et al., 2015). Our findings suggest that defects in Nrg and BDNF signal transduction caused by the loss of miR-137 may further contribute to defects in hippocampal synaptic plasticity and thereby contribute cognitive deficits in 1p21.3 microdeletion patients.

6.3.2 miR-137 and schizophrenia

Our data suggest several mechanisms by which miR-137 might contribute to the etiology of schizophrenia. As previously discussed, it is unclear whether miR-137 gain- or loss-of-function contribute to schizophrenia, but our data suggest that either might be disruptive to Nrg or BDNF signaling in neurons. First, miR-137 might contribute to schizophrenia by targeting proteins within the PI3K-Akt-mTOR pathway. Variants in the human *AKT3* gene have been linked to schizophrenia in recent studies (Ripke et al., 2014). Furthermore, the antipsychotic haloperidol may work, in part, through the stimulation of mTORC1 signaling, and inhibition of the p110δ subunit of PI3K rescues cognitive defects in a mouse model of schizophrenia (Bonito-Oliva et al., 2013; Papaleo et al., 2016). Together these studies suggest that defects in PI3K-Akt-mTOR signaling may contribute to schizophrenia and that pharmacological manipulation of this pathway may have therapeutic potential for the treatment of schizophrenia. Our data in Chapter 2 suggest that dysregulation of miR-137 may contribute to dysregulation PI3K-Akt-mTOR signaling in schizophrenia patients.

miR-137 may also contribute to schizophrenia by disrupting Nrg/ErbB signaling. As discussed in Chapter 3, genetic studies have repeatedly linked genes encoding Nrgs and the ErbB family of receptors to schizophrenia, suggesting that dysregulation of Nrg/ErbB signaling contributes to schizophrenia (Mei and Nave, 2014). Our data in Chapter 3 suggest that dysregulation of miR-137 may disrupt neuronal responses to Nrg/ErbB signaling, even in the absence of genetic risk factors at Nrg or ErbB loci.

Genetic studies have also linked *GRIA1* to schizophrenia (Ripke et al., 2014). In Chapter 4, we demonstrated that miR-137 directly targets mouse *Gria1* mRNA and that inhibition of miR-137 blocks Nrg1α-induced GluA1 synthesis. Dysregulation of miR-137 may thus contribute to dysregulation of GluA1 in the absence of genetic risk factors at the *GRIA1* locus by two mechanisms: through the dysregulation of miR-137 and *GRIA1* mRNA interactions and through the dysregulation of Nrg1α-induced GluA1 synthesis. GluA1 protein synthesis is also tightly

controlled by synaptic signaling, suggesting dysregulation of GluA1 protein synthesis may contribute to synaptic dysfunction in schizophrenia patients.

Similarly, BDNF-induced protein synthesis is critical for several forms of synaptic plasticity. In Chapter 5, we demonstrated that inhibition of miR-137 blocks BDNF-induced protein synthesis in the dendrite of primary hippocampal neurons. Furthermore, inhibition or overexpression of miR-137 blocked BDNF-induced dendrite outgrowth, suggesting that dysregulation of miR-137 may contribute to structural defects in the brains of schizophrenia through the dysregulation of BDNF signaling. Similarly, GluA1 and Nrg/ErbB signaling also regulate dendritic outgrowth. Dysregulation of miR-137 may contribute to structural defects through the dysregulation of GluA1 expression or Nrg/ErbB signaling as well.

Finally, as discussed in Chapter 1 several recent neuroimaging studies suggest that the total genetic risk contributed through risk variants at *MIR137* and miR-137 target genes may shed light on how miR-137 contributes to schizophrenia etiology (Cosgrove et al., 2017; Wright et al., 2016). Our observation that miR-137 regulates PI3K-Akt-mTOR dependent responses to Nrg/ErbB and BDNF signaling suggests that genetic risk at loci associated with these pathways may also interact with genetic risk at the *MIR137* locus in schizophrenia etiology. Additional human studies, like those described in Wright et al., 2016 and Cosgrove et al., 2017, are needed to test this hypothesis, however.

6.3.3 miR-137 and Fragile X Syndrome

Our data suggest that miR-137 regulates BDNF and Nrg/ErbB signaling through a common mechanism: through the targeting of proteins within the PI3K-Akt-mTOR pathway. The PI3K-Akt-mTOR pathway responds to a number of other receptor pathways that have been linked to neurodevelopmental disorders including Fragile X Syndrome (FXS), which is associated with disruption of group 1 mGluR signaling. The mGluR theory of FXS postulates that the loss of FMRP enhances mGluR-dependent protein synthesis and causes enhanced long term synaptic

depression in the hippocampus of FXS patients (Bear et al., 2004). FMRP represses the translation of several proteins within the PI3K pathway that mediate neuronal responses to mGluR signaling, and the loss of FMRP enhances mTORC1 signaling under basal conditions and blocks mGluR-induced stimulation of protein synthesis in neurons derived from FXS model mice (Gross et al., 2010, 2015a, Muddashetty et al., 2007, 2011; Weiler et al., 2004). Kovács et al., 2014 also demonstrated that Nrg1-induced Akt phosphorylation is ablated in peripheral B lymphoblasts derived from FXS patients, whereas Nrg1-induced Erk phosphorylation is intact. This suggests that the loss of FMRP may specifically disrupt PI3K-Akt-mTOR-dependent responses to Nrg1 signaling, as we observed with the loss of miR-137. Whether Nrg signaling is disrupted in FXS model mice is currently unknown but may be an interesting direction for future research. Furthermore, the similarity between the consequences of miR-137 and FMRP loss suggest that they may contribute to neurodevelopmental disease through related mechanisms. Notably, both 1p21.3 microdeletion syndrome and FXS are associated with intellectual disability and the increased risk of autism (Carter et al., 2011; Tsiouris and Brown, 2004; Willemsen et al., 2011). It is possible that dysregulation of miR-137 aggravates signaling deficits in FXS patients, or conversely that the enhancement of miR-137 activity may rescue signaling defects in FXS patients by restoring normal PI3K-Akt-mTOR signaling.

In the following sections, we will describe a series of experiments that could be used to further explore how miR-137 might contribute to the etiology of 1p21.3 microdeletion syndrome, schizophrenia, Fragile X Syndrome, and other neurodevelopmental disorders. We will also propose experiments to further explore the mechanism by which inhibition of miR-137 disrupts PI3K-Akt-mTOR signaling.

6.4 Future Directions

6.4.1 Examine the regulation of neuronal signaling by miR-137 in disease models

In the present study, we used primary cortical and hippocampal neurons derived from wild-type mice to examine the consequences of miR-137 overexpression and inhibition on neuronal signaling. However, a number of additional model systems may be useful for examining the effects of miR-137 manipulation within a neurodevelopmental disease context. We will now explore potential model systems for specifically examining the role of miR-137 in 1p21.3 microdeletion syndrome, schizophrenia, and Fragile X Syndrome.

miR-137 levels are significantly reduced in LCLs derived from patients with 1p21.3 microdeletion syndrome, since these patients only possess one functional copy of the *MIR137* gene (Willemsen et al., 2011). This suggests that miR-137 may also be reduced within the brains of patients; however, postmortem brain tissue is not currently available from 1p21.3 patients. Recent attempts to generate a *MIR137* knockout mouse have revealed that complete miR-137 knockout is embryonic lethal in mice (Crowley et al., 2015). By contrast, heterozygous mice, which possess one functional copy of the miR-137 gene, are phenotypically normal and possess normal levels of miR-137. Therefore, these mice may be a poor model system for studying 1p21.3 microdeletion syndrome. However, an alternative mouse model might be to inhibit miR-137 through viral vectors containing a miR-137 sponge, similar to the vectors we used in Chapters 3-5, or to inhibit miR-137 using LNA inhibitors, similar to our approach in Chapter 2 but with LNA inhibitors modified for *in vivo* use. In addition, cell lines may be generated from 1p21.3 microdeletion patients and compared to cell lines generated from neurotypical subjects. For example, fibroblasts may be acquired from patients, converted to induced pluripotent stem cells (iPSCs) and differentiated into cortical neurons. If neurons derived from 1p21.3 microdeletion patients display reduced levels of miR-137, then these neurons could be used in experiments similar to those described in this dissertation to assess the integrity of PI3K-Akt-

mTOR, Nrg/ErbB, and BDNF signaling and assess whether signaling defects contribute to 1p21.3 microdeletion associated neurological phenotypes.

Because controversy surrounds whether miR-137 gain- or loss-of-function contributes to schizophrenia, modeling miR-137 dysfunction in schizophrenia is less straightforward. One option is to generate iPSC-derived neurons from schizophrenia patients and control subjects, sequence the *MIR137* locus in each subject, measure miR-137 levels, and examine the effects of schizophrenia diagnosis and genotype on neuronal signaling. The effects of miR-137 overexpression and inhibition may also be assessed within existing schizophrenia mouse models. For example, Papaleo et al., 2016 recently described a transgenic mouse model that overexpresses Nrg1-IV that displays cognitive deficits reminiscent of schizophrenia that are reversible by p110δ inhibitors. miR-137 overexpression or inhibition in these mice might exacerbate or rescue these deficits by further altering Nrg/ErbB signaling and might shed further light on interactions between miR-137 and the Nrg/ErbB signaling pathway in schizophrenia etiology.

Fmr1 knockout mice are a well-established model for Fragile X Syndrome, and primary neuronal cultures may be generated from these knockout mice and used to examine miR-137 in the absence of FMRP, the protein encoded by *Fmr1*. miR-137 might be examined with two purposes in mind: 1) to determine whether miR-137 dysregulation contributes to FXS disease etiology, and 2) to determine whether targeting miR-137 might have some therapeutic benefit.

Basal miR-137 expression has not been assessed within this model system or within the brains of *Fmr1* knockout mice, and if miR-137 expression is dysregulation, it might contribute to signaling and synaptic defects associated with FXS. FMRP also regulates miRNA interactions with target mRNAs (Muddashetty et al., 2011), so it is possible that miR-137 targeting is disrupted in FXS and contributes to aberrant protein synthesis.

Alternatively, targeting miR-137 might be useful for rescuing FXS deficits associated with aberrant LTD. Olde Loohuis et al., 2015 reported that mGluR5 signaling transiently increases miR-137 levels in primary hippocampal neurons, suggesting that both miR-137 and

FMRP are necessary for normal mGluR signaling and normal expression of LTD. Overexpression of miR-137 might also reduce the availability of target proteins such as Akt2 that enhance PI3K-Akt-mTOR signaling, thereby normalizing PI3K-Akt-mTOR signaling downstream of mGluR receptors. However, miR-137 also targets mRNAs that encode proteins such as PTEN that inhibit PI3K-Akt-mTOR signaling, so overexpression of miR-137 might also exacerbate phenotypes caused by the loss of FMRP. Alternatively, miR-137 overexpression is necessary for the expression of LTD in the hippocampus (Olde Loohuis et al 2015), and LTD is enhanced in the hippocampus of *Fmr1* knockout mice. Inhibition of miR-137 might, therefore, rescue hippocampal LTD in *Fmr1* knockout mice.

6.4.2 Explore the relationship between miR-137 and FMRP

Exploring the relationship between miR-137 and FMRP has obvious significance for the study of Fragile X Syndrome, but it also may be particularly relevant to understanding schizophrenia etiology. As we noted previously, Nrg1-induced Akt phosphorylation is ablated in peripheral B lymphoblasts derived from Fragile X Syndrome patients (Kovács et al., 2014), and defects in Nrg1 signaling are strongly linked to schizophrenia (Mei and Nave, 2014). FMRP levels are reduced in the cerebella and peripheral blood lymphocytes of schizophrenia patients who lack disruptive *FMR1* mutations, suggesting FMRP may be dysregulated in schizophrenia (Fatemi et al., 2010, 2013; Kelemen et al., 2013; Kovács et al., 2014). In schizophrenia patients, genes that encode mRNA targets of FMRP are also enriched with rare, disruptive mutations (Purcell et al., 2014). Folsom et al., 2015 also observed reduced expression of several FMRP targets, e.g. STEP, in the cerebella of schizophrenia patients. Together, these studies suggest that dysregulation of FMRP may contribute to schizophrenia etiology.

First, future research might examine whether FMRP regulates Nrg signaling in neurons. To do so, the experiments described in Chapters 3 and 4 might be repeated with neurons derived from *Fmr1* knockout mice or in neurons in which FMRP has been knocked down by siRNA or

overexpressed using plasmids. We predict that FMRP loss-of-function will mimic the effects of miR-137 inhibition, disrupt PI3K-Akt-mTOR signaling, and ablate Nrg-induced induced increases in phospho-S6, mRNA translation, GluA1 synthesis, and dendritic outgrowth.

Dysregulation of the mGluR pathway as a result of the loss of FMRP is well-documented (Bear et al., 2004; Gross et al., 2010; Muddashetty et al., 2007; Niere et al., 2012). We found that miR-137 regulates PI3K-Akt-mTOR-dependent signaling downstream of Nrg/ErbB and BDNF. We propose that PI3K-Akt-mTOR-dependent responses to mGluR signaling will also be blocked by inhibition of miR-137. By repeating the acute stimulation experiments described in Chapter 3, future research might examine the effects of inhibition of miR-137 on mGluR signal transduction. We predict that inhibition of miR-137 will ablate mGluR-induced increases in dendritic phospho-S6 and dendritic protein synthesis.

Also, FMRP co-immunoprecipitation experiments should be used to determine whether miR-137 and FMRP associate in mouse brain and cultured neurons. We predict that miR-137 and FMRP share mRNA targets and may cooperate or compete to regulate the translation of these targets. FMRP phosphorylation might also regulate miR-137 binding to mRNA targets as described for FMRP and miR-125a by Muddashetty et al., 2011. The loss of FMRP might ablate signaling induced changes in miR-137 activity by such a mechanism. Conversely, miR-137 might be necessary for FMRP-mediated translational repression of some mRNA targets and for the induction of protein synthesis in response to mGluR, Nrg/ErbB, and other signaling cascades. In either case, the identification of common mRNA target of miR-137 and FMRP might suggest common molecular mechanisms underlying intellectual disability and autism associated with 1p21.3 microdeletion syndrome and Fragile X Syndrome and perhaps underlying schizophrenia etiology as well.

Finally, we propose that FMRP and miR-137 interactions should be examined within the context of PI3K-Atk-mTOR and mGluR signaling. Both pathways appear to require FMRP and miR-137 activity for normal signal transduction. Both FMRP and miR-137 target mRNAs that

encode proteins within the PI3K-Akt-mTOR pathway that regulate mGluR signal transduction. Both are regulated by changes in mGluR signaling: FMRP is dephosphorylated in response to mGluR signaling whereas miR-137 levels are increased by mGluR signaling (Narayanan et al., 2007; Olde Loohuis et al., 2015). One interesting possibility is if mGluR signaling causes a selective increase in FMRP target synthesis while selectively inhibiting miR-137 target synthesis, thus providing an additional layer of selectivity in mGluR-induced protein synthesis. This selectivity could be elucidated using proteomic analysis of primary neurons following mGluR stimulation in the presence of FMRP and miR-137 gain- and loss-of-function.

6.4.3 Identify the mechanism by which miR-137 disrupts PI3K-Akt-mTOR signaling

In Chapter 2, we demonstrated that miR-137 regulates the protein levels of p55γ, PTEN, Akt2, GSK3β, mTOR, and rictor. This suggests that miR-137 regulates PI3K-Akt-mTOR signaling by directly targeting mRNAs that encode proteins within the pathway. However, we did not identify the specific mechanism by which miR-137 disrupts signaling. For this purpose, we propose the following series of experiments.

First, we propose to assess Nrg-induced changes in phosphatidylinositol(PtdIns)(3,4,5)P_3 in neurons in which miR-137 is overexpressed and inhibited. miR-137 targeting of p55γ and PTEN may have opposing effects on PtdIns(3,4,5)P_3, with p55γ stimulating phosphorylation and PTEN opposing. PtdIns(3,4,5)P_3 levels may be assessed by western blot (Gross et al., 2010) and should elucidate whether miR-137 regulates basal phosphorylation (whether miR-137 effects on p55γ or PTEN "win") and whether Nrg1-induced phosphorylation is intact in neurons with miR-137 gain- or loss-of-function.

The phosphorylation states of proteins at each stage of PI3K-Akt-mTOR may also be assessed by western blot or quantitative immunofluorescence using antibodies specific to phospho-proteins. The stage at which Nrg-induced phosphorylation is impaired should suggest where in the pathway signal transduction fails. For example, if Nrg-induced Akt phosphorylation

is intact in neurons expressing the miR-137 sponge but the Nrg-induced phosphorylation for mTORC1 components is impaired, this would suggest that miR-137 specifically inhibits Nrg-induced changes in mTOR activity. We would then focus on this stage of the pathway for further experiments.

We might also assess Nrg signal transduction using rescue experiments. For example, if we determine that Nrg-induced Akt phosphorylation is intact in neurons in which miR-137 is inhibited but Nrg-induced stimulation of mTORC1 activity is not, we might hypothesize that inhibition of miR-137 inhibits mTORC1 activity by increasing GSK3β and/or rictor activity. We could then inhibit GSK3β or mTORC2 activity using small molecule inhibitors or siRNA-mediated knockdown of the target protein. If Nrg-induced activation of mTORC1 is then restored, this would support our hypothesis that increased GSK3β or rictor activity disrupts Nrg signal transduction in neurons in which miR-137 is inhibited.

Target protectors might also prove useful for assessing Nrg signal transduction. Target protectors are modified single stranded RNAs that shield a specific miRNA binding site on a specific target mRNA from miRNA mediated regulation without affecting miRNA interactions with other targets(Choi et al., 2007). In theory, we could develop target protectors for the miRNA binding site for each protein within the PI3K-Akt-mTOR pathway, then assess Nrg signaling integrity. If, for example, the target protector specific for the miR-137 target site(s) in the *GSK3B*-3'UTR disrupted Nrg signaling, while others left signaling intact, this would suggest that inhibition of miR-137 blocks Nrg/ErbB signal transduction specifically through the dysregulation of GSK3β synthesis.

If the mechanism(s) by which miR-137 regulates Nrg/ErbB and BDNF signaling were successfully identified, these findings might be applied to models of neurodevelopmental diseases associated with dysregulation of miR-137. This might yield further insight into the role of miR-137 in neurodevelopmental disease etiology. If we could successfully rescue signaling deficits in

animal models, we might then be closer to our ultimate goal: the development of novel therapies for patients with miR-137-associated disorders.

miRNA-based therapeutic strategies have been increasingly explored in recent years. miRNA mimics and antagomirs may be used to increase or inhibit miRNA activity, respectively, though these strategies face significant technical challenges (Bader and Lammers, 2012; Ishida and Selaru, 2013). The miR-122 inhibitor RG-101 is currently in Phase II clinical trials for the treatment of hepatitis C, however, suggesting that miRNAs may be viable therapeutic targets (van der Ree et al., 2017). Targeting of miR-137 in schizophrenia may not be a useful strategy as no clear up- or downregulation of miR-137 has been observed in schizophrenia patients. However, we predict that restoration of miR-137 in 1p21.3 patients may improve neurological symptoms. Alternatively, miRNAs often target mRNAs that encode proteins that may serve as therapeutic targets themselves. miR-137's targeting of the mTOR pathway may be of particular interest, since several drugs have been approved to target mTOR in human cancer patients (AlQurashi et al., 2013; Don and Zheng, 2011). Further research is needed to elucidate the roles of miR-137 in brain function before we can really begin to explore miR-137-based therapies.

6.5 Concluding Remarks

The results presented here demonstrate a novel requirement for miR-137 in neurodevelopmental signal transduction. We found that miR-137 regulates the levels of proteins within the PI3K-Atk-mTOR pathway. Inhibition of miR-137 ablates Nrg1α-induced increases in dendritic phospho-S6, mRNA translation, GluA1 synthesis, and outgrowth. Furthermore, inhibition of miR-137 blocks BDNF-induced changes in mTORC1-dependent responses, i.e. mRNA translation and dendritic outgrowth, while leaving mTORC1-independent S6 phosphorylation intact. Our results demonstrate a novel mechanism by which dysregulation of miR-137 might contribute to neurodevelopmental disease etiology: through the dysregulation of PI3K-Akt-mTOR, Nrg/ErbB, and BDNF signaling. This work, therefore, has important

implications for our understanding of neurodevelopmental disorders associated with miR-137 dysregulation.

6.6 Figures

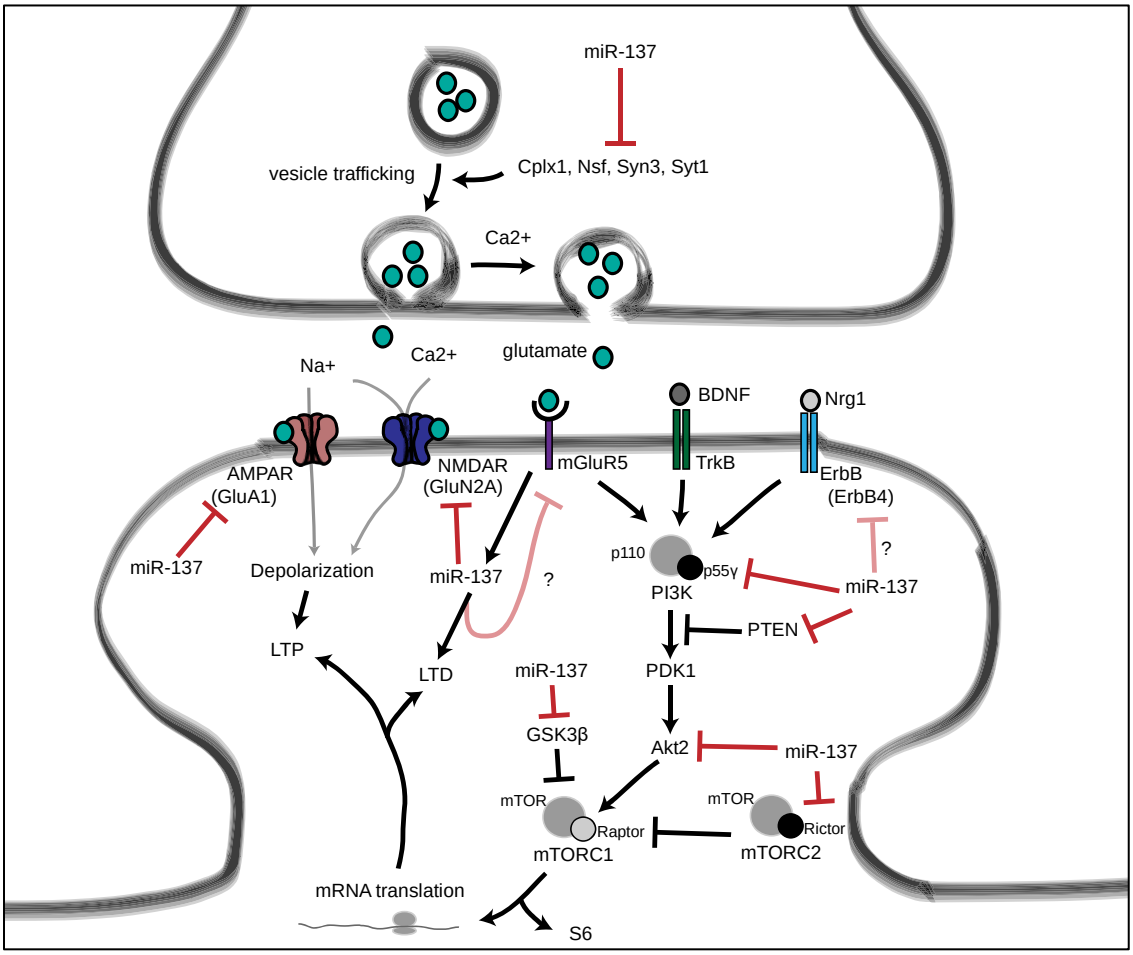

Figure 6.1 Proposed roles for miR-137 at the glutamatergic synapse

The figure above summarizes the findings of Siegert et al., 2015, Olde Loohuis et al., 2015, Zhao et al., 2013, and this dissertation. We propose that miR-137 regulates presynaptic signaling by regulating vesicle trafficking in the axon terminus. miR-137 also regulates GluA1 and GluN2A protein levels, and bioinformatics predictions suggest that miR-137 may also target mGluR5 and ErbB4. mGluR5 signaling, in turn, increases miR-137 levels. We found that miR-137 also regulates proteins within the PI3K-Akt-mTOR pathway, e.g. p55γ, to regulate neuronal responses to BDNF and Nrg1 signaling. We propose that miR-137 may also regulates PI3K-Akt-mTOR signaling downstream of mGluR receptors as well.

References

Abe, Y., Namba, H., Kato, T., Iwakura, Y., and Nawa, H. (2011). Neuregulin-1 signals from the periphery regulate AMPA receptor sensitivity and expression in GABAergic interneurons in developing neocortex. J. Neurosci. *31*, 5699–5709.

Alisch, R.S., Jin, P., Epstein, M., Caspary, T., and Warren, S.T. (2007). Argonaute2 is essential for mammalian gastrulation and proper mesoderm formation. PLoS Genet. *3*, 2565–2571.

AlQurashi, N., Hashimi, S., and Wei, M. (2013). Chemical Inhibitors and microRNAs (miRNA) Targeting the Mammalian Target of Rapamycin (mTOR) Pathway: Potential for Novel Anticancer Therapeutics. Int. J. Mol. Sci. *14*, 3874–3900.

Angelucci, F., Brenè, S., and Mathé, a a (2005). BDNF in schizophrenia, depression and corresponding animal models. Mol. Psychiatry *10*, 345–352.

Angelucci, F., Gruber, S.H.M., El Khoury, A., Tonali, P.A., and Mathé, A.A. (2007). Chronic amphetamine treatment reduces NGF and BDNF in the rat brain. Eur. Neuropsychopharmacol. *17*, 756–762.

Ashraf, S.I., McLoon, A.L., Sclarsic, S.M., and Kunes, S. (2006). Synaptic protein synthesis associated with memory is regulated by the RISC pathway in Drosophila. Cell *124*, 191–205.

Audesirk, G., Cabell, L., and Kern, M. (1997). Modulation of neurite branching by protein phosphorylation in cultured rat hippocampal neurons. Dev. Brain Res. *102*, 247–260.

Autry, A.E., and Monteggia, L.M. (2012). Brain-derived neurotrophic factor and neuropsychiatric disorders. Pharmacol Rev *64*, 238–258.

Babiarz, J.E., Ruby, J.G., Wang, Y., Bartel, D.P., and Blelloch, R. (2008). Mouse ES cells express endogenous shRNAs , siRNAs , and other Microprocessor-independent, Dicer-dependent small RNAs. 2773–2785.

Bader, A.G., and Lammers, P. (2012). The Therapeutic Potential of microRNAs. Innov. Pharm. Technol. 52–55.

Ballas, N., and Mandel, G. (2005). The many faces of REST oversee epigenetic programming of neuronal genes. Curr. Opin. Neurobiol. *15*, 500–506.

Banerjee, S., Neveu, P., and Kosik, K.S. (2009). A Coordinated Local Translational Control Point at the Synapse Involving Relief from Silencing and MOV10 Degradation. Neuron *64*, 871–884.

Bao, J., Wolpowitz, D., Role, L.W., and Talmage, D.A. (2003). Back signaling by the Nrg-1 intracellular domain. J. Cell Biol. *161*, 1133–1141.

Bao, J., Lin, H., Ouyang, Y., Lei, D., Osman, A., Kim, T.-W.W., Mei, L., Dai, P., Ohlemiller, K.K., and Ambron, R.T. (2004). Activity-dependent transcription regulation of {PSD-95} by neuregulin-1 and Eos. Nat. Neurosci. *7*, 1250–1258.

Barkus, C., Sanderson, D.J., Rawlins, J.N.P., Walton, M.E., Harrison, P.J., and Bannerman, D.M. (2014). What causes aberrant salience in schizophrenia? A role for impaired short-term habituation and the GRIA1 (GluA1) AMPA receptor subunit. Mol. Psychiatry *19*, 1060–1070.

Bartel, D.P. (2009). MicroRNAs: Target Recognition and Regulatory Functions. Cell *136*, 215–233.

Bassell, G.J., and Warren, S.T. (2008). Fragile X Syndrome: Loss of Local mRNA Regulation Alters Synaptic Development and Function. Neuron *60*, 201–214.

Baudry, A., Mouillet-Richard, S., Schneider, B., Launay, J.-M., and Kellermann, O. (2010). MiR-16 Targets the Serotonin Transporter: A New Facet for Adaptive Responses to Antidepressants. Science (80-.). *329*, 1537–1541.

Bear, M.F., Huber, K.M., and Warren, S.T. (2004). The mGluR theory of fragile X mental retardation. Trends Neurosci. *27*, 370–377.

Behm-Ansmant, I., Rehwinkel, J., Doerks, T., Stark, A., Bork, P., and Izaurralde, E. (2006). mRNA degradation by miRNAs and GW182 requires both CCR4:NOT deadenylase and DCP1:DCP2 decapping complexes. Genes Dev. *20*, 1885–1898.

Berezikov, E., Chung, W.J., Willis, J., Cuppen, E., and Lai, E.C. (2007). Mammalian Mirtron Genes. Mol. Cell *28*, 328–336.

Bernstein, H.-G., and Bogerts, B. (2013). Neuregulin-1 alpha, the underestimated molecule: emerging new roles in normal brain function and the pathophysiology of schizophrenia? Genome *56*, 703–704.

Bernstein, H.-G., Lendeckel, U., Bertram, I., Bukowska, A., Kanakis, D., Dobrowolny, H., Stauch, R., Krell, D., Mawrin, C., Budinger, E., et al. (2006). Localization of neuregulin-1α (heregulin-α) and one of its receptors, ErbB-4 tyrosine kinase, in developing and adult human brain. Brain Res. Bull. *69*, 546–559.

Bernstein, H.-G., Stricker, R., Dobrowolny, H., Steiner, J., Bogerts, B., Trübner, K., and Reiser, G. (2013). Nardilysin in human brain diseases: both friend and foe. Amino Acids *45*, 269–278.

Bertram, I., Bernstein, H.-G., Lendeckel, U., Bukowska, A., Dobrowolny, H., Keilhoff, G., Kanakis, D., Mawrin, C., Bielau, H., Falkai, P., et al. (2007). Immunohistochemical Evidence for Impaired Neuregulin-1 Signaling in the Prefrontal Cortex in Schizophrenia and in Unipolar Depression. Ann. N. Y. Acad. Sci. *1096*, 147–156.

Bicker, S., Khudayberdiev, S., Weiß, K., Zocher, K., Baumeister, S., and Schratt, G. (2013). The DEAH-box helicase DHX36 mediates dendritic localization of the neuronal precursor-microRNA-134. Genes Dev. *27*, 991–996.

Biswas, A.B., and Furniss, F. (2016). Cognitive phenotype and psychiatric disorder in 22q11.2 deletion syndrome: A review. Res. Dev. Disabil. *53–54*, 242–257.

Bohnsack, M.T., Czaplinski, K., and Gorlich, D. (2004). Exportin 5 is a RanGTP-dependent dsRNA-binding protein that mediates nuclear export of pre-miRNAs. RNA *10*, 185–191.

Bonito-Oliva, A., Pallottino, S., Bertran-Gonzalez, J., Girault, J.A., Valjent, E., and Fisone, G. (2013). Haloperidol promotes mTORC1-dependent phosphorylation of ribosomal protein S6 via dopamine- and cAMP-regulated phosphoprotein of 32 kDa and inhibition of

protein phosphatase-1. Neuropharmacology *72*, 197–203.

Borchert, G.M., Lanier, W., and Davidson, B.L. (2006). RNA polymerase III transcribes human microRNAs. Nat. Struct. Mol. Biol. *13*, 1097–1101.

Bowling, H., Zhang, G., Bhattacharya, A., Pérez-cuesta, L.M., Hoeffer, C.A., Neubert, T.A., Gan, W., Klann, E., Bowling, H., Zhang, G., et al. (2014). Antipsychotics activate mTORC1-dependent translation to enhance neuronal morphological complexity. *7*, 1–15.

Bredt, D.S., and Nicoll, R.A. (2003). AMPA Receptor Trafficking at Excitatory Synapses. Neuron *40*, 361–379.

Broadbelt, K., Byne, W., and Jones, L.B. (2002). Evidence for a decrease in basilar dendrites of pyramidal cells in schizophrenic medial prefrontal cortex. *58*, 75–81.

Cahill, M.E., Jones, K.A., Rafalovich, I., Xie, Z., Barros, C.S., Müller, U., and Penzes, P. (2012). Control of interneuron dendritic growth through NRG1/erbB4-mediated kalirin-7 disinhibition. Mol. Psychiatry *17*, 99–107.

Cahill, M.E., Remmers, C., Jones, K.A., Xie, Z., Sweet, R.A., and Penzes, P. (2013). Neuregulin1 signaling promotes dendritic spine growth through kalirin. J. Neurochem. *126*, 625–635.

Cai, X., Hagedorn, C.H., and Cullen, B.R. (2004). Human microRNAs are processed from capped, polyadenylated transcripts that can also function as mRNAs. RNA *10*, 1957–1966.

Cajigas, I.J., Tushev, G., Will, T.J., Tom Dieck, S., Fuerst, N., and Schuman, E.M. (2012). The Local Transcriptome in the Synaptic Neuropil Revealed by Deep Sequencing and High-Resolution Imaging. Neuron *74*, 453–466.

Caputo, V., Sinibaldi, L., Fiorentino, A., Parisi, C., Catalanotto, C., Pasini, A., Cogoni, C., and Pizzuti, A. (2011). Brain derived neurotrophic factor (BDNF) expression is regulated by microRNAs miR-26a and miR-26b allele-specific binding. PLoS One *6*.

Carter, M., Nikkel, S., Fernandez, B., Marshall, C., Noor, A., Lionel, A., Prasad, A., Pinto, D., Joseph-George, A., Noakes, C., et al. (2011). Hemizygous deletions on chromosome

1p21.3 involving the DPYD gene in individuals with autism spectrum disorder. Clin. Genet. *80*, 435–443.

Chamak, B., Fellous, A., Glowinski, J., and Prochiantz, A. (1987). MAP2 expression and neuritic outgrowth and branching are coregulated through region-specific neuro-astroglial interactions. J. Neurosci. *7*, 3163–3170.

Chang, Q., Khare, G., Dani, V., Nelson, S., and Jaenisch, R. (2006). The disease progression of Mecp2 mutant mice is affected by the level of BDNF expression. Neuron *49*, 341–348.

Chatterjee, S., and Grosshans, H. (2009). Active turnover modulates mature microRNA activity in Caenorhabditis elegans. Nature *461*, 546–549.

Cheloufi, S., Dos Santos, C.O., Chong, M.M., and Hannon, G.J. (2010). A dicer-independent miRNA biogenesis pathway that requires Ago catalysis. Nature *465*, 584–589.

Chen, Y.L., and Shen, C.K. (2013). Modulation of mGluR-dependent MAP1B translation and AMPA receptor endocytosis by microRNA miR-146a-5p. J Neurosci *33*, 9013–9020.

Chen, C., Jeon, S., Bhaskar, P.T., Nogueira, V., Tonic, I., Park, Y., and Hay, N. (2011). FoxOs inhibit mTORC1 and activate Akt by inducing the expression of Sestrin3 and Rictor. Dev. Cell *18*, 592–604.

Chen, L., Zheng, H., and Zhang, S. (2016a). Involvement of upregulation of miR-210 in a rat epilepsy model. Neuropsychiatr. Dis. Treat. *12*, 1731–1737.

Chen, T., Wu, Q., Zhang, Y., Lu, T., Yue, W., and Zhang, D. (2016b). Tcf4 Controls Neuronal Migration of the Cerebral Cortex through Regulation of Bmp7. Front. Mol. Neurosci. *9*, 1–9.

Chendrimada, T.P., Gregory, R.I., Kumaraswamy, E., Norman, J., Cooch, N., Nishikura, K., and Shiekhattar, R. (2005). TRBP recruits the Dicer complex to Ago2 for microRNA processing and gene silencing. Nature *436*, 740–744.

Cheng, Y., Li, Y., Liu, D., Zhang, R., and Zhang, J. (2014). MiR-137 effects on gastric carcinogenesis are mediated by targeting Cox-2-activated PI3K/AKT signaling pathway.

FEBS Lett. *588*, 3274–3281.

Choi, W.-Y., Giraldez, A.J., and Schier, A.F. (2007). Target protectors reveal dampening and balancing of Nodal agonist and antagonist by miR-430. Science (80-.). *318*, 271–275.

Chun, S., Westmoreland, J.J., Bayazitov, I.T., Eddins, D., Pani, A.K., Smeyne, R.J., Yu, J., Blundon, J.A., and Zakharenko, S.S. (2014). Specific disruption of thalamic inputs to the auditory cortex in schizophrenia models. Science (80-.). *344*, 1178–1182.

Chun, S., Du, F., Westmoreland, J.J., Han, S.B., Wang, Y.-D., Eddins, D., Bayazitov, I.T., Devaraju, P., Yu, J., Mellado Lagarde, M.M., et al. (2016). Thalamic miR-338-3p mediates auditory thalamocortical disruption and its late onset in 22q11.2 microdeletion models. Nat. Med. *23*, 1–39.

Cifuentes, D., Xue, H., Taylor, D.W., Patnode, H., Mishima, Y., Cheloufi, S., Ma, E., Mane, S., Hannon, G.J., Lawson, N.D., et al. (2010). A novel miRNA processing pathway independent of Dicer requires Argonaute2 catalytic activity. Science *328*, 1694–1698.

Connor, C.M., Guo, Y., and Akbarian, S. (2009). Cingulate White Matter Neurons in Schizophrenia and Bipolar Disorder. Biol. Psychiatry *66*, 486–493.

Corcoran, D.L., Pandit, K. V., Gordon, B., Bhattacharjee, A., Kaminski, N., and Benos, P. V. (2009). Features of mammalian microRNA promoters emerge from polymerase II chromatin immunoprecipitation data. PLoS One *4*, 1–10.

Cosgrove, D., Harold, D., Mothersill, O., Anney, R., Hill, M.J., Bray, N.J., Blokland, G., Petryshen, T., Donnelly, P., Bates, L., et al. (2017). MiR-137-derived polygenic risk: effects on cognitive performance in patients with schizophrenia and controls. Transl. Psychiatry *7*, e1012.

Courter, L.A., Shaffo, F.C., Ghogha, A., Parrish, D.J., Lorentz, C.U., Habecker, B.A., and Lein, P.J. (2016). BMP7-induced dendritic growth in sympathetic neurons requires p75NTR signaling. Dev. Neurobiol. *76*, 1003–1013.

Cousijn, H., Eissing, M., Fernández, G., Fisher, S.E., Franke, B., Zwiers, M., Harrison, P.J., and

Arias-Vásquez, A. (2014). No effect of schizophrenia risk genes MIR137, TCF4, and ZNF804A on macroscopic brain structure. Schizophr. Res. *159*, 329–332.

Coyle, J.T. (2006). Glutamate and schizophrenia: beyond the dopamine hypothesis. Cell. Mol. Neurobiol. *26*, 365–384.

Crino, P.B. (2016). The mTOR signalling cascade: paving new roads to cure neurological disease. Nat. Rev. Neurol. *12*, 379–392.

Crowley, J.J., Collins, A.L., Lee, R.J., Nonneman, R.J., Farrell, M.S., Ancalade, N., Mugford, J.W., Agster, K.L., Nikolova, V.D., Moy, S.S., et al. (2015). Disruption of the MicroRNA 137 Primary Transcript Results in Early Embryonic Lethality in Mice. Biol. Psychiatry *77*, e5–e7.

Cummings, E., Donohoe, G., Hargreaves, A., Moore, S., Fahey, C., Dinan, T.G., McDonald, C., O'Callaghan, E., O'Neill, F.A., Waddington, J.L., et al. (2013). Mood congruent psychotic symptoms and specific cognitive deficits in carriers of the novel schizophrenia risk variant at MIR-137. Neurosci. Lett. *532*, 33–38.

Dajas-Bailador, F., Bonev, B., Garcez, P., Stanley, P., Guillemot, F., and Papalopulu, N. (2012). microRNA-9 regulates axon extension and branching by targeting Map1b in mouse cortical neurons. Nat. Neurosci. *15*, 697–699.

Denli, A.M., Tops, B.B.J., Plasterk, R.H. a, Ketting, R.F., and Hannon, G.J. (2004). Processing of primary microRNAs by the Microprocessor complex. Nature *432*, 231–235.

Djukic, A., Holtzer, R., Shinnar, S., Muzumdar, H., Rose, S.A., Mowrey, W., Galanopoulou, A.S., Shinnar, R., Jankowski, J.J., Feldman, J.F., et al. (2016). Pharmacologic Treatment of Rett Syndrome With Glatiramer Acetate. Pediatr. Neurol. *61*, 51–57.

Don, A.S.A., and Zheng, X.F.S. (2011). Recent clinical trials of mTOR-targeted cancer therapies. Rev. Recent Clin. Trials *6*, 24–35.

Duan, J., Shi, J., Fiorentino, A., Leites, C., Chen, X., Moy, W., Chen, J., Alexandrov, B.S., Usheva, A., He, D., et al. (2014). A rare functional noncoding variant at the GWAS-

Implicated MIR137/MIR2682 locus might confer risk to schizophrenia and bipolar disorder. Am. J. Hum. Genet. *95*, 744–753.

Earls, L.R., Fricke, R.G., Yu, J., Berry, R.B., Baldwin, L.T., and Zakharenko, S.S. (2012). Age-Dependent MicroRNA Control of Synaptic Plasticity in 22q11 Deletion Syndrome and Schizophrenia. J. Neurosci. *32*, 14132–14144.

Easow, G., Teleman, A.A., and Cohen, S.M. (2007). Isolation of microRNA targets by miRNP immunopurification. RNA *13*, 1198–1204.

Eckert, J.M., Byer, S.J., Clodfelder-Miller, B.J., and Carroll, S.L. (2009). Neuregulin-1β and neuregulin-1α differentially affect the migration and invasion of malignant peripheral nerve sheath tumor cells. Glia *57*, 1501–1520.

Edbauer, D., Neilson, J.R., Foster, K.A., Wang, C.F., Seeburg, D.P., Batterton, M.N., Tada, T., Dolan, B.M., Sharp, P.A., and Sheng, M. (2010). Regulation of Synaptic Structure and Function by FMRP-Associated MicroRNAs miR-125b and miR-132. Neuron *65*, 373–384.

Ender, C., Krek, A., Friedländer, M.R., Beitzinger, M., Weinmann, L., Chen, W., Pfeffer, S., Rajewsky, N., and Meister, G. (2008). A Human snoRNA with MicroRNA-Like Functions. Mol. Cell *32*, 519–528.

English, J.A., Fan, Y., Föcking, M., Lopez, L.M., Hryniewiecka, M., Wynne, K., Dicker, P., Matigian, N., Cagney, G., Mackay-Sim, A., et al. (2015). Reduced protein synthesis in schizophrenia patient-derived olfactory cells. Transl. Psychiatry *5*, e663.

van Erp, T.G.M., Guella, I., Vawter, M.P., Turner, J., Brown, G.G., McCarthy, G., Greve, D.N., Glover, G.H., Calhoun, V.D., Lim, K.O., et al. (2014). Schizophrenia miR-137 Locus Risk Genotype Is Associated with Dorsolateral Prefrontal Cortex Hyperactivation. Biol. Psychiatry *75*, 398–405.

Eulalio, A., Tritschler, F., and Izaurralde, E. (2009). The GW182 protein family in animal cells: new insights into domains required for miRNA-mediated gene silencing. RNA *15*, 1433–

1442.

Fabian, M.R., Mathonnet, G., Sundermeier, T., Mathys, H., Zipprich, J.T., Svitkin, Y. V., Rivas, F., Jinek, M., Wohlschlegel, J., Doudna, J.A., et al. (2009). Mammalian miRNA RISC Recruits CAF1 and PABP to Affect PABP-Dependent Deadenylation. Mol. Cell *35*, 868–880.

Fabian, M.R., Sonenberg, N., and Filipowicz, W. (2010). Regulation of mRNA translation and stability by microRNAs. Annu. Rev. Biochem. *79*, 351–379.

Fatemi, S.H., Kneeland, R.E., Liesch, S.B., and Folsom, T.D. (2010). Fragile X mental retardation protein levels are decreased in major psychiatric disorders. Schizophr. Res. *124*, 246–247.

Fatemi, S.H., Folsom, T.D., Rooney, R.J., and Thuras, P.D. (2013). mRNA and protein expression for novel GABAA receptors θ and ρ2 are altered in schizophrenia and mood disorders; relevance to FMRP-mGluR5 signaling pathway. Transl. Psychiatry *3*, e271.

Filipowicz, W., Bhattacharyya, S.N., and Sonenberg, N. (2008). Mechanisms of post-transcriptional regulation by microRNAs: are the answers in sight? Nat Rev Genet *9*, 102–114.

Fiore, R., Khudayberdiev, S., Christensen, M., Siegel, G., Flavell, S.W., Kim, T.K., Greenberg, M.E., and Schratt, G. (2009). Mef2-mediated transcription of the miR379-410 cluster regulates activity-dependent dendritogenesis by fine-tuning Pumilio2 protein levels. Embo J *28*, 697–710.

Folsom, T.D., Thuras, P.D., and Fatemi, S.H. (2015). Protein expression of targets of the FMRP regulon is altered in brains of subjects with schizophrenia and mood disorders. Schizophr. Res. *165*, 201–211.

Fortin, D.A., Davare, M.A., Srivastava, T., Brady, J.D., Nygaard, S., Derkach, V.A., and Soderling, T.R. (2010). Long-Term Potentiation-Dependent Spine Enlargement Requires Synaptic Ca 2 ∂ -Permeable AMPA Receptors Recruited by CaM-Kinase I. *30*, 11565–

11575.

Fortin, D.A., Srivastava, T., Dwarakanath, D., Pierre, P., Nygaard, S., Derkach, V.A., and Soderling, T.R. (2012). Brain-derived neurotrophic factor activation of CaM-kinase kinase via transient receptor potential canonical channels induces the translation and synaptic incorporation of GluA1-containing calcium-permeable AMPA receptors. J. Neurosci. *32*, 8127–8137.

Franke, K., Otto, W., Johannes, S., Baumgart, J., Nitsch, R., and Schumacher, S. (2012). miR-124-regulated RhoG reduces neuronal process complexity via ELMO/Dock180/Rac1 and Cdc42 signalling. EMBO J. *31*, 2908–2921.

Garcia, R.A., Vasudevan, K., and Buonanno, A. (2000). The neuregulin receptor ErbB-4 interacts with PDZ-containing proteins at neuronal synapses. Proc. Natl. Acad. Sci. U. S. A. *97*, 3596–3601.

Gerecke, K.M., Wyss, J.M., and Carroll, S.L. (2004). Neuregulin-1beta induces neurite extension and arborization in cultured hippocampal neurons. Mol. Cell. Neurosci. *27*, 379–393.

Giraldez, A.J., Cinalli, R.M., Glasner, M.E., Enright, A.J., Thomson, J.M., Baskerville, S., Hammond, S.M., Bartel, D.P., and Schier, A.F. (2005). MicroRNAs regulate brain morphogenesis in zebrafish. Science (80-.). *308*, 833–838.

Giusti, S. a, Vogl, A.M., Brockmann, M.M., Vercelli, C. a, Rein, M.L., Trümbach, D., Wurst, W., Cazalla, D., Stein, V., Deussing, J.M., et al. (2014). MicroRNA-9 controls dendritic development by targeting REST. Elife *3*, 1–22.

Golden, R.J., Chen, B., Li, T., Braun, J., Manjunath, H., Chen, X., Wu, J., Schmid, V., Chang, T.-C., Kopp, F., et al. (2017). An Argonaute phosphorylation cycle promotes microRNA-mediated silencing. Nature 1–6.

Gong, R., Park, C.S., Abbassi, N.R., and Tang, S.-J. (2006). Roles of glutamate receptors and the mammalian target of rapamycin (mTOR) signaling pathway in activity-dependent dendritic protein synthesis in hippocampal neurons. J. Biol. Chem. *281*, 18802–18815.

Graber, T.E., Hébert-Seropian, S., Khoutorsky, A., David, A., Yewdell, J.W., Lacaille, J.-C., and Sossin, W.S. (2013). Reactivation of stalled polyribosomes in synaptic plasticity. Proc. Natl. Acad. Sci. U. S. A. *110*, 1–6.

Greco, S.J., and Rameshwar, P. (2007). MicroRNAs regulate synthesis of the neurotransmitter substance P in human mesenchymal stem cell-derived neuronal cells. Proc. Natl. Acad. Sci. U. S. A. *104*, 15484–15489.

Green, M.J., Matheson, S.L., Shepherd, a, Weickert, C.S., and Carr, V.J. (2011). Brain-derived neurotrophic factor levels in schizophrenia: a systematic review with meta-analysis. Mol. Psychiatry *16*, 960–972.

Gregory, R.I., Yan, K.-P., Amuthan, G., Chendrimada, T., Doratotaj, B., Cooch, N., and Shiekhattar, R. (2004). The Microprocessor complex mediates the genesis of microRNAs. Nature *432*, 235–240.

Gregory, R.I., Chendrimada, T.P., Cooch, N., and Shiekhattar, R. (2005). Human RISC couples microRNA biogenesis and posttranscriptional gene silencing. Cell *123*, 631–640.

Gross, C., and Bassell, G.J. (2014). Neuron-specific regulation of class I PI3K catalytic subunits and their dysfunction in brain disorders. Front. Mol. Neurosci. *7*, 12.

Gross, C., Nakamoto, M., Yao, X., Chan, C.-B., Yim, S.Y., Ye, K., Warren, S.T., and Bassell, G.J. (2010). Excess phosphoinositide 3-kinase subunit synthesis and activity as a novel therapeutic target in fragile X syndrome. J. Neurosci. *30*, 10624–10638.

Gross, C., Chang, C.W., Kelly, S.M., Bhattacharya, A., McBride, S.M.J., Danielson, S.W., Jiang, M.Q., Chan, C.B., Ye, K., Gibson, J.R., et al. (2015a). Increased Expression of the PI3K Enhancer PIKE Mediates Deficits in Synaptic Plasticity and Behavior in Fragile X Syndrome. Cell Rep. *11*, 727–736.

Gross, C., Raj, N., Molinaro, G., Allen, A.G., Whyte, A.J., Gibson, J.R., Huber, K.M., Gourley, S.L., and Bassell, G.J. (2015b). Selective Role of the Catalytic PI3K Subunit p110β in Impaired Higher Order Cognition in Fragile X Syndrome. Cell Rep. *11*, 681–688.

Gross, C., Yao, X., Engel, T., Tiwari, D., Xing, L., Rowley, S., Danielson, S.W., Thomas, K.T., Jimenez-Mateos, E.M., Schroeder, L.M., et al. (2016). MicroRNA-Mediated Downregulation of the Potassium Channel Kv4.2 Contributes to Seizure Onset. Cell Rep. *17*, 37–45.

Gu, S., Jin, L., Zhang, F., Sarnow, P., and Kay, M.A. (2009). Biological basis for restriction of microRNA targets to the 3' untranslated region in mammalian mRNAs. Nat Struct Mol Biol *16*, 144–150.

Guella, I., Sequeira, A., Rollins, B., Morgan, L., Torri, F., van Erp, T.G.M., Myers, R.M., Barchas, J.D., Schatzberg, A.F., Watson, S.J., et al. (2013). Analysis of miR-137 expression and rs1625579 in dorsolateral prefrontal cortex. J. Psychiatr. Res. *47*, 1215–1221.

Guo, C., Sah, J.F., Beard, L., Willson, J.K. V., Markowitz, S.D., and Guda, K. (2008). The noncoding RNA, miR-126, suppresses the growth of neoplastic cells by targeting phosphatidylinositol 3-kinase signaling and is frequently lost in colon cancers. Genes, Chromosom. Cancer *47*, 939–946.

Guo, W., Polich, E.D., Su, J., Gao, Y., Christopher, D.M., Allan, A.M., Wang, M., Wang, F., Wang, G., and Zhao, X. (2015). Fragile X Proteins FMRP and FXR2P Control Synaptic GluA1 Expression and Neuronal Maturation via Distinct Mechanisms. Cell Rep. *11*, 1651–1666.

Haijma, S. V., Van Haren, N., Cahn, W., Koolschijn, P.C.M.P., Hulshoff Pol, H.E., and Kahn, R.S. (2013). Brain volumes in schizophrenia: A meta-analysis in over 18 000 subjects. Schizophr. Bull. *39*, 1129–1138.

Han, J.M., and Sahin, M. (2011). TSC1/TSC2 signaling in the CNS. FEBS Lett. *585*, 973–980.

Han, J., Lee, Y., Yeom, K., Kim, Y., Jin, H., and Kim, V.N. (2004). The Drosha – DGCR8 complex in primary microRNA processing. Genes Dev. 3016–3027.

Han, L., Wen, Z., Lynn, R.C., Baudet, M.-L., Holt, C.E., Sasaki, Y., Bassell, G.J., and Zheng,

J.Q. (2011). Regulation of chemotropic guidance of nerve growth cones by microRNA. Mol. Brain *4*, 40.

Hancock, M.L., Preitner, N., Quan, J., and Flanagan, J.G. (2014). MicroRNA-132 is enriched in developing axons, locally regulates Rasa1 mRNA, and promotes axon extension. J. Neurosci. *34*, 66–78.

Harada, A., Teng, J., Takei, Y., Oguchi, K., and Hirokawa, N. (2002). MAP2 is required for dendrite elongation, PKA anchoring in dendrites, and proper PKA signal transduction. J. Cell Biol. *158*, 541–549.

Hassan, T., Smith, S.G.J., Gaughan, K., Oglesby, I.K., O'Neill, S., McElvaney, N.G., and Greene, C.M. (2013). Isolation and identification of cell-specific microRNAs targeting a messenger RNA using a biotinylated anti-sense oligonucleotide capture affinity technique. Nucleic Acids Res. *41*, 1–13.

Hauberg, M.E., Roussos, P., Grove, J., Børglum, A.D., and Mattheisen, M. (2016). Analyzing the Role of MicroRNAs in Schizophrenia in the Context of Common Genetic Risk Variants. JAMA Psychiatry *73*, 369–377.

Hawkins, P.T., Anderson, K.E., Davidson, K., and Stephens, L.R. (2006). Signalling through Class I PI3Ks in mammalian cells. Biochem. Soc. Trans. *34*, 647–662.

He, M., Liu, Y., Wang, X., Zhang, M.Q., Hannon, G.J., and Huang, Z.J. (2012). Cell-Type-Based Analysis of MicroRNA Profiles in the Mouse Brain. Neuron *73*, 35–48.

Higa, G.S.V., De Sousa, E., Walter, L.T., Kinjo, E.R., Resende, R.R., and Kihara, A.H. (2014). MicroRNAs in neuronal communication. Mol. Neurobiol. *49*, 1309–1326.

Horman, S.R., Janas, M.M., Litterst, C., Wang, B., MacRae, I.J., Sever, M.J., Morrissey, D. V., Graves, P., Luo, B., Umesalma, S., et al. (2013). Akt-mediated phosphorylation of argonaute 2 downregulates cleavage and upregulates translational repression of MicroRNA targets. Mol. Cell *50*, 356–367.

Hu, Z., Zhao, J., Hu, T., Luo, Y., Zhu, J., and Li, Z. (2015). miR-501-3p mediates the activity-

dependent regulation of the expression of AMPA receptor subunit GluA1. J. Cell Biol. *208*, 949–959.

Huang, Y.W.A., Ruiz, C.R., Eyler, E.C.H., Lin, K., and Meffert, M.K. (2012). Dual regulation of miRNA biogenesis generates target specificity in neurotrophin-induced protein synthesis. Cell *148*, 933–946.

Hutvágner, G., McLachlan, J., Pasquinelli, A.E., Bálint, E., Tuschl, T., and Zamore, P.D. (2001). A cellular function for the RNA-interference enzyme Dicer in the maturation of the let-7 small temporal RNA. Science *293*, 834–838.

Iadevaia, V., Huo, Y., Zhang, Z., Foster, L.J., and Proud, C.G. (2012). Roles of the mammalian target of rapamycin, mTOR, in controlling ribosome biogenesis and protein synthesis. Biochem. Soc. Trans. *40*, 168–172.

Impey, S., Davare, M., Lasiek, A., Fortin, D., Ando, H., Varlamova, O., Obrietan, K., Soderling, T.R., Goodman, R.H., and Wayman, G.A. (2010). An activity-induced microRNA controls dendritic spine formation by regulating Rac1-PAK signaling. Mol. Cell. Neurosci. *43*, 146–156.

Irie, K., Tsujimura, K., Nakashima, H., and Nakashima, K. (2016). MicroRNA-214 promotes dendritic development by targeting the schizophrenia-associated gene quaking (Qki). J. Biol. Chem. *291*, 13891–13904.

Ishida, M., and Selaru, F.M. (2013). miRNA-Based Therapeutic Strategies. Curr. Anesthesiol. Rep. *1*, 63–70.

Jan, Y.-N., and Jan, L.Y. (2010). Branching out: mechanisms of dendritic arborization. Nat. Rev. Neurosci. *11*, 316–328.

Jin, P., Zarnescu, D.C., Ceman, S., Nakamoto, M., Mowrey, J., Jongens, T. a, Nelson, D.L., Moses, K., and Warren, S.T. (2004). Biochemical and genetic interaction between the fragile X mental retardation protein and the microRNA pathway. Nat. Neurosci. *7*, 113–117.

Johnstone, E.C., Frith, C.D., Crow, T.J., Husband, J., and Kreel, L. (1976). Cerebral Ventricular Size and Cognitive Impairment in Chronic Schizophrenia. Lancet *308*, 924–926.

Jovičić, A., Roshan, R., Moisoi, N., Pradervand, S., Moser, R., Pillai, B., and Luthi-Carter, R. (2013). Comprehensive expression analyses of neural cell-type-specific miRNAs identify new determinants of the specification and maintenance of neuronal phenotypes. Ann. Intern. Med. *158*, 5127–5137.

Ju, W., Morishita, W., Tsui, J., Gaietta, G., Deerinck, T.J., Adams, S.R., Garner, C.C., Tsien, R.Y., Ellisman, M.H., and Malenka, R.C. (2004). Activity-dependent regulation of dendritic synthesis and trafficking of AMPA receptors. Nat. Neurosci. *7*, 244–253.

Ka, M., Condorelli, G., Woodgett, J.R., and Kim, W.-Y. (2014). mTOR regulates brain morphogenesis by mediating GSK3 signaling. Development *141*, 4076–4086.

Kainulainen, V., Sundvall, M., Määttä, J.A., Santiestevan, E., Klagsbrun, M., and Elenius, K. (2000). A natural ErbB4 isoform that does not activate phosphoinositide 3-kinase mediates proliferation but not survival or chemotaxis. J. Biol. Chem. *275*, 8641–8649.

Kalus, P., Bondzio, J., Federspiel, A., Muller, T.J., and Zuschratter, W. (2002). Cell-type specific alterations of cortical interneurons in schizophrenic patients. *13*, 713–717.

Katoh, T., Sakaguchi, Y., Miyauchi, K., Suzuki, T., Suzuki, T., Kashiwabara, S.I., and Baba, T. (2009). Selective stabilization of mammalian microRNAs by 3’ adenylation mediated by the cytoplasmic poly(A) polymerase GLD-2. Genes Dev. *23*, 433–438.

Kedde, M., van Kouwenhove, M., Zwart, W., Oude Vrielink, J. a F., Elkon, R., and Agami, R. (2010). A Pumilio-induced RNA structure switch in p27-3’ UTR controls miR-221 and miR-222 accessibility. Nat. Cell Biol. *12*, 1014–1020.

Kelemen, O., Kovács, T., and Kéri, S. (2013). Contrast, motion, perceptual integration, and neurocognition in schizophrenia: The role of fragile-X related mechanisms. Prog. Neuro-Psychopharmacology Biol. Psychiatry *46*, 92–97.

Kim, A.H., Parker, E.K., Williamson, V., McMichael, G.O., Fanous, A.H., and Vladimirov, V.I.

(2012). Experimental validation of candidate schizophrenia gene ZNF804A as target for hsa-miR-137. Schizophr. Res. *141*, 60–64.

Kim, J., Krichevsky, A., Grad, Y., Hayes, G.D., Kosik, K.S., Church, G.M., and Ruvkun, G. (2004). Identification of many microRNAs that copurify with polyribosomes in mammalian neurons. Proc. Natl. Acad. Sci. U. S. A. *101*, 360–365.

Kim, W., Lee, Y., McKenna, N.D., Yi, M., Simunovic, F., Wang, Y., Kong, B., Rooney, R.J., Seo, H., Stephens, R.M., et al. (2014). MiR-126 contributes to Parkinson's disease by dysregulating the insulin-like growth factor/phosphoinositide 3-kinase signaling. Neurobiol. Aging *35*, 1712–1721.

Kim, W., Noh, H., Lee, Y., Jeon, J., Shanmugavadivu, A., McPhie, D.L., Kim, K.S., Cohen, B.M., Seo, H., and Sonntag, K.C. (2016). MiR-126 Regulates Growth Factor Activities and Vulnerability to Toxic Insult in Neurons. Mol. Neurobiol. *53*, 95–108.

Kinjo, E.R., Higa, G.S. V, Santos, B.A., de Sousa, E., Damico, M. V, Walter, L.T., Morya, E., Valle, A.C., Britto, L.R.G., and Kihara, A.H. (2016). Pilocarpine-induced seizures trigger differential regulation of microRNA-stability related genes in rat hippocampal neurons. Sci. Rep. *6*, 20969.

Kong, Y., Liang, X., Liu, L., Zhang, D., Wan, C., Gan, Z., and Yuan, L. (2015). High Throughput Sequencing Identifies MicroRNAs Mediating α-Synuclein Toxicity by Targeting Neuroactive-Ligand Receptor Interaction Pathway in Early Stage of Drosophila Parkinson's Disease Model. PLoS One *10*, e0137432.

Koshimizu, H., Hazama, S., Hara, T., Ogura, A., and Kojima, M. (2010). Distinct signaling pathways of precursor BDNF and mature BDNF in cultured cerebellar granule neurons. Neurosci. Lett. *473*, 229–232.

Kovács, T., Bánsági, B., Kelemen, O., and Kéri, S. (2014). Neuregulin 1-Induced AKT and ERK Phosphorylation in Patients with Fragile X Syndrome (FXS) and Intellectual Disability Associated with Obstetric Complications. J. Mol. Neurosci. *54*, 119–124.

Krichevsky, A.M., King, K.S., Donahue, C.P., Khrapko, K., and Kosik, K.S. (2004). A microRNA array reveals extensive regulation of microRNAs during brain development A microRNA array reveals extensive regulation of microRNAs during brain development. Rna 1274–1281.

Krivosheya, D., Tapia, L., Levinson, J.N., Huang, K., Kang, Y., Hines, R., Ting, A.K., Craig, A.M., Mei, L., Bamji, S.X., et al. (2008). ErbB4-neuregulin signaling modulates synapse development and dendritic arborization through distinct mechanisms. J. Biol. Chem. *283*, 32944–32956.

Krol, J., Busskamp, V., Markiewicz, I., Stadler, M.B., Ribi, S., Richter, J., Duebel, J., Bicker, S., Fehling, H.J., Schübeler, D., et al. (2010). Characterizing Light-Regulated Retinal MicroRNAs Reveals Rapid Turnover as a Common Property of Neuronal MicroRNAs. Cell *141*, 618–631.

van Kuilenburg, A.B.P., Meijer, J., Mul, A.N.P.M., Meinsma, R., Schmid, V., Dobritzsch, D., Hennekam, R.C.M., Mannens, M.M.A.M., Kiechle, M., Etienne-Grimaldi, M.-C., et al. (2010). Intragenic deletions and a deep intronic mutation affecting pre-mRNA splicing in the dihydropyrimidine dehydrogenase gene as novel mechanisms causing 5-fluorouracil toxicity. Hum. Genet. *128*, 529–538.

Kumar, V., Zhang, M., Swank, M.W., Kunz, J., and Wu, G. (2005). Regulation of dendritic morphogenesis by Ras–PI3K–Akt–mTOR and Ras–MAPK signaling pathways. *25*, 11288–11299.

Kundu, P., Fabian, M.R., Sonenberg, N., Bhattacharyya, S.N., and Filipowicz, W. (2012). HuR protein attenuates miRNA-mediated repression by promoting miRISC dissociation from the target RNA. Nucleic Acids Res. *40*, 5088–5100.

Kuswanto, C.N., Sum, M.Y., Qiu, A., Sitoh, Y.Y., Liu, J., and Sim, K. (2015). The impact of genome wide supported microRNA-137 (MIR137) risk variants on frontal and striatal white matter integrity, neurocognitive functioning, and negative symptoms in

schizophrenia. Am. J. Med. Genet. Part B Neuropsychiatr. Genet. *168*, 317–326.

Kwon, E., Wang, W., and Tsai, L.-H. (2011). Validation of schizophrenia-associated genes CSMD1, C10orf26, CACNA1C and TCF4 as miR-137 targets. Mol. Psychiatry *18*, 11–12.

Lagos-Quintana, M., Rauhut, R., Lendeckel, W., and Tuschl, T. (2001). Identification of novel genes Coding for RNAs of Small expressed RNAs. Science (80-.). *294*, 853–858.

Lagos-Quintana, M., Rauhut, R., Yalcin, A., Meyer, J., Lendeckel, W., and Tuschl, T. (2002). Identification of tissue-specific MicroRNAs from mouse. Curr. Biol. *12*, 735–739.

Lambert, T.J., Storm, D.R., and Sullivan, J.M. (2010). MicroRNA132 Modulates Short-Term Synaptic Plasticity but Not Basal Release Probability in Hippocampal Neurons. PLoS One *5*.

Landthaler, M., Yalcin, A., and Tuschl, T. (2004). The Human DiGeorge Syndrome Critical Region Gene 8 and Its D. melanogaster Homolog Are Required for miRNA Biogenesis. Curr. Biol. *14*, 2162–2167.

Laplante, M., and Sabatini, D.M. (2009). mTOR signaling at a glance. J Cell Sci *122*, 3589–3594.

Lau, A.G., Irier, H.A., Gu, J., Tian, D., Ku, L., Liu, G., Xia, M., Fritsch, B., Zheng, J.Q., Dingledine, R., et al. (2010). Distinct 3'UTRs differentially regulate activity-dependent translation of brain-derived neurotrophic factor (BDNF). Proc. Natl. Acad. Sci. *107*, 15945–15950.

Lau, N.C., Lim, L.P., Weinstein, E.G., and Bartel, D.P. (2001). An abundant class of tiny RNAs with probable regulatory roles in Caenorhabditis elegans. Science (80-.). *294*, 858–862.

Law, A.J., Wang, Y., Sei, Y., O'Donnell, P., Piantadosi, P., Papaleo, F., Straub, R.E., Huang, W., Thomas, C.J., Vakkalanka, R., et al. (2012). Neuregulin 1-ErbB4-PI3K signaling in schizophrenia and phosphoinositide 3-kinase-p110δ inhibition as a potential therapeutic strategy. Proc. Natl. Acad. Sci. U. S. A. *109*, 12165–12170.

Leal, G., Comprido, D., and Duarte, C.B. (2014). BDNF-induced local protein synthesis and

synaptic plasticity. Neuropharmacology *76*, 639–656.

Ledonne, a, Nobili, a, Latagliata, E.C., Cavallucci, V., Guatteo, E., Puglisi-Allegra, S., D'Amelio, M., and Mercuri, N.B. (2014). Neuregulin 1 signalling modulates mGluR1 function in mesencephalic dopaminergic neurons. Mol. Psychiatry 1–15.

Lee, R.C., and Ambros, V. (2001). An extensive class of small RNAs in Caenorhabditis elegans. Science *294*, 862–864.

Lee, H.Y., Zhou, K., Smith, A.M., Noland, C.L., and Doudna, J.A. (2013). Differential roles of human Dicer-binding proteins TRBP and PACT in small RNA processing. Nucleic Acids Res. *41*, 6568–6576.

Lee, R.C., Feinbaum, R.L., and Ambros, V. (1993). The C. elegans heterochronic gene lin-4 encodes small RNAs with antisense complementarity to lin-14. Cell *75*, 843–854.

Lee, S.-T., Chu, K., Jung, K.-H., Kim, J.H., Huh, J.-Y., Yoon, H., Park, D.-K., Lim, J.-Y., Kim, J.-M., Jeon, D., et al. (2012). miR-206 regulates brain-derived neurotrophic factor in Alzheimer disease model. Ann. Neurol. *72*, 269–277.

Lee, Y., Ahn, C., Han, J., Choi, H., Kim, J., Yim, J., Lee, J., Provost, P., Rådmark, O., Kim, S., et al. (2003). The nuclear RNase III Drosha initiates microRNA processing. Nature *425*, 415–419.

Lee, Y., Kim, M., Han, J., Yeom, K.-H., Lee, S., Baek, S.H., and Kim, V.N. (2004). MicroRNA genes are transcribed by RNA polymerase II. Embo J *23*, 4051–4060.

Lessmann, V., Gottmann, K., and Malcangio, M. (2003). Neurotrophin secretion: Current facts and future prospects. Prog. Neurobiol. *69*, 341–374.

Lett, T., Chakravarty, M., Chakavarty, M., Felsky, D., Brandl, E., Tiwari, A., Gonçalves, V., Rajji, T., Daskalakis, Z., Meltzer, H., et al. (2013). The genome-wide supported microRNA-137 variant predicts phenotypic heterogeneity within schizophrenia. Mol. Psychiatry *18*, 443–450.

Levine, E.S., Dreyfus, C.F., Black, I.B., and Plummer, M.R. (1995). Brain-derived neurotrophic

factor rapidly enhances synaptic transmission in hippocampal neurons via postsynaptic tyrosine kinase receptors. Proc. Natl. Acad. Sci. U. S. A. *92*, 8074–8077.

Li, M., and Su, B. (2013). Impact of the genome-wide schizophrenia risk single nucleotide polymorphism (rs1625579) in miR-137 on brain structures in healthy individuals. Psychiatr. Genet. *23*, 267.

Li, B., Woo, R.S., Mei, L., and Malinow, R. (2007). The Neuregulin-1 Receptor ErbB4 Controls Glutamatergic Synapse Maturation and Plasticity. Neuron *54*, 583–597.

Li, C.J., Chang, J.K., Wang, G.J., and Ho, M.L. (2011). Constitutively expressed COX-2 in osteoblasts positively regulates Akt signal transduction via suppression of PTEN activity. Bone *48*, 286–297.

Li, W., Xu, X., and Pozzo-Miller, L. (2016). Excitatory synapses are stronger in the hippocampus of Rett syndrome mice due to altered synaptic trafficking of AMPA-type glutamate receptors. Proc. Natl. Acad. Sci. 201517244.

Liu, J., Carmell, M.A., Rivas, F. V, Marsden, C.G., Thomson, J.M., Song, J.-J., Hammond, S.M., Joshua-Tor, L., and Hannon, G.J. (2004). Argonaute2 is the catalytic engine of mammalian RNAi. Science *305*, 1437–1441.

Liu, L.-L., Lu, S.-X., Li, M., Li, L.-Z., Fu, J., Hu, W., Yang, Y.-Z., Luo, R.-Z., Zhang, C.Z., and Yun, J.-P. (2014). FoxD3-regulated microRNA-137 suppresses tumour growth and metastasis in human hepatocellular carcinoma by targeting AKT2. Oncotarget *5*, 5113–5124.

Liu, M., Lang, N., Qiu, M., Xu, F., Li, Q., Tang, Q., Chen, J., Chen, X., Zhang, S., Liu, Z., et al. (2011). MiR-137 targets Cdc42 expression, induces cell cycle G1 arrest and inhibits invasion in colorectal cancer cells. Int. J. Cancer *128*, 1269–1279.

Liu-Yesucevitz, L., Bassell, G.J., Gitler, a. D., Hart, a. C., Klann, E., Richter, J.D., Warren, S.T., and Wolozin, B. (2011). Local RNA Translation at the Synapse and in Disease. J. Neurosci. *31*, 16086–16093.

Llorens-Martín, M., Fuster-Matanzo, A., Teixeira, C.M., Jurado-Arjona, J., Ulloa, F., Defelipe, J., Rábano, A., Hernández, F., Soriano, E., and Avila, J. (2013). GSK-3β overexpression causes reversible alterations on postsynaptic densities and dendritic morphology of hippocampal granule neurons in vivo. Mol. Psychiatry *18*, 451–460.

López-Bendito, G., Cautinat, A., Sánchez, J.A., Bielle, F., Flames, N., Garratt, A.N., Talmage, D.A., Role, L.W., Charnay, P., Marín, O., et al. (2006). Tangential Neuronal Migration Controls Axon Guidance: A Role for Neuregulin-1 in Thalamocortical Axon Navigation. Cell *125*, 127–142.

Lugli, G., Larson, J., Martone, M.E., Jones, Y., and Smalheiser, N.R. (2005). Dicer and eIF2c are enriched at postsynaptic densities in adult mouse brain and are modified by neuronal activity in a calpain-dependent manner. J. Neurochem. *94*, 896–905.

Lund, E., Güttinger, S., Calado, A., Dahlberg, J.E., and Kutay, U. (2004). Nuclear export of microRNA precursors. Science (80-.). *303*, 95–98.

Lyu, J., Yuan, B., Cheng, T., Qiu, Z., and Zhou, W. (2016). Reciprocal regulation of autism-related genes MeCP2 and PTEN via microRNAs. Sci. Rep. *6*, 20392.

Ma, G., Yin, J., Fu, J., Luo, X., Zhou, H., Tao, H., Cui, L., Li, Y., Lin, Z., Zhao, B., et al. (2014). Association of a miRNA-137 Polymorphism with Schizophrenia in a Southern Chinese Han Population. Biomed Res. Int. *2014*.

Mathonnet, G., Fabian, M.R., Svitkin, Y. V, Parsyan, A., Huck, L., Murata, T., Biffo, S., Merrick, W.C., Darzynkiewicz, E., Pillai, R.S., et al. (2007). MicroRNA Inhibition of Translation Initiation in Vitro by Targeting the Cap-Binding Complex eIF4F. Science (80-.). *317*, 1764–1767.

Mei, L., and Nave, K.A. (2014). Neuregulin-ERBB signaling in the nervous system and neuropsychiatric diseases. Neuron *83*, 27–49.

Mei, L., and Xiong, W.-C. (2008). Neuregulin 1 in neural development, synaptic plasticity and schizophrenia. Nat. Rev. Neurosci. *9*, 437–452.

Meister, G., Landthaler, M., Patkaniowska, A., Dorsett, Y., Teng, G., and Tuschl, T. (2004). Human Argonaute2 mediates RNA cleavage targeted by miRNAs and siRNAs. Mol. Cell *15*, 185–197.

Mellios, N., Sugihara, H., Castro, J., Banerjee, A., Le, C., Kumar, A., Crawford, B., Strathmann, J., Tropea, D., Levine, S.S., et al. (2011). miR-132, an experience-dependent microRNA, is essential for visual cortex plasticity. Nat. Neurosci. *14*, 1240–1242.

Miska, E.A., Alvarez-Saavedra, E., Townsend, M., Yoshii, A., Sestan, N., Rakic, P., Constantine-Paton, M., and Horvitz, H.R. (2004). Microarray analysis of microRNA expression in the developing mammalian brain. Genome Biol. *5*, R68.

Morita, S., Horii, T., Kimura, M., Goto, Y., Ochiya, T., and Hatada, I. (2007). One Argonaute family member, Eif2c2 (Ago2), is essential for development and appears not to be involved in DNA methylation. Genomics *89*, 687–696.

Muddashetty, R.S., Kelić, S., Gross, C., Xu, M., and Bassell, G.J. (2007). Dysregulated metabotropic glutamate receptor-dependent translation of AMPA receptor and postsynaptic density-95 mRNAs at synapses in a mouse model of fragile X syndrome. J. Neurosci. *27*, 5338–5348.

Muddashetty, R.S., Nalavadi, V.C., Gross, C., Yao, X., Xing, L., Laur, O., Warren, S.T., and Bassell, G.J. (2011). Reversible Inhibition of PSD-95 mRNA Translation by miR-125a, FMRP Phosphorylation, and mGluR Signaling. Mol. Cell *42*, 673–688.

Narayanan, U., Nalavadi, V., Nakamoto, M., Pallas, D.C., Ceman, S., Bassell, G.J., and Warren, S.T. (2007). FMRP Phosphorylation Reveals an Immediate-Early Signaling Pathway Triggered by Group I mGluR and Mediated by PP2A. J. Neurosci. *27*, 14349–14357.

Niere, F., Wilkerson, J.R., and Huber, K.M. (2012). Evidence for a Fragile X Mental Retardation Protein-Mediated Translational Switch in Metabotropic Glutamate Receptor-Triggered Arc Translation and Long-Term Depression. J. Neurosci. *32*, 5924–5936.

Noland, C.L., and Doudna, J.A. (2013). Multiple sensors ensure guide strand selection in human

RNAi pathways. RNA *19*, 639–648.

Nudelman, A.S., Dirocco, D.P., Lambert, T.J., Garelick, M.G., Le, J., Nathanson, N.M., and Storm, D.R. (2010). Neuronal activity rapidly induces transcription of the CREB-regulated microRNA-132, in vivo. Hippocampus *20*, 492–498.

O'Carroll, D., and Schaefer, A. (2013). General principals of miRNA biogenesis and regulation in the brain. Neuropsychopharmacology *38*, 39–54.

O'Connor, J., and Hemby, S. (2007). Elevated GRIA1 mRNA expression in Layer II/III and V pyramidal cells of the DLPFC in schizophrenia. Schizophr. Res. *97*, 277–288.

Okamura, K., Hagen, J.W., Duan, H., Tyler, D.M., and Lai, E.C. (2007). The Mirtron Pathway Generates microRNA-Class Regulatory RNAs in Drosophila. Cell *130*, 89–100.

Okamura, K., Liu, N., and Lai, E.C. (2009). Distinct Mechanisms for MicroRNA Strand Selection by Drosophila Argonautes. Mol. Cell *36*, 431–444.

Olde Loohuis, N.F.M., Ba, W., Stoerchel, P.H., Kos, A., Jager, A., Schratt, G., Martens, G.J.M., van Bokhoven, H., Nadif Kasri, N., and Aschrafi, A. (2015). MicroRNA-137 controls AMPA-receptor-mediated transmission and mGluR-dependent LTD. Cell Rep. *11*, 1876–1884.

Ørom, U.A., Nielsen, F.C., and Lund, A.H. (2008). MicroRNA-10a Binds the 5'UTR of Ribosomal Protein mRNAs and Enhances Their Translation. Mol. Cell *30*, 460–471.

Packer, A.N., Xing, Y., Harper, S.Q., Jones, L., and Davidson, B.L. (2008). The bifunctional microRNA miR-9/miR-9* regulates REST and CoREST and is downregulated in Huntington's disease. J. Neurosci. *28*, 14341–14346.

Panja, D., and Bramham, C.R. (2014). BDNF mechanisms in late LTP formation: A synthesis and breakdown. Neuropharmacology *76*, 664–676.

Papaleo, F., Yang, X.F., Paterson, C., Palumbo, X.S., Carr, G. V, Wang, Y., Floyd, K., Huang, W., Thomas, C.J., Chen, J., et al. (2016). Behavioral, neurophysiological, and synaptic impairment in a transgenic neuregulin1 (NRG1-IV) murine schizophrenia model. *36*,

4859–4875.

Paroo, Z., Ye, X., Chen, S., and Liu, Q. (2009). Phosphorylation of the Human MicroRNA-Generating Complex Mediates MAPK/Erk Signaling. Cell *139*, 112–122.

Pasquinelli, A.E., Reinhart, B.J., Slack, F., Martindale, M.Q., Kuroda, M.I., Maller, B., Hayward, D.C., Ball, E.E., Degnan, B., Müller, P., et al. (2000). Conservation of the sequence and temporal expression of let-7 heterochronic regulatory RNA. Nature *408*, 86–89.

Patranabis, S., and Bhattacharyya, S.N. (2016). Phosphorylation of Ago2 and Subsequent Inactivation of let-7a miRNPs Control Differentiation of Mammalian Sympathetic Neurons. Mol. Cell. Biol. *36*, MCB.00054-16.

Patterson, M.A., Szatmari, E.M., and Yasuda, R. (2010). AMPA receptors are exocytosed in stimulated spines and adjacent dendrites in a Ras-ERK-dependent manner during long-term potentiation. Proc Natl Acad Sci U S A *107*, 15951–15956.

Petersen, C.P., Bordeleau, M.E., Pelletier, J., and Sharp, P.A. (2006). Short RNAs repress translation after initiation in mammalian cells. Mol. Cell *21*, 533–542.

Poopal, A.C., Schroeder, L.M., Horn, P.S., Bassell, G.J., and Gross, C. (2016). Increased expression of the PI3K catalytic subunit p110δ underlies elevated S6 phosphorylation and protein synthesis in an individual with autism from a multiplex family. Mol. Autism *7*, 3.

Purcell, S.M., Moran, J.L., Fromer, M., Ruderfer, D., Solovieff, N., Roussos, P., Duncan, L., Stahl, E., Genovese, G., Dushlaine, C.O., et al. (2014). A polygenic burden of rare disruptive mutations in schizophrenia.

Qin, M., Kang, J., Vurlin, T., Jiang, C., and Smith, C. (2005). Postadolescent Changes in Regional Cerebral Protein Synthesis: An In Vivo Study in the Fmr1 Null Mouse. J. Neurosci. *25*, 5087–5095.

Raab-Graham, K.F., Haddick, P.C.G., Jan, Y.N., and Jan, L.Y. (2006). Activity- and mTOR-dependent suppression of Kv1.1 channel mRNA translation in dendrites. Science *314*, 144–148.

Rao, A., Kim, E., Sheng, M., and Craig, A.M. (1998). Heterogeneity in the molecular composition of excitatory postsynaptic sites during development of hippocampal neurons in culture. J. Neurosci. *18*, 1217–1229.

van der Ree, M.H., de Vree, J.M., Stelma, F., Willemse, S., van der Valk, M., Rietdijk, S., Molenkamp, R., Schinkel, J., van Nuenen, A.C., Beuers, U., et al. (2017). Safety, tolerability, and antiviral effect of RG-101 in patients with chronic hepatitis C: a phase 1B, double-blind, randomised controlled trial. Lancet *389*, 709–717.

Reinhart, B.J., Slack, F.J., Basson, M., Pasquinelli, a E., Bettinger, J.C., Rougvie, a E., Horvitz, H.R., and Ruvkun, G. (2000). The 21-nucleotide let-7 RNA regulates developmental timing in Caenorhabditis elegans. Nature *403*, 901–906.

Ripke, S., Sanders, A., Kendler, K., Levinson, D., Sklar, P., Holmans, P., Lin, D., Duan, J., Ophoff, R., Andreassen, O., et al. (2011). Genome-wide association study identifies five new schizophrenia loci. Nat. Genet. *43*, 969–976.

Ripke, S., O'Dushlaine, C., Chambert, K., Moran, J.L., Kähler, A.K., Akterin, S., Bergen, S.E., Collins, A.L., Crowley, J.J., Fromer, M., et al. (2013). Genome-wide association analysis identifies 13 new risk loci for schizophrenia. Nat. Genet. *45*, 1150–1159.

Ripke, S., Neale, B.M., Corvin, A., Walters, J.T.R., Farh, K.-H., Holmans, P. a., Lee, P., Bulik-Sullivan, B., Collier, D. a., Huang, H., et al. (2014). Biological insights from 108 schizophrenia-associated genetic loci. Nature *511*, 421–427.

Rodriguez, A., Griffiths-Jones, S., Ashurst, J., and Bradley, A. (2004). Identification of Mammalian microRNA Host Genes and Transcription Units. Genome Res. *14*, 1902–1910.

Rose, E.J., Morris, D.W., Fahey, C., Cannon, D., Mcdonald, C., Scanlon, C., Kelly, S., Gill, M., Corvin, A., and Donohoe, G. (2014). The miR-137 schizophrenia susceptibility variant rs1625579 does not predict variability in brain volume in a sample of schizophrenic patients and healthy individuals. Am. J. Med. Genet. Part B Neuropsychiatr. Genet. *165*,

467–471.

Rosoklija, G., Toomayan, G., Ellis, S., Keilp, J., Mann, J., Latov, N., Hays, A., and Dwork, A. (2000). Structural abnormalities of subicular dendrites in subjects with schizophrenia and mood disorders. Arch. Gen. Psychiatry *57*, 349–356.

Roux, P.P., Shahbazian, D., Vu, H., Holz, M.K., Cohen, M.S., Taunton, J., Sonenberg, N., and Blenis, J. (2007). RAS/ERK signaling promotes site-specific ribosomal protein S6 phosphorylation via RSK and stimulates cap-dependent translation. *282*, 14056–14064.

Ruby, J.G., Jan, C.H., and Bartel, D.P. (2007). Intronic microRNA precursors that bypass Drosha processing. Nature *448*, 83–86.

Rui, Y., Myers, K.R., Yu, K., Wise, A., De Blas, A.L., Hartzell, H.C., and Zheng, J.Q. (2013). Activity-dependent regulation of dendritic growth and maintenance by glycogen synthase kinase 3β. Nat. Commun. *4*, 2628.

Ryu, H.S., Park, S.-Y., Ma, D., Zhang, J., and Lee, W. (2011). The induction of microRNA targeting IRS-1 is involved in the development of insulin resistance under conditions of mitochondrial dysfunction in hepatocytes. PLoS One *6*, e17343.

Saba, R., Störchel, P.H., Aksoy-Aksel, A., Kepura, F., Lippi, G., Plant, T.D., and Schratt, G.M. (2012). Dopamine-regulated microRNA MiR-181a controls GluA2 surface expression in hippocampal neurons. Mol. Cell. Biol. *32*, 619–632.

Sampathkumar, C., Wu, Y.-J., Vadhvani, M., Trimbuch, T., Eickholt, B., Rosenmund, C., Abuhatzira, L., Makedonski, K., Kaufman, Y., Razin, A., et al. (2016). Loss of MeCP2 disrupts cell autonomous and autocrine BDNF signaling in mouse glutamatergic neurons. Elife *5*, 214–222.

Sang, L., Liu, T., Liu, H., Li, H., Zhang, H., and Jiang, F. (2016). MicroRNA-137 suppresses cell migration and invasion in renal cell carcinoma by targeting PIK3R3. *9*, 7160–7167.

Sarbassov, D.D., Ali, S.M., Kim, D.-H., Guertin, D.A., Latek, R.R., Erdjument-Bromage, H., Tempst, P., and Sabatini, D.M. (2004). Rictor, a Novel Binding Partner of mTOR,

Defines a Rapamycin-Insensitive and Raptor-Independent Pathway that Regulates the Cytoskeleton. Curr. Biol. *14*, 1296–1302.

Sarbassov, D.D., Guertin, D. a, Ali, S.M., and Sabatini, D.M. (2005). Phosphorylation and regulation of Akt/PKB by the rictor-mTOR complex. Science *307*, 1098–1101.

Sarbassov, D.D., Ali, S.M., Sengupta, S., Sheen, J.H., Hsu, P.P., Bagley, A.F., Markhard, A.L., and Sabatini, D.M. (2006). Prolonged Rapamycin Treatment Inhibits mTORC2 Assembly and Akt/PKB. Mol. Cell *22*, 159–168.

Sasaki, Y., Gross, C., Xing, L., Goshima, Y., and Bassell, G.J. (2014). Identification of axon-enriched MicroRNAs localized to growth cones of cortical neurons. Dev. Neurobiol. *74*, 397–406.

Schratt, G.M., Nigh, E.A., Chen, W.G., Hu, L., and Greenberg, M.E. (2004). BDNF Regulates the Translation of a Select Group of mRNAs by a Mammalian Target of Rapamycin-Phosphatidylinositol 3-Kinase-Dependent Pathway during Neuronal Development. J. Neurosci. *24*, 7366–7377.

Schratt, G.M., Tuebing, F., Nigh, E.A., Kane, C.G., Sabatini, M.E., Kiebler, M., and Greenberg, M.E. (2006). A brain-specific microRNA regulates dendritic spine development. Nature *439*, 283–289.

Scott, E.K., Reuter, J.E., and Luo, L. (2003). Small GTPase Cdc42 is required for multiple aspects of dendritic morphogenesis. J. Neurosci. *23*, 3118–3123.

Scott, H.L., Tamagnini, F., Narduzzo, K.E., Howarth, J.L., Lee, Y.B., Wong, L.F., Brown, M.W., Warburton, E.C., Bashir, Z.I., and Uney, J.B. (2012). MicroRNA-132 regulates recognition memory and synaptic plasticity in the perirhinal cortex. Eur. J. Neurosci. *36*, 2941–2948.

Sempere, L.F., Freemantle, S., Pitha-Rowe, I., Moss, E., Dmitrovsky, E., and Ambros, V. (2004). Expression profiling of mammalian microRNAs uncovers a subset of brain-expressed microRNAs with possible roles in murine and human neuronal differentiation. Genome

Biol. *5*, R13.

Sengupta, J.N., Pochiraju, S., Kannampalli, P., Bruckert, M., Addya, S., Yadav, P., Miranda, A., Shaker, R., and Banerjee, B. (2013). MicroRNA-mediated GABAAα-1 receptor subunit down-regulation in adult spinal cord following neonatal cystitis-induced chronic visceral pain in rats. Pain *154*, 59–70.

Seshadri, S., Kamiya, A., Yokota, Y., Prikulis, I., Kano, S., Hayashi-Takagi, A., Stanco, A., Eom, T.Y., Rao, S., Ishizuka, K., et al. (2010). Disrupted-in-Schizophrenia-1 expression is regulated by beta-site amyloid precursor protein cleaving enzyme-1-neuregulin cascade. Proc Natl Acad Sci U S A *107*, 5622–5627.

Shaked, I., Meerson, A., Wolf, Y., Avni, R., Greenberg, D., Gilboa-Geffen, A., and Soreq, H. (2009). MicroRNA-132 Potentiates Cholinergic Anti-Inflammatory Signaling by Targeting Acetylcholinesterase. Immunity *31*, 965–973.

Shaltiel, G., Hanan, M., Wolf, Y., Barbash, S., Kovalev, E., Shoham, S., and Soreq, H. (2013). Hippocampal microRNA-132 mediates stress-inducible cognitive deficits through its acetylcholinesterase target. Brain Struct. Funct. *218*, 59–72.

Shen, J., Xia, W., Khotskaya, Y.B., Huo, L., Nakanishi, K., Lim, S.O., Du, Y., Wang, Y., Chang, W.C., Chen, C.H., et al. (2013). EGFR modulates microRNA maturation in response to hypoxia through phosphorylation of AGO2. Nature *497*, 383–387.

Shi, F., Dong, Z., Li, H., Liu, X., Liu, H., and Dong, R. (2017). MicroRNA-137 protects neurons against ischemia/reperfusion injury through regulation of the Notch signaling pathway. Exp. Cell Res.

Siegert, S., Seo, J., Kwon, E.J., Rudenko, A., Cho, S., Wang, W., Flood, Z., Martorell, A.J., Ericsson, M., Mungenast, A.E., et al. (2015). The schizophrenia risk gene product miR-137 alters presynaptic plasticity. Nat. Neurosci. *18*, 1008–1016.

Slipczuk, L., Bekinschtein, P., Katche, C., Cammarota, M., Izquierdo, I., and Medina, J.H. (2009). BDNF activates mTOR to regulate GluR1 expression required for memory

formation. PLoS One *4*.

Smoller, J.W. (2013). Identification of risk loci with shared effects on five major psychiatric disorders: a genome-wide analysis. Lancet *381*, 1371–1379.

Smrt, R.D., Szulwach, K.E., Pfeiffer, R.L., Li, X., Guo, W., Pathania, M., Teng, Z.Q., Luo, Y., Peng, J., Bordey, A., et al. (2010). MicroRNA miR-137 regulates neuronal maturation by targeting ubiquitin ligase mind bomb-1. Stem Cells *28*, 1060–1070.

Sosanya, N.M., Huang, P.P.C., Cacheaux, L.P., Chen, C.J., Nguyen, K., Perrone-Bizzozero, N.I., and Raab-Graham, K.F. (2013). Degradation of high affinity HuD targets releases Kv1.1 mRNA from miR-129 repression by mTORC1. J. Cell Biol. *202*, 53–69.

Stephan, K.E., Baldeweg, T., and Friston, K.J. (2006). Synaptic Plasticity and Dysconnection in Schizophrenia. Biol. Psychiatry *59*, 929–939.

Strazisar, M., Cammaerts, S., van der Ven, K., Forero, D.A., Lenaerts, A., Nordin, A., Almeida-Souza, L., Genovese, G., Timmerman, V., Liekens, A., et al. (2014). MIR137 variants identified in psychiatric patients affect synaptogenesis and neuronal transmission gene sets. Mol. Psychiatry *20*, 1–10.

Sturgeon, M., Davis, D., Albers, A., Beatty, D., Austin, R., Ferguson, M., Tounsel, B., and Liebl, F.L.W. (2016). The Notch ligand E3 ligase, Mind Bomb1, regulates glutamate receptor localization in Drosophila. Mol. Cell. Neurosci. *70*, 11–21.

Sullivan, P.F., Kendler, K.S., and Neale, M.C. (2003). Schizophrenia as a Complex Trait. Arch. Gen. Psychiatry *60*, 1187–1192.

Sullivan, P.F., Daly, M.J., and O'Donovan, M. (2012). Genetic architectures of psychiatric disorders: the emerging picture and its implications. Nat. Rev. Genet. *13*, 537–551.

Sutton, M.A., and Schuman, E.M. (2005). Local Translational Control in Dendrites and Its Role in Long-Term Synaptic Plasticity. 116–131.

Sutton, M.A., Ito, H.T., Cressy, P., Kempf, C., Woo, J.C., and Schuman, E.M. (2006). Miniature Neurotransmission Stabilizes Synaptic Function via Tonic Suppression of Local

Dendritic Protein Synthesis. 785–799.

Swanger, S.A., and Bassell, G.J. (2013). Dendritic protein synthesis in the normal and diseased brain. Neuroscience *232*, 106–127.

Szulwach, K.E., Li, X., Smrt, R.D., Li, Y., Luo, Y., Lin, L., Santistevan, N.J., Li, W., Zhao, X., and Jin, P. (2010). Cross talk between microRNA and epigenetic regulation in adult neurogenesis. J. Cell Biol. *189*, 127–141.

Tandon, R., Keshavan, M.S., and Nasrallah, H.A. (2008). Schizophrenia, "just the facts" what we know in 2008. 2. Epidemiology and etiology. Schizophr. Res. *102*, 1–18.

Tandon, R., Nasrallah, H.A., and Keshavan, M.S. (2009). Schizophrenia, “just the facts” 4. Clinical features and conceptualization. Schizophr. Res. *110*, 1–23.

Thermann, R., and Hentze, M.W. (2007). Drosophila miR2 induces pseudo-polysomes and inhibits translation initiation. Nature *447*, 875–878.

Ting, A.K., Chen, Y., Wen, L., Yin, D.-M., Shen, C., Tao, Y., Liu, X., Xiong, W.-C., and Mei, L. (2011). Neuregulin 1 promotes excitatory synapse development and function in GABAergic interneurons. J. Neurosci. *31*, 15–25.

Tognini, P., Putignano, E., Coatti, A., and Pizzorusso, T. (2011). Experience-dependent expression of miR-132 regulates ocular dominance plasticity. Nat. Neurosci. *14*, 1237–1239.

tom Dieck, S., Kochen, L., Hanus, C., Heumüller, M., Bartnik, I., Nassim-Assir, B., Merk, K., Mosler, T., Garg, S., Bunse, S., et al. (2015). Direct visualization of newly synthesized target proteins in situ. Nat. Methods *12*, 411–414.

Traynelis, S.F., Wollmuth, L.P., Mcbain, C.J., Menniti, F.S., Vance, K.M., Ogden, K.K., Hansen, K.B., Yuan, H., Myers, S.J., and Dingledine, R. (2010). Glutamate Receptor Ion Channels : Structure , Regulation , and Function. *62*, 405–496.

Tsiouris, J. a, and Brown, W.T. (2004). Neuropsychiatric Symptoms of Fragile X Syndrome.

CNS Drugs *18*, 687–703.

Tucci, A., Ciaccio, C., Scuvera, G., Esposito, S., and Milani, D. (2016). MIR137 is the key gene mediator of the syndromic obesity phenotype of patients with 1p21.3 microdeletions. Mol. Cytogenet. *9*, 80.

Uchida, N., Hoshino, S. ichi, Imataka, H., Sonenberg, N., and Katada, T. (2002). A novel role of the mammalian GSPT/eRF3 associating with poly(A)-binding protein in cap/poly(A)-dependent translation. J. Biol. Chem. *277*, 50286–50292.

Vallès, A., Martens, G.J.M., De Weerd, P., Poelmans, G., and Aschrafi, A. (2014). MicroRNA-137 regulates a glucocorticoid receptor-dependent signalling network: Implications for the etiology of schizophrenia. J. Psychiatry Neurosci. *39*, 312–320.

Vo, N., Klein, M.E., Varlamova, O., Keller, D.M., Yamamoto, T., Goodman, R.H., and Impey, S. (2005). A cAMP-response element binding protein-induced microRNA regulates neuronal morphogenesis. Proc. Natl. Acad. Sci. U. S. A. *102*, 16426–16431.

Warburton, A., Breen, G., Rujescu, D., Bubb, V.J., and Quinn, J.P. (2015). Characterization of a REST-regulated internal promoter in the schizophrenia genome-wide associated gene MIR137. Schizophr. Bull. *41*, 698–707.

Wayman, G. a, Davare, M., Ando, H., Fortin, D., Varlamova, O., Cheng, H.-Y.M., Marks, D., Obrietan, K., Soderling, T.R., Goodman, R.H., et al. (2008). An activity-regulated microRNA controls dendritic plasticity by down-regulating p250GAP. Proc. Natl. Acad. Sci. U. S. A. *105*, 9093–9098.

Wei, C., Thatcher, E.J., Olena, A.F., Cha, D.J., Perdigoto, A.L., Marshall, A.F., Carter, B.D., Broadie, K., and Patton, J.G. (2013). miR-153 Regulates SNAP-25, Synaptic Transmission, and Neuronal Development. PLoS One *8*.

Weiler, I.J., Spangler, C.C., Klintsova, A.Y., Grossman, A.W., Kim, S.H., Bertaina-Anglade, V., Khaliq, H., de Vries, F.E., Lambers, F. a E., Hatia, F., et al. (2004). Fragile X mental retardation protein is necessary for neurotransmitter-activated protein translation at

synapses. Proc. Natl. Acad. Sci. U. S. A. *101*, 17504–17509.

Wen, D., Suggs, S. V, Karunagaran, D., Liu, N., Cupples, R.L., Luo, Y., Janssen, A.M., Ben-Baruch, N., Trollinger, D.B., and Jacobsen, V.L. (1994). Structural and functional aspects of the multiplicity of Neu differentiation factors. Mol. Cell. Biol. *14*, 1909–1919.

Wenger, T.L., Miller, J.S., DePolo, L.M., de Marchena, A.B., Clements, C.C., Emanuel, B.S., Zackai, E.H., McDonald-McGinn, D.M., and Schultz, R.T. (2016). 22Q11.2 Duplication Syndrome: Elevated Rate of Autism Spectrum Disorder and Need for Medical Screening. Mol. Autism *7*, 27.

Wibrand, K., Panja, D., Tiron, A., Ofte, M.L., Skaftnesmo, K.O., Lee, C.S., Pena, J.T.G., Tuschl, T., and Bramham, C.R. (2010). Differential regulation of mature and precursor microRNA expression by NMDA and metabotropic glutamate receptor activation during LTP in the adult dentate gyrus in vivo. Eur. J. Neurosci. *31*, 636–645.

Wightman, B., Bürglin, T.R., Gatto, J., Arasu, P., and Ruvkun, G. (1991). Negative regulatory sequences in the lin-14 3′-untranslated region are necessary to generate a temporal switch during Caenorhabditis elegans development. Genes Dev. *5*, 1813–1824.

Wightman, B., Ha, I., and Ruvkun, G. (1993). Posttranscriptional regulation of the heterochronic gene lin-14 by lin-4 mediates temporal pattern formation in C. elegans. Cell *75*, 855–862.

Willemsen, M.H., Vallès, A., Kirkels, L.A.M.H., Mastebroek, M., Olde Loohuis, N., Kos, A., Wissink-Lindhout, W.M., de Brouwer, A.P.M., Nillesen, W.M., Pfundt, R., et al. (2011). Chromosome 1p21.3 microdeletions comprising DPYD and MIR137 are associated with intellectual disability. J. Med. Genet. *48*, 810–818.

Williams, K.R., McAninch, D.S., Stefanovic, S., Xing, L., Allen, M., Li, W., Feng, Y., Mihailescu, M.R., and Bassell, G.J. (2016). hnRNP-Q1 represses nascent axon growth in cortical neurons by inhibiting Gap-43 mRNA translation. Mol. Biol. Cell *27*, 518–534.

Woldemichael, B.T., Jawaid, A., Kremer, E.A., Gaur, N., Krol, J., Marchais, A., and Mansuy, I.M. (2016). The microRNA cluster miR-183/96/182 contributes to long-term memory in

a protein phosphatase 1-dependent manner. Nat. Commun. *7*, 12594.

Wright, C., Gupta, C.N., Chen, J., Patel, V., Calhoun, V.D., Ehrlich, S., Wang, L., Bustillo, J.R., Perrone-Bizzozero, N.I., and Turner, J.A. (2016). Polymorphisms in MIR137HG and microRNA-137-regulated genes influence gray matter structure in schizophrenia. Transl. Psychiatry *6*, e724.

Xu, B., Hsu, P., Stark, K.L., Karayiorgou, M., and Gogos, J.A. (2012). Derepression of a Neuronal Inhibitor due to miRNA Dysregulation in a Schizophrenia-Related Microdeletion. Cell *152*, 262–275.

Xue, Q., Yu, C., Wang, Y., Liu, L., Zhang, K., Fang, C., Liu, F., Bian, G., Song, B., Yang, A., et al. (2016). miR-9 and miR-124 synergistically affect regulation of dendritic branching via the AKT/GSK3β pathway by targeting Rap2a. Sci. Rep. *6*, 26781.

Yang, J.-S., Maurin, T., Robine, N., Rasmussen, K.D., Jeffrey, K.L., Chandwani, R., Papapetrou, E.P., Sadelain, M., O'Carroll, D., and Lai, E.C. (2010). Conserved vertebrate mir-451 provides a platform for Dicer-independent, Ago2-mediated microRNA biogenesis. Proc. Natl. Acad. Sci. U. S. A. *107*, 15163–15168.

Yang, Y.-R., Li, Y.-X., Gao, X.-Y., Zhao, S.-S., Zang, S.-Z., and Zhang, Z.-Q. (2015). MicroRNA-137 inhibits cell migration and invasion by targeting bone morphogenetic protein-7 (BMP7) in non-small cell lung cancer cells. Int. J. Clin. Exp. Pathol. *8*, 10847–10853.

Yao, J., Sun, J., Zhao, Q., Wang, C., Mei, Y., Jj, Y., Sun, J., Qr, Z., Cy, W., and Erbb, M.Y.A.N.- (2013). Neuregulin-1 / ErbB4 signaling regulates Kv4 . 2-mediated transient outward K 2 current through the Akt / mTOR pathway. 197–206.

Yi, R., Qin, Y., Macara, I.G., and Cullen, B.R. (2003). Exportin-5 mediates the nuclear export of pre-microRNAs and short hairpin RNAs Exportin-5 mediates the nuclear export of pre-microRNAs and short hairpin RNAs. 3011–3016.

Yoon, K.-J., Lee, H.-R., Jo, Y.S., An, K., Jung, S.-Y., Jeong, M.-W., Kwon, S.-K., Kim, N.-S.,

Jeong, H.-W., Ahn, S.-H., et al. (2012). Mind bomb-1 is an essential modulator of long-term memory and synaptic plasticity via the Notch signaling pathway. Mol. Brain *5*, 40.

Yoshii, A., and Constantine-Paton, M. (2010). Postsynaptic BDNF-TrkB signaling in synapse maturation, plasticity, and disease. Dev. Neurobiol. *70*, 304–322.

Yudowski, G.A., Olsen, O., Adesnik, H., Marek, K.W., and Bredt, D.S. (2013). Acute Inactivation of PSD-95 Destabilizes AMPA Receptors at Hippocampal Synapses. PLoS One *8*, 1–9.

Yurek, D.M., Zhang, L., Fletcher-Turner, A., and Seroogy, K.B. (2004). Supranigral injection of neuregulin1-β induces striatal dopamine overflow. Brain Res. *1028*, 116–119.

Zdanowicz, A., Thermann, R., Kowalska, J., Jemielity, J., Duncan, K., Preiss, T., Darzynkiewicz, E., and Hentze, M.W. (2009). Drosophila miR2 Primarily Targets the m7GpppN Cap Structure for Translational Repression. Mol. Cell *35*, 881–888.

Zeng, Y., Sankala, H., Zhang, X., and Graves, P.R. (2008). Phosphorylation of Argonaute 2 at serine-387 facilitates its localization to processing bodies. Biochem. J. *413*, 429–436.

Zhang, J., and Abdullah, J.M. (2013). The role of GluA1 in central nervous system disorders. Rev. Neurosci. *24*, 499–505.

Zhang, J., Du, Y., Lin, Y., Chen, Y., Yang, L., Wang, H., and Ma, D. (2008). The cell growth suppressor, mir-126, targets IRS-1. Biochem. Biophys. Res. Commun. *377*, 136–140.

Zhang, Q., Yu, Y., and Huang, X. (2016). Olanzapine prevents the PCP-induced reduction in the neurite outgrowth of prefrontal cortical neurons via NRG1. Sci. Rep. *6*, 19581.

Zhao, L., Li, H., Guo, R., Ma, T., Hou, R., Ma, X., and Du, Y. (2013). miR-137, a new target for post-stroke depression? Neural Regen. Res. *8*, 2441–2448.

Zhu, N., Zhang, D., Xie, H., Zhou, Z., Chen, H., Hu, T., Bai, Y., Shen, Y., Yuan, W., Jing, Q., et al. (2011). Endothelial-specific intron-derived miR-126 is down-regulated in human breast cancer and targets both VEGFA and PIK3R2. Mol. Cell. Biochem. *351*, 157–164.

Zoghbi, H.Y., and Bear, M.F. (2012). Synaptic dysfunction in neurodevelopmental disorders

associated with autism and intellectual disabilities. Cold Spring Harb. Perspect. Biol. *4*, 1–22.

Zou, Y., Chiu, H., Domenger, D., Chuang, C.F., and Chang, C. (2012). The lin-4 microRNA targets the LIN-14 transcription factor to inhibit netrin-mediated axon attraction. Sci Signal *5*, ra43.